

8-2012

Cell-Matrix Adhesion in Muscle Development and Disease

Michelle F. Goody

Follow this and additional works at: <http://digitalcommons.library.umaine.edu/etd>

 Part of the [Biomechanics Commons](#), [Medical Biochemistry Commons](#), [Musculoskeletal Diseases Commons](#), [Musculoskeletal, Neural, and Ocular Physiology Commons](#), and the [Musculoskeletal System Commons](#)

Recommended Citation

Goody, Michelle F, "Cell-Matrix Adhesion in Muscle Development and Disease" (2012). *Electronic Theses and Dissertations*. 1801.
<http://digitalcommons.library.umaine.edu/etd/1801>

This Open-Access Dissertation is brought to you for free and open access by DigitalCommons@UMaine. It has been accepted for inclusion in Electronic Theses and Dissertations by an authorized administrator of DigitalCommons@UMaine.

CELL-MATRIX ADHESION IN MUSCLE

DEVELOPMENT AND DISEASE

by

Michelle F. Goody

B.S. The University of Maine, 2007

A DISSERTATION

Submitted in Partial Fulfillment of the

Requirements for the Degree of

Doctor of Philosophy

(in Biomedical Sciences)

The Graduate School

The University of Maine

August, 2012

Advisory Committee:

Clarissa Henry, Associate Professor, School of Biology and Ecology, University of Maine, Advisor

Dorothy E. Croall, Professor of Biochemistry, Department of Molecular and Biomedical Sciences, University of Maine

Leif Oxburgh, Principal Investigator, Maine Medical Center Research Institute

Roger Sher, Associate Research Scientist, The Jackson Laboratory

Mary Tyler, Professor, School of Biology and Ecology, University of Maine

DISSERTATION ACCEPTANCE STATEMENT

On behalf of the Graduate Committee for Michelle F. Goody I affirm that this manuscript is the final and accepted dissertation. Signatures of all committee members are on file with the Graduate School at the University of Maine, 42 Stodder Hall, Orono, Maine.

Clarissa Henry, PhD, Advisor

Date

Copyright Michelle F. Goody 2012

LIBRARY RIGHTS STATEMENT

In presenting this dissertation in partial fulfillment of the requirements for an advanced degree at the University of Maine, I agree that the Library shall make it freely available for inspection. I further agree that permission for “fair use” copying of this dissertation for scholarly purposes may be granted by the Librarian. It is understood that any copying or publication of this dissertation for financial gain shall not be allowed without my written permission.

Signature:

Date:

**CELL-MATRIX ADHESION IN MUSCLE
DEVELOPMENT AND DISEASE**

By Michelle F. Goody

Advisor: Dr. Clarissa Henry

An Abstract of the Dissertation Presented
in Partial Fulfillment of the Requirements for the
Degree of Doctor of Philosophy
(in Biomedical Sciences)
August, 2012

A variety of diseases, both inherited and acquired, affect muscle tissues in humans. The anchoring of muscle fibers to their surrounding environment is critical for muscle homeostasis. Muscle fibers attach to their microenvironment through cell-matrix adhesion complexes. These anchoring complexes are placed under repeated stress during muscle contraction. Genetic mutations in these complexes weaken the attachment between muscle fibers and their microenvironment, making fibers more susceptible to damage and death. This increased fiber degeneration eventually leads to progressive muscle wasting diseases, known as congenital muscular dystrophies. Although clinical trials are ongoing, there is presently no way to cure the loss of muscle structure and function associated with congenital muscular dystrophies.

Animal models of human diseases are used to gain insights into mechanisms of disease pathogenesis and to screen for potential therapeutic compounds. The zebrafish model system, well-known for its use in developmental biological studies, is rapidly

becoming widely-accepted as a useful model for biomedical research. We utilized zebrafish embryos to study the initial morphogenesis of substructures in the muscle microenvironment and the initial stable cell-matrix adhesions formed in muscle tissue. As the muscle fiber microenvironment is abnormal in congenital muscular dystrophies and cell-matrix adhesions are weakened, studies elucidating how strong, stable cell-matrix adhesions form in development could be informative in the effort to treat congenital muscular dystrophies.

Using this approach, we identified a previously undescribed cell-matrix adhesion pathway required for normal organization of an important substructure in the muscle tissue microenvironment. We show that activation of this cell-matrix adhesion pathway in dystrophic zebrafish not only significantly reduces muscle degeneration, but also improves swimming ability. The results presented in this dissertation identify proteins that function in this cell-matrix adhesion pathway and use dystrophic zebrafish to show the benefits and limitations of this pathway in treating symptoms of congenital muscular dystrophies. Our findings suggest that activation of this pathway has the potential to ameliorate loss of muscle structure and function in multiple muscular dystrophies.

ACKNOWLEDGEMENTS

Thank you to my committee members, Drs. Croall, Oxburgh, Sher and Tyler, for your perspectives, feedback and guidance during my graduate education and graduate research experience. I would especially like to thank Mary Tyler. Mary - not only was it a pleasure to be your student and learn from you, but your recommendation to introduce myself to Dr. Clarissa Henry changed the path that I was on and resulted in me embarking on the adventure of graduate school.

I can only begin to express my gratitude for my advisor, Dr. Clarissa Henry. Clarissa - it was an absolute joy to be trained by you and to conduct my graduate research project in your lab under your guidance. I feel the top-notch, well-rounded training that I received from you at UMaine has provided me with a solid foundation to competitively pursue any science-related career. I am thankful for the opportunities that you afforded me to travel to scientific conferences and for teaching me how to effectively communicate my work. The atmosphere in your lab, an ideal balance between productivity and fun, made me motivated and genuinely excited to be at the lab each day.

I would like to thank all the members of the Henry lab that I got to work with, past and present. Thanks to a wonderful technician, Mary Astumian, for experimental help as well as keeping the day-to-day operations of the lab running smoothly. Thank you to former Henry lab graduate students Matt Peterson, Molly Jenkins and Erik McCarthy for collaborations and helpful discussions of my project (especially Erik for piecing together that MIBP2 and NrK2b are the same protein, which resulted in a whole new direction to explore). I would like to thank the outstanding undergraduate researchers that

I got the opportunity to work with and help train, including Judi Azevedo, Kevin Lessard, Sam Entwisle, Christine Reynolds and Anna Burgess. Also, thanks to Cindi Gousse, an undergraduate worker, for doing the unglorified, but necessary chores that keep a lab running. I owe a debt of gratitude to Meghan Kelly. Meghan - my time in graduate school was so enjoyable in large part because you were right there next to me, whether we were in class, at a conference or seminar, writing at our desks, injecting embryos, imaging at the microscopes, cross-country skiing or at the movie theatre. Your input and support, professionally and personally, are invaluable to me and I am truly grateful that graduate school introduced us to one another.

I found a home in UMaine's Graduate School of Biomedical Sciences and would like to thank the GSBS director Dr. Carol Kim. Carol - you have put so much thought and effort into making the GSBS a student-centered, intellectually stimulating, collaborative and fun experience and you have succeeded in your vision. Also, thanks to my fellow GSBS peers and members of nearby laboratories, especially Kim Brothers, Dr. Remi Gratacap, Kristin Gabor, Jeremy Charette and Rachel Palmer, for helpful advice, discussions of science and fun times.

I would like to thank UMaine's Thesis Studio co-founder, Dr. Dylan Dryer, and the members of my particular Thesis Studio, especially Robert Hodges, for making the writing of my dissertation enjoyable. It was a wonderful experience to receive helpful critiques of my writing and to be able to help others improve their writing.

Thanks to Mark Nilan for outstanding care and maintenance of the UMaine zebrafish facility. The health and fecundity of the zebrafish at UMaine are unparalleled in

large part to your ingenuity and meticulousness; the value of this resource is not taken for granted.

Lastly, I would like to thank my extremely supportive family. Thank you to my parents for the importance you place on education and for loving and supporting me in everything I do, to my sisters for being my best friends, and to my husband, Brad, and his family for constant love and encouragement. Thank you Brad for all the times that you have listened to me explain what I did at work that day and waited in the car for me while I just had to run into the lab for “five” minutes. Brad, I have loved every minute of raising our five, furry, four-legged children with you and can not wait to start raising our daughter together very soon; your personality is the perfect compliment to mine and your humor and outlook remind me what is important in life. Thank you!

TABLE OF CONTENTS

ACKNOWLEDGEMENTS.....	iv
LIST OF TABLES.....	xii
LIST OF FIGURES.....	xiii
Chapter	
1. THE TRANSLATIONAL SCIENCE IMPLICATIONS OF DEVELOPMENTAL BIOLOGY.....	1
1.1. Perspective.....	1
1.2. Introduction.....	3
1.2.1. The Extracellular Matrix Microenvironment in Development and Disease.....	3
1.2.2. Cell-Matrix Adhesion Complexes in Dynamic Reciprocity, Basement Membrane Assembly and Disease.....	6
1.2.3. Zebrafish Muscle: A Paradigm to Study Cell-Matrix Adhesion during Muscle Development and Disease.....	10
2. NRK2B AND NAD ⁺ REGULATE CELL ADHESION AND ARE REQUIRED FOR MUSCLE MORPHOGENESIS <i>IN VIVO</i>	13
2.1. Chapter Abstract.....	13
2.2. Introduction.....	14
2.3. Materials and Methods.....	18
2.3.1. Zebrafish Husbandry/Mutant/Transgenic Lines.....	18

2.3.2. Morpholino Injections.....	19
2.3.3. NAD ⁺ Treatment.....	19
2.3.4. Antibody Staining/Immunohistochemistry.....	20
2.3.5. Whole Mount <i>In Situ</i> Hybridization.....	20
2.3.6. Westerns.....	21
2.3.7. Genetic Mosaics.....	21
2.3.8. Comparative qRT-PCR.....	21
2.3.9. Imaging.....	23
2.3.10. Measuring Myotome Boundary Angles.....	23
2.3.11. Normalized Fluorescence Intensity.....	23
2.3.12. The 2D Wavelet Transform Modulus Maxima Method.....	24
2.4. Results.....	24
2.4.1. Characterization of <i>nrk2b</i> Expression and Morpholinos Targeting <i>nrk2b</i>	24
2.4.2. MTJs are Disrupted in <i>nrk2b</i> Morphants.....	30
2.4.3. Exogenous NAD ⁺ Rescues MTJ Deterioration in <i>nrk2b</i> Morphants.....	35
2.4.4. Nrk2b is Required Non-Cell Autonomously for Basement Membrane Polymerization at the MTJ.....	39
2.4.5. CMAC Assembly is Aberrant in <i>nrk2b</i> Morphants.....	48
2.4.6. Paxillin is Sufficient for Boundary Capture in <i>nrk2b</i> Morphants.....	54

2.5. Discussion.....	59
2.5.1. A Novel Morphogenetic Role for NAD+.....	62
2.5.2. Dynamic Reciprocity and Musculoskeletal Homeostasis.....	65
2.5.3. Nr2f1 and Specificity of Cell Adhesion Function.....	66
2.5.4. Paxillin at the MTJ is Not Required for Subcellular Localization of FAK to the MTJ.....	68
2.5.5. Quantitative Analysis of Morphogenesis.....	69
2.6. Chapter Conclusions.....	70
3. NAD+ AMELIORATES MUSCULAR DYSTROPHY IN ZEBRAFISH.....	72
3.1. Chapter Abstract.....	72
3.2. Introduction.....	73
3.3. Materials and Methods.....	77
3.3.1. Zebrafish Husbandry/Mutant/Transgenic Lines.....	77
3.3.2. Morpholino Injection.....	78
3.3.3. NAD+ and Emergen-C Treatment.....	78
3.3.4. Phalloidin Staining and Immunohistochemistry.....	79
3.3.5. Genetic Mosaic Analysis.....	80
3.3.6. Westerns.....	80
3.3.7. <i>In Situ</i> Hybridization.....	80
3.3.8. Two-Dimensional Wavelet Transform Modulus Maxima.....	80
3.3.9. Motility Assay.....	80
3.3.10. Imaging.....	81

3.3.11. Statistical Analyses.....	81
3.3.12. Measuring Myotome Boundary Angles.....	81
3.3.13. Electron Microscopy.....	81
3.4. Results.....	82
3.4.1. NAD ⁺ Supplementation Reduces Muscle Degeneration in <i>dystroglycan</i> Morphants.....	82
3.4.2. A Normal MTJ BM Microenvironment is Sufficient to Rescue the Structure of Dystrophic Muscle.....	86
3.4.3. Itga7 is Required for NAD ⁺ -Mediated Reduction of Dystrophy in <i>dag1</i> Morphants.....	90
3.4.4. Itga6 is Required for NAD ⁺ -Mediated Improvement of Muscle Tissue Structure.....	94
3.4.5. Paxillin Overexpression is Sufficient to Increase MTJ BM Structure and Decrease Fiber Detachment in <i>dag1</i> Morphants.....	102
3.4.6. NAD ⁺ Supplementation Improves the Mobility of Dystrophic Zebrafish.....	108
3.5. Discussion.....	111
3.5.1. The ECM Microenvironment: A Dynamic Structure Sufficient to Guide Morphological Change.....	112
3.5.2. Unique and Redundant Roles for the Laminin Receptor Proteins Integrin alpha7, Integrin alpha6, and Dystroglycan.....	114
3.5.3. Paxillin and Basement Membrane Organization.....	117

3.5.4. Moving Toward Viable Therapeutic Options for Myopathies.....	118
3.6. Chapter Conclusions.....	121
4. FUTURE DIRECTIONS.....	123
4.1. Molecular Functions of Zebrafish Nr2b.....	124
4.2. Molecular Functions and Regulation of NAD+.....	126
4.3. Elucidating the Molecular Function of NAD+ in Basement Membrane Organization.....	129
4.4. Elucidating the Molecular Function of Paxillin in Basement Membrane Organization.....	132
4.5. Potential of the Nr2b Pathway in Therapeutics.....	136
4.6. Concluding Remarks.....	140
REFERENCES.....	141
APPENDIX A.....	160
APPENDIX B.....	174
BIOGRAPHY OF THE AUTHOR.....	192

LIST OF TABLES

Table 2.1.	Primer Sequences, Product Sizes and Concentrations.....	22
Table 2.2.	Quantitative Real-Time PCR Results.....	22

LIST OF FIGURES

Figure 2.1.	<i>nrk2b</i> Expression and MO Characterization.....	28
Figure 2.2.	Disrupted MTJs in <i>nrk2b</i> Morphants are Not Due to Discontinuous Initial Somite Boundaries.....	34
Figure 2.3.	Exogenous NAD ⁺ Treatment Rescues the <i>nrk2b</i> Morphant Muscle Phenotype.....	38
Figure 2.4.	Nrk2b is Required for Normal Basement Membrane Development.....	43
Figure 2.5.	Nrk2b is Non-Cell Autonomously Required for Normal Basement Membrane Polymerization.....	47
Figure 2.6.	Nrk2b is Required for Normal Subcellular Localization of Paxillin, but Not Beta-Dystroglycan or FAK.....	52
Figure 2.7.	Nrk2b is Cell Autonomously Required for Paxillin Localization to MTJs.....	54
Figure 2.8.	Paxillin Overexpression Rescues MTJ Integrity in <i>nrk2b</i> Morphants.....	58
Figure 2.9.	Roles for Cell–Matrix Adhesion during Muscle Morphogenesis.....	62
Figure 3.1.	Exogenous NAD ⁺ Improves the Structure of Muscle in <i>dag1</i> Morphants.....	84
Figure 3.2.	An Organized ECM Microenvironment Rescues Fiber Resiliency in Dag1-Deficient Cells.....	90

Figure 3.3.	Itga7 is Required for NAD ⁺ -Mediated Reduction of Fiber Degeneration in <i>dag1</i> Morphants.....	94
Figure 3.4.	<i>itga6</i> is Upregulated in Regenerating Muscle and Characterization of <i>itga6</i> MOs.....	98
Figure 3.5.	Itga6 is Required for NAD ⁺ -Mediated Rescue of MTJ Morphogenesis and Dystrophy.....	102
Figure 3.6.	Paxillin Overexpression Increases Laminin Organization and Ameliorates Dystrophy in <i>dag1</i> Morphants.....	105
Figure 3.7.	Paxillin Action, but Not Subcellular Localization, Requires Functional Integrin Receptors for Laminin.....	108
Figure 3.8.	NAD ⁺ Supplementation, but Not Paxillin Overexpression, Improves Motility of Dystrophic Zebrafish.....	111

CHAPTER 1

**THE TRANSLATIONAL SCIENCE IMPLICATIONS OF DEVELOPMENTAL
BIOLOGY**

1.1. Perspective

Research in the basic sciences (e.g. physics, chemistry, biology) attempts to better understand the phenomena occurring in our natural world. In addition to being intrinsically interesting, findings from basic sciences research can be applicable to translational scientific efforts to improve the human condition. This dissertation provides an example of how findings from developmental biology can begin to be translated into novel potential treatments for human diseases.

Development encompasses an organism's journey from an egg cell to its adult form. A process so complex, yet so vitally important to life, must be exquisitely orchestrated and tightly regulated both spatially and temporally. Developmental biologists study how biological processes are regulated over developmental time by chemical and mechanical signals to give rise to the proper size, shape, organization and function of a new life form. Developmental biology is both inherently interdisciplinary and fractal in nature. Mechanisms of development bridge scientific fields and occur simultaneously across different size scales, ranging from molecular level biochemical reactions to cell biological tissue interactions to whole organism level fitness and survival. Thus, findings from developmental biology have great potential to apply to and inform a broad range of scientific disciplines.

This dissertation will provide examples of two ways in which developmental biological findings can be used to guide translational science research. First, one aim of developmental biological studies is to elucidate what genes are necessary and/or sufficient for certain developmental processes to occur normally. Chapter 2 details a study in which a novel pathway involved in cell-matrix adhesion, the ‘NrK2b pathway,’ was elucidated and components in this pathway are shown to be necessary and/or sufficient for development of the myotendinous junction basement membrane in zebrafish. Findings such as these not only lead to a better understanding of the mechanisms underlying development, but as developmental processes are often disrupted in disease, these data provide insights into mechanisms of disease pathogenesis and genes that could potentially serve as therapeutic targets.

Second, developmental biologists aim to elucidate ‘intrinsic compensatory mechanisms’ through challenging embryos and characterizing the innate adaptations that occur in response to developmental perturbations. As cell adhesion contributes to virtually every developmental process and must be robust, disruptions in cell adhesion invoke many innate adaptations, such as changes in the expression or functionality of other cell adhesion components or complexes. Activation of these intrinsic compensatory mechanisms in disease models is yet another developmental biological approach that can be employed to potentially provide protection against disease progression and new treatment options to pursue. Chapter 3 describes a study in which activation of the NrK2b pathway was tested as an intrinsic compensatory mechanism and potential therapy in multiple cell-matrix adhesion-deficient zebrafish models of muscle disease.

A valuable lesson learned over the course of my graduate research experience is the translational science implications of developmental biological findings. Without building off of developmental biology research, manipulation of the Nr2b pathway may not have emerged at the present time as a potential therapeutic avenue for treatment of muscle diseases. Therefore, as is usually the case, the synergy of findings across scientific disciplines will best inform and guide translational science and optimize the benefits to people in need.

1.2. Introduction

The overall aim of my graduate research project was to investigate how proteins involved in cell adhesion to the extracellular matrix contribute to the development of muscle tissue in zebrafish embryos. Because developmental biology findings have the potential to apply to human health and diseases, an additional aim of my research became to investigate manipulation of certain cell-extracellular matrix adhesion molecules as novel, potential therapies using zebrafish models of congenital muscle diseases.

1.2.1. The Extracellular Matrix Microenvironment in Development and Disease

In multicellular organisms, in addition to the vital functions carried out by cells themselves, important processes occur in the region between cells, an area containing what is known as the extracellular matrix. The extracellular microenvironment consists of proteins and other molecules that are secreted by cells. Extracellular matrices form specific 3D structures with differing relative molecular compositions and therefore physical characteristics and functions. These structures external to cells provide scaffolds on which cells can migrate or stably adhere. However, the extracellular matrix is more

than just a static scaffold for cell adhesion and migration. Extracellular matrices with certain physical properties can regulate the availability of molecules involved in cell signaling. Extracellular matrix proteins themselves can also act as signaling molecules, relaying instructive or permissive cues to cells and modulating processes such as development, morphogenesis, homeostasis and aging (reviewed in ¹⁻⁶). Cells, in turn, affect their extracellular microenvironment and can remodel the physical attributes (e.g. molecular composition, density, rigidity) of their surrounding extracellular matrix. This bi-directional co-regulation between cells and the extracellular microenvironment is referred to as dynamic reciprocity (⁷).

One example of dynamic reciprocity in development and homeostasis is illustrated through the interactions that occur between cells and a specialized extracellular matrix substructure called the basement membrane. Basement membranes are layered, sheet-like structures densely packed with concentrated extracellular matrix proteins, primarily Laminin and Collagen type IV. Basement membranes surround some individual cell types and sit below all epithelia, separating epithelia from their underlying mesenchymal tissues. Basement membranes act to anchor cells within tissues and serve as a mechanical barrier between tissue types. Additionally, adhesion between cells and extracellular matrix ligands in the basement membrane result in bi-directional signaling that is essential for cell survival and proliferation as well as the proper form and functioning of all epithelia.

In skeletal muscle tissue, basement membranes both surround individual muscle fibers and concentrate to form the basement membrane at the myotendinous junction

(which is the site of force transmission from muscle to the skeletal system). During human skeletal muscle development, basement membranes first assemble at myotendinous junctions and then form around individual muscle fibers; the Laminin isoform composition of these basement membranes also continually changes over developmental time (8). Throughout the developmental remodeling of skeletal muscle basement membranes and the 'life' of a muscle cell, adhesion to the basement membrane must be maintained. These adhesions and the dynamic reciprocity that occurs through these adhesions are vital for the survival of muscle cells and thus the ability of skeletal muscle to perform its function of voluntarily contracting and relaxing to move the skeletal system.

Given the importance of maintained adhesion to the basement membrane for muscle cell survival and proper muscle tissue function, it is not surprising that disruptions in this adhesion cause muscle diseases. Basement membrane abnormalities are one way in which this adhesion and dynamic reciprocity can be perturbed in muscle tissue. Consequently, basement membrane defects are known to be associated with some human early-onset muscle diseases, such as Fukuyama congenital muscular dystrophy, Merosin-deficient congenital muscular dystrophy and Walker-Warburg syndrome (9-13). Despite the critical need for adhesion to the basement membrane in muscle tissue, as well as in other tissues, relatively little is known about how muscle tissue basement membranes develop normally *in vivo*. In Chapter 2, a novel cell-matrix adhesion pathway operating during zebrafish skeletal muscle development is shown to be required for normal *in vivo* development of the basement membrane at the myotendinous junction.

As described in Section 1.1, the genes discovered to be required for *in vivo* basement membrane development could potentially serve as therapeutic targets to strengthen or better repair basement membranes in muscle diseases where basement membranes are compromised. Basement membrane augmentation has been shown to be protective in zebrafish or mouse models of Laminin alpha2-, Laminin beta2-, Integrin alpha7- and Dystrophin-deficient muscle diseases (14-24). Despite these exciting advances, these previous gene therapy-based methods of basement membrane augmentation have not been translated into human muscle disease therapies. In Chapter 3, an alternate, chemical-based approach to basement membrane augmentation is explored in zebrafish models of human muscle diseases.

1.2.2. Cell-Matrix Adhesion Complexes in Dynamic Reciprocity, Basement Membrane Assembly and Disease

Dynamic reciprocity is the bi-directional signaling between cells and their extracellular matrix. In order for cells to communicate with their extracellular matrix and vice versa, groups of proteins are assembled into functional units called cell-matrix adhesion complexes. These complexes span from extracellular matrix ligands through the plasma membrane to the intracellular actin cytoskeleton. Thus, these adhesions form a mechanical link between the cytoskeleton of cells and the extracellular matrix which can bi-directionally transduce signals that result in biochemical reactions. The protein composition of these adhesions can differ depending on the specific extracellular matrix ligand(s) to which they bind and different protein compositions lead to adhesions with differing functions. The proteins associated with an adhesion can change over

developmental time or in response to stimuli, thus creating adhesions with functions that are dynamic and capable of being modulated. Very little is known about how assembly, disassembly or regulation of the protein composition of these adhesion complexes affects their function *in vivo*. Findings presented in Chapter 2 begin to tease apart cell-matrix adhesion complex regulation by showing that the localization of a ubiquitously-expressed cell-matrix adhesion protein can be regulated in a cell-autonomous and tissue-specific manner.

For adhesion between muscle cells and the basement membrane ligand Laminin, two varieties of cell-matrix adhesion complexes are utilized. The Dystrophin-glycoprotein complex links the basement membrane to the actin cytoskeleton through the extracellular, Laminin-binding protein alpha-Dystroglycan, plasma membrane-spanning proteins (beta-Dystroglycan, the Sarcoglycans and Sarcospan), and intracellular proteins (the Syntrophins and F-actin-binding Dystrophin). The other Laminin-binding receptor complexes, Integrin heterodimers, consist of one alpha and one beta Integrin subunit, which span the plasma membrane and bind Laminin extracellularly and numerous adaptor proteins intracellularly. These Integrin-associated adaptor proteins, namely Paxillin, Focal Adhesion Kinase, Src, Vinculin and Talin, can bind one another and some bind F-actin.

Given that the Dystrophin-glycoprotein complex and Integrins mediate dynamic reciprocity between cells and basement membranes, it is logical that proteins in these receptor complexes would play roles in basement membrane formation *in vivo*. While Laminin and Collagen type IV can self-assemble into meshworks *in vitro* ^(25,26),

interactions between these proteins and other extracellular matrix molecules as well as cell-matrix adhesion receptor proteins add layers of complexity and regulation to *in vivo* basement membrane assembly (reviewed in ²⁷). Dystroglycan and Integrin beta1 are known to be required for normal basement membrane formation in mouse embryos or embryoid bodies (²⁸⁻³²). In mouse embryoid bodies, the basement membrane assembly roles of Dystroglycan and Integrin beta1 were shown to be unique: Dystroglycan is required for initial adhesion between cells and Laminin and Integrin beta1 is required for assembly of higher order Laminin structures (³³). It is likely that other proteins involved in cell adhesion to Laminin also contribute to the regulation of basement membrane assembly *in vivo*. Elucidating unknown roles for other cell adhesion proteins in this poorly understood developmental process (as is done in Chapter 2) will enhance our understanding of *in vivo* basement membrane formation.

Disruption (e.g. genetic mutation) to any of the components of cell-matrix adhesion complexes can affect intracellular signaling downstream of these adhesions as well as the physical characteristics of the extracellular microenvironment and contribute to the onset or progression of a disease. Mutations that affect Laminin, transmembrane receptors for Laminin or some intracellular proteins involved in adhesion to Laminin are known to cause muscle diseases in humans (reviewed in ³⁴). *In vivo* studies utilizing animal models of human muscle diseases have suggested that an intrinsic compensatory mechanism (see Section 1.1) exists between the Dystrophin-glycoprotein complex and Integrins, such that when one is disrupted the expression or functionality of the other is increased.

Multiple lines of evidence lend support to the idea of compensation between the Dystrophin-glycoprotein complex and Integrins in adhesion to Laminin. First, in cultured mouse myoblasts, Integrin alpha7 and alpha-Dystroglycan were shown to bind distinct regions in the G-domain of Laminin ⁽³⁵⁾ and disruption of both Laminin receptors in mice results in more severe muscle disease than disruption of either complex alone ^(36,37). Together, these findings suggest that these two receptor complexes cooperate in Laminin adhesion. Second, expression of components in the uncompromised Laminin receptor complex are frequently upregulated in mouse models of muscle disease ⁽³⁸⁻⁴¹⁾ and overexpression of components of the uncompromised receptor complex can reduce disease severity ⁽⁴²⁻⁴⁶⁾. These findings not only describe an intrinsic compensatory mechanism involved in adhesion to Laminin, but also begin to test the use of these innate adaptations as disease therapies. Identification of additional intrinsic compensatory mechanisms that occur in response to developmental disruptions or alternate approaches to activate previously characterized innate adaptations will provide new therapeutic avenues and potential therapeutic molecules to investigate. The discovery of a novel, Integrin-based cell adhesion pathway involved in zebrafish muscle development (see Chapter 2) inspired a study to explore components in this pathway as activators of the intrinsic compensatory mechanism between the Dystrophin-glycoprotein complex and Integrins in zebrafish muscle disease models where muscle cell-Laminin adhesion is compromised (see Chapter 3).

1.2.3. Zebrafish Muscle: A Paradigm to Study Cell-Matrix Adhesion during Muscle Development and Disease

Given the complexity of the contributions of cell-matrix adhesion to muscle development and diseases, there is a need for simple model organisms in which cell-matrix adhesion can be studied and manipulated. Mutations in or ‘pseudo-genetic’ manipulation of the same cell-matrix adhesion component genes that cause the human muscle diseases described in Section 1.2.2 result in similar muscle diseases in animal model organisms, such as mice (reviewed in ⁴⁷) and zebrafish (reviewed in ⁴⁸⁻⁵¹). Despite being more evolutionarily distant from humans than mice, there are numerous advantages to using zebrafish (*Danio rerio*) as a model organism. Due to the overlap between developmental biology and translational science described in Section 1.1, the same advantages that make zebrafish embryos attractive for developmental biological studies (i.e. genetic and embryological tractability) also make zebrafish an advantageous model for biomedical research (reviewed in ⁵¹).

The common embryonic origin, conserved genetic regulatory networks of muscle development and abundance of skeletal muscle tissue make zebrafish embryos a well-suited system in which to study muscle form and function. Most skeletal muscle in vertebrates, including zebrafish, mice and humans, is derived from conserved, transient embryonic structures called somites. Somites are comprised of sclerotome, myotome and dermatome cell lineages, which give rise to vertebrae, skeletal muscle and dermis, respectively. Zebrafish somites consist of these three cell types, but contain a smaller proportion of sclerotome cells and a greater proportion of myotome cells compared to

mouse or human somites (reviewed in ^{52,53}). Muscle tissue structures with analogous functions in fish, mice and humans also add to the power of using zebrafish to study skeletal muscle development and disease. Basement membranes and myotendinous junctions serve analogous functions across vertebrates (⁵⁴⁻⁵⁶) and cell-matrix adhesion proteins and their functions are conserved from invertebrates to vertebrates (⁵⁷). As in human skeletal muscle development, zebrafish muscle tissue basement membranes first form at myotendinous junctions (^{21,58-60}) and then assemble around individual muscle fibers (⁵⁵) and the expression of *laminin* chains changes over developmental time (⁶¹). Zebrafish muscle tissue architecture is simplified and more homogeneous compared to humans, however, conserved transcriptional regulators (reviewed in ^{62,63}), muscle tissue structures and cell adhesion proteins allow findings from zebrafish muscle research to have great potential to apply to human muscle development and disease.

Zebrafish muscle disease models not only recapitulate symptoms of human muscle diseases, but have also led to novel insights into muscle disease pathogenesis that would have been difficult or impossible to achieve using other model organisms. Common skeletal muscle disease phenotypes in mammals (including muscle degeneration, fibrosis, inflammation, muscle regeneration, fiber size variation and fibers with centralized nuclei) all occur in zebrafish muscle disease, with the exception of fibers with centralized nuclei (⁶⁴). The ability to watch muscle degeneration in zebrafish embryos identified, for the first time, the myotendinous junction as the site of adhesion failure in *dystrophin* mutants (⁶⁵). While the myotendinous junction as a site of muscle disease pathology has not been confirmed in human patients because muscle biopsies are

taken at a distance from the tendon to avoid damaging it, MRI studies have shown that muscle damage can be more severe near the myotendinous junction (^{66,67}).

Therapeutic insights into muscle diseases also come from the ability to conduct rapid and thorough chemical-genetic screens using zebrafish. Kawahara et al. used *sapje* mutant zebrafish and a library of chemicals approved for human use to identify novel therapeutics for Dystrophin-deficient muscle diseases. They found a compound affecting cAMP-dependent PKA signaling to be the most effective therapeutic in the Prestwick chemical library (⁶⁸). This finding not only implicates PKA signaling pathway components as potential drug targets for the treatment of Dystrophin-deficient muscle diseases, but is also of interest to developmental biologists as it suggests the operation of PKA-dependent mechanisms in muscle tissue development and homeostasis. Taken all together, the published findings discussed above show that zebrafish muscle development and the resulting muscle tissue structure is similar to that in humans, thus making zebrafish an ideal model organism in which to investigate cell-matrix adhesion in skeletal muscle development and disease.

CHAPTER 2

NRK2B AND NAD⁺ REGULATE CELL ADHESION AND ARE REQUIRED FOR MUSCLE MORPHOGENESIS *IN VIVO*

2.1. Chapter Abstract

Cell–matrix adhesion complexes (CMACs) play fundamental roles during morphogenesis. Given the ubiquitous nature of CMACs and their roles in many cellular processes, one question is how specificity of CMAC function is modulated. The clearly defined cell behaviors that generate segmentally reiterated axial skeletal muscle during zebrafish development comprise an ideal system with which to investigate CMAC function during morphogenesis. We find that Nicotinamide riboside kinase 2b (Nr2b) cell autonomously modulates the molecular composition of CMACs *in vivo*. Nr2b is required for normal Laminin polymerization at the myotendinous junction (MTJ). In Nr2b-deficient embryos, at MTJ loci where Laminin is not properly polymerized, muscle fibers elongate into adjacent myotomes and are abnormally long. In cultured mouse myoblasts, MIBP/Nrk2 binds the cytoplasmic tail of Integrin beta1 and in yeast and human cells, an alternate function of Nrk2 is phosphorylation of Nicotinamide Riboside to generate NAD⁺ through a salvage pathway⁽⁶⁹⁻⁷²⁾. We find exogenous NAD⁺ treatment rescues MTJ development in Nr2b-deficient embryos, but not in *laminin* mutant embryos. Both Nr2b and Laminin are required for localization of Paxillin, but not beta-Dystroglycan, to CMACs at the MTJ. Overexpression of Paxillin in Nr2b-deficient embryos is sufficient to rescue MTJ integrity. Taken together, these data show that Nr2b plays a specific role in modulating subcellular localization of discrete CMAC

components that in turn play roles in musculoskeletal development. Furthermore, these data suggest that NAD⁺ regulates Laminin assembly/polymerization and Paxillin subcellular localization during MTJ development. These results indicate a previously unrecognized complexity to CMAC assembly *in vivo* and also elucidate a novel role for NAD⁺ during morphogenesis.

2.2. Introduction

One fundamental question in developmental biology is how tissue architecture is generated and maintained. Both cell–cell adhesion and cell–matrix adhesion are critical for organogenesis. However, despite the spatial and temporal regulation of cell adhesion in nearly all morphogenetic events, the dynamic modulation of cell adhesion during morphogenesis is not well understood. Zebrafish axial skeletal muscle, because of its reiterated nature and simple structure, is an ideal model system with which to analyze cell adhesion complex assembly and specificity of cell adhesion dynamics during different cellular behaviors.

Cell–matrix adhesion mechanically links cells to the extracellular matrix (ECM) through transmembrane receptors (e.g. Integrins). *In vitro*, these adhesion sites have different names depending on their size and composition (⁷³). A recent review proposed use of the umbrella term Cell–Matrix Adhesion Complexes (CMACs, pronounced seeMACs) to refer to all cell–matrix adhesion structures (⁷⁴). CMACs are dynamic structures that are alternately formed and disassembled during cell migration. CMAC assembly involves Integrin clustering and the recruitment and phosphorylation of numerous cytoplasmic proteins that link to the cytoskeleton. Two well known

cytoplasmic proteins that modulate dynamic adhesion are Focal Adhesion Kinase (FAK) and Paxillin. FAK is a non-receptor tyrosine kinase that is phosphorylated upon adhesion to the ECM (75). FAK is over expressed in many types of cancerous cells (76) and is thought to promote cell motility by facilitating CMAC turnover (77). Counter intuitively, FAK also plays a role in stabilizing adhesion: FAK is required for costamereogenesis in muscle cells (78) and FAK concentration increases subsequent to muscle loading (79). Similarly, the scaffolding protein Paxillin can also promote both CMAC assembly and disassembly. Paxillin is one of the first proteins recruited to nascent CMACs and is hypothesized to play a role in mediating the molecular composition of assembling CMACs (80). However, Paxillin is also required for adhesion turnover: cells without Paxillin exhibit stabilized adhesions (81). Many *in vitro* studies have looked at the order in which intracellular proteins are recruited to CMACs. The unifying conclusion from these studies is that the order of recruitment is context dependent. Even less is known about CMAC dynamics *in vivo*. Given the complexity of CMACs *in vitro*, along with the fact that the same proteins can promote different cellular behaviors, it is likely that a complex combinatorial code of the post-translational modifications and interactions of CMAC proteins mediates cell behavior *in vivo*.

One important question is how an adhesion code mediates interaction of cells with their ECM microenvironment. The bidirectional signaling that occurs between cells and their ECM through CMACs is called “dynamic reciprocity” (7). Signaling from the ECM modifies intracellular signaling, gene expression and cell morphology. Signals from within the cell modify the molecular composition and structure of the ECM. The

basement membrane is one specialized compartment of the ECM and is required for muscle development and physiology. Basement membranes surround individual muscle fibers and concentrate at the myotendinous junction (MTJ). Adhesion to Laminin in basement membranes is required for normal muscle development in both zebrafish and mice (reviewed in ^{48,51,82,83}). Multiple human myopathies result from disruption of muscle to basement membrane adhesion (^{82,83}). Despite the critical importance of adhesion between muscle and the basement membrane, the mechanisms that mediate initial attachment and assembly/polymerization of the basement membrane are not known.

Given the ubiquitous and dynamic nature of cell adhesion, one fundamental question is how cell adhesion modulates multiple cell behaviors. Muscle Integrin Binding Protein (MIBP) is a novel, muscle-specific protein that binds to the Laminin receptor Integrin alpha7beta1 (⁶⁹). MIBP is a splice variant of Nicotinamide riboside kinase 2 (Nr2), which has also been designated Integrin beta1 Binding Protein 3 (ITGB1BP3). Human Nr1 and Nr2 phosphorylate Nicotinamide Riboside to generate Nicotinamide Adenine Dinucleotide (⁷⁰⁻⁷²). Several lines of evidence suggest that Nr2 plays a critical role in muscle development and physiology: (1) overexpression of *mibp* disrupts myotube formation *in vitro* (⁸⁴), (2) *itgb1bp3* is the second most upregulated muscle transcript in *myostatin* $-/-$ cows (⁸⁵), and (3) *nr2* is the most highly upregulated tissue-restricted transcript in alveolar soft-part sarcoma (⁸⁶). Taken together, these data suggest that Nr2 is a critical regulator of muscle growth and development. Thus, we asked whether Nr2 is required for animal development in general and zebrafish muscle development specifically.

There are at least two zebrafish orthologs of Nrk2. We focused on Nrk2b (a.k.a. MIBP2) because it is expressed during muscle development. We used morpholino-mediated knockdown to ask whether Nrk2b is required for muscle development *in vivo*. Embryos injected with morpholinos targeted to *nrk2b* resemble *laminin* mutants, suggesting that Nrk2b functions in adhesion to Laminin *in vivo*. In support of this, injecting *laminin* mutants with *nrk2b* morpholinos resulted in a *laminin* mutant phenotype and not a more developmentally disrupted phenotype. This epistasis analysis suggests that Nrk2b functions in the Laminin pathway. Although a basement membrane at the MTJ does form in *nrk2b* morphants, it is significantly less organized than in control embryos. Genetic mosaic analysis suggests that Nrk2b is non-cell autonomously required for proper basement membrane polymerization. However, Nrk2b is cell autonomously sufficient for localization of Paxillin to CMACs at the MTJ. To our knowledge, this is the first identification of a vertebrate protein that cell autonomously mediates the molecular complexity of CMACs *in vivo*. Human and yeast Nrk proteins function in an alternative salvage pathway to generate NAD⁺ (70,71,87-89). Exogenous NAD⁺ rescues discontinuous MTJs in *nrk2b* morphants but not in *laminin* mutants. These data suggest that NAD⁺ functions upstream of Laminin adhesion/signaling during zebrafish muscle morphogenesis. Taken together, these data show that this understudied protein and NAD⁺ are novel cell adhesion regulators that impart specificity to the assembly of cell adhesion complexes.

2.3. Materials and Methods

2.3.1. Zebrafish Husbandry/Mutant/Transgenic Lines

Adult zebrafish were kept at 28.5 °C on a 16 hour light/8 hour dark cycle. Zebrafish embryos were collected from natural spawnings of these adult fish. Embryos were staged according to ⁽⁹⁰⁾. *Gup/laminin beta1tg210* and *sly/laminin gamma1ti263A* mutants were a generous gift from the Tuebingen stock center. A transgenic line expressing GFP fused to the C-terminus of Paxillin was generated by cloning full length Paxillin from 24 hours post fertilization (hpf) zebrafish cDNA, cloning the PCR product into the pDONR221 plasmid (Invitrogen) and then cloning, along with p5E-bactin2 (ubiquitous beta-actin promoter, a 5' entry clone vector from the Tol2Kit ⁹¹) and p3E-EGFPpA (EGFP for C-terminal fusions, plus SV40 late polyA, a 3' entry clone vector from the Tol2Kit ⁹¹), into a pDestTol2pA plasmid (a destination vector from the Tol2Kit ⁹¹) via a recombination reaction. Linearized pCS2-TP plasmid (kindly provided by Koichi Kawakami) was used as a template to generate capped mRNA encoding Tol2 transposase by *in vitro* transcription using SP6 polymerase (Message Machine, Ambion). Plasmids were co-injected with mRNA encoding Tol2 transposase into embryos at the single cell stage. GFP expressing zebrafish from the F0 generation were grown up and then spawned to detect for germ line incorporation of the transgene. The F1 generation, offspring of the F0 generation with germ line incorporation of the transgene, stably over expressing Paxillin was used for experimentation.

2.3.2. Morpholino Injections

MOs were obtained from Gene Tools, LLC. The nucleotide sequence of the *nrk2bm1* MO is 5'-GAACTTCATCCTCGACGTGATTTT G-3' and the sequence of the *nrk2bm2* MO is 5'-CGTCAAAGTAGAGAAAAATTGG CTA-3'. The sequence of the standard control MO is 5'-CCTCTTACCTCAGTTACAATTTATA-3'. All MOs were diluted in sterile water to a stock concentration of 6 mM. The *nrk2b* MO cocktail was 12 ng *nrk2bm1* plus 6 ng *nrk2bm2*. 12 ng of the standard control MO was injected. *dystroglycan* MO was injected according to (⁹²). The *p53* MO sequence is 5'-CCCTTGCGAACTTACATCAAATTCT-3'. Equal amounts of *nrk2b* MOs and the *p53* MO were combined and co-injected. MOs were injected with a MPPI-2 Pressure Injector from ASI. Embryos were injected in the yolk at the 1-cell stage. The *laminin* MOs used have been previously described and recapitulate the mutant phenotype (⁹³).

Suppression of GFP fluorescence when the target sequence is co-injected with MOs: full length *nrk2b* was amplified using cDNA from 24 hpf zebrafish. The PCR product was cloned using the Tol2Kit and injected as above, with or without *nrk2b* MOs.

2.3.3. NAD⁺ Treatment

Beta-NAD (Sigma) was dissolved in Embryo Rearing Medium to a stock concentration of 15 mM. The treatments used were 100 μ M and 1 mM NAD⁺ (⁹⁴). Embryos were treated from shield stage through live imaging/fixation.

2.3.4. Antibody Staining/Immunohistochemistry

All Abs were diluted in block (5% w/v Bovine Serum Albumin (BSA) in Phosphate Buffered Saline (PBS) with 0.1% Tween20). Alexa Fluor 488 phalloidin (Molecular Probes) staining involved fixing embryos in 4% Paraformaldehyde (PFA) for 4h at room temperature (RT), washing 5 times for 5 min each (5×5) in 0.1% PBS-Tween, permeabilizing for 1.5h in 2% PBS-Triton, washing 5×5 and then incubating in phalloidin (1:20) for 1–4 h at RT. Ab staining followed phalloidin staining or started with blocking for 1 h at RT, incubating in 1° Ab overnight at 4 °C, washing for 2–8 h at RT, incubating in 2° Ab overnight at 4 °C, then washing for 1 h. 1° Abs: anti-beta-Catenin 1:500 (Sigma); anti-beta-Dystroglycan 1:50 (Novocastra); anti-Laminin-111 1:50 (Sigma); anti-Paxillin 1:50 (BD Biosciences); anti-pan-FAK-c-20 1:50 (Santa Cruz Biotechnology); anti-pY-397-FAK, anti-pY-861-FAK 1:50 (Biosource). 2° Abs: GAM/GAR 488, 546, 633 1:200 (Invitrogen).

2.3.5. Whole Mount *In Situ* Hybridization

Dechorionated embryos were fixed and washed as above, treated with Proteinase K (Fisher) for 1 to 15 min and then fixed (20 min) and washed 5×5 . Embryos were incubated in prehybridization solution (50% Formamide, $5 \times$ sodium chloride–sodium citrate buffer, 50 µg/mL Heparin, 500 µg/mL Yeast tRNA, 0.1% Tween20, pH of 6.0 with citric acid) for 4 h at 65 °C, and then hybridized overnight at 65 °C with a digoxigenin-labeled probe. Embryos were washed using serial dilutions into and out of 2X SSC, then incubated in anti-digoxigenin Ab (Roche) for 2 h at RT, washed and then developed in a

0.45% NBT/0.35% BCIP (Roche) in PBS-Tween solution until the desired color was obtained. Controls and morphants hybridized with the same probe were developed for the same amount of time. The developing process was stopped by fixing or rinsing 4 times in sterile water.

2.3.6. Westerns

Protein was prepared from 24h post fertilization zebrafish embryos using previously described methods (⁹⁵). Protein was resolved on a 10% SDS-PAGE gel, transferred to PVDF membrane, blocked in 5% dry milk, incubated in 1° Ab (anti-Paxillin 1:1000, BD Biosciences) at 4 °C overnight, washed, incubated in 2° Ab, washed, detected with Supersignal West Dura (Pierce) and developed on a CCD LAS 4000 Fuji camera.

2.3.7. Genetic Mosaics

Embryos were injected with MOs as described above and 10,000 MW fluorescent (wavelength 546 or 633) dextrans (Molecular Probes). Transplants were performed as described in (⁹⁶).

2.3.8. Comparative qRT-PCR

RNA was isolated from whole embryos at 24 hpf via Qiagen's RNeasy Mini Kit. One-step comparative qRT-PCR was conducted with Quanta kit reagents and Rox reference dye. A Mx400 machine was used and the annealing temperature was 60 °C. Approximately 50 ng of RNA template was used per reaction. We used *beta-actin* as our normalizing transcript. See Table 2.1 for a complete list of primer information.

Table 2.1. Primer Sequences, Product Sizes and Concentrations.

Primer	Sequence	Product size	Final conc.
<i>beta-actin</i> forward	5'-TCGTGACCTGACAGACTACCTGAT-3'	84 base pairs	250 nM
<i>beta-actin</i> reverse	5'-CGGACAATTTCTCCTTCGGCTGTG-3'		
<i>laminin alpha1</i> forward	5'-TGCTGGAGCTCATCAACAAC-3'	220 base pairs	150 nM
<i>laminin alpha1</i> reverse	5'-TTTTCCAGCACAGACTGC-3'		
<i>laminin beta1</i> forward	5'-GCAGCTCAAAAAGGATCTGG-3'	160 base pairs	150 nM
<i>laminin beta1</i> reverse	5'-AAGTTTCTCGCTGGCCTGTA-3'		
<i>laminin gamma1</i> forward	5'-GGTTGCAAACCATGTGACTG-3'	231 base pairs	150 nM
<i>laminin gamma1</i> reverse	5'-CAAATTCTGCAGGTCAAGCA-3'		
<i>paxillin</i> forward	5'-CAGCAACACCCAACGATATG-3'	184 base pairs	75 nM
<i>paxillin</i> reverse	5'-TGATGAGACAGGGACAGCAG-3'		

The qRT-PCR results shown are the averages of the three biological replicates for each primer and RNA treatment (each biological replicate being an average of three technical replicates) and the error is standard error of the mean. See Table 2.2 for qRT-PCR results.

Table 2.2. Quantitative Real-Time PCR Results.

Primer	RNA Treatment	Average $\Delta\Delta\text{ct}$	S.E.M.	$\Delta\Delta\text{ct}$ Range
<i>laminin alpha1</i>	<i>nrk2b</i> MO injected	2.65	0.18	2.43-3.01
<i>laminin beta1</i>	<i>nrk2b</i> MO injected	1.53	0.21	1.21-1.94
<i>laminin gamma1</i>	<i>nrk2b</i> MO injected	1.37	0.11	1.17-1.55
<i>paxillin</i>	<i>nrk2b</i> MO injected	1.26	0.09	1.16-1.44

2.3.9. Imaging

All images were obtained on a Zeiss Axio Imager Z1 microscope with a Zeiss ApoTome attachment. Embryos were deyolged in PBS, side mounted in 80% glycerol/20% PBS and viewed with the 10×, 20× or 40× objective. For images where fluorescence levels were to be compared, exposure times were kept constant throughout the imaging of that experiment. Images were optimized by averaging up to 5 frames.

For ISH images, embryos older than 16 somites were deyolged and side mounted as above. Younger embryos were whole mounted by clearing their yolks in MeOH for 15 min followed by 1:2 Benzyl Alcohol: Benzyl Benzoate for 15 min, then dorsally orienting them in Permount. Image modifications in Adobe Photoshop were one round of linear adjustments, Gaussian filtering (0.3 pixel) and unsharp mask (50%, 1 pixel) prior to being collated in Adobe Illustrator.

2.3.10. Measuring Myotome Boundary Angles

Zeiss Inside 4D software was used to calculate the angle of the chevron shaped myotome boundary from brightfield images. The angle degrees were averaged within in a treatment and then graphed and statistically analyzed for significance.

2.3.11. Normalized Fluorescence Intensity

Images were imported into ImageJ (freely available online) and the profiles were plotted. The resulting data were imported into Excel for normalization. For each panel, in order to control for varied exposure times, the maximum intensity of phalloidin was

determined and the values were all normalized to this intensity. Thus, what is shown is a “percentage of maximum intensity.”

2.3.12. The 2D Wavelet Transform Modulus Maxima Method

The 2D WTMM method is a multifractal image analysis formalism that has been adapted to perform a structural, multi-scale anisotropic analysis of image features having a complex geometry (^{97,98}). At a given scale a , the WTMM are defined by the positions where the Wavelet Transform Modulus is locally maximum in the direction A of the gradient vector. These WTMM lie on connected chains called maxima chains. Vectors along the maxima chains corresponding to positions where the image gradient is locally maximal on the maxima chain are the WTMM maxima, or WTMMM. Their angle indicates locally the direction where the signal has the sharpest variation.

At all size scales a , the probability density functions (pdfs), $P_a(A)$, of the angles, A , are associated to each WTMM vector. A flat pdf indicates random directions of sharpest intensity variation (i.e. isotropy). The anisotropy factor has been defined in such a way that a theoretically isotropic surface will have a value of $F_a = 0$, while any value greater than 0 quantifies a departure from isotropy.

2.4. Results

2.4.1. Characterization of *nrk2b* Expression and Morpholinos Targeting *nrk2b*

nrk2b is expressed in muscle tissue at 26 hpf (⁹⁹). We found that *nrk2b* expression is initiated in the paraxial mesoderm at tailbud stage (data not shown) and persists

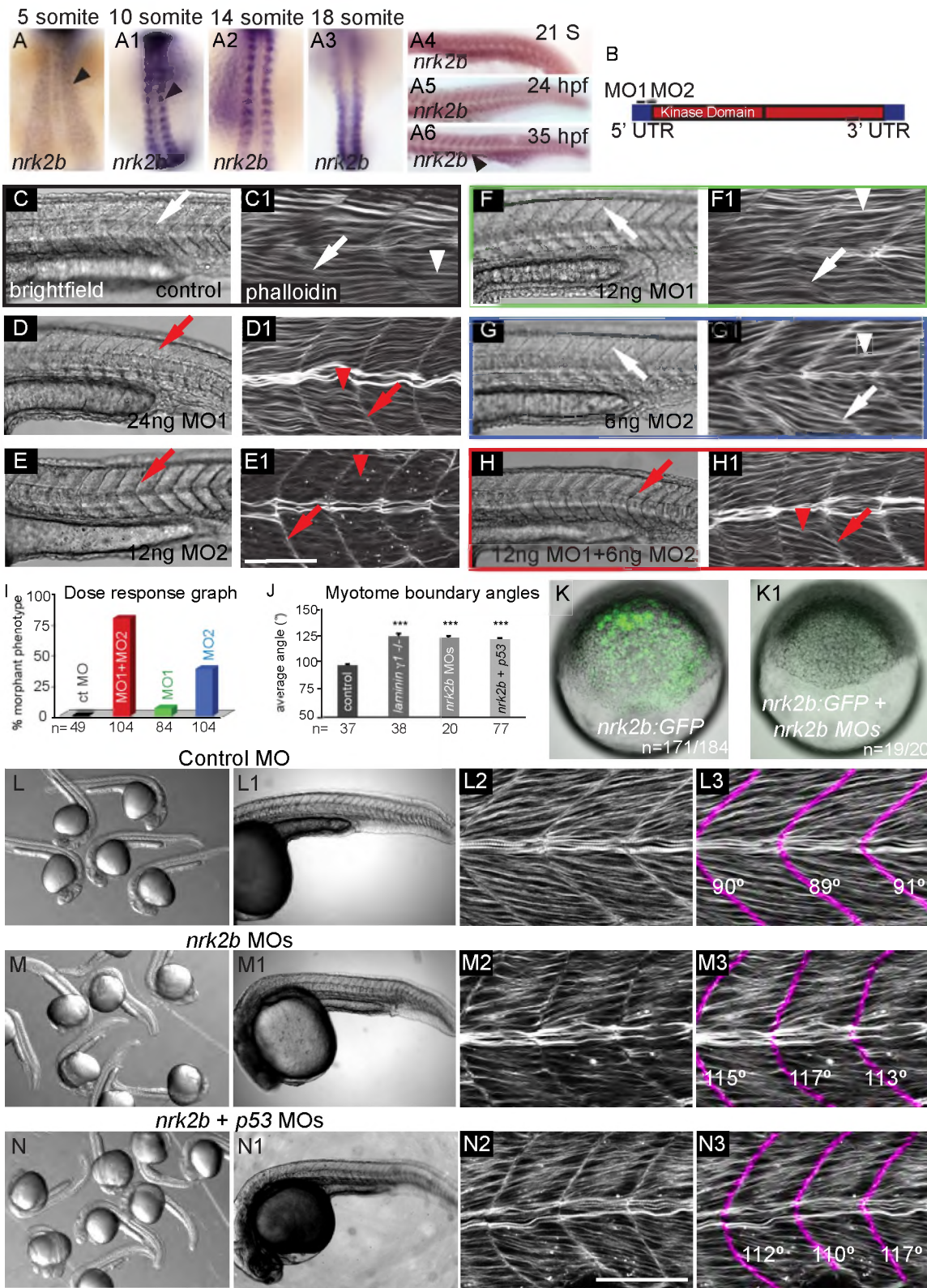
through at least 35 hpf (Fig. 2.1 panels A-A6). In order to determine the function of NrK2b in muscle development, we designed two non-overlapping, translation-blocking MOs targeting *nrk2b* (Fig. 2.1 panel B). Injection of 12 ng of control MO did not elicit a phenotype (Fig. 2.1 panels C-C1). Injection of either 24 ng MO1 or 12 ng MO2 disrupted muscle development: myotomes were U-shaped and thinner in the anterior–posterior dimension than in controls (Fig 2.1 panels D-E1). Injection of half the functional amount of MO1 or MO2 did not disrupt muscle development (Fig. 2.1 panels F-G1). Co-injection of 12 ng MO1 + 6 ng MO2 elicited the same phenotype as embryos injected with higher levels of single MOs (compare Fig. 2.1 panels H-H1 to D-E1). This synergy suggests that these MOs disrupt translation of the same gene product⁽¹⁰⁰⁾. The MO cocktail of 12 ng MO1 + 6 ng MO2 was injected in all the ensuing experiments.

A *nrk2b:gfp* fusion construct containing the MO target sequences was generated using the Tol2Kit⁽⁹¹⁾ to test the effectiveness of the *nrk2b* MO cocktail in blocking translation of NrK2b protein. This fusion construct was injected with and without the *nrk2b* MO cocktail. *nrk2b* MOs dramatically decreased translation of the NrK2b:GFP fusion protein in all embryos observed (Fig. 2.1 panels K-K1, 3 experiments, 1 representative experiment: 93% of *nrk2b:gfp* injected embryos expressed GFP (n=171 out of 184 embryos) whereas only 5% of *nrk2b:gfp* + *nrk2b* MO-injected embryos expressed any GFP (n=1 out of 20 embryos, *nrk2b* MOs knocked down NrK2b:GFP protein for at least 26 h, data not shown). These data indicate that two separate, non-overlapping *nrk2b* MOs synergize and are sufficient to disrupt NrK2b translation.

Because injection of MOs can activate the p53 pathway and cause non-specific effects

(¹⁰¹), we co-injected the *nrk2b* MO cocktail 1:1 with *p53* MO (¹⁰¹). Co-injection of *p53* MO rescued necrosis in the head, but not U-shaped myotomes and shorter body axes (Fig. 2.1 panels N-N3). Myotome boundary angles in *nrk2b* morphants are significantly wider than controls (Fig. 2.1 panel J, Student t-test, $p < 0.001$). Myotome boundary angles in *nrk2b:p53* double morphants are also significantly wider than controls (Fig. 2.1 panel J, Student t-test, $p < 0.001$) and are not significantly different than boundary angles in *nrk2b* morphants (Fig. 2.1 panel J). Thus, co-injection of *p53* MO does not rescue the paraxial mesoderm phenotype of *nrk2b* morphants.

Fig. 2.1. *nrk2b* Expression and MO Characterization. (A–A6) ISH with *nrk2b* probe. (A–A3) Dorsal mount, anterior top. (A4–A6) Side mount, anterior left, dorsal top. Black arrowheads denote *nrk2b* expression. (B) Cartoon of *nrk2b* and MO target sites. (C–H1) Side mount, anterior left, dorsal top, 26 hpf embryos, lettered panels are DIC images, numbered panels are phalloidin stained to visualize actin. (C, C1) Injection of a standard control MO did not elicit a phenotype. Myotomes are V-shaped (white arrows) and muscle fibers are normal (white arrowheads). Injection of the functional dose of MO1 (D, D1) or MO2 (E, E1) resulted in U-shaped myotomes (red arrows) and wavy muscle fibers (red arrowheads). Injection of half the functional dose of MO1 (F, F1) or MO2 (G, G1) did not disrupt muscle development. (H, H1) Injection of both low doses of MO1+MO2 recapitulated the phenotype. (I) Dose response graph. Injection of low doses of MO1 + MO2 resulted in more embryos with the phenotype than injection of either low dose alone (n of embryos injected is listed on the x-axis). (J) Average myotome boundary angles of 26 hpf control, *laminin gamma1* mutants, *nrk2b* morphant, and *nrk2b + p53* MO-injected embryos. *laminin gamma1* mutants, *nrk2b* morphants, and *nrk2b + p53* morphants have myotome boundaries of a similar angle and all have myotome boundary angles that are significantly wider than controls, $p < 0.001$ (n of MTJs measured is listed on the x-axis). (K–K1) Brightfield images of shield stage embryos. Animal pole to the top. (K) Embryo injected with the *nrk2b:gfp* plasmid that contains both MO target sites. (K1) Embryo injected with the *nrk2b:gfp* plasmid and *nrk2b* MOs. Note that expression of GFP-tagged Nrk2b is drastically decreased by injection of *nrk2b* MOs (3 experiments, 1 representative experiment: 93% of *nrk2b:gfp* injected embryos expressed GFP (n = 171 out of 184 embryos) whereas only 5% of *nrk2b:gfp + nrk2b* MO-injected embryos expressed any GFP (n = 1 out of 20 embryos)). (L–N) Brightfield images of a dish of 26 hpf embryos. (L–L1) Control MO-injected embryos. (M–M1) *nrk2b* morphants. (N–N1) *nrk2b + p53* morphants. (L1–N1) Side mount, anterior left, dorsal top, 26 hpf embryos, DIC imaging. Higher magnification images of one representative embryo from each of the corresponding dishes. Note that the control morphant (L1) has a longer body axis than both *nrk2b* morphants (M1) and *nrk2b + p53* double morphants (N1). (L2–N3) Side mount, anterior left, dorsal top, 26 hpf embryos, phalloidin staining to visualize actin. Higher magnification views of embryos from the corresponding dishes. In panels numbered 3, myotome boundaries were pseudocolored fuchsia and the myotome boundary angle is given with the corresponding boundary. Note that while injection of *p53* MO did rescue the cell death seen in the head of *nrk2b* morphants, it did not rescue the shorter body axis (compare M1 to N1) or the U-shaped myotomes (compare M3 to N3). Scale bars are 50 μm , *** $p < 0.001$.



Nrk2 was identified in a yeast two-hybrid screen for proteins that interact with the Laminin receptor Integrin alpha7beta1. It was subsequently shown that ectopic Nrk2 expression in C2C12 myoblasts disrupts adhesion to Laminin, but not the ECM protein Fibronectin (⁶⁹). The fact that the phenotype of the paraxial mesoderm in *nrk2b* morphants resembles that of *laminin beta1* and *gamma1* mutants (⁹³), in that myotome boundary angles in *laminin* mutants and *nrk2b* morphants are not significantly different (Student t-test, $p = 0.3$) and both are significantly wider compared to controls (Fig. 2.1 panel J, Student t-test, $p < 0.001$), suggests that Nrk2 is involved in adhesion to Laminin *in vivo* as well as *in vitro*. These data, however, do not clarify whether Nrk2b also functions in other pathways operating during development. We thus conducted pseudo-genetic epistasis analysis. If the function(s) of Nrk2b is/are solely in adhesion to Laminin, then knock down of Nrk2b and Laminin in the same embryo will result in a *laminin* mutant phenotype. If Nrk2b additionally functions outside of Laminin adhesion, then knock down of Nrk2b in *laminin* mutants will result in a more severe phenotype, such as when Hedgehog signaling is inhibited in *laminin* mutants (¹⁰²). Injection of *nrk2b* MOs into *laminin* mutants phenocopied *laminin* mutants (Fig. 2.2 panels A-D). This result suggests that Nrk2b participates in the Laminin signaling pathway during early development.

The preceding data provide evidence that *nrk2b* MOs are specific. First, two MOs targeting *nrk2b* generate a similar phenotype, suggesting that they disrupt translation of *nrk2b*. Second, the phenotype is recapitulated by co-injection of sub-functional doses of both MOs. Third, *nrk2b* MOs block translation of a Nrk2b:GFP fusion protein containing the target sequences for the MOs. Fourth, co-injection of *p53* MO with the *nrk2b* MO

cocktail rescues the cell death seen in the head of *nrk2b* morphants, but does not rescue the disrupted muscle phenotype. Fifth, injection of *nrk2b* MOs into wild-type or *laminin* mutants phenocopies the *laminin* mutant phenotype. Taken together, these results suggest that *nrk2b* MOs disrupt translation of Nrk2b protein and do not cause significant “off-target” effects⁽¹⁰⁰⁾.

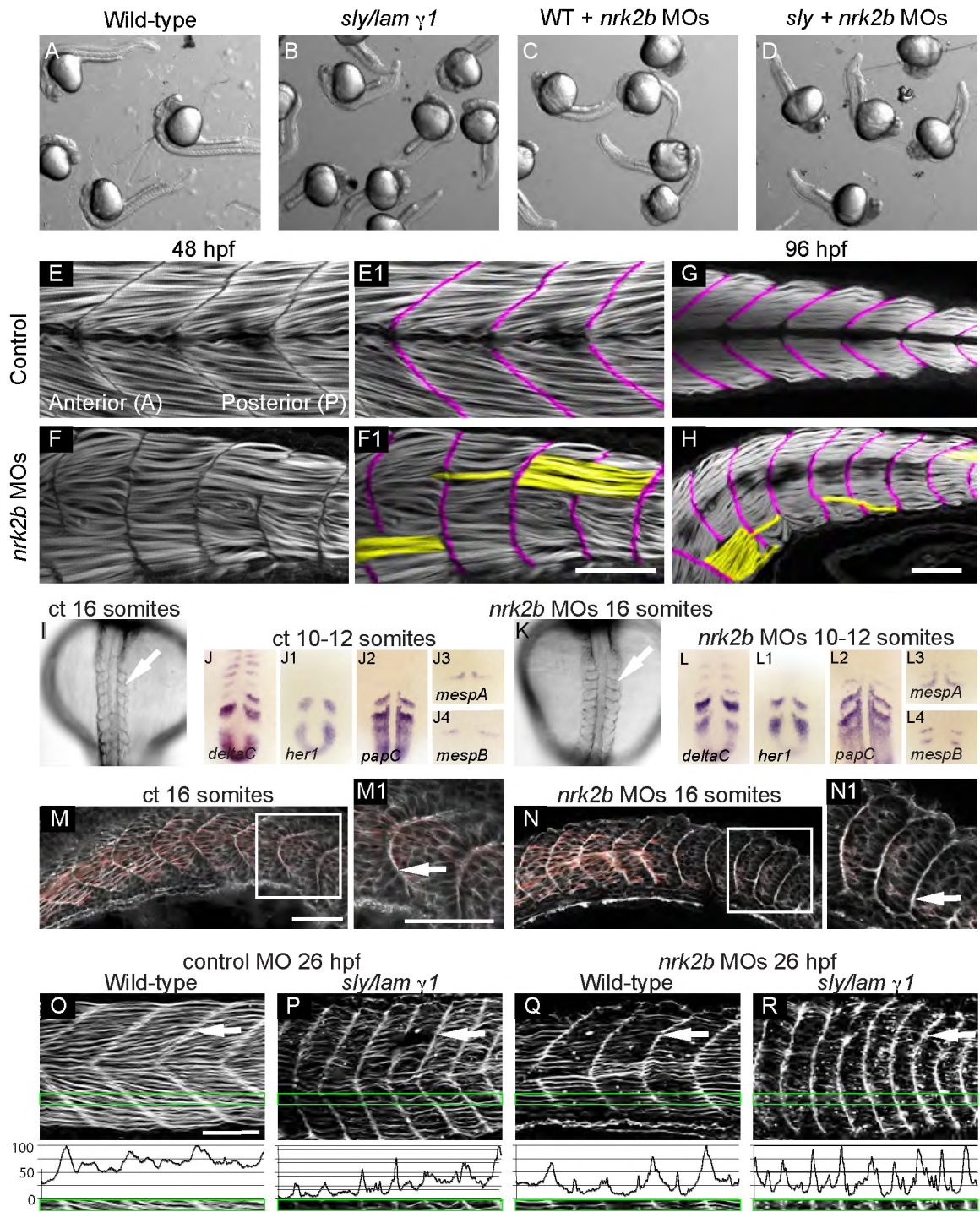
2.4.2. MTJs are Disrupted in *nrk2b* Morphants

MTJ development is disrupted by 48 hpf in *laminin beta1* and *gamma1* mutants⁽¹⁰³⁾. Given the above data suggesting that Nrk2b participates in Laminin signaling/adhesion, we asked whether MTJ development is also disrupted in *nrk2b* morphants. Phalloidin staining, to visualize filamentous-actin, showed organized elongated muscle fibers in 48 hpf controls (Fig. 2.2 panel E). The MTJ is the dark region devoid of actin staining (pseudocolored purple in Fig. 2.2 panel E1). In contrast, about one third (71/212, 33%) of MTJs in every 48 hpf *nrk2b* morphant contained foci where MTJs were disrupted and muscle fibers were abnormally long (pseudocolored yellow in Fig. 2.2 panels F-F1). Approximately the same proportion of MTJs (19/67, 28%) were disrupted in all 96 hpf *nrk2b* morphants (Fig. 2.2 panel H). Similar proportions of disrupted MTJs in 48 and 96 hpf *nrk2b* morphants indicates that there is no age-dependent degeneration of the MTJ. This phenotype of disrupted MTJs is also observed in *nrk2b:p53* double morphants (data not shown). These data show that Nrk2b is required for normal muscle development and raise the question of why *nrk2b* morphant MTJs are discontinuous.

In teleosts, MTJs are derived from initial epithelial somite boundaries. Therefore, we asked if discontinuous MTJs at 48 hpf are a direct consequence of discontinuous initial somite boundary formation. Although somites are misshapen in *nrk2b* morphants, segmentally reiterated boundaries form (Fig. 2.2 panels I, K) and the expression of somite patterning genes appears normal (Fig. 2.2 panels J-J4, L-L4). Similar to *laminin beta1* and *gamma1* mutants (¹⁰³), initial somites are narrower in the anterior–posterior dimension (Fig. 2.2 panels N-N1). These abnormally shaped but continuous somite boundaries are clearly visible when phalloidin staining is used to outline cells (Fig. 2.2 panels N-N1). In controls at 26 hpf, MTJs are clearly V-shaped and actin is slightly enriched at the terminal ends of muscle fibers attached to MTJs, (Fig. 2.2 panel O, white arrow). In contrast, actin is strikingly enriched at the terminal ends of muscle fibers at the MTJ and depleted within myotubes in 26 hpf *laminin* mutants (Fig. 2.2 panel P). Similar actin distribution is observed in both *nrk2b* morphants and *nrk2b* MO-injected *laminin* mutants (Fig. 2.2 panels Q-R). These differences in actin distribution are clear when normalized fluorescence intensity in the anterior–posterior dimension is graphed (Fig. 2.2 panels O-R). Note that the peaks and valleys of fluorescence intensity in controls (Fig. 2.2 panel O) are less extreme than those in the other panels (Fig. 2.2 panels P-R). These data suggest that adhesion to Laminin may be required for normal cellular distribution of F-actin. In addition, this higher resolution analysis of *nrk2b* morphant-*laminin* mutants indicates that injection of *nrk2b* MOs into *laminin* mutants does slightly affect the *laminin* mutant phenotype. Boundaries are more U-shaped than *laminin* mutants injected with control MO (compare Fig. 2.2 panels P and R). Both *laminin beta1* and *laminin*

gamma1 are maternally expressed (⁹³), and we have found that injection of *laminin* MOs into *laminin* mutants worsens the *laminin* mutant phenotype, resulting in early embryonic lethality (data not shown). We hypothesize that injection of *nrk2b* MOs into *laminin* mutants disrupts adhesion to maternally provided *laminin* and thus results in a slightly worse phenotype, as opposed to the alternate explanation of Laminin-independent functions for Nrk2b. Taken together, these data indicate that discontinuous MTJs at 48 hpf in *nrk2b* morphants are not due to discontinuous somite boundary formation earlier in development. In addition, these data further show that the *nrk2b* morphant phenotype resembles that of *laminin* mutants, supporting the hypothesis that Nrk2b functions in Laminin-mediated adhesion/signaling.

Fig. 2.2. Disrupted MTJs in *nrk2b* Morphants are Not Due to Discontinuous Initial Somite Boundaries. (A–D) Brightfield images of a dish of 26 hpf embryos. (A) Wild-types. (B) *sly/laminin gamma1* mutants. (C) *nrk2b* morphants. (D) *nrk2b* MO-injected-*laminin gamma1* mutants. Note that injection of *nrk2b* MOs into *laminin* mutants does not drastically worsen their phenotype or result in death. (E–H) Side mount, anterior left, dorsal top, phalloidin stained embryos, MTJ boundaries are pseudocolored fuchsia and abnormally long muscle fibers are pseudocolored yellow. (E–E1) 48 hpf control. (F–F1) 48 hpf *nrk2b* morphant (71/212, 33% of MTJs are crossed by muscle fibers). (G) 96 hpf control. (H) 96 hpf *nrk2b* morphant (19/67, 28% of MTJs are crossed by muscle fibers). (I, K) Dorsal mount, anterior top, 16 S, brightfield images. Note that somite boundaries form (white arrows) in *nrk2b* morphants (K). (Panels J and L) Dorsal mount, anterior top, 10–12 S, ISH for known somite patterning and somite boundary formation genes. Note that the domains and patterns of expression are similar between controls (panel J) and *nrk2b* morphants (panel L). (M–N) Side mount, anterior left, dorsal top, 16 S, phalloidin staining. Note concentrated actin at the initial somite boundary (white arrows). These data show that discontinuous MTJs are not due to discontinuous initial somite boundaries. (O–R) Side view, anterior left, dorsal top, 26 hpf embryos, phalloidin stained to visualize actin. (O–P) Control MO-injected. (Q–R) *nrk2b* MO-injected. (O, Q) Wild-types. (P, R) *sly/laminin gamma1* mutants. Note that in *laminin* mutants and *nrk2b* morphants, actin is enriched at the MTJ (white arrows) and lacking in the myotome. Green boxes correspond to normalized fluorescence intensity (see Section 2.3.11) plots. These graphs support the qualitative actin disruption seen in *laminin* mutants and *nrk2b* morphants. Scale bars are 50 μ m.

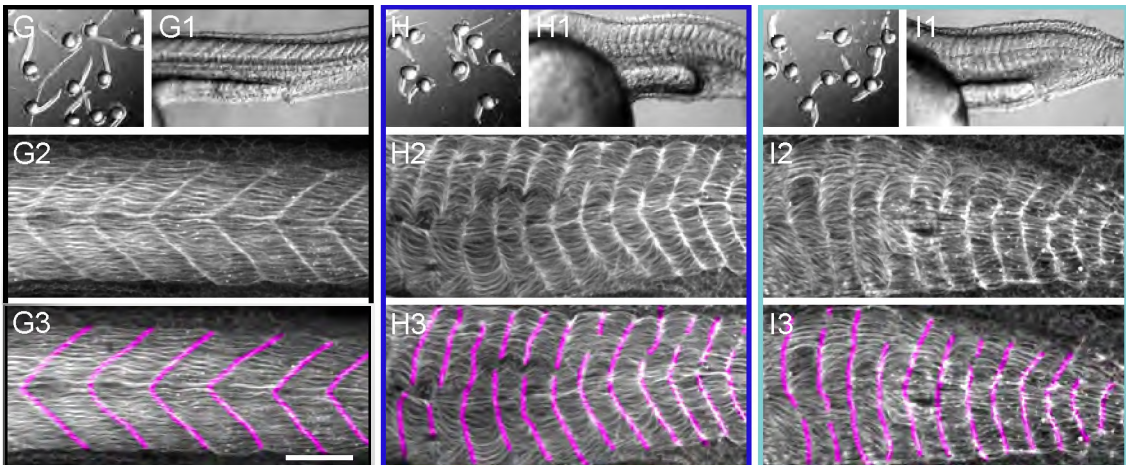
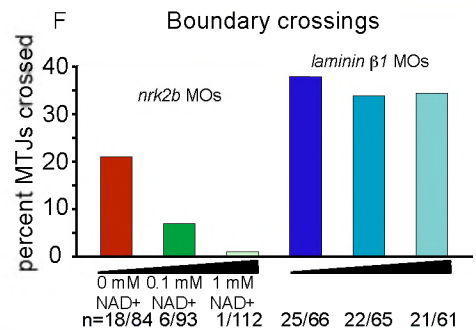
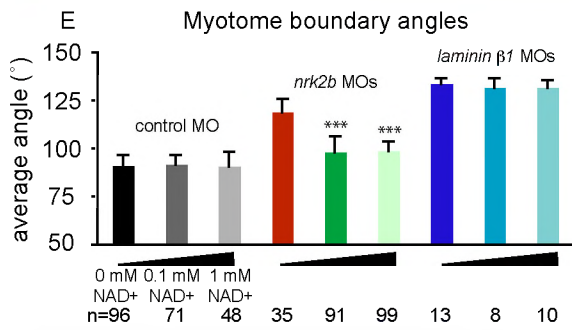
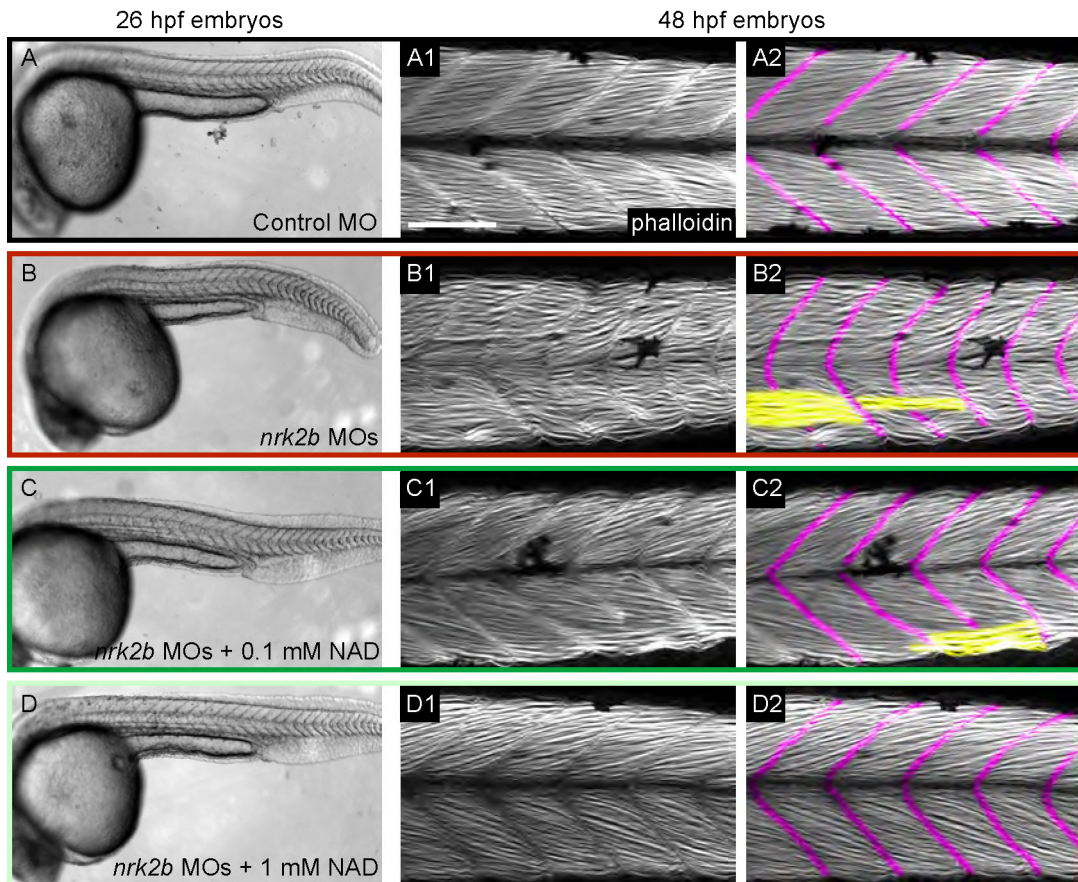


2.4.3. Exogenous NAD⁺ Rescues MTJ Deterioration in *nrk2b* Morphants

Yeast and human Nrk2 phosphorylate Nicotinamide Riboside to generate NAD⁺ through an alternative salvage pathway (71). We hypothesized that addition of exogenous NAD⁺ would rescue the *nrk2b* morphant phenotype. We incubated control and *nrk2b* MO-injected embryos in 100 μ M or 1 mM exogenous NAD⁺ beginning at shield stage. Addition of NAD⁺ to control MO-injected embryos did not affect muscle development (Fig. 2.3 panels A-A2). Body axes are again shorter, somites are U-shaped, and MTJs are discontinuous in *nrk2b* morphants (Fig. 2.3 panels B-B2). Exogenous NAD⁺ rescued the *nrk2b* morphant paraxial mesoderm phenotype. Morphants incubated in 100 μ M or 1 mM NAD⁺ had longer body axes and greatly decreased boundary angles that were significantly different from angles in *nrk2b* morphants (Fig. 2.3 panels C-C2, D-D2, $p < 0.001$ for both concentrations). Approximately 7% of MTJs were discontinuous in morphants treated with 100 μ M NAD⁺ (Fig. 2.3 panel C2). Discontinuous MTJs in NAD⁺-treated *nrk2b* morphants with normal boundary angles indicate that MTJ disruption is not a non-specific side effect of wider MTJs. Although myotome boundary angles were not significantly different in *nrk2b* morphants grown in 100 μ M and 1 mM NAD⁺, there was a difference in MTJ integrity. Far fewer MTJs were discontinuous in morphants treated with 1 mM NAD⁺ than treated with 100 μ M NAD⁺ (Fig. 2.3 panel F). Thus, there is a dose dependent rescue of MTJ integrity when *nrk2b* morphants are supplemented with NAD⁺. Treatment of *laminin* morphants with exogenous NAD⁺ did not rescue wider myotome boundary angles or MTJ crossings (Fig. 2.3 panels E, F, H-H3, I-I3).

Taken together, these data suggest NAD⁺ is functionally upstream of Laminin adhesion/
signaling.

Fig. 2.3. Exogenous NAD⁺ Treatment Rescues the *nrk2b* Morphant Muscle Phenotype. (A–D) Brightfield images, side mount, anterior left, dorsal top, 26 hpf embryos. (Numbered panels A–D) Side mount, anterior left, dorsal top, 48 hpf embryos, phalloidin stained to visualize actin. In panels numbered 2, MTJs are pseudocolored fuchsia. (Panel A) Control MO-injected. (Panel B) *nrk2b* MO-injected. (Panel C) *nrk2b* MO-injected embryos incubated in 0.1 mM NAD⁺. (Panel D) *nrk2b* MO-injected embryos incubated in 1 mM NAD⁺. (E) Graph of average myotome boundary angles in controls, NAD⁺-treated controls, *nrk2b* morphants, NAD⁺-treated *nrk2b* morphants, *laminin* morphants, and NAD⁺-treated *laminin* morphants. The average myotome boundary angle of *nrk2b* morphants is significantly different than controls (Student t-test, p<0.001) and the average myotome boundary angle of NAD⁺-treated *nrk2b* morphants is significantly different than untreated *nrk2b* morphants and controls (Student t-test, p<0.001, n of myotome boundaries measured on x-axis). (F) Graph of the percent of MTJs crossed by muscle fibers in *nrk2b* morphants, NAD⁺-treated *nrk2b* morphants, *laminin* morphants, and NAD⁺-treated *laminin* morphants. NAD⁺ treatment rescues boundary crossings in a dose dependent manner in *nrk2b* morphants, but not *laminin* morphants (n of MTJs crossed over total MTJs analyzed is listed on the x-axis). (Panel G) Controls. (Panel H) *laminin* morphants. (Panel I) 1 mM NAD⁺-treated *laminin* morphants. (Lettered panels) Brightfield images of a dish of embryos. (Panels numbered 1) Side mount, brightfield images, 26 hpf embryos, anterior left, dorsal top. (Panels numbered 2) Side mount, 48 hpf embryos, anterior left, dorsal top, phalloidin stained to visualize actin. (Panels numbered 3) MTJs are pseudocolored fuchsia. Scale bars are 50 μm, ***p<0.001.



2.4.4. Nr2f1 is Required Non-Cell Autonomously for Basement Membrane

Polymerization at the MTJ

We showed that discontinuous MTJs in *nr2f1* morphants at 48 hpf are not due to discontinuous somite boundaries. Somite boundary morphogenesis into nascent MTJs occurs around 24 hpf⁽⁹⁶⁾ and polymerized Laminin-111, indicative of basement membrane assembly, robustly concentrates throughout the MTJ at this time^(58,60). We asked if Nr2f1 is required for basement membrane formation because Nr2f1 interacts specifically with the Laminin receptor, Integrin alpha7beta1, *in vitro*⁽⁶⁹⁾. In controls, Laminin-111 at the basement membrane is clear as a distinct line between adjacent myotomes (Fig. 2.4 panels A1-3, small square panels). In 3D projections, the organization and continuous nature of Laminin-111 in the medial-lateral dimension is clear (Fig. 2.4 panels A1-3, large square panels). When the 3D projections are rotated to generate a transverse view, high levels of Laminin-111 are observed throughout the medial-lateral extent of the MTJ except for the horizontal myoseptum (dark vertical line, Fig. 2.4 A1-3, tall rectangular panels, Laminin is observed at the MTJ adjacent to slow-twitch fibers in blue, but also medially in the fast-twitch muscle domain). In contrast, the MTJ basement membrane in *nr2f1* morphants is disorganized and discontinuous. At a lower magnification view, Laminin-111 at the MTJ in *nr2f1* morphants appears similar to controls (compare Fig. 2.4 panels A to B). Upon closer inspection, however, it is clear that Laminin-111 is not laid down in a straight and organized line (Fig. 2.4 panels B1-3, small square panels). The basement membrane is not always continuous, i.e. there are holes in Laminin-111 at the MTJ (Fig. 2.4 panel B3, white arrow in large square panel,

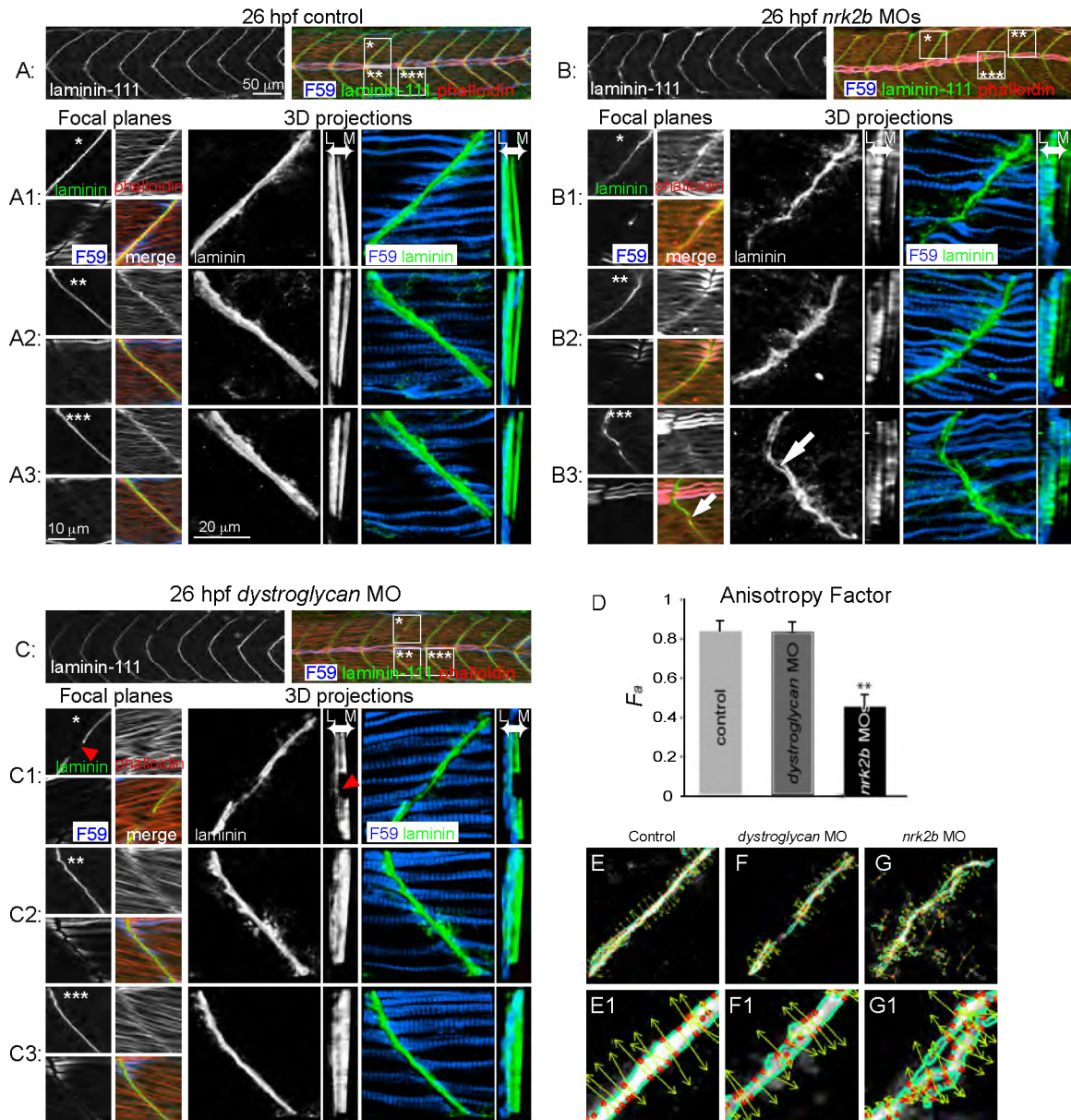
note gap in Laminin-111 staining in the top left small square panel, this gap appears as a hole in Laminin-111 staining when 3D projected). These holes do not represent gaps within muscle tissue because staining for phalloidin, which outlines cells, showed that muscle fibers terminated adjacent to the gaps/holes (Fig. 2.4 panel B3, white arrow in small square panel). This disorganization of the basement membrane is especially clear in 3D projections (Fig. 2.4 panels B1-3, large square panels). The transverse view shows that levels of Laminin-111 are not uniform throughout the medial–lateral extent of the MTJ (Fig. 2.4 panels B1-3, tall rectangular panels). Interestingly, Laminin-111 deposition appears to be particularly poor in the MTJ adjacent to the medial fast-twitch muscle domain (Fig. 2.4 panels B1-3, tall rectangular panels).

The above data indicate that basement membrane assembly at the MTJ is disrupted in *nrk2b* morphants. To test whether this disruption is a common phenotype when adhesion to Laminin-111 is disrupted, we assayed basement membrane assembly in *dystroglycan* morphants. Dystroglycan is a component of the Dystrophin–Glycoprotein Complex (DGC), a transmembrane receptor for Laminin, and is crucial for maintenance of muscle fiber attachment to the ECM. It has previously been shown that *dystroglycan* morphants have muscular dystrophy (⁹²), but the age of onset has not been closely investigated. We find that MTJs in *dystroglycan* morphants at 26 hpf are fairly normal (Fig. 2.4 panel C). Very few MTJs are discontinuous and crossed by abnormally long muscle fibers (2 experiments, 13 embryos, 4/110 MTJs crossed). Careful inspection of the basement membrane in *dystroglycan* morphants corroborates this conclusion. 3D and transverse projections show robust basement membrane polymerization (Fig. 2.4, panel

C). Even when the MTJ is discontinuous and there is a hole in the basement membrane that is crossed by muscle fibers, the adjacent basement membrane is robust (Fig. 2.4 panel C1, square panels, red arrowhead). Importantly, transverse views show that basement membrane assembly in the fast-twitch muscle domain is robust adjacent to the gap in the MTJ that is crossed by muscle fibers (Fig. 2.4 panel C, tall rectangular panel, red arrowhead).

By applying the 2D Wavelet Transform Modulus Maxima (WTMM) method ^(60,97,98,103) we performed a structural, multi-scale anisotropy analysis to rigorously and objectively assess CMAC components at the MTJ in *nrk2b* morphants. The 2D WTMM method can be used to quantify the amount of structure (order) of objects that do not have a well-defined boundary by calculating the angle of steep gradients in pixel intensity, at different size scales. This is perhaps most apparent in controls, where most of the arrows plotting this angle are parallel to each other (Fig. 2.4 panel E). Angles are also mostly parallel in *dystroglycan* morphants (Fig. 2.4 panel F). However, arrows are far less organized in *nrk2b* morphants (Fig. 2.4 panel G). This organization is quantified by calculating the probability density function of the angles, from which we obtain the anisotropy factor. The anisotropy factor is the departure from isotropy or randomness. A higher anisotropy factor indicates a more ordered structure. We found that control and *dystroglycan* morphants have similar anisotropy factors (Fig. 2.4 panel D). The anisotropy factor of Laminin-111 staining in *nrk2b* morphants is significantly lower, indicating a more random structure (Student t-test, $p < 0.01$, Fig. 2.4 panel D). These data indicate that *Nrk2b* is required for normal basement membrane assembly.

Fig. 2.4. Nr2f2 is Required for Normal Basement Membrane Development. (A, B, C) 26 hpf embryos, side mount, anterior left, dorsal top, F59 antibody stained to visualize slow-twitch muscle, phalloidin stained to visualize actin and Laminin-111 antibody stained to visualize the basement membrane of the MTJ. (A) Control. (B) *nr2f2* morphant. (C) *dystroglycan* morphant. Numbered panels 1–3 are examples of different MTJs within an embryo from each treatment (*, ** or *** indicates the location of the MTJ). Small square panels are focal planes of each antibody/stain used as well as a merged view. Large square panels are 3D reconstructed Laminin-111 antibody staining (in black and white) or F59 and Laminin-111 antibody staining (in color). Tall rectangular panels are transverse views of the 3D reconstructed antibody staining with lateral to the left and medial to the right. Note in the MTJ examples in *nr2f2* morphants (panel B) that Laminin-111 is not laid down in a straight line and is not always continuous (white arrows). In the transverse views, note that Laminin-111 is especially disrupted in the medial fast-twitch fiber domain. In *dystroglycan* morphants, MTJs can still be discontinuous (red arrowheads), but Laminin-111 is robust in the lateral and medial domains. (D) Graph of the anisotropy factor (see Section 2.3.12) in Laminin-111 stained images. A lower anisotropy value in *nr2f2* morphant images indicates that there is less order/ structure in Laminin-111 staining in these morphants. (E–G) Side mount, anterior left, dorsal top, 26 hpf embryos, Laminin-111 antibody staining. Numbered panels are higher magnification views of corresponding panels. Images were analyzed with the 2D Wavelet Transform Modulus Maxima (2DWTMM) method. (Panel E) Controls. (Panel F) *dystroglycan* morphants. (Panel G) *nr2f2* morphants. In controls and *dystroglycan* morphants, the vectors are more parallel indicating more order than in *nr2f2* morphants. Scale bars are labeled on the figure, **p<0.01.



Possible explanations for the apparent decrease in Laminin-111 at *nrk2b* morphant MTJs are: (1) reduced *laminin* transcription, (2) increased Laminin-111 degradation or (3) less efficient assembly/polymerization of Laminin-111. We used multiple experimental approaches to distinguish between these possible mechanisms. We first analyzed *laminin* transcription at 24 hpf because this is the earliest time that basement membranes at the MTJ are reliably robust in controls and disrupted in *nrk2b* morphants.

Neither of these *laminin* chains is highly expressed in controls at 24 hpf (Fig. 2.5 panels B, C). Expression of both chains appears increased in 24 hpf *nrk2b* morphants (Fig. 2.5 panels B1, C1). Because expression levels are somewhat low, we also quantitatively analyzed transcription of the three *laminin* chains that make up Laminin-111.

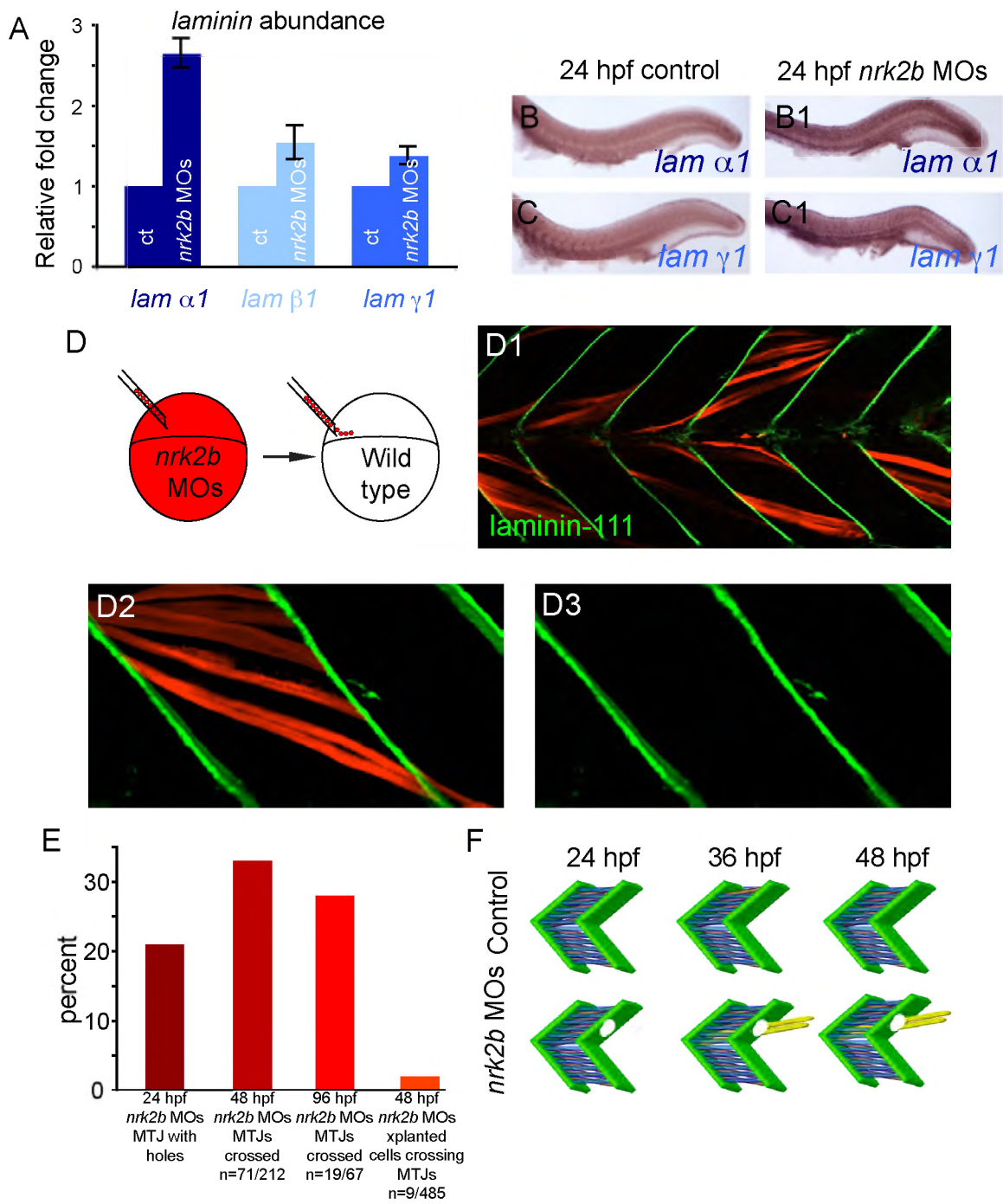
Comparative quantitative Reverse Transcriptase-Polymerase Chain Reaction (qRT-PCR) of controls and *nrk2b* morphants indicated that these three *laminin* chains are not down regulated in *nrk2b* morphants (Fig. 2.5 panel A, Table 2.2). If anything, transcription of these *laminin* chains is increased. Transcription of *laminin alpha1* is upregulated approximately 2.5 fold compared to controls. Because all three chains are required for Laminin-111 assembly, it is not clear whether dramatically increased transcription of one chain affects levels of Laminin-111 protein (we have been unsuccessful at using Westerns to detect Laminin-111 with the above antibody, this is probably due to the fact that the antibody recognizes assembled and polymerized Laminin-111). However, these data allow us to conclude that the disruption in Laminin-111 at the MTJ basement membrane is not due to decreased *laminin* transcription.

Another mechanism that could account for the holes in the MTJ basement membrane in *nrk2b* morphants is increased degradation of Laminin-111. We used genetic mosaic analysis to ask whether *nrk2b* morphant cells are sufficient for Laminin-111 degradation. *Nrk2b*-deficient cells were transplanted into wild-type hosts and the MTJ basement membrane was assessed at 48 hpf. No holes in the MTJ basement membrane were observed adjacent to *Nrk2b*-deficient cells in control hosts (Fig. 2.5 panels D-D3, n = 68 cells). We also asked whether *Nrk2b*-deficient cells were able to elongate across

MTJ boundaries. Only 9/485 (2%) cells crossed control MTJ boundaries (Fig. 2.5 panel E). Genetic mosaic analysis of myotubes is complicated by their multinucleate nature. However, we can conclude that *Nrk2b*-deficient cells are not sufficient, even in large quantities, to frequently induce Laminin degradation. Taken together, the above data suggest that *Nrk2b* is non-cell autonomously required for basement membrane polymerization and that basement membrane polymerization is a phenomenon mediated by communities of cells. To our knowledge, this is the first example of an intracellular protein critical for basement membrane assembly during muscle development *in vivo*.

The percentage of holes in Laminin-111 at 24 hpf is similar to the percentage of MTJs crossed at 48 hpf (Fig. 2.5 panel E). Muscle integrity does not degenerate through time in *nrk2b* morphants: the percentage of MTJs crossed at 96 hpf is similar to the percentage crossed at 48 hpf (Fig. 2.5 panel E). These results suggest that initial defects in basement membrane assembly precede muscle fibers crossing through the defective basement membrane later in development, resulting in discontinuous MTJs (Fig. 2.5 panel F).

Fig. 2.5. Nr2f2 is Non-Cell Autonomously Required for Normal Basement Membrane Polymerization. (A) qRT-PCR for relative transcript abundance of the three *laminin* chains that comprise Laminin-111 in 24 hpf embryos. (B–C) Side mount, anterior left, dorsal top, 24 hpf. ISH for *laminin* transcripts in controls (lettered panels) and *nr2f2* morphants (numbered panels), (panel B) *laminin alpha1*, (panel C) *laminin gamma1*. ISH and qRT-PCR suggest that Laminin-111 defects in *nr2f2* morphants are not due to a *laminin* transcription deficiency. (D) Model of dextran labeled *nr2f2* morphant cells being transplanted into a wild-type host at blastula stage. (D1–D3) Side mount, anterior left, dorsal top, 48 hpf, red cells are dextran labeled Nr2f2-deficient cells. Laminin-111 antibody staining (in green) is normal adjacent to Nr2f2-deficient cells (red) in a wild-type background. This suggests that basement membrane polymerization is a phenomenon mediated by communities of cells and that Nr2f2 is non-cell autonomously required for basement membrane polymerization. (E) Graph of the percentage of MTJs with holes in Laminin-111 or with boundary crossings over time. The observation that the percentage of MTJs with defects does not steadily increase over time suggests that boundary crossings are not due to age-dependent degeneration of the MTJ. Note that a very small percentage of Nr2f2-deficient cells cross MTJs in wild-type hosts suggesting that these cells do not actively degrade Laminin-111 and that Nr2f2 functions non-cell autonomously in basement membrane development. (F) Model of MTJ basement membrane defects in *nr2f2* morphants leading to fibers crossing MTJs as time progresses.



2.4.5. CMAC Assembly is Aberrant in *nrk2b* Morphants

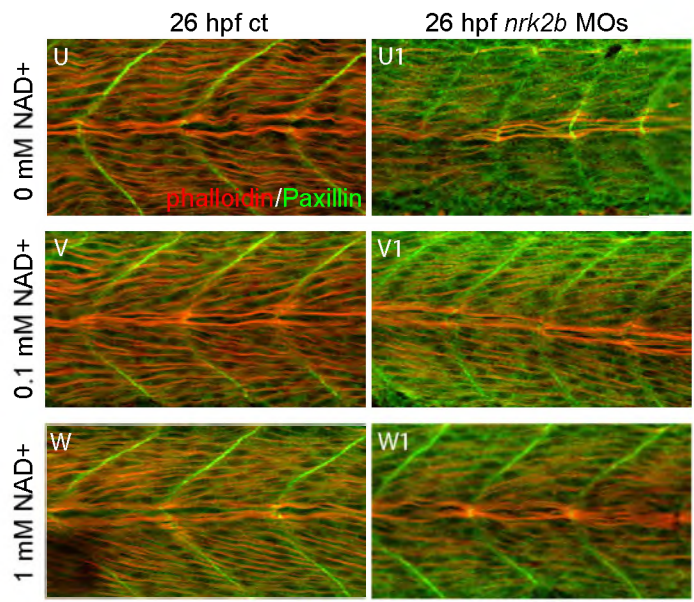
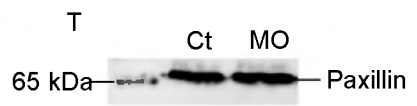
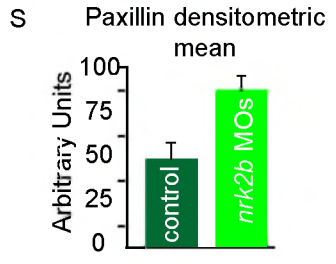
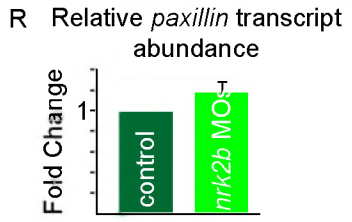
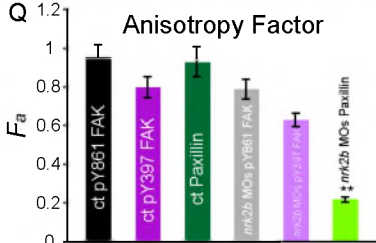
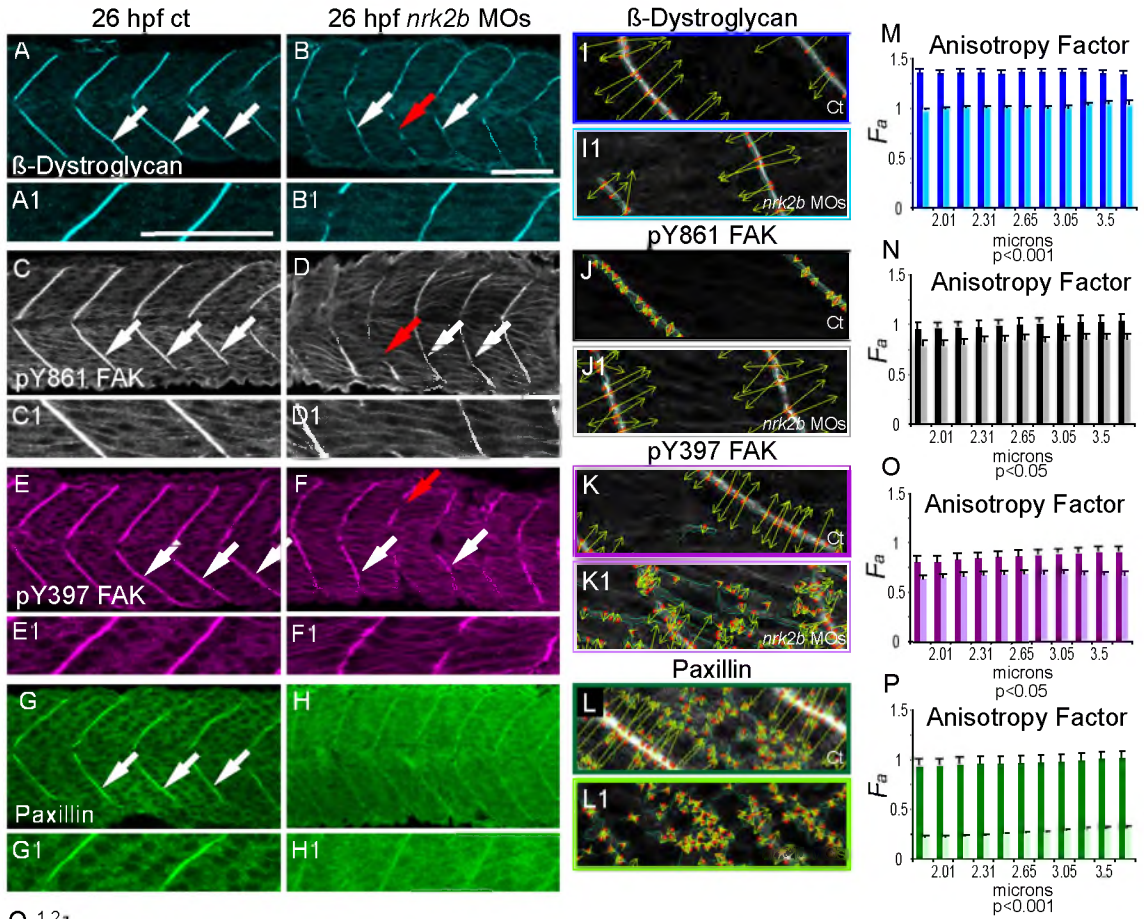
The above data show that Laminin-111 is not efficiently polymerized at the MTJ basement membrane in *nrk2b* morphants. Recruitment of intracellular scaffolding and signaling proteins, like Focal Adhesion Kinase (FAK), Paxillin and beta-Dystroglycan, to CMACs is critical for the assembly and maintenance of the ECM^(74,104,105). Thus, we assessed CMAC assembly at the MTJ both qualitatively and quantitatively, with the WTMM formalism. The WTMM formalism was applied to images for beta-Dystroglycan, pY861 FAK, pY397 FAK, and Paxillin. In order to best assess structure at the MTJ, we analyzed wavelets between 1.88 and 3.75 μm . Beta-Dystroglycan robustly concentrates at the MTJ in controls at 26 hpf (Fig. 2.6 panel A, white arrows). This organized staining is reflected in a relatively high anisotropy factor, approximately 1.3, across all size scales analyzed (Fig. 2.6 panel M, dark blue bars). Beta-Dystroglycan concentrates at *nrk2b* morphant MTJs, but is slightly less robust than in controls (Fig. 2.6 panel B, ct n=31 MTJs, *nrk2b* MOs n = 44 MTJs). This difference is clear when the anisotropy factor is calculated (Fig. 2.6 panel M, light blue bars): beta-Dystroglycan is significantly less organized in *nrk2b* morphants for all size scales examined ($p < 0.001$). Both FAK (data not shown, ct n = 48 MTJs; *nrk2b* MOs n = 43 MTJs) and tyrosine phosphorylated FAK concentrated at the MTJ in controls and *nrk2b* morphants (Fig. 2.6 panels C-F, white arrows, pY861 FAK ct n = 52 MTJs, *nrk2b* MOs n=75 MTJs; pY397 FAK ct n=55 MTJs, *nrk2b* MOs n=83 MTJs). Gaps in FAK staining in *nrk2b* morphants correlated with gaps in MTJs and abnormally long muscle fibers (Fig. 2.6 panels D, F, red arrows). Anisotropy factors reflecting organization of pY FAK between control and *nrk2b*

morphants were more similar to each other, but still significantly different (Fig. 2.6 panel N, O, p values ranged from 0.02 to 0.05, there was no correlation of size scale with p value). These results indicate that although concentration of beta-Dystroglycan and pY FAK appear qualitatively similar to controls, subcellular localization of these proteins at the MTJ is less organized in *nrk2b* morphants than in controls.

Strikingly, the localization of a different CMAC component, Paxillin, was disrupted in all *nrk2b* morphants analyzed (Fig. 2.6 panels G-H, imaging parameters were the same for controls and morphants, ct n = 200 MTJs; *nrk2b* MOs n = 181 MTJs). Note that Paxillin is concentrated at MTJs in controls, but is not highly concentrated at the MTJ in *nrk2b* morphants. Interestingly, similar to Laminin-111 staining, Paxillin staining at the MTJ within slow-twitch muscle fibers was not affected (data not shown), but was disrupted in the more medial fast-twitch fiber domain. The anisotropy factor was strikingly lower for *nrk2b* morphants than controls over all size scales (Fig. 2.6 panel P, $p < 0.001$). In controls, the anisotropy factors for pY FAK and Paxillin are not significantly different (Fig. 2.6 panel Q). In contrast, the anisotropy factor for Paxillin in *nrk2b* morphants was significantly different than pY FAK ($p < 0.01$). Addition of exogenous NAD⁺ rescues Paxillin concentration at the MTJ in the medial fast-twitch muscle domain in *nrk2b* morphants (Fig. 2.6 panels U-W). Taken together, the qualitative and quantitative assessments of CMAC formation in *nrk2b* morphants indicate that Paxillin concentration at MTJ CMACs is dramatically disrupted in *nrk2b* morphants.

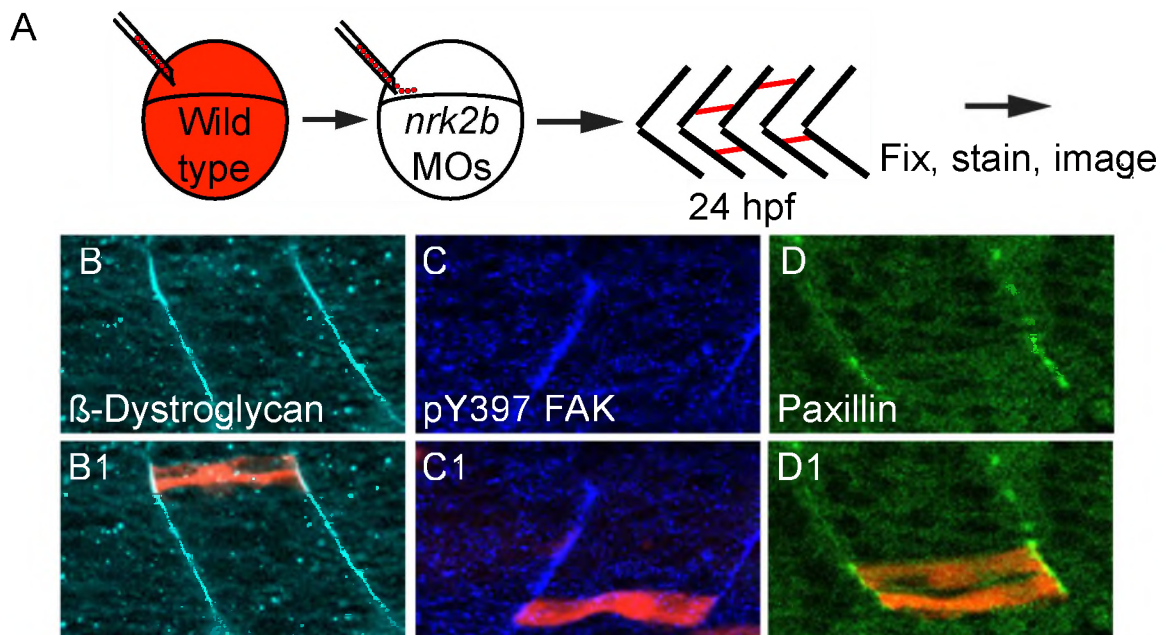
The lack of robust Paxillin concentration at MTJs in *nrk2b* morphants could be due to: (1) decreased *paxillin* transcription, (2) less Paxillin protein or (3) reduced recruitment/retention of Paxillin to MTJ CMACs. qRT-PCR for *paxillin* transcript levels show that *paxillin* transcription is normal in *nrk2b* morphants (Fig. 2.6 panel R, Table 2.2). Densitometry measurements of Paxillin antibody staining and Western analysis suggested that there is not a reduction in Paxillin protein in *nrk2b* morphants (Fig. 2.6 panels S, T). One caveat, however, is that densitometry is qualitative and qRT-PCR and Westerns represent levels within entire embryos. Thus, although it does not appear to be the case, there could be a physiologically significant reduction of Paxillin levels in muscle tissue. These data suggest the hypothesis that Nrk2b is required for recruitment and/or retention of cytoplasmic Paxillin to MTJ CMACs.

Fig. 2.6. Nr2b is Required for Normal Subcellular Localization of Paxillin, but Not Beta-Dystroglycan or FAK. (A–H) Side mount, anterior left, dorsal top, 26 hpf. Panels A, C, E, and G are controls. Panels B, D, F, and H are *nr2b* morphants. Panels numbered 1 are magnifications of the corresponding lettered panels. (A–B1) - Dystroglycan antibody staining. (C–D1) pY861 FAK antibody staining. (E–F1) pY397 FAK antibody staining. (G–H1) Paxillin antibody staining. White arrows indicate normal localization of proteins to MTJs. Red arrows in *nr2b* morphants (B, D, F) indicate discontinuous MTJs crossed by muscle fibers. Note that in *nr2b* morphants (H, H1), Paxillin does not robustly concentrate to MTJs. (I–L) Side mount, anterior left, dorsal top, 26 hpf controls (lettered panels) and *nr2b* morphants (numbered panels). Application of 2D WTMM method showing maxima chains (dark green), nodes (red), and vectors (light green) for CMAC component antibody staining. (M–Q) Graphs of anisotropy or the amount of order in a structure over a range of applicable size scales. (R) qRT-PCR, (S) average densitometric mean of Paxillin antibody-stained images and (T) Western analysis suggest that Paxillin levels are not decreased in *nr2b* morphants. (U–W) Side mount, anterior left, dorsal top, 26 hpf embryos, phalloidin staining in red, Paxillin antibody staining in green. Lettered panels are controls and numbered panels are *nr2b* morphants. (Panel U) No exogenous NAD⁺. (Panel V) 0.1 mM exogenous NAD⁺. (Panel W) 1 mM exogenous NAD⁺. Note that exogenous NAD⁺ treatment rescues medial Paxillin concentration at the MTJ in *nr2b* morphants in a dose dependent manner. Scale bars are 50 μm.



The above data indicate a specific requirement for Nrk2b in Paxillin localization at MTJ CMACs. This represents a novel model system with which to ask important questions about CMAC assembly *in vivo*. We used genetic mosaic analysis to ask whether Paxillin localization to MTJ CMACs was restored in wild-type cells transplanted into *nrk2b* morphants. Normal beta-Dystroglycan localization indicated that cells are not appreciably perturbed by transplantation (Fig. 2.7 panel B). Similar results were obtained when pY397 FAK concentration at the MTJ was analyzed (Fig. 2.7 panel C). Strikingly, Paxillin localization to MTJs was rescued in wild-type cells, but not in the Nrk2b-deficient cells surrounding them (Fig. 2.7 panel D) The multinucleate nature of fast-twitch muscle fibers and the possibility that wild-type cells fused with Nrk2b-deficient cells implies that even reduced amounts of Nrk2b are sufficient for Paxillin concentration at the MTJ. This result indicates that the protein composition of CMACs can be modulated cell autonomously *in vivo*.

Fig. 2.7. Nr2b is Cell Autonomously Required for Paxillin Localization to MTJs. (A) Cartoon showing dextran labeled wild-type cells being transplanted into a *nrk2b* morphant host at blastula stage. (B–D) Side mount, anterior left, 26 hpf *nrk2b* morphant hosts with transplanted wild-type cells (red), beta-Dystroglycan antibody staining (light blue, panel B), pY397 FAK antibody staining (dark blue, panel C), and Paxillin antibody staining (green, panel D). Note that beta-Dystroglycan and pY397 FAK robustly localize to MTJs in *nrk2b* morphants in the presence and the absence of transplanted wild-type cells. Note that robust Paxillin localization to the MTJ in *nrk2b* morphants is rescued in the transplanted wild-type cells, but not in the Nr2b-deficient cells surrounding them. Numbered panels are merged images showing both antibody staining and transplanted, dextran-labeled cells.



2.4.6. Paxillin is Sufficient for Boundary Capture in *nrk2b* Morphants

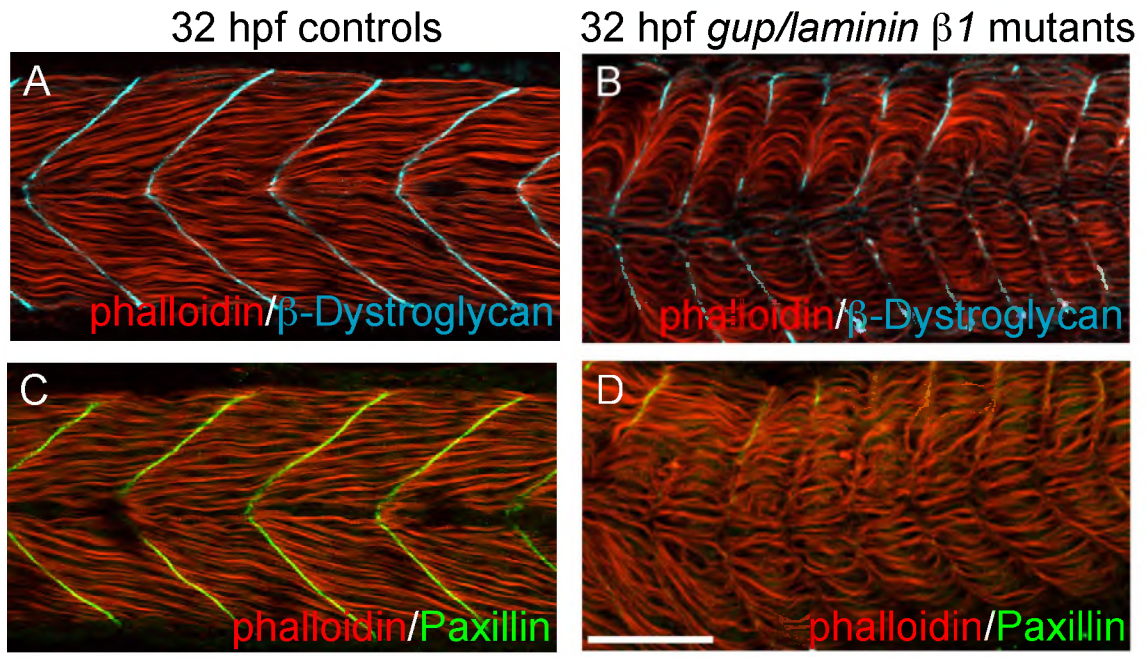
The data thus far suggest multiple hypotheses, including: (1) Paxillin concentration at the MTJ promotes normal basement membrane assembly and boundary capture, (2) Paxillin concentration at the MTJ is a read-out of robust CMAC assembly, (3) adhesion to Laminin-111 is critical for Paxillin concentration at the MTJ, or (4) Paxillin concentration at the MTJ and basement membrane assembly are linked through

inside-out and outside-in signaling. Unfortunately we do not currently possess the tools for dynamic, *in vivo* analysis of basement membrane assembly and are unable to definitively discriminate between these hypotheses. However, analysis of Paxillin subcellular localization in *laminin* mutants could be informative. If Paxillin concentrates at the MTJ in *laminin* mutants, hypotheses (2) and (3) could be eliminated. Beta-Dystroglycan concentrates at the MTJ in *laminin* mutants as previously reported (Fig. 2.8 panel B, ⁹³). We find that Paxillin concentration at the MTJ is nearly abrogated in *laminin* mutants (Fig. 2.8 panel D). This result suggests that Paxillin concentration to the MTJ requires Laminin for its stability and is thus functionally downstream of Laminin.

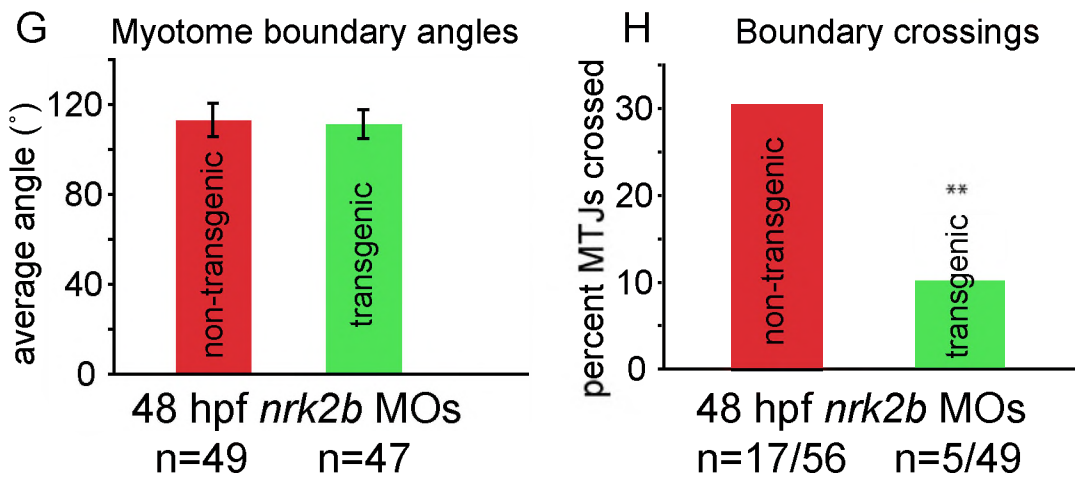
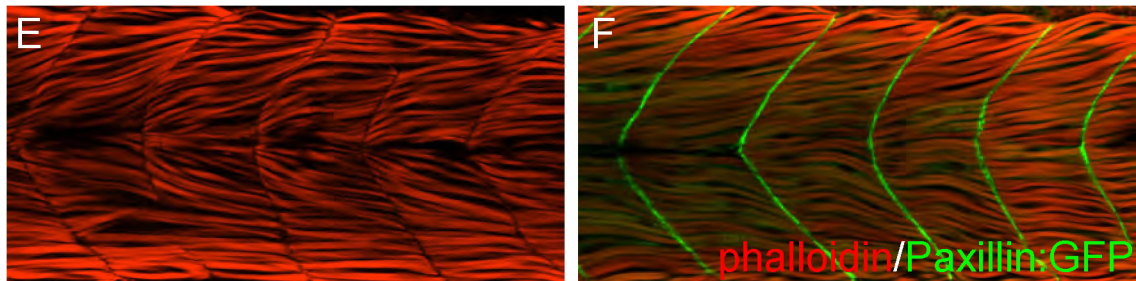
We asked whether overexpression of Paxillin was sufficient to rescue the *nrk2b* morphant phenotype using a transgenic line that ubiquitously over expresses Paxillin:GFP. Paxillin:GFP concentrates robustly at MTJs in control transgenic embryos and Paxillin overexpression does not disrupt early development (data not shown). Interestingly, Paxillin:GFP also robustly concentrates at MTJs in transgenic embryos injected with *nrk2b* MOs. Overexpression of Paxillin:GFP did not significantly decrease wider MTJ angles in *nrk2b* morphants (Fig. 2.8 panel G, Student t-test, $p = 0.17$). However, overexpression of Paxillin:GFP did significantly reduce the percentage of MTJs crossed by muscle fibers in *nrk2b* morphants (Fig. 2.8 panel H, Student t-test, $p < 0.01$). These data indicate that MTJ angle and MTJ integrity can be uncoupled. Furthermore, these data implicate Paxillin as a major regulator of boundary capture *in vivo*. Whether rescue of the *nrk2b* morphant phenotype by Paxillin overexpression is

dependent on or independent of changes in NAD^+ concentration remains to be determined.

Fig. 2.8. Paxillin Overexpression Rescues MTJ Integrity in *nrk2b* Morphants. (A–D) Side mount, anterior left, dorsal top, 32 hpf controls (panels A and C) *gup/laminin beta1* mutants (panels B and D) stained with phalloidin (red), beta-Dystroglycan (blue) and Paxillin (green). Note that the Paxillin is severely disrupted in *gup/laminin beta1* mutants, suggesting that adhesion to Laminin plays a role in Paxillin localization. (E–F) Side mount, anterior left, dorsal top, 48 hpf embryos. (E) *nrk2b* morphant. Note that approximately 1/3 of MTJs are crossed by muscle fibers. (F) *nrk2b*-MO-injected Paxillin:GFP transgenic zebrafish. Note that overexpression of Paxillin:GFP greatly reduces the frequency of boundary crossings in *nrk2b* morphants. (G) Graph of myotome boundary angles. Note that overexpression of Paxillin:GFP does not rescue the wider myotome boundary angles observed in *nrk2b* morphants (n of myotome boundary angles measured is on the x-axis). (H) Graph of percentage of MTJs crossed by muscle fibers. Note that overexpression of Paxillin:GFP does significantly rescue boundary crossings in *nrk2b* morphants (n of crossed MTJs over total MTJs analyzed is on the x-axis). Scale bar is 50 μm , **p<0.01.



48 hpf *nrk2b* MOs



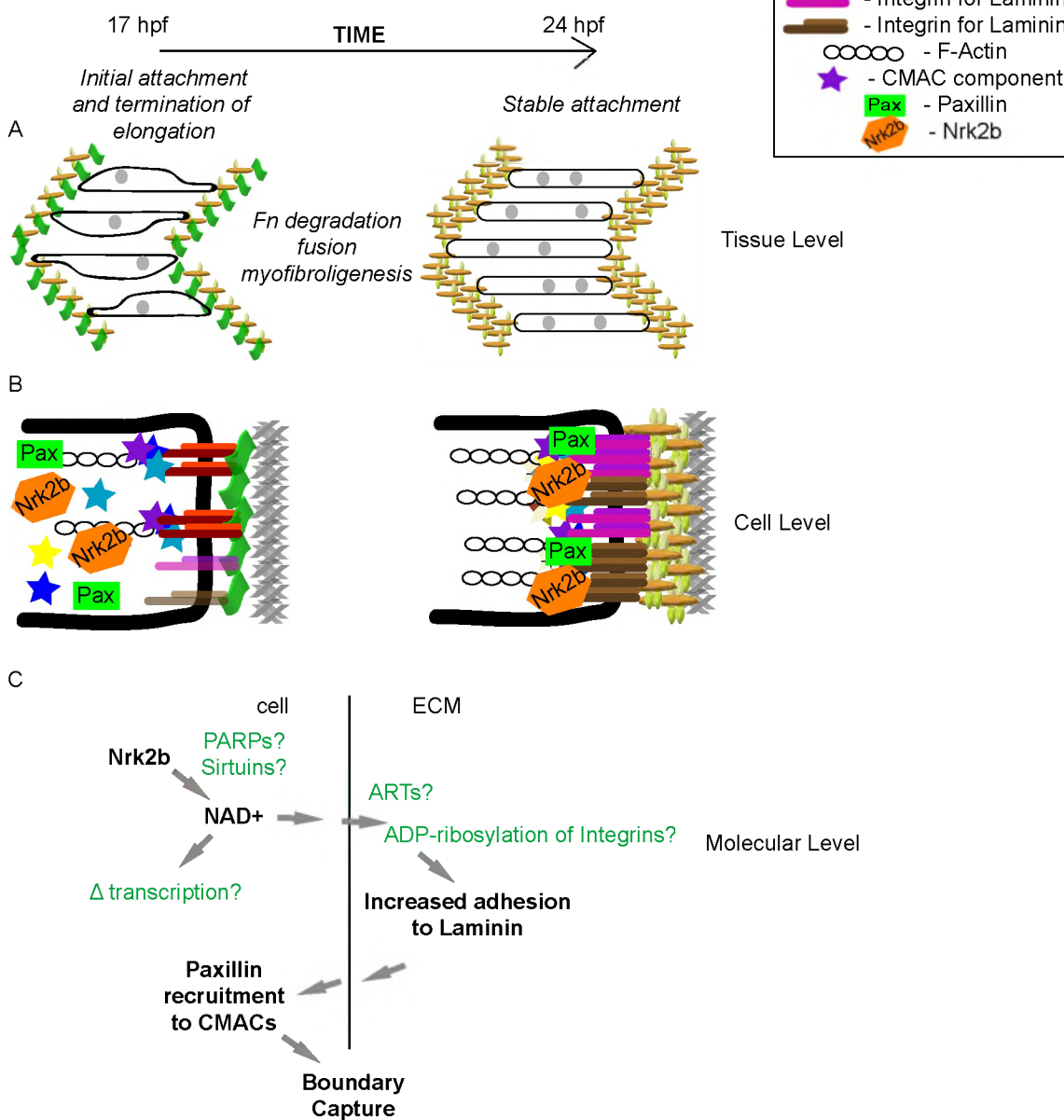
2.5. Discussion

Signaling through cell adhesion complexes not only mediates cell migration and cell shape changes, but also influences all other major cellular functions. Thus, these complexes are best thought of as flexible and dynamic information handling machines (74). Elucidating how adhesion complexes mediate the cellular and molecular mechanisms underlying myotube formation and tendon attachment is critical to understanding musculoskeletal development and the transition to disease states. We show that a novel protein, Nr2f1, is required for muscle development *in vivo*. Importantly, we identify Nr2f1 functions at the tissue and cellular levels (Fig. 2.9). Nr2f1 is required for normal basement membrane assembly at the MTJ. In the absence of Nr2f1, MTJs are discontinuous, resulting in abnormally long muscle fibers. Nr2f1 also regulates the molecular composition of CMACs. Nr2f1 is required for normal FAK and beta-Dystroglycan organization at the MTJ and localization of Paxillin to the MTJ is nearly abolished in *nr2f1* morphants. Finally, we show that addition of exogenous NAD⁺ rescues the *nr2f1* morphant phenotype. Multiple lines of evidence suggest that Nr2f1, although little studied, is a highly significant protein with important functions in muscle growth and disease. Microarray analysis of “double muscled” *myostatin* ^{-/-} cows found that *itgb1bp3/nr2f1* is the second most upregulated muscle transcript, second only to troponin T type 1 (85). *nr2f1* transcription is also highly upregulated in alveolar soft-part sarcoma (86), a rare and highly metastatic cancer with poor prognosis. These data do not determine whether *nr2f1* upregulation is a cause or an effect of increased muscle growth/

proliferation. However, they do suggest that *in vivo* functional analysis may identify conserved functions of Nrk2 with therapeutic relevance.

Fig. 2.9. Roles for Cell–Matrix Adhesion during Muscle Morphogenesis. (A) Cartoon of steps involved in muscle morphogenesis between 17 hpf and 24 hpf at the tissue level. During this time, myotube shape becomes more regular, fusion occurs, Fn is degraded, and Laminin polymerization increases. (B) Cartoon of CMAC formation and the modulation of the specificity of CMACs between 17 hpf and 24 hpf. Note the increase in cell–matrix adhesion complex formation. (C) Cartoon of hypothesized molecular level events during muscle morphogenesis involving Nrk2b and NAD⁺. Speculative interactions are in green lettering. NAD⁺ is an obligatory substrate for enzymes such as poly-ADP-ribose polymerases (PARPs), and Sirtuins. Ecto-mono-ADP-ribosyltransferases (ARTs) are hypothesized to ADP-ribosylate Integrins, increasing their binding affinity for Laminin in an irreversible reaction. NAD⁺ is also believed to modulate gene transcription via regulation of Sirtuin activity. Increased adhesion to Laminin can promote Paxillin recruitment to CMACs. Paxillin, in turn, mediates boundary capture and termination of muscle cell elongation.

“Inside-out” and “Outside-in” signaling comprise a positive feedback loop that reinforces and stabilizes muscle fiber-myotendinous junction adhesion



2.5.1. A Novel Morphogenetic Role for NAD⁺

NAD⁺ is a ubiquitous coenzyme best known for its role in metabolic electron transfer reactions, but is also a critical coenzyme for many different reactions. For

example, NAD⁺ is an obligatory substrate in ADP-ribosylation reactions that influence processes ranging from DNA repair to cell signaling and adhesion (¹⁰⁶⁻¹¹²). Although recent data have identified a novel NAD(H) binding protein that links metabolic cues with cell cycle regulation, roles for NAD⁺ during morphogenesis have not been identified. We show that NAD⁺ regulates muscle morphogenesis. It was traditionally thought that the only mechanism for NAD⁺ synthesis was *de novo* synthesis from amino acids. Within the last decade, however, an alternative salvage pathway that generates NAD⁺ has been identified (⁷¹). This pathway involves salvage of Nicotinic acid, Nicotinamide, or Nicotinamide Riboside (^{72,88}). Nicotinamide riboside kinases, Nrks, phosphorylate Nicotinamide Riboside, a critical step towards NAD⁺ synthesis. The question that remains, however, is how NAD⁺ regulates morphogenesis. Because a role for NAD⁺ during morphogenesis has not previously been shown, we can only speculate. We hypothesize that Nrk2b post-translationally promotes basement membrane assembly by providing a local source of NAD⁺ used to ADP-ribosylate Integrins (for discussion of the alternative hypothesis that Nrk2b regulates basement membranes through its Integrin binding function, see Section 4.1). ART1 is an ecto-mono-ADP-ribosyltransferase that ADP-ribosylates Integrin alpha7 at multiple sites, depending upon NAD⁺ concentration (^{113,114}). This ADP-ribosylation by ART1 is not readily reversible and leads to an increased Laminin-binding affinity of Integrin alpha7beta1 in differentiated myotubes. Given that NAD⁺ is an obligatory substrate in ADP-ribosylation reactions, the authors hypothesized that Integrin alpha7 ADP-ribosylation might be a protective mechanism that increases Integrin alpha7beta1 adhesion to Laminin when the sarcolemma has been

compromised and intracellular NAD⁺ leaks into the extracellular space. However, it is also possible that Integrin ADP-ribosylation and the subsequent increased affinity for Laminin is a morphogenetic mechanism that promotes basement membrane polymerization. We have identified two ART1 orthologs expressed in developing zebrafish skeletal muscle (unpublished data). Preliminary data indicate that expression of these ARTs is NrK2b dependent, they are required for basement membrane assembly, and act within the same pathway as NrK2b (Peterson and Henry, unpublished data). Thus, one interesting avenue of research is development of fluorescent tools that would allow visualization of ADP-ribosylation and basement membrane assembly *in vivo*. This model is clearly very speculative. However, two recent findings establish some precedent for compartmentalized NAD⁺ usage and NAD⁺-dependent enzymes in morphogenesis. Transgenic Arabidopsis expressing reporter constructs for three NAD⁺ kinases, or NADKs, show tissue-specific expression (¹¹⁵). Expression of GFP-tagged versions of the NADKs in suspension cultures showed that one of the three localized to the peroxisomal matrix (¹¹⁵). These data suggest that localized NAD⁺ usage may play roles in plant development and/or physiology. Data that potentially implicate NAD⁺ in morphogenesis were obtained by identifying a potential locus underlying isolated congenital nail clubbing (ICNC). ICNC is a rare autosomal recessive disorder characterized by abnormal connective tissue growth and matrix that lead to enlargement of digit terminal segments (¹¹⁶). In one large Pakistani family, a nonsense mutation in the gene encoding NAD⁺-dependent 15-hydroxyprostaglandin dehydrogenase is thought to underlie ICNC (¹¹⁶). Taken together, our findings implicating NAD⁺ in morphogenesis, as well as clear roles

for NAD⁺ in modulating Integrin affinity for Laminin in cell culture, localized usage of NAD⁺ in Arabidopsis, and roles for a NAD⁺-dependent enzyme in a connective tissue disease all suggest that NAD⁺ may be a little recognized yet important morphogenetic mediator.

2.5.2. Dynamic Reciprocity and Musculoskeletal Homeostasis

Adhesion of muscle cells to the surrounding basement membrane is one of the most important aspects of musculoskeletal structure. When genes whose protein products are involved in muscle cell-basement membrane adhesion are mutated, myopathies can occur. Zebrafish models of muscular dystrophies have both validated the model and provided novel insights into pathogenesis (^{59,65,92,117-121}). One important insight is that the MTJ is a major site of failure in *sapje/dystrophin* mutants (⁶⁵). It has also recently been shown that muscle fibers detach from the basement membrane at the MTJ prior to membrane disruption and apoptosis in *laminin alpha2* mutants (⁵⁹), *laminin beta2* mutants (²¹), and *dystroglycan* mutants (¹²²). One less appreciated but critically important aspect of musculoskeletal homeostasis is initial MTJ morphogenesis. Multiple studies have shown that disruption of ECM at the MTJ can result in the formation of aberrant and discontinuous MTJs (^{60,103,123,124}). In this study, we elucidate some of the underlying mechanisms that govern ECM remodeling and allow cells to integrate signaling and differentiation with the structure of their local microenvironment. This dynamic, bidirectional relationship between cells and their local ECM environment mediate basement membrane assembly at the MTJ and reinforces muscle fiber-MTJ adhesion. We

show that Nr2b plays a critical role in basement membrane assembly. This is a novel mechanism of “inside-out” signaling. We also show that Laminin itself is critical for recruitment of Paxillin to cell–matrix adhesion complexes at the MTJ — “outside-in” signaling. Overexpression of Paxillin:GFP promotes boundary capture and termination of muscle fiber elongation, representing another example of “inside-out” signaling. These results provide a mechanistic framework for future studies investigating the positive feedback loop between cells and their matrix that reinforces and stabilizes muscle fiber-MTJ adhesion.

2.5.3. Nr2b and Specificity of Cell Adhesion Function

Although it is not known how CMACs regulate disparate cellular processes such as motility, stable adhesion, proliferation, survival and invasion, it is likely that changes in their size, localization, stability and molecular composition mediate different cellular outputs. Recent advances in imaging technology (fluorescent speckle microscopy, spatio-temporal image correlation spectroscopy) have allowed new insights into the CMAC to F-actin linkage *in vitro* (74). However, analysis of the molecular composition and size of CMACs during development is difficult, if not impossible. Analysis of the phenotypes of mice, *Xenopus* and zebrafish deficient for different CMAC components has increased understanding of CMAC function during development. These studies show that one mechanism contributing to CMAC functional specificity is tissue-restricted expression of CMAC components. But what about a CMAC component such as Paxillin, which is ubiquitously expressed during zebrafish development (58)? How is Paxillin function

within CMACs modulated in different contexts? Here, we provide one paradigm by which specificity can be achieved. We show that *nrk2b* is expressed in axial skeletal muscle and is required for Paxillin localization to MTJ CMACs. Interestingly, we also provide evidence that Nr2b-mediated Paxillin concentration is modulated in a cell autonomous fashion. To our knowledge, this is the first mechanistic understanding of cell autonomous CMAC molecular composition regulation *in vivo*. Our data do not indicate whether Nr2b is required for Paxillin recruitment or retention/stabilization of Paxillin at MTJs. Given the absolutely critical role of Paxillin in mediating cell adhesion and migration *in vitro* (¹²⁵), it is perhaps not surprising that Paxillin localization to the MTJ can be modulated in a tissue-specific manner. Importantly, the fact that Nr2b was shown to regulate the protein level and tyrosine phosphorylation of Paxillin in C2C12 myoblasts (⁶⁹) suggests some conservation of Nr2b function. Thus, an *in vivo* model of Nr2b function may provide relevant insights into human health and disease.

Basement membranes, primarily composed of Laminin, are specialized compartments within the ECM that provide mechanical support and regulate multiple cellular activities. Laminins are heterotrimeric proteins composed of an alpha, beta and gamma chain. It is thought that once assembled, most Laminins polymerize via interactions between the three N-terminal short arms (¹²⁶). The mechanisms that regulate Laminin polymerization *in vivo* are not well understood. We show that despite normal/increased levels of *laminin* chain transcription, the MTJ basement membrane is significantly disorganized in *nrk2b* morphants. The fact that *nrk2b* morphant cells in control hosts are unable to induce basement membrane defects indicates that basement

membrane assembly at the MTJ is a community-mediated phenomenon. This result suggests that the basement membrane is not disorganized because of unusually high degradation in *nrk2b* morphants. If Nrk2b deficiency results in increased matrix proteolysis, one would predict that large cohorts of Nrk2b-deficient cells in control hosts would be sufficient to induce basement membrane disruption. Thus, taken together, these data suggest that Nrk2b is a novel regulator of basement membrane assembly during early MTJ morphogenesis.

2.5.4. Paxillin at the MTJ is Not Required for Subcellular Localization of FAK to the MTJ

Paxillin and FAK were among the first identified focal adhesion proteins and, as such, the focus of thousands of studies elucidating their molecular structure and function. FAK has a central kinase domain and a C-terminal domain that targets FAK to focal adhesions. Paxillin is a scaffolding protein replete with protein–protein binding domains: SH2 and SH3 domain binding sites, four C-terminal LIM domains, and five N-terminal LD motifs (¹²⁵). Paxillin and FAK directly interact and FAK phosphorylation and localization to focal adhesions are reduced in *paxillin* *-/-* cells (^{127,128}). LD motifs 2 and 4 of Paxillin bind to the alpha-helix 1/4 and alpha-helix 2/3 Paxillin-binding sites within the Focal Adhesion Targeting (FAT) domain of FAK (¹²⁹⁻¹³¹). A recent *in vitro* study analyzed the function of these two Paxillin-binding sites within FAK. In the absence of both sites, only about 10% of FAK localizes to focal adhesions. The presence of either Paxillin-binding site is sufficient for FAK targeting to focal adhesions. However, both

Paxillin-binding sites are necessary for maximal FAK activation and phosphorylation of downstream substrates (¹³²). Given these *in vitro* data, it is curious that FAK phosphorylation and concentration at the MTJ are not more disrupted in *nrk2b* morphants that show disrupted Paxillin. In this regard, there is evidence from *in vitro* studies that secondary mechanisms for FAK subcellular localization may exist. Notably, although glutamic acid 997 of FAK does not normally play a role in FAK localization to focal adhesions, this residue is required for FAK localization to focal adhesions when FAK binding to Paxillin is abrogated (¹³²). Thus, it is possible that within the complex *in vivo* environment, there are multiple mechanisms mediating FAK concentration at CMACs. Alternatively, it is possible that FAK at the MTJ is primarily localized to the Dystrophin-Glycoprotein Complex (DGC) that also anchors the intracellular cytoskeleton to Laminin in the ECM. Far less is known about dynamics of DGC assembly and it is not known if Paxillin is required for FAK recruitment to DGC based adhesions. Regardless, our data show that normal Paxillin localization is not required for robust concentration of FAK to CMACs at the MTJ *in vivo*.

2.5.5. Quantitative Analysis of Morphogenesis

The ability to quantify phenotypes is critical when investigating development or disease. A mathematical approach facilitates both an understanding of experimental/developmental variability and also aids in identifying subtle differences that could otherwise be construed as noise (¹³³). For example, morphometric analyses determined that adult zebrafish haploinsufficient for *Fgf8* have craniofacial defects (¹³⁴). The authors

posit that one approach to identifying later developmental roles for homozygous lethal mutations is to quantitatively analyze morphogenesis in heterozygous embryos. Quantification is also important for comparing the efficacy of different treatments in animal models of disease. Towards this end, the minimal “Feret's diameter” has been identified as an excellent tool for reliable measure of fiber size in *mdx* $-/-$ mice (135). Multiple laboratories have developed excellent methodologies for quantification of morphogenesis (136,137). In this manuscript, we used the 2D WTMM method (60,97,98,103) to characterize the anisotropic signature (order/structure) of muscle architecture. Use of the 2D WTMM formalism showed that the basement membrane at the MTJ is significantly less organized in *nrk2b* morphants than in control or *dystroglycan* morphants. Importantly, however, we also showed that the 2D WTMM can be invaluable in parsing out subtle differences in CMAC organization. Although recruitment of both pY FAK and beta-Dystroglycan to the MTJ appears normal in *nrk2b* morphants, there is a significant difference in CMAC organization.

2.6. Chapter Conclusions

Zebrafish axial muscle development is an ideal paradigm for quantitatively integrating functions for cell adhesion in morphogenesis. We show that *Nrk2b* and NAD^+ regulate basement membrane assembly and boundary capture at the MTJ, regulate Paxillin concentration at the MTJ, and exogenous Paxillin expression is sufficient to rescue boundary capture in *nrk2b* morphants. Thus, we have identified novel roles for NAD^+ during morphogenesis and for Paxillin during boundary capture *in vivo*. Taken

together, these data provide novel insight into contributions of cell adhesion to morphogenesis.

CHAPTER 3

NAD⁺ AMELIORATES MUSCULAR DYSTROPHY IN ZEBRAFISH

3.1. Chapter Abstract

Muscular dystrophies are common, currently incurable diseases. A subset of dystrophies result from genetic disruptions in complexes that attach muscle fibers to their surrounding extracellular matrix microenvironment. Cell-matrix adhesions are exquisite sensors of physiological conditions and mediate responses that allow cells to adapt to changing conditions. Thus, one approach towards finding targets for future therapeutic applications is to identify cell adhesion pathways that mediate these dynamic, adaptive responses *in vivo*. We find that NAD⁺, which functions as a small molecule agonist of muscle fiber-extracellular matrix adhesion, corrects dystrophic phenotypes in zebrafish lacking either a primary component of the Dystrophin-glycoprotein complex or Integrin alpha7. Exogenous NAD⁺ or a vitamin precursor to NAD⁺ reduce muscle fiber degeneration and result in significantly faster escape responses in dystrophic embryos. Overexpression of Paxillin, an intracellular, Integrin-associated protein, reduces muscle degeneration in zebrafish with intact Integrin receptors but does not improve motility. NAD⁺ and Paxillin significantly increase organization of Laminin, a major component of the extracellular matrix basement membrane. Our results indicate that the primary protective effects of NAD⁺ result from changes to the basement membrane, as a wild-type basement membrane is sufficient to increase resilience of dystrophic muscle fibers to damage. The surprising result that NAD⁺ supplementation ameliorates dystrophy in Dystrophin-glycoprotein complex- or Integrin alpha7-deficient zebrafish suggests the

existence of an additional Laminin receptor complex that anchors muscle fibers to the basement membrane. We identify this receptor as Integrin alpha6, but show that either Integrin alpha7 or the Dystrophin-glycoprotein complex are required in conjunction with Integrin alpha6 to reduce muscle degeneration. Taken together, these results define a novel cell adhesion pathway that may have future therapeutic relevance for a broad spectrum of muscular dystrophies.

3.2. Introduction

The extracellular matrix (ECM) connects to the intracellular actin cytoskeleton via transmembrane receptor complexes. These adhesion complexes not only serve as scaffolds for tissue architecture, but also function as sensors of physiological change and signal transduction hubs. Thus, adhesion complexes facilitate cell adaptation to changing conditions during development, aging, injury response, and disease. Perhaps not surprisingly, the onset and progression of many diseases is affected by disrupted cell-ECM interactions. Despite the fact that modulating cell-ECM adhesion could be exploited for therapeutic purposes, the dynamic regulation of cell-ECM adhesion *in vivo* is not well understood.

Muscles and tendons function as an integrated unit to transduce force to the skeletal system and stabilize joints. Cell-ECM adhesions mechanically link muscles to tendons and are required for muscle physiology and homeostasis. Many muscle diseases, such as Duchenne, Becker, Merosin-deficient muscular dystrophies and congenital muscular dystrophy (CMD) with Integrin deficiency, result from mutations that disrupt adhesion of muscle fibers to their surrounding basement membrane (BM), a substructure within the

ECM. This weakened link between muscle fibers and the BM results in increased susceptibility to fiber damage and death during repeated cycles of contraction and relaxation. Due to the continuous bidirectional communication between cells and their surrounding BM, muscle atrophy is also accompanied by degeneration of the ECM microenvironment⁽¹³⁾. As the BM also provides support for satellite cells that mediate muscle repair, augmenting the BM is a potential strategy to improve muscle structure and regenerative capacity^(14,15,21).

Muscle fibers are known to utilize two receptor complexes to adhere to Laminin in the BM, the Dystrophin-glycoprotein complex (DGC) and Integrin alpha7beta1 heterodimers. Disruption of components in either complex can lead to muscle disease. Dystroglycan (UniProtKB accession number Q8JHU7_DANRE) is a major component of the DGC and consists of two subunits (alpha and beta) transcribed from the same locus, *DAG1*⁽¹³⁸⁾. Beta-Dystroglycan is a transmembrane subunit that indirectly links to the intracellular cytoskeleton, and alpha-Dystroglycan binds to Laminin and again in the BM⁽¹³⁹⁻¹⁴¹⁾. Humans with mutations in *DAG1* have cognitive impairment and mild myopathy^(142,143). Alpha-Dystroglycan is heavily glycosylated and these post-translational modifications are critical for binding of alpha-Dystroglycan to BM ligands and BM deposition^(139,144). Mutations in six genes required for normal glycosylation of alpha-Dystroglycan have been identified thus far and the resultant diseases are commonly referred to as the dystroglycanopathies (reviewed in¹⁴⁵). These diseases show a wide clinical spectrum with only modest correlation between genotype and clinical phenotype^(145,146). Screening patient populations suggests that there are as yet unidentified genes

involved in dystroglycanopathies (¹⁴⁷). There are zebrafish orthologues of all six dystroglycanopathy genes (^{49,148}). Morpholinos (MOs) against two of these genes have been characterized and both lead to muscle degeneration (Fukutin related protein QOPIP5_DANRE, LARGE 2 LARG2_DANRE) (^{122,148}). Thus, the zebrafish system may provide a genetically and embryologically accessible model to complement investigations in mammalian model systems.

Both the DGC and Integrin alpha7beta1 heterodimers contribute to force production in mouse muscle, but only the DGC is required to maintain the attachment between the muscle cell membrane (sarcolemma) and the surrounding BM during lengthening contractions (¹⁴⁹). Integrin alpha7 (E7FGC7_DANRE), in contrast, functions primarily at MTJs (^{150,151}). Despite their differing roles in sarcolemma-BM attachment, these two receptor complexes can partially compensate for one another (^{41,43,44}) and mutations in components of both receptor complexes greatly exacerbate the extent of muscle atrophy in mice (^{36,37}). These data suggest that dynamic cell-ECM signaling mediates adaptive responses when normal muscle architecture is perturbed. Thus, one therapeutic approach is to enhance the intrinsic compensatory relationships between cell adhesion proteins and their ECM microenvironment by potentiating the adhesion of the alternate complex to the BM.

Vertebrate muscle is derived from somites, segmentally reiterated structures delineated by the formation of somite boundaries. As development proceeds, a subset of somitic cells generate muscle and the somite boundary gives rise to the myotendinous junction (MTJ), which is the major site of force transmission from muscle to the skeletal

system. In zebrafish, elongation of fast-twitch muscle fibers and their subsequent attachment to the MTJ correlates with an increase in Laminin polymerization at the MTJ⁽⁶⁰⁾. We have identified a novel cell adhesion pathway required for Laminin polymerization at the MTJ *in vivo*. We found that Nicotinamide riboside kinase 2b (NrK2b Q7ZUR6_DANRE) and NAD⁺ potentiate Laminin polymerization and subcellular localization of Paxillin (Q6R3L1_DANRE), an Integrin-associated adaptor protein⁽¹⁵²⁾. Yeast and human Nrks function in an alternative salvage pathway that generates Nicotinamide Adenine Dinucleotide (NAD⁺)^(71,72). Exogenous NAD⁺ rescues MTJ morphogenesis in NrK2b-deficient zebrafish embryos. Our previous results showing a requirement for NrK2b and NAD⁺ in initial BM morphogenesis led us to hypothesize that activation of the NrK2b pathway, either through chemical (NAD⁺ supplementation) or gene therapy (Paxillin overexpression) approaches, would be sufficient to activate the intrinsic compensation between cell-ECM adhesion proteins and result in a novel method of BM augmentation. Herein we will investigate whether the NrK2b pathway can be exploited to augment Laminin polymerization and thus improve muscle tissue structure and function in dystrophic embryos.

Zebrafish deficient for *Dag1* display progressive muscle atrophy⁽⁹²⁾. Here, we show that muscle atrophy is preceded by degeneration of the MTJ BM. As we previously showed that NrK2b is necessary for MTJ BM organization during development, we hypothesized that exogenous NAD⁺ would improve MTJ BM organization in *dag1* morphants. Indeed, supplementation of *dag1* morphants with NAD⁺ or a vitamin precursor of NAD⁺ significantly improved muscle structure. Muscle function was also

improved: NAD⁺- or Emergen-C-supplemented *dag1* morphants swam faster after a touch stimulus. Nr2 interacts with the cytoplasmic tail of Integrin beta1 in the Integrin alpha7beta1 complex (⁶⁹). Surprisingly, exogenous NAD⁺ reduced muscle degeneration in *integrin alpha7 (itga7)* morphants, indicating that Itga7 is not the only Integrin in the Nr2b pathway. We find that the mechanism of action of zebrafish Nr2b involves a different Integrin receptor for Laminin, Integrin alpha6 (Itga6 A8WHQ8_DANRE). The intracellular cell-ECM adhesion protein Paxillin is downstream of NAD⁺ during MTJ development (¹⁵²). Paxillin overexpression was sufficient to improve Laminin organization and significantly reduce muscle defects in *dag1* morphants. Taken together, these results suggest manipulation of NAD⁺ precursors/biosynthetic enzymes and Paxillin as new potential therapeutic approaches for treatment of not only muscle diseases, but also diseases/syndromes that affect Laminin integrity.

3.3. Materials and Methods

3.3.1. Zebrafish Husbandry/Mutant/Transgenic Lines

Embryos were obtained from natural spawnings of zebrafish kept on a 16 hour light/8 hour dark cycle. Embryos were kept at 28.5°C in ERM and staged according to (⁹⁰). Embryos stably overexpressing Paxillin fused to GFP were obtained from pairwise spawnings of carriers from the F1 generation of the *Tg:paxillin:GFP* line described in (¹⁵²). *wi390/laminin gamma1*^{-/-} embryos (¹⁵³) were obtained from natural spawnings of identified heterozygotes.

3.3.2. Morpholino Injection

Stable antisense MO oligonucleotides were obtained from Gene Tools, LLC and hydrated with sterile water to form 1 mM stocks. The *dag1* translation-blocking MO sequence has been published (⁹²) and 12.5 ng was injected per embryo. A splice blocking *itga7* MO has been described (¹¹⁹) and 12.5 ng was injected per embryo. In our hands the phenotype was subtle and dystrophy varied between biological replicates. Two *itga6* translation-blocking MOs had the following sequences: MO1 5'-AGCTCCATTGCCTGAAATGAATG-3' and MO2 5'-CTGTTGTATGAAAATATAGCCCTT-3'. These two MOs were co-injected so that embryos received 9 ng MO1 and 8 ng MO2. The Gene Tools standard control MO sequence is: 5'-CCTCTTACCTCAGTTACAAGGGATA-3'. 17 ng of control MO was injected as a control for *itga6* MO injections. The *p53* MO sequence is: 5'-CCCTTGCGAACTTACATCAAATTCT-3'. *p53* MO was co-injected 1:1 with *itga6* MOs. MOs were injected into the yolk of 1-2 cell stage embryos using a MPPI-2 pressure injector from ASI. For experiments where Paxillin:GFP transgenic and wild-type zebrafish were injected with *dag1*, *itga7* or *itga6* MOs, embryos from separate spawnings of each line were combined prior to injection and separated during imaging based on GFP fluorescence.

3.3.3. NAD⁺ and Emergen-C Treatment

Beta-NAD (10 mg aliquots, Sigma, stored at -20°C) were dissolved to 15 mM stocks in ERM. Twenty five embryos per 60 mm Petri dish were grown in 5 mL of ERM with a final concentration of either 0 or 0.1 mM NAD. Embryos were treated from shield

stage (6 hpf) through live imaging/fixation and the media were made fresh and changed every 24 hours. A new aliquot was used for each change of the NAD-containing media. Emergen-C (original formula, registered trademark of Alacer Corporation) supplementation followed the above protocol. Emergen-C powder was dissolved in ERM such that the final concentration of niacin that embryos were exposed to was 6.77 micromolar. This concentration was chosen because it is roughly equivalent to what the concentration of niacin would be in an adult human bloodstream after consuming the contents of one Emergen-C packet (assuming 6 L of blood volume).

3.3.4. Phalloidin Staining and Immunohistochemistry

Embryos were fixed using 4% paraformaldehyde for four hours at room temperature or overnight at 4°C. Embryos were washed out of 4% paraformaldehyde at least three times with Phosphate Buffered Saline-0.1% Tween20 (PBS-0.1%Tw). Prior to phalloidin staining, embryos were permeabilized for 1.5 hours at room temperature with PBS-2%Triton. Embryos were incubated in Alexa fluor 488 or 546 phalloidin (Molecular Probes) at a 1:20 dilution overnight at 4°C. Antibody staining followed phalloidin staining or began with an incubation in block (5% w/v Bovine Serum Albumin in PBS-Tw) for at least one hour at room temperature. Embryos were incubated in primary antibody overnight at 4°C, washed in block for two to eight hours at room temperature, and then incubated in secondary antibody overnight at 4°C. Embryos were washed in PBS-0.1%Tw prior to imaging. Primary antibodies: polyclonal anti-Laminin-111 (Thermo Scientific, 1:50 dilution in block), monoclonal anti-Paxillin (BD

Biosciences, 1:50 dilution in block). Secondary antibodies: GAM/GAR 488, 546, 633 (Invitrogen, 1:200 dilution in block).

3.3.5. Genetic Mosaic Analysis

Embryos (1-2 cell stage) were injected with *dag1* MOs and 10,000 MW dextrans (Molecular Probes). Morphant cells were removed at the sphere stage and transplanted into unlabeled control hosts. Hosts were grown to the appropriate stage, fixed and stained with phalloidin.

3.3.6. Westerns

Immunodetection of Paxillin was conducted using preparations from 2 dpf embryos as previously described (¹⁵²). Protein concentration was quantified using a Nanodrop spectrophotometer and sample concentrations were normalized prior to loading. Band intensities were quantified in NIH Image J (<http://lukemiller.org/journal/2007/08/quantifying-western-blot-without.html>).

3.3.7. *In Situ* Hybridization

ISHs were done as previously described (¹⁵²) with serial washes into and out of 2X SSC occurring before incubation in anti-digoxigenin antibody.

3.3.8. Two-Dimensional Wavelet Transform Modulus Maxima

This rigorous and objective method of image quantification was applied as previously described in (^{103,152}).

3.3.9. Motility Assay

Two concentric circles were drawn on an overhead projector transparency. The inner circle with a diameter of 5 mm and the outer circle with a diameter of 10 mm. A 60

mm Petri dish containing ERM was placed on top of the concentric circles. An embryo was placed in the Petri dish and aligned to the middle of the inner circle. A video was recorded (see Imaging section below) of each embryo being poked with the end of fishing wire and the time that it took for the embryo to leave the field of view was documented. Embryos with abnormal escape responses were poked multiple times and the most robust escape response was recorded and used for analysis. For comparison of average escape response time between groups, embryos that were unable to exit the field of view were assigned a time value equal to that of the slowest embryo within an experiment that could exit the field of view (the value was determined after biological replicates of the same experiment had been combined).

3.3.10. Imaging

Images were collected and processed as described in ⁽¹⁵²⁾. Videos were acquired on a Zeiss Discovery.V12 microscope with a high-speed digital camera.

3.3.11. Statistical Analyses

Error is reported as standard error of the mean and significance was calculated using two-tailed, paired, student t-tests with $p < 0.05$ being considered significant.

3.3.12. Measuring Myotome Boundary Angles

Early MTJ morphogenesis was assayed through MTJ angle measurements as previously described in ⁽¹⁵²⁾.

3.3.13. Electron Microscopy

Transmission electron microscopy was performed by Dr. Bryan D. Crawford, University of Fredericton, New Brunswick. Samples were fixed in Karnovsky's fixative

(2% paraformaldehyde from 16% stock, 2.5% glutaraldehyde from 25% stock, 5% sucrose, and 0.1% CaCl₂ in 0.1 M cacodylate buffer (from 0.2 M cacodylate stock at pH 7.2)). Embryos in Karnovsky's fixative were shipped to the University of Fredericton, New Brunswick where they were post-fixed in osmium, dehydrated, embedded, sectioned (70 nm), stained and imaged.

3.4. Results

3.4.1. NAD⁺ Supplementation Reduces Muscle Degeneration in *dystroglycan*

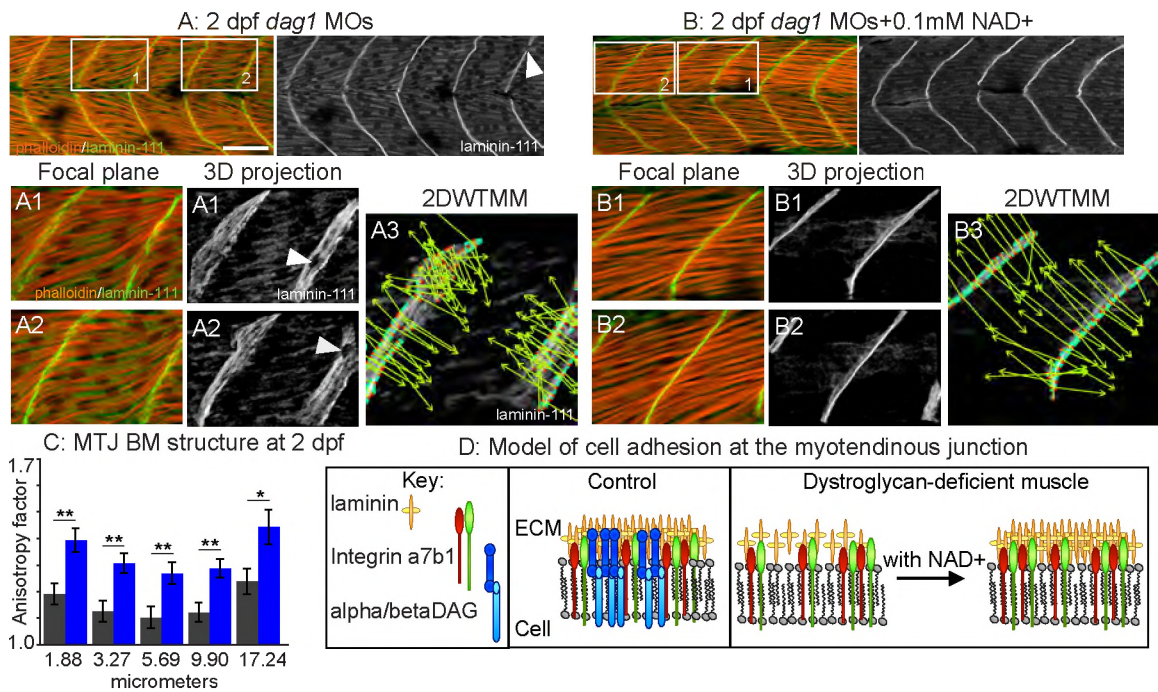
Morphants

Dystroglycan null mice die around the time of implantation ⁽³¹⁾. In contrast, zebrafish *dag1* is maternally expressed, *Dag1*-deficient zebrafish gastrulate and initial muscle fiber development is normal ⁽⁹²⁾. Staining for Laminin-111 in the ECM microenvironment of *Dag1*-deficient zebrafish muscle showed that initial BM development is also normal at 1 day post fertilization (dpf) ⁽¹⁵²⁾. At this point in time, Laminin-111 is thought to be the major Laminin heterotrimer present ⁽⁶¹⁾. Given the critical role of the ECM microenvironment in maintaining fiber integrity, we asked whether the MTJ BM degenerates over time. Although Laminin concentrated at the MTJ BM in 2 dpf *dag1* morphants, staining intensity was variable (white arrowhead, Fig. 3.1 panel A). 3D reconstruction of Laminin-111 highlighted inconsistencies in the MTJ BM in *dag1* morphants (Fig. 3.1 panels A1-A2, white arrowheads show holes in the MTJ BM). Because we have shown that *Nrk2b* is *necessary* for normal organization of the MTJ BM at 1 dpf, we asked whether exogenous NAD⁺ would be *sufficient* to improve MTJ BM structure at 2 dpf in *dag1* morphants. Qualitatively, MTJ BM structure appeared

to be better aligned in the medial-lateral dimension in *dag1* morphants supplemented with NAD⁺ compared to untreated *dag1* morphants (Fig. 3.1 panel B, Laminin-111 panels). To quantify these observations, we used a mathematical formalism, the 2DWTMM (^{97,98,103,152}), to interrogate MTJ BM structure. The MTJ BM was significantly more organized in NAD⁺-supplemented *dag1* morphants compared to untreated morphants. This increased organization is visually represented by the parallel alignment of vectors oriented in the direction of the maximal intensity gradient (Fig. 3.1 panels A3, B3). The anisotropy factor (a readout of organization) is derived from the sum of the vectors and is significantly higher in NAD⁺-supplemented *dag1* morphants (Fig. 3.1 panel C, **p < 0.01, *p<0.05). Therefore, NAD⁺ supplementation increases organization of the BM in *dag1* morphants.

It is not known if detachment of muscle fibers from the MTJ BM contributes to human muscular dystrophies because biopsies are excised from the musculature to avoid injury to the tendon, but MRI studies do suggest that muscle damage is more severe closer to the MTJ (^{66,67}). In dystrophic zebrafish, muscle fibers detach from the MTJ prior to apoptosis in *laminin alpha2* (⁵⁹), *laminin beta2* (²¹), and *dag1* mutants (¹²²), implicating failure of muscle fiber-MTJ adhesion as the primary etiology in these models of muscular dystrophy. We hypothesized that the increased organization of the MTJ BM in NAD⁺-supplemented *Dag1*-deficient zebrafish would reduce the frequency of muscle fiber detachment. The ordered array of myofibers in wild-type skeletal muscle results in birefringence of polarized light (¹⁵⁴). Muscle degeneration in *dag1* morphants results in gaps in birefringence (Fig. 3.2 panel A, white arrowheads). Birefringence was improved

Figure 3.1. Exogenous NAD⁺ Improves the Structure of Muscle in *dag1* Morphants. (A-B) Anterior left, dorsal top, side mounted 2 dpf embryos stained for actin (phalloidin, red) and Laminin-111 (green or white). Qualitatively, Laminin-111 antibody staining appears to be within myotomes and less well aligned at the MTJ BM in *dag1* morphants (A) compared to *dag1* morphants treated with 0.1 mM NAD⁺ (B). White boxes in A and B correspond to numbered panels below. White arrowheads indicate holes in the MTJ BM. (A3, B3) 2DWTMM analysis of Laminin-111 stained *dag1* morphants (A3) and NAD⁺-supplemented *dag1* morphants (B3). Maxima nodes are in red, maxima chains are in blue and vectors pointing in the direction of the maximum intensity gradient are in green. Parallel vectors reflect greater organization. (C) Quantification of the anisotropy factor. The anisotropy factor is the sum of the vector angles. A greater anisotropy factor denotes more organization. NAD⁺ treatment of *dag1* morphants (blue bars) significantly increases organization of Laminin-111 compared to *dag1* morphants (gray bars) over multiple size scales, *p<0.05, **p<0.01. (D) Model of the MTJ. Transmembrane receptors, Integrins and the DGC bind extracellular Laminin. In *dag1* morphants, Laminin is less organized at the MTJ BM. Exogenous NAD⁺ improves Laminin organization in the MTJ BM in *Dag1*-deficient zebrafish. Scale bar is 50 micrometers.



in NAD⁺-supplemented *dag1* morphants (Fig. 3.2 panel A). We next used phalloidin staining to visualize detached muscle fibers and quantitatively assess muscle degeneration. The percent of muscle segments per embryo with detached muscle fibers

was significantly reduced in *dag1* morphants supplemented with NAD⁺ compared to untreated *dag1* morphants (Fig. 3.2 panels B-D, white arrowheads indicate detached fibers, **p<0.01). These data show that NAD⁺ is sufficient to improve birefringence and reduce detachment of muscle fibers.

NAD⁺ is synthesized via multiple different pathways. Nrk2 is part of an alternative salvage pathway that mediates NAD⁺ biosynthesis (^{71,72}). In addition, Tryptophan and vitamin B3 (niacin, niacinamide, nicotinamide or nicotinic acid) are NAD⁺ precursors. We next asked whether vitamin supplementation would result in an outcome similar to addition of exogenous NAD⁺. We choose Emergen-C packets for vitamin B3 supplementation because they: (1) are soluble in Embryo Rearing Medium (ERM) and do not disrupt development (data not shown), and (2) contain 5 mg niacin. As shown in Figure 3.2 panel D, addition of Emergen-C significantly reduced muscle degeneration in *dag1* morphants compared to non-supplemented morphants. This result implicates the complex of B vitamins in Emergen-C as potent precursors of NAD⁺ in zebrafish and in promoting muscle health in genetic diseases.

In addition to using the 2DWTMM, polarized light and phalloidin staining assays to visualize and quantify changes in muscle tissue structure, we also utilized transmission electron microscopy. Electron microscopy showed that NAD⁺ supplementation did not affect muscle structure in control embryos (Fig. 3.2 panels E-F), but improved structure in *dag1* morphants. Electron microscopy revealed deficiencies in the MTJ of *dag1* morphant muscle. Abnormal gaps in the MTJ BM were observed (Fig. 3.2 panel G, red

arrows). In NAD⁺-supplemented *dag1* morphants, BM structure was improved (Fig. 3.2 panel H, white arrow).

3.4.2. A Normal MTJ BM Microenvironment is Sufficient to Rescue the Structure of Dystrophic Muscle

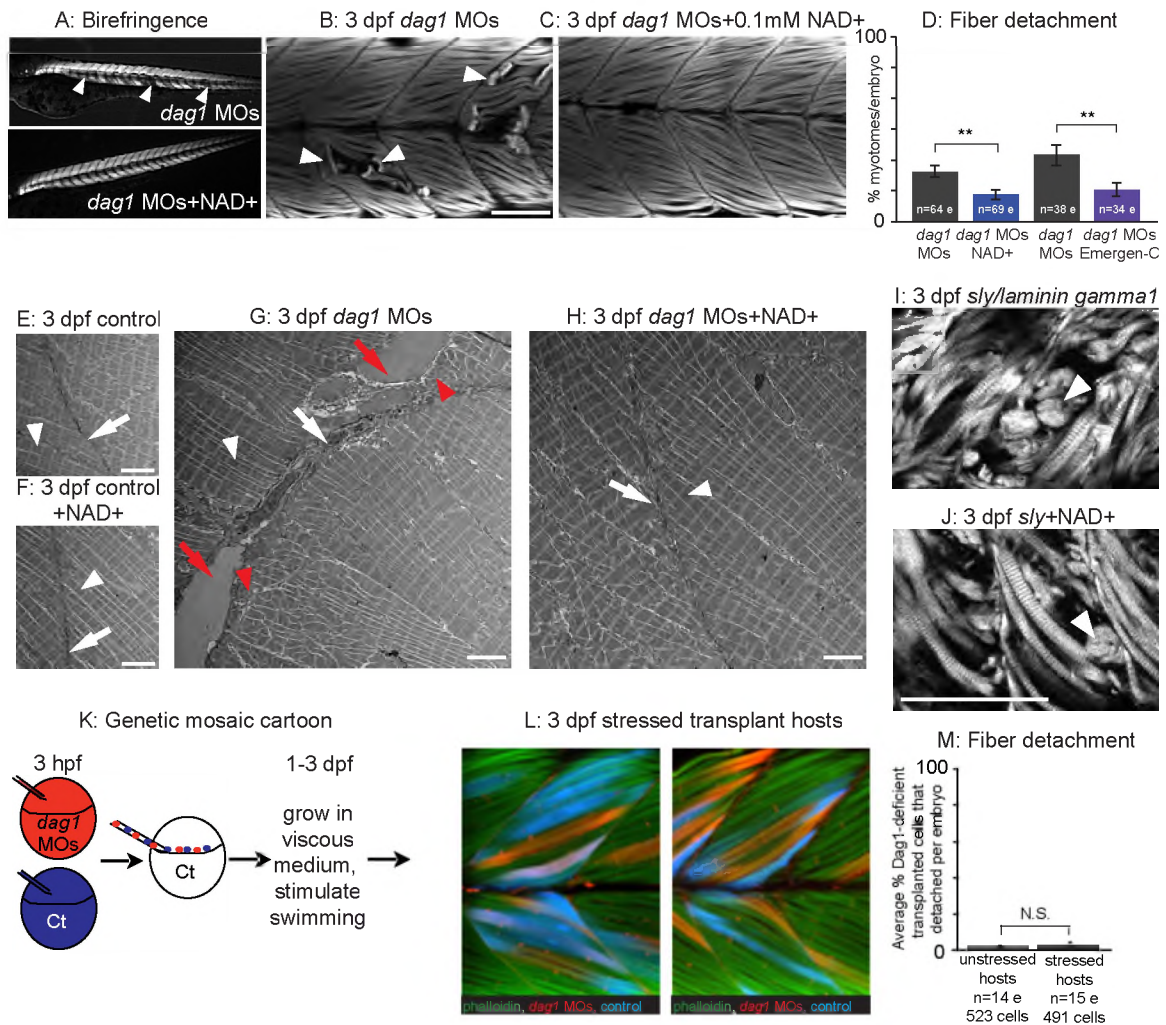
NAD⁺ supplementation significantly increases MTJ BM organization *prior* to the onset of dystrophy. This result suggests that the mechanism of action of NAD⁺ could be through BM augmentation. If NAD⁺ supplementation reduces the incidence of dystrophy via Laminin augmentation, NAD⁺ would not protect against muscle degeneration in *laminin* mutant zebrafish. We asked if Laminin is required for NAD⁺-mediated amelioration of dystrophy by utilizing *laminin gamma1* mutant zebrafish, which display muscle degeneration starting at 3 dpf (Fig. 3.2 panel I, Laminin gamma1 UniProtKB accession number Q1LVF0 LAMC1_DANRE). *laminin gamma1* mutants supplemented with exogenous NAD⁺ showed no improvement in the incidence of dystrophy compared to untreated mutants (Fig. 3.2 panels I-J). This result shows that Laminin is required for NAD⁺-mediated reduction of fiber detachment and supports our hypothesis that the protective effects of NAD⁺ occur through BM augmentation. This result also aligns with our previous finding that NAD⁺ reduces MTJ failure in 2 dpf *nrk2b* morphants, but not *laminin beta1* morphants (¹⁵²). Together, these results strongly suggest that the protective effects of NAD⁺ supplementation on MTJ failure and fiber detachment result from augmentation of Laminin in the BM.

We used genetic mosaic analysis to further test our hypothesis. If the DGC is

required cell autonomously for maintenance of muscle fiber adhesion, we would predict that *dag1* morphant cells in control hosts would degenerate as observed in *dag1* morphants. If, however, a normal BM provides a supportive environment for muscle fibers, we would predict that *dag1* morphant cells would be less likely to degenerate in control embryos. To discriminate between these two outcomes, we transplanted fluorescent dextran-labeled *dag1* morphant cells into control embryo hosts at the blastula stage, grew the embryos until 3 dpf, and asked whether *dag1* morphant cells were viable (Fig. 3.2 panel K). The vast majority of *dag1* morphant cells were viable (Fig. 3.2 panel L). Only 10 out of 523 transplanted *dag1* morphant cells (1.9%) detached from the MTJ BM. The incidence of fiber detachment per embryo in transplant hosts was significantly less than in *dag1* morphant embryos ($p < 0.001$). In addition, *dag1* morphant cells fused with fluorescent dextran-labeled control cells (Fig. 3.2 panel L, fusion indicated by pink cells). A more rigorous test of our hypothesis would be to ask whether Dag1-deficient cells are more likely to detach in control hosts when muscle tissue is stressed. We repeatedly stimulated transplant host embryos to swim through a viscous medium as described previously (⁵⁹). Of the 491 Dag1-deficient cells analyzed in 15 stressed host embryos, only 12 cells (2.4%) detached from the MTJ. Although a higher percentage of morphant cells detached in stressed hosts versus non-stressed hosts, the incidence of dystrophy per embryo did not significantly differ depending on stress (Fig. 3.2 panel M, $p=0.81$) and was still significantly different than in *dag1* morphants ($p<0.001$). These data clearly indicate that local integrity of the ECM microenvironment is sufficient for

muscle cell adhesion and that Dag1 is not required cell autonomously for maintenance of this adhesion.

Figure 3.2. An Organized ECM Microenvironment Rescues Fiber Resiliency in Dag1-Deficient Cells. (A) Anterior left, dorsal top, side mounted, 3 dpf embryos. Polarized light microscopy shows loss of birefringence in *dag1* morphant myotomes (white arrowheads). Birefringence is rescued in NAD⁺-supplemented *dag1* morphants. (B, C, I, J, L) Anterior left, dorsal top, side mounted, 3 dpf embryos stained with phalloidin (white or green). Fiber detachment is readily observed in *dag1* morphants (B, white arrowheads) whereas *dag1* morphants supplemented with NAD⁺ display less fiber detachment (C). (D) Compared to *dag1* morphants (gray bars), NAD⁺ supplementation (blue bar) and vitamin supplementation with Emergen-C (purple bar) significantly reduce fiber detachment, **p<0.01. (E-H) Transmission electron micrographs showing normal BMs (white arrows), normal sarcomeres (white arrowheads), disrupted BMs (red arrows) and disrupted sarcomeres (red arrowheads). Note that sarcomeres are disrupted adjacent to abnormal BMs in *dag1* morphants (G) and that NAD⁺ rescues these disruptions (H). (I) The dystrophic phenotype of 3 dpf *sly/laminin gamma1* mutant zebrafish. White arrowhead points to detached fibers. (J) NAD⁺ does not rescue the dystrophic phenotype in *sly* mutants, suggesting that NAD⁺-mediated amelioration of dystrophy requires Laminin. (K) Genetic mosaic cartoon depicting transplantation of fluorescent dextran-labeled *dag1* morphant (red) and control (blue) cells into unlabeled, control hosts. Some embryos were stressed (frequently stimulated to swim in a viscous medium) and all hosts were reared to 3 dpf. (L) Transplanted control cells (blue) and *dag1* morphant cells (red) remain attached to MTJs, even when hosts are stressed. This suggests that a normal host ECM microenvironment is sufficient for resiliency of *dag1* morphant cells and supports that NAD⁺ functions via augmentation of the ECM microenvironment. (M) The vast majority of Dag1-deficient cells remain attached in unstressed (513/523 Dag1-deficient cells were attached) and stressed hosts (479/491 Dag1-deficient cells were attached), N.S. = not significant. Scale bars are 50 micrometers in B and J and 5 micrometers in E-H.



3.4.3. *Itga7* is Required for NAD⁺-Mediated Reduction of Dystrophy in *dag1*

Morphants

The two ‘canonical’ Laminin receptors in muscle tissue are the DGC and Integrin alpha7beta1 receptor complexes. *Itga7* is disrupted in CMD with Integrin deficiency (¹⁵⁵). As the DGC is not required for NAD⁺-mediated reduction of dystrophy (Fig. 2), we asked if *Itga7* is required for the amelioration of dystrophy in *dag1* morphants by exogenous NAD⁺. A zebrafish model of CMD with Integrin deficiency has been generated (^{119,150}). Muscle degeneration in *itga7* morphants is apparent at approximately

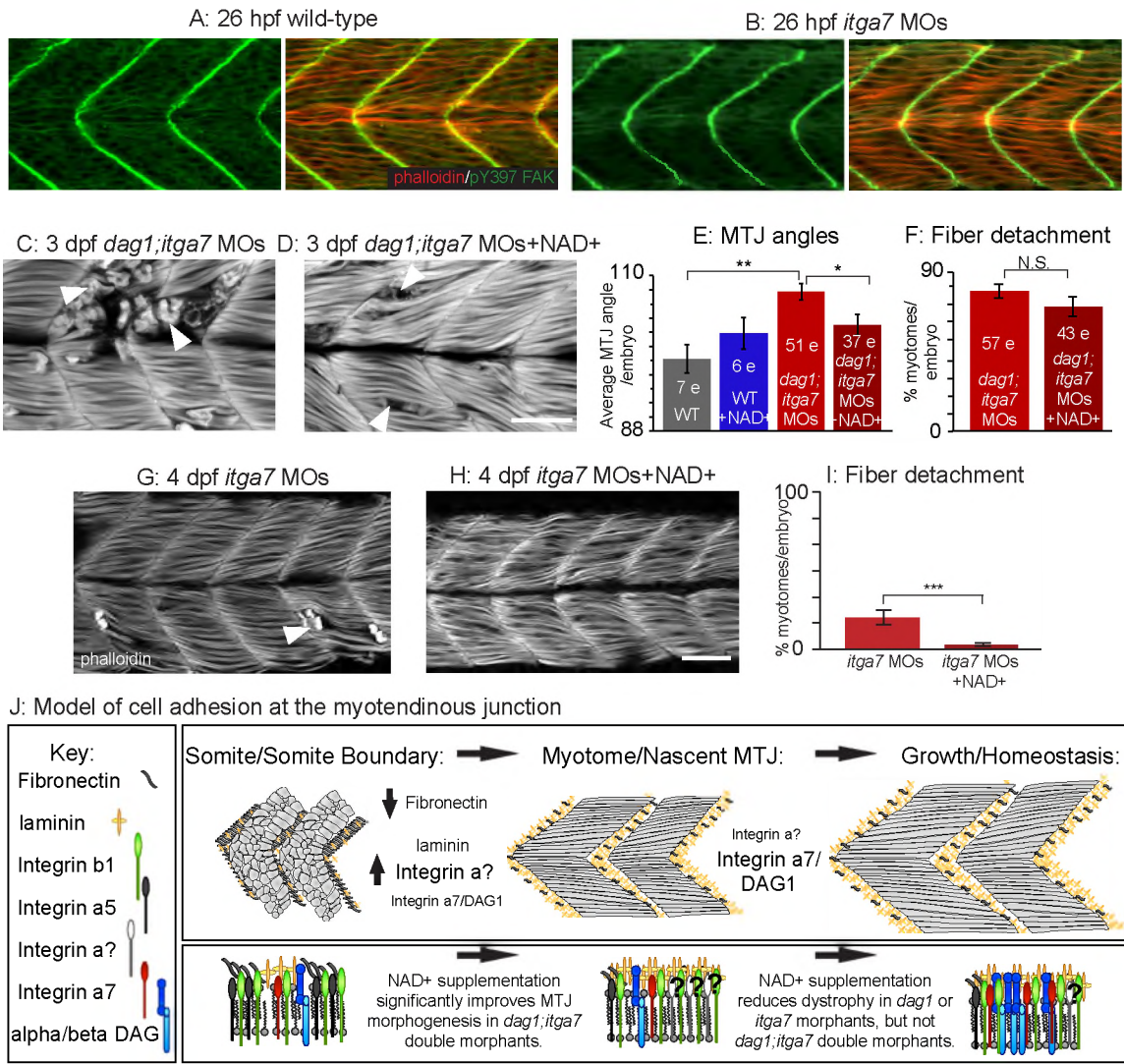
4.5 dpf. One critical axis to consider when evaluating muscle homeostasis is whether initial muscle morphogenesis is disrupted. It is not known if initial muscle development proceeds normally in *itga7* morphants. We analyzed muscle morphogenesis at 26 hpf and found that both MTJ and muscle fiber development appeared normal (Fig. 3.3 panels A-B). We next generated *dag1;itga7* double morphant embryos by co-injecting half the functional doses of *dag1* and *itga7* MOs. Surprisingly, given that early MTJ morphogenesis appears grossly unaffected in single morphants, MTJ morphogenesis was disrupted in double morphants. MTJ angles were abnormally wide (Fig. 3.3 panels C, E), similar to *laminin beta1* and *gamma1* mutant embryos (⁹³). This disruption in MTJ development is dramatically greater than would be predicted based upon the individual phenotypes and suggests Dag1 and Itga7-mediated adhesion to Laminin is synergistically required for MTJ morphogenesis. This was surprising given that MTJ morphogenesis appears normal in single morphants. We next asked whether exogenous NAD⁺ would rescue initial MTJ morphogenesis in *dag1;itga7* morphants (Fig. 3.3 panel D). We found that MTJ angles in NAD⁺-supplemented *dag1;itga7* morphants were significantly different from untreated double morphants (Fig. 3.3 panel E, 103.03 +/- 1.41 degrees vs. 107.74 +/- 1.16 degrees respectively, **p < 0.01, *p < 0.05). Thus, NAD⁺ supplementation is sufficient to rescue early morphogenetic events that require adhesion to Laminin in a Dag1 and Itga7-independent manner.

The above data indicate that Itga7 and Dag1 are synergistic with regards to initial muscle development but NAD⁺ supplementation is sufficient to improve MTJ development in *itga7;dag1* double morphant embryos. We next asked whether Itga7 is

required for NAD⁺-mediated reduction of dystrophy in *dag1* morphants. We found that NAD⁺ supplementation was not sufficient to significantly reduce the percent of muscle segments with fiber detachment in double morphants (Fig. 3.3 panel F, p=0.2). However, qualitatively, fewer fibers per myotome were detached (compare Fig. 3.3 panels C to D, we were unable to reliably count detached fibers in myotomes with severe degeneration and thus could not quantitate this observation). Taken together, these data indicate that *Itga7* is required for NAD⁺-mediated reduction of dystrophy in *dag1* morphants and that NAD⁺ supplementation is not sufficient to reduce the frequency of myotomes with muscle degeneration when both canonical Laminin receptors (*Dag1*, *Itga7*) are compromised.

The above data clearly show that *Itga7* plays a role in NAD⁺-mediated reduction of dystrophy in *dag1* morphants. Interestingly, two results suggest that an additional Laminin receptor participates in muscle development and homeostasis: (1) NAD⁺ supplementation rescues early MTJ morphogenesis in *dag1;itga7* double morphants, and (2) overall muscle structure is qualitatively improved with NAD⁺ supplementation in *dag1;itga7* double morphants. A key experiment to clarify whether an additional Laminin receptor also participates is to ask whether NAD⁺ supplementation is sufficient to reduce dystrophy in *itga7* morphants. NAD⁺ supplementation significantly reduced the incidence of dystrophy in *itga7* morphants (Fig. 3.3 panels G-I, ***p<0.001). This result indicates that there is an additional, “non-canonical” Laminin receptor that mediates Laminin signaling downstream of NAD⁺ during musculoskeletal homeostasis.

Figure 3.3. *Itga7* is Required for NAD⁺-Mediated Reduction of Fiber Degeneration in *dag1* Morphants. (A-D, G-H) Anterior left, dorsal top, side mounted embryos stained with phalloidin (red or white) or pY397 FAK (green). (A-B) Muscle morphogenesis proceeds normally in *itga7* morphants. Phosphorylated FAK (green) outlines fibers and concentrates at the MTJ and actin distribution in slow- and fast-twitch muscle fibers (red) appears normal in 26 hpf *itga7* morphants compared to wild-types. (C) 3 dpf *dag1;itga7* double morphant. (D) 3 dpf NAD⁺-supplemented *dag1;itga7* double morphant. MTJ morphogenesis is disrupted in *dag1;itga7* double morphants as displayed by wider MTJ angles (C). MTJ morphogenetic defects were rescued by NAD⁺ in *dag1;itga7* double morphants (D), suggesting that another Laminin receptor is sufficient for NAD⁺-mediated MTJ improvements. (E) Quantification of MTJ angles shows that *dag1;itga7* double morphants have significantly wider MTJ angles than wild-types and NAD⁺ significantly reduces this defect, **p<0.01, *p<0.05. (F) Quantification of incidence of dystrophy per embryo shows no significant difference in *dag1;itga7* double morphants upon addition of exogenous NAD⁺, suggesting that *Itga7* is required for NAD⁺-mediated reduction of dystrophy in *dag1* morphants, N.S. = not significant. However, fewer fibers appeared to detach in *dag1;itga7* double morphants supplemented with NAD⁺ (D), again suggesting the involvement of another receptor for Laminin in NAD⁺ action. (G-H) Mild fiber detachment is readily observed in 4 dpf *itga7* morphants (G) and reduced in NAD⁺-treated *itga7* morphants (H). (I) NAD⁺ treatment significantly decreases fiber degeneration in *itga7* morphants, ***p<0.001. (J) Model of cell adhesion at the MTJ. The transition from a somite boundary to a MTJ involves the downregulation of Fibronectin and the upregulation of Laminin and Laminin receptors. Our results suggest that Laminin receptors, *Itga7* and *Dag1*, play a role in this transition, but the primary receptor involved is an unknown Integrin. In maintenance of fiber adhesion at the MTJ, our data show that either *Itga7* or *Dag1* is required, but also suggest the involvement of an additional Laminin receptor. Scale bar is 50 micrometers.



3.4.4. *Itga6* is Required for NAD⁺-Mediated Improvement of Muscle Tissue

Structure

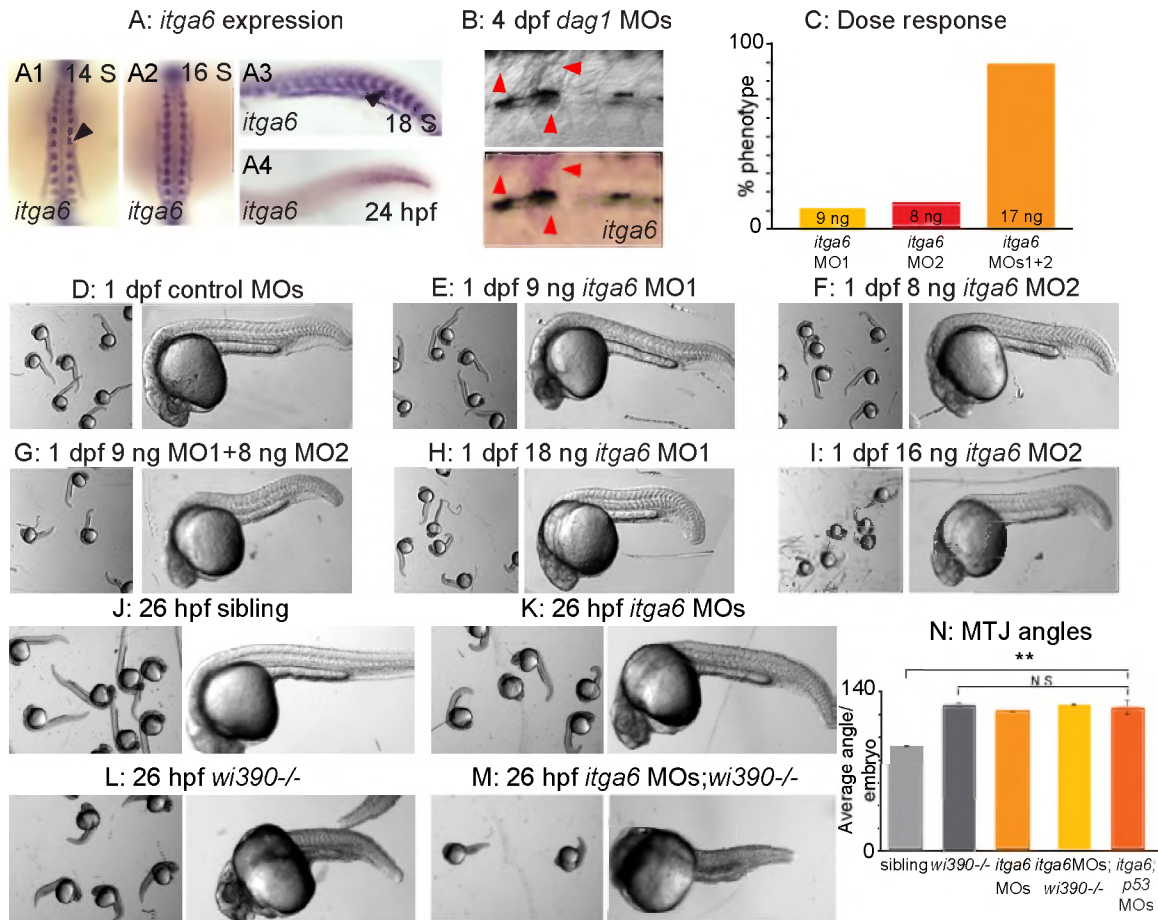
The above data indicate that the primary beneficial effect of NAD⁺ on muscle architecture is increased organization of Laminin in the BM. However, neither of the two Laminin receptors known to be required for muscle structure (*Dag1*, *Itga7*) are required individually for NAD⁺-mediated reduction of dystrophy (Figs. 3.2, 3.3). In order to identify mechanisms downstream of Laminin, we focused on identifying the relevant

Laminin receptor. The Laminin-binding family of Integrin alpha chains that partner with Integrin beta1 includes alpha3, alpha6, and alpha7 (¹⁵⁶). Only two of these chains, *itga6* and *itga7*, are expressed during zebrafish muscle development (¹¹⁹, Thisse, B. and Thisse C., <http://zfin.org>, Fig. 3.4 panel A). Expression of *itga6* is high during initial muscle development, and then declines. This correlates with the low level expression of *itga6* in human muscle (¹⁵⁷).

Interestingly, *itga6* has recently been implicated in muscle development and regeneration in multiple mammalian species (¹⁵⁸⁻¹⁶¹). We asked whether *itga6* expression is upregulated in *dag1* morphant zebrafish in dystrophic lesions where regeneration is occurring. As in other vertebrates, *itga6* expression was low in zebrafish muscle, but clearly visible in dystrophic lesions (Fig. 3.4 panel B, red arrowheads). Given these recent results, combined with our data showing upregulation of *itga6* in *dag1* morphants, we hypothesized that Itga6 is involved in the Nr2b-NAD⁺-Laminin pathway. We tested this hypothesis by using morpholino (MO)-mediated knockdown. We first characterized MOs against *itga6*. Injection of varying amounts/combinations of two different, non-overlapping, translation-blocking MOs showed that both MOs generated the same phenotype and acted synergistically (Fig. 3.4 panels C-I). The *itga6* morphant phenotype was nearly identical to that of *laminin beta1* and *gamma1* mutants and *nr2b* morphants (^{103,152}). This striking phenotypic similarity suggested that *itga6* may function in the Nr2b-NAD⁺-Laminin pathway. To confirm that Itga6 acts in Laminin signaling/adhesion, we conducted pseudo-genetic epistasis analysis. The transcripts for *laminin beta1* and *gamma1* are maternally expressed. Thus injection of *laminin beta1/gamma1*

MOs into *laminin beta1/gamma1* mutants slightly worsens the phenotype (¹⁶²). Injection of *itga6* MOs into *laminin gamma1* mutants also slightly worsened the phenotype (Fig. 3.4 panels J-M), but average MTJ angles were not significantly different in *itga6;laminin gamma1* morphant/mutants compared to *laminin gamma1* mutants (Fig. 3.4 panel N). Together, these data indicate that these MOs are specific and do not cause off target effects (¹⁰⁰). The above results also suggest that Itga6 does participate in Laminin signaling/adhesion.

Figure 3.4. *itga6* is Upregulated in Regenerating Muscle and Characterization of *itga6* MOs. (A) *In situ* hybridizations showing *itga6* expression (purple). (A1-2) Dorsal view, anterior top. (A3-4, B) Side view, anterior left, dorsal top. (A1-4) Black arrowheads denote somitic expression. *itga6* expression is high during early muscle development, then decreases. (B) *itga6* is re-expressed in regenerating muscle. *itga6*, not normally expressed in muscle at 4 dpf, is observed in dystrophic lesions of 4 dpf *dag1* morphants (red arrowheads). (C) *itga6* MO characterization. Dose response graph. MO1 and MO2 generate the same phenotype and synergize when co-injected. (D-M) Brightfield images, side view, anterior left, dorsal top, 1 dpf embryos. (D-I) Phenotypic analysis of *itga6* MOs 1 and 2. Embryos injected with low doses of MO1 (E) or MO2 (F) are morphologically similar to controls (D). Combining the two lower doses of MOs 1 and 2 results in a truncated body axis with myotomes that are narrower in the anterior-posterior dimension (G). The identical phenotype is obtained when higher doses of either MO1 (H) or MO2 (I) are injected. (J-M) Pseudo-genetic epistasis analysis. (J) Siblings, (K) *itga6* morphants, (L) *wi390*^{-/-}/*laminin gamma1* mutants, (M) *itga6* MOs;*wi390*^{-/-}. Note that injection of *itga6* MOs into *laminin* mutants does not change their phenotype, suggesting Itga6 functions in Laminin signaling and adhesion. (N) Average MTJ angles of 1 dpf embryos. MTJ angles in morphants, mutants and morphant/mutants do not significantly differ from one another and are all significantly wider than in sibling controls, **p<0.01, N.S. = not significant.



Although somite patterning was relatively normal and somite boundaries formed in these embryos (data not shown), by 2 dpf approximately 25% of the MTJs had failed (Fig. 3.5 panel B red arrows, 3.5 panel D). Abnormally long muscle fibers crossed the MTJ at sites of MTJ failure (Fig. 3.5 panel B1, MTJs pseudocolored blue and crossing fibers pseudocolored red). One possible side affect of MOs is that they can activate p53-dependent apoptosis and cause non-specific cell death⁽¹⁰¹⁾. Co-injection with *p53* MO did not alter the phenotype of *itga6* morphants (Fig. 3.5 panels C, D). Co-injection of *itga6* MOs with *itga6* cDNA lacking the MO target sites rescued the morphant phenotype (Fig. 3.5 panels E, F), further suggesting that these *itga6* MOs are specific⁽¹⁰⁰⁾.

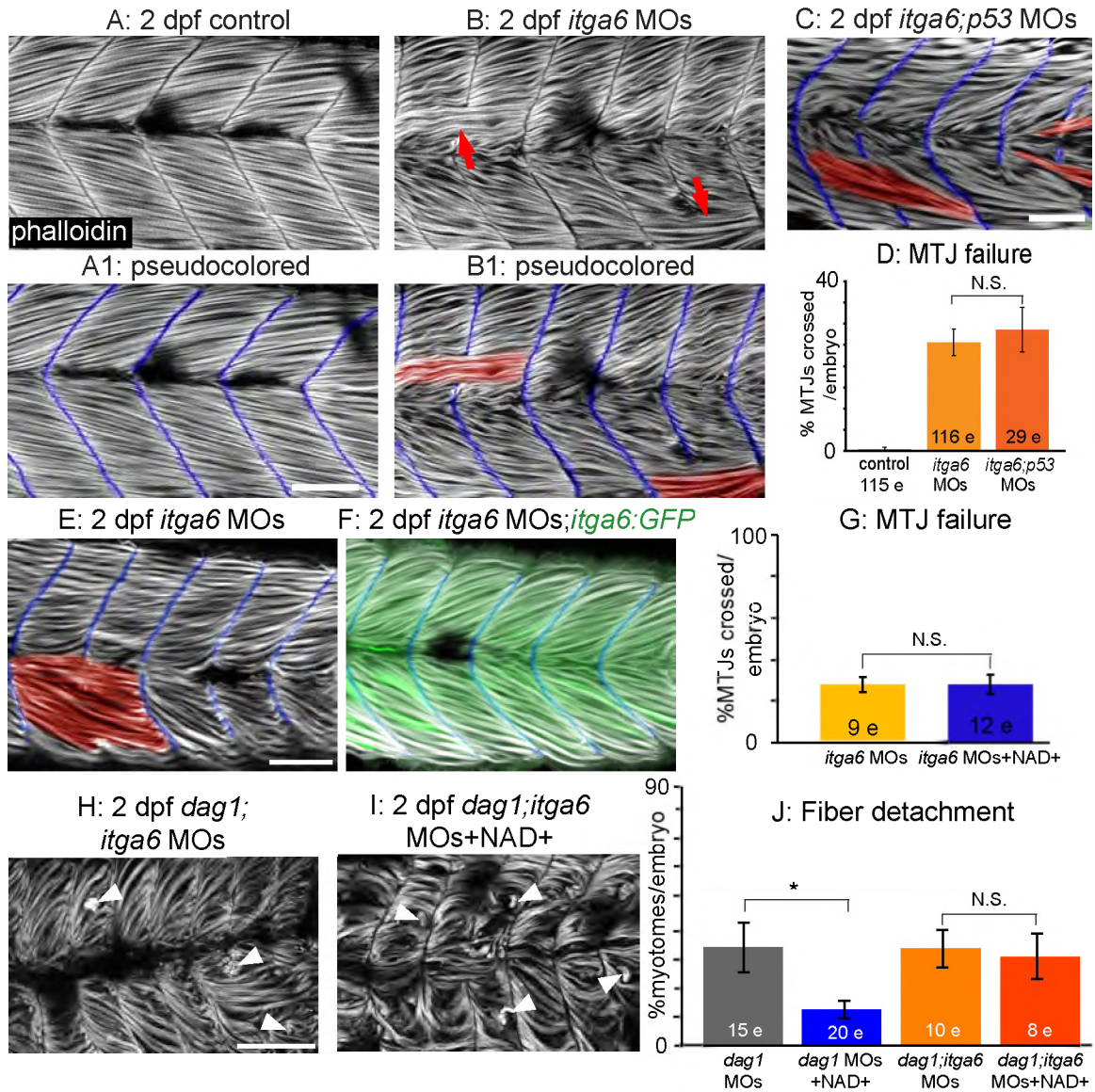
NAD⁺ functions upstream of Laminin polymerization during MTJ development

(¹⁵²), thus, we hypothesized that *itga6* morphants would not be rescued by NAD⁺ supplementation. Neither exogenous NAD⁺ nor Emergen-C (data not shown) were sufficient to rescue MTJ failure at 2 dpf in *itga6* morphants, indicating that Itga6 functions in this pathway downstream of NAD⁺ (Fig. 3.5 panel G, p=0.99 for NAD⁺). Although *itga6* morphants were slightly dystrophic (data not shown), the frequency of dystrophy was too rare to readily ask whether NAD⁺ supplementation is sufficient to reduce dystrophy in *itga6* morphants. Taken together, these data suggest that Itga6 functions in this pathway downstream of NAD⁺.

Given the requirements for Itga6 in muscle development in mouse (¹⁵⁸) and our data showing that Itga6 is required in zebrafish muscle development, we asked whether Itga6 is required to mediate reduction of dystrophy in *dag1* morphants. We co-injected *itga6* and *dag1* MOs and assayed the incidence of dystrophy in response to NAD⁺ supplementation (Fig. 3.5 panels H-I). As with co-injection of *itga7* and *dag1* MOs, initial MTJ morphogenesis was disrupted: myotomes were narrower in the anterior-posterior dimension and wider in the medial-lateral dimension. In contrast to *dag1;itga7* double morphants, NAD⁺ supplementation was not sufficient to improve MTJ morphogenesis in *dag1;itga6* double morphants (data not shown, average MTJ angle for *dag1;itga6* morphants: 143.98 +/- 3.08 degrees, average MTJ angle for NAD⁺-treated *dag1;itga6* morphants: 139.50 +/- 3.52 degrees, p=0.35). This result indicates that Itga6 is the Laminin receptor required for the role of NAD⁺ in MTJ morphogenesis. NAD⁺ supplementation also did not ameliorate muscle degeneration in *dag1;itga6* double

morphants (Fig. 3.5 panel J, $p=0.78$). This result indicates that *Itga6* is also required for NAD⁺-mediated amelioration of dystrophy in *dag1* morphants.

Figure 3.5. Itga6 is Required for NAD⁺-Mediated Rescue of MTJ Morphogenesis and Dystrophy. (A-C, E-F, H-I) Anterior left, dorsal top, side mounted, 2 dpf embryos stained with phalloidin (white) to visualize actin. In pseudocolored panels (A1, B1, C, E, F), MTJ boundaries are blue and abnormally long muscle fibers are red. (A) MTJs are V-shaped and continuous in control embryos. (B) In *itga6* morphants, MTJs are U-shaped, discontinuous and crossed by abnormally long muscle fibers (red arrows). (C) Co-injection of *p53* MOs does not rescue MTJ failure in *itga6* morphants. (D) Quantification of MTJ failure at 2 dpf in controls, *itga6* morphants and *itga6;p53* double morphants. (E-F) Co-injection of *itga6* cDNA that does not contain the MO target sites with *itga6* MOs rescues the *itga6* morphant phenotype. (G) Quantification of MTJ failure shows that NAD⁺ treatment does not rescue MTJ failure in *itga6* morphants, suggesting that NAD⁺ requires Itga6 for rescue of MTJ failure. (H) *dag1;itga6* double morphants have U-shaped MTJs and dystrophy (white arrowheads). (I) NAD⁺ does not reduce MTJ angles (not shown) or dystrophy in *dag1;itga6* double morphants, suggesting that Itga6 is also required for NAD⁺-mediated rescue of MTJ angles and dystrophy. (J) Quantification of dystrophy shows significant rescue by exogenous NAD⁺ in *dag1* morphants, but not *dag1;itga6* double morphants, *p < 0.05, N.S. = not significant. Scale bars are 50 micrometers.

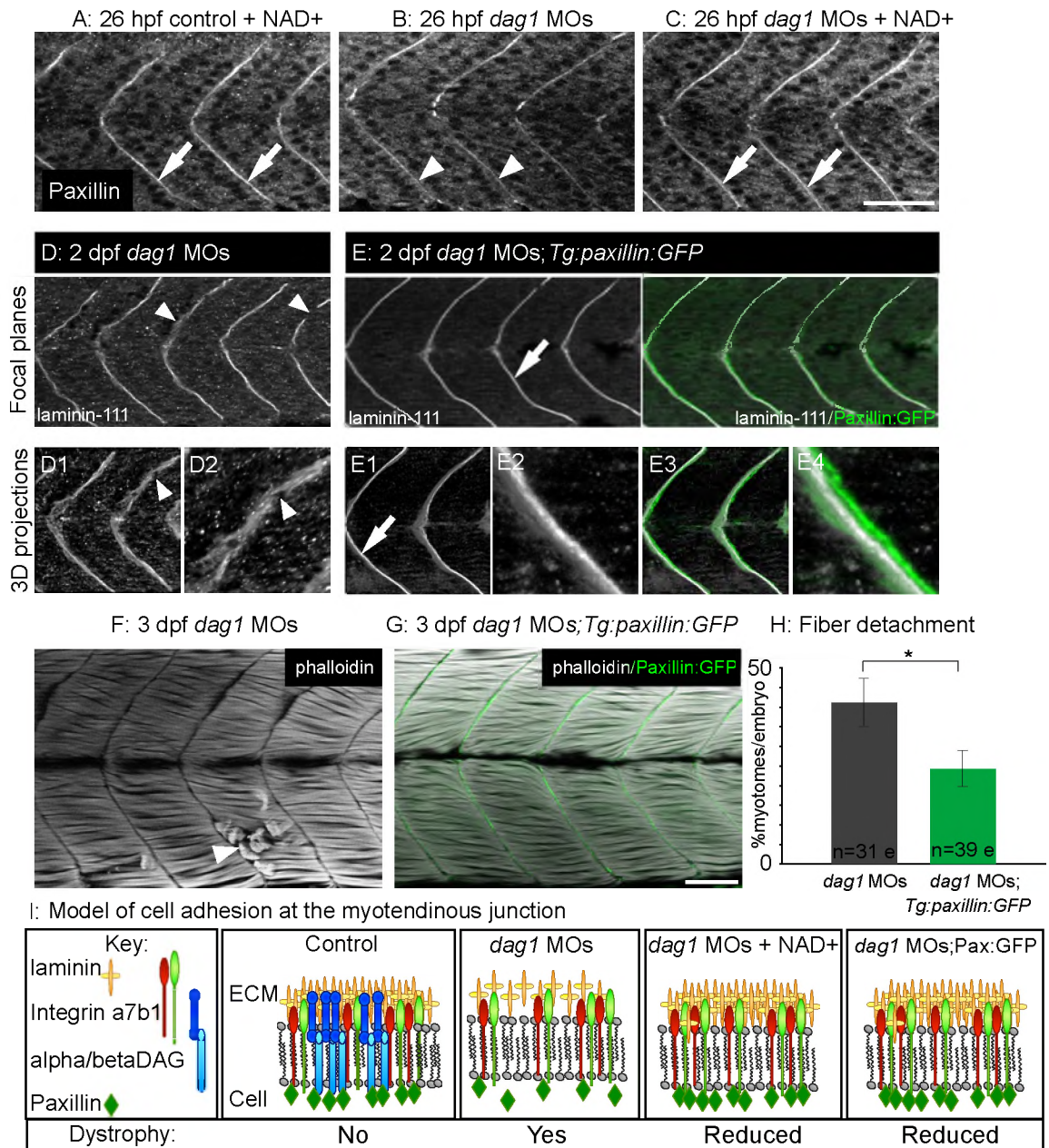


3.4.5. Paxillin Overexpression is Sufficient to Increase MTJ BM Structure and Decrease Fiber Detachment in *dag1* Morphants

We previously showed that the Integrin-associated adaptor protein Paxillin functions downstream of NAD⁺ during MTJ development: Paxillin overexpression is sufficient to rescue MTJ morphogenesis in *nrk2b* morphants⁽¹⁵²⁾. Thus, likely through “inside-out” signaling via Laminin receptors, Paxillin is sufficient to affect the ECM

microenvironment. We asked whether overexpression of Paxillin would be sufficient to augment MTJ BM organization in dystrophic embryos. Paxillin concentration at the MTJ was slightly disrupted in *dag1* morphants at 26 hpf (Fig. 3.6 panel B). NAD⁺ supplementation improved Paxillin concentration at the MTJ in 26 hpf *dag1* morphants (Fig. 3.6 panel C). Next, we overexpressed Paxillin in *dag1* morphants by injecting *dag1* MOs into *Tg:paxillin:GFP* embryos. Paxillin:GFP accounted for approximately 66.05 +/- 8% of total Paxillin expressed at 2 dpf in *Tg:paxillin:GFP* embryos (data not shown). Paxillin overexpression increased organization of Laminin-111 at the MTJ in 2 dpf *dag1* morphants (compare Fig. 3.6 panel E to D, 2DWTMM analysis not shown: *p < 0.05 for wavelets from 1.88 to 4.02 micrometers). Paxillin overexpression also significantly reduced the incidence of fiber detachment in 3 dpf *Dag1*-deficient embryos (Fig. 3.6 panels F-H, *p<0.05).

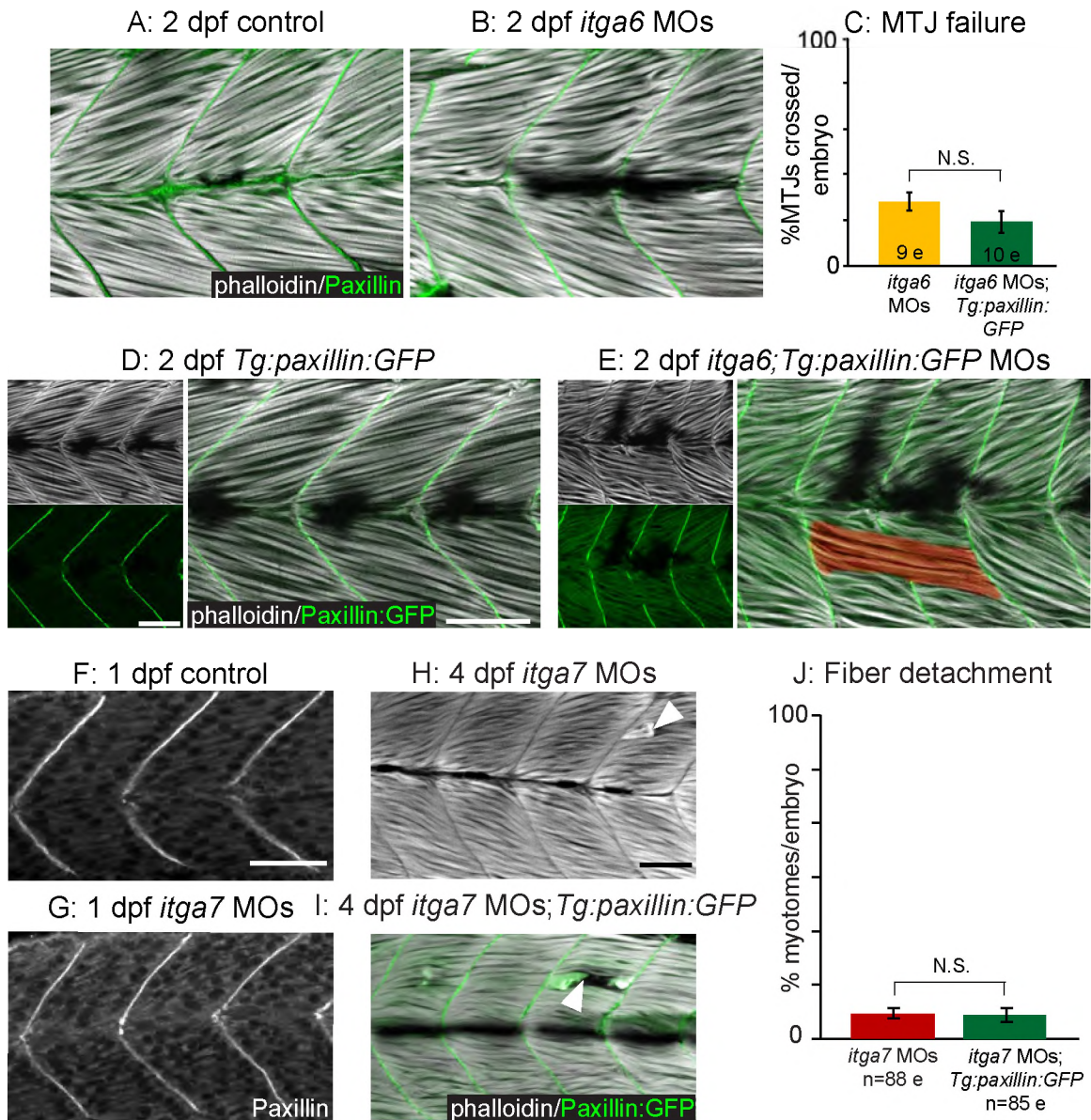
Figure 3.6. Paxillin Overexpression Increases Laminin Organization and Ameliorates Dystrophy in *dag1* Morphants. (A-C) Anterior left, dorsal top, side mounted, 1 dpf embryos antibody stained for Paxillin (white). (A) Paxillin concentrates at the MTJ in both untreated (not shown) and NAD⁺-treated controls (white arrows). (B) Paxillin is less concentrated at the MTJ in *dag1* morphants (white arrowheads). (C) NAD⁺ rescues the disrupted concentration of Paxillin at the MTJ in *dag1* morphants (white arrows). (D-E) Anterior left, dorsal top, side mounted, 2 dpf embryos stained with Laminin-111 antibody (white). Numbered panels are 3D reconstructions. (D) *dag1* morphant. Laminin-111 appears within myotomes and the MTJ BM is poorly aligned medially-laterally and contains holes (white arrowheads). (E) In contrast, Paxillin overexpression (green) in *dag1* morphants reduces Laminin-111 within myotomes and enhances organization of Laminin-111 at the MTJ BM (white arrows). (F-G) Anterior left, dorsal top, side mounted, 3 dpf embryos stained for actin (phalloidin, white). (F) *dag1* morphant with detached fibers (white arrowhead). (G) Transgenic overexpression of Paxillin (green) in *dag1* morphants reduces fiber detachment. (H) Paxillin overexpression significantly reduces the frequency of fiber detachment in *dag1* morphants, *p<0.05. (I) Model of cell adhesion at the MTJ in response to Nr2b pathway activation via exogenous NAD⁺ or Paxillin overexpression. Scale bars are 50 micrometers.



As Paxillin does not require Dag1 for BM augmentation-mediated reduction of dystrophy (Fig. 3.6), we asked whether Integrin receptors are required. We analyzed both the subcellular localization of Paxillin upon *Itga6* or *Itga7* knockdown as well as the ability of transgenic Paxillin overexpression to rescue the muscle defects observed in *itga6* or *itga7* morphants. In *itga6* morphants, Paxillin concentrated at the MTJ as in

control embryos (Fig. 3.7 panels A-B). Paxillin overexpression in *itga6* morphants (Fig. 3.7 panel E) did not reduce the incidence of MTJ failure (Fig. 3.7 panel C, $p=0.18$). Paxillin also localized to the MTJ in *itga7* morphants (Fig. 3.7 panel G) and Paxillin overexpression in *itga7* morphants had no effect on the percent of myotomes per embryo with dystrophic lesions (Fig. 3.7 panels H-J, $p=0.9$). As Paxillin is an Integrin adaptor protein, it is perhaps not surprising that Paxillin-mediated BM augmentation requires functional Integrin receptors for Laminin. Our results suggest that *Dag1*, but not *Itga6* or *Itga7*, is required for localization of Paxillin to the MTJ and that the beneficial effects of overexpressing Paxillin in *Dag1*-deficient muscle tissue may result from increasing the amount of MTJ-proximal Paxillin involved in inside-out signaling via Integrin receptors for Laminin.

Figure 3.7. Paxillin Action, but Not Subcellular Localization, Requires Functional Integrin Receptors for Laminin. (A-B, D-E) Side mounted, anterior left, dorsal top, 2 dpf embryos stained with phalloidin (white). (A-B) Antibody staining shows that Paxillin (green) concentrates at the MTJ in *itga6* morphants (B) as in controls (A). (C) Quantification of MTJ failure shows that Paxillin overexpression does not rescue *itga6* morphants. (D-E) Transgenic overexpression of Paxillin:GFP (green) does not affect MTJ development in controls (D) and is not sufficient to rescue MTJ failure in *itga6* morphants (E). (F-G) Anterior left, dorsal top, side mounted, 26 hpf embryos stained for Paxillin (white). Paxillin concentrates at the MTJ in *itga7* morphants (G) as in controls (F). (H-I) Side mounted, anterior left, dorsal top, 4 dpf embryos stained with phalloidin (white). Fiber detachment is readily observed in *itga7* morphants (H) and *itga7* morphants transgenically overexpressing Paxillin (I, white arrowheads). (J) Paxillin overexpression does not affect fiber detachment frequency in *itga7* morphants. Together, these results suggest that *Itga6* and *Itga7* are required for Paxillin-mediated improvements in muscle tissue. N.S. = not significant. Scale bars are 50 micrometers.

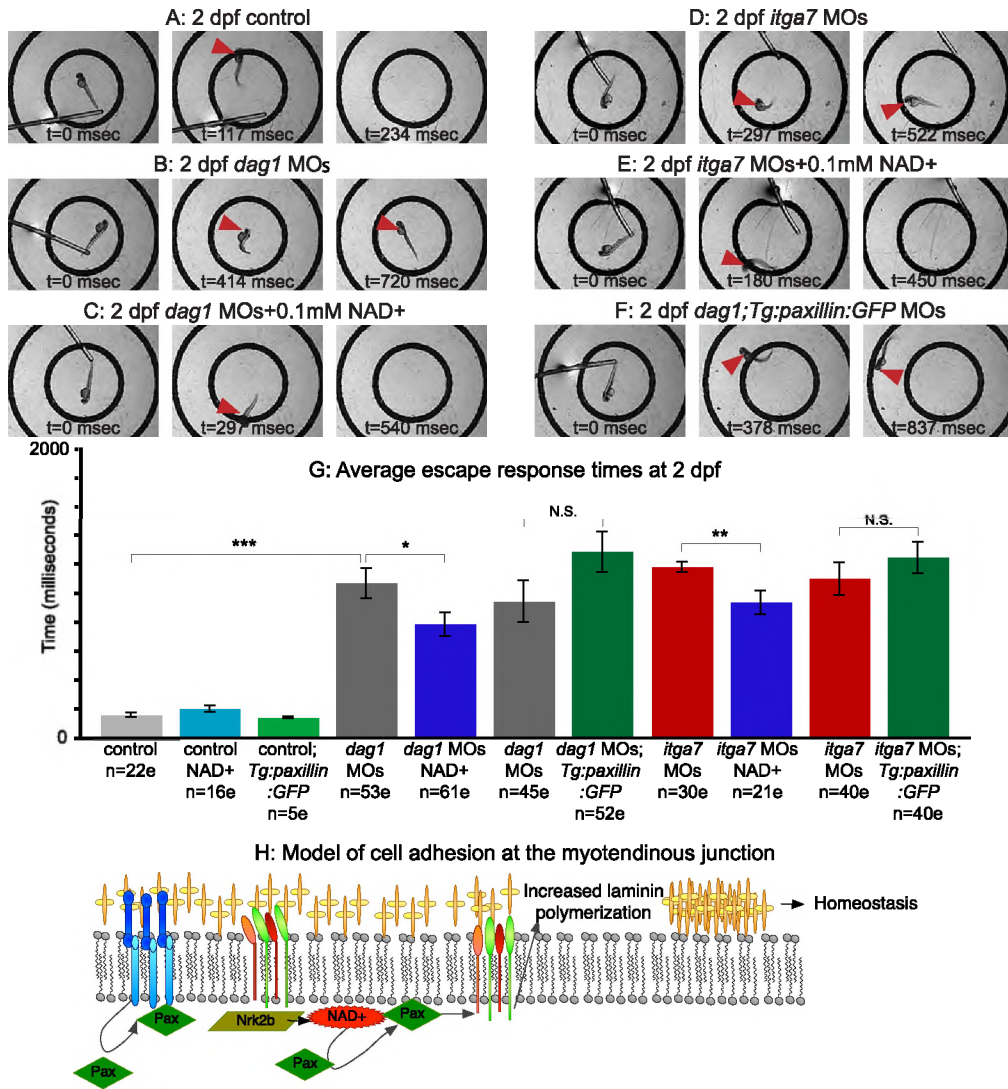


3.4.6. NAD⁺ Supplementation Improves the Mobility of Dystrophic Zebrafish

We next asked whether improvements in MTJ BM structure and maintenance of fiber attachment in dystrophic zebrafish correlated with physiological improvements by assaying the average time it takes for dystrophic embryos to swim a predetermined distance following a touch stimulus. Whereas control, NAD⁺-treated, Emergen-C-supplemented (not shown) or *Tg:Paxillin:GFP* control embryos always rapidly exited a

10 mm diameter circle (Fig. 3.8 panel G), only approximately half of *dag1* morphants swam out of the circle and were, on average, significantly slower than controls (Fig. 3.8 panels B, G, *** $p < 0.001$). *Dag1* morphants supplemented with NAD⁺ (Fig. 3.8 panel C) or Emergen-C (not shown) were more likely to exit the circle compared to untreated *dag1* morphants and were, on average, significantly faster than untreated *dag1* morphants (Fig. 3.8 panel G, * $p < 0.05$ for NAD⁺, ** $p < 0.01$ for Emergen-C). Similarly, NAD⁺-treated or Emergen-C-supplemented (not shown) *itga7* morphants were more likely to exit the circle (Fig. 3.8 panel E) and were, on average, significantly faster (Fig. 3.8 panel G, ** $p < 0.01$ for NAD⁺, * $p < 0.05$ for Emergen-C) than unsupplemented *itga7* morphants (Fig. 3.8 panel D). These data suggest that NAD⁺ or Emergen-C treatment is sufficient to improve mobility in *Dag1* or *Itga7*-deficient zebrafish. Interestingly, however, *Tg:paxillin:GFP* embryos injected with *dag1* MOs or *itga7* MOs actually tended to be slower than *dag1* or *itga7* morphants, respectively (Fig. 3.8 panels F, G). These results indicate that improving basement membrane structure in dystrophic zebrafish by overexpressing Paxillin is not sufficient to improve mobility.

Figure 3.8. NAD⁺ Supplementation, but Not Paxillin Overexpression, Improves Motility of Dystrophic Zebrafish. (A-F) Individual panels from videos of escape responses after a touch stimulus at 2 dpf, time in milliseconds is denoted on panels. The outer circle is 10 mm in diameter. Red arrowheads point to the embryo's location. (A) Control embryo. (B) *dag1* morphant. (C) NAD⁺-supplemented *dag1* morphant. (D) *itga7* morphant. (E) NAD⁺-supplemented *itga7* morphant. (F) *dag1* MOs;*Tg:paxillin:GFP* embryo. (G) Average escape response times of 2 dpf dystrophic zebrafish after exogenous NAD⁺ treatment or overexpression of Paxillin. Exogenous NAD⁺ or Emergen-C (not shown) significantly reduced the escape times of both *dag1* and *itga7* morphants. Overexpression of Paxillin, however, did not reduce escape times of *dag1* or *itga7* morphants. * p<0.05, **p<0.01, ***p<0.001, N.S. = not significant. (H) Model of cell adhesion at the MTJ. Our data show that Laminin polymerization is necessary and sufficient for muscle fiber homeostasis and that NAD⁺ and Paxillin increase Laminin polymerization. We find that *Dag1* and *Nrk2b* are required for Paxillin localization to the MTJ. We hypothesize that NAD⁺, through mediating Paxillin concentration at MTJs, invokes 'inside-out' signaling through Laminin receptors that results in increased Laminin polymerization.



3.5. Discussion

Tissue homeostasis, especially when tissue is stressed, requires cellular adaptations. Such adaptations are executed by a variety of mechanisms and lead to numerous potential outcomes such as hypertrophy, hyperplasia, and metaplasia, among others. Interactions between cells and their ECM microenvironment may play roles in skeletal muscle adaptation because cell-ECM adhesion complexes sense multiple types of physiological changes and interface with every major signaling pathway. Thus, cell-ECM adhesion

complexes are in a prime position to facilitate appropriate responses to physiological change. However, in muscle disorders such as muscular dystrophies, sarcopenia, and denervation injuries, tissue structure is disrupted to such a degree that normal cellular adaptive responses are not sufficient to compensate. In zebrafish embryos deficient for Dag1 or Itga7, transmembrane receptor proteins involved in anchoring the sarcolemma of muscle cells to the BM, the consequence of disrupted cell adhesion is detachment and death of muscle fibers^(92,119). Here, we show that addition of a small molecule, NAD⁺, is sufficient to increase the organization of the muscle cell microenvironment in dystrophic zebrafish. Exogenous NAD⁺ is sufficient to reduce dystrophy when either Itga7 or Dag1 is compromised because this pathway also functions through a different Laminin receptor, Itga6. Pseudo-genetic epistasis experiments show that either Dag1 or Itga7 is required with Itga6 for the effects of exogenous NAD⁺ on reduction of dystrophy. Finally, we show that NAD⁺ plays a dual role in ameliorating dystrophy: NAD⁺-mediated Paxillin clustering improves muscle structure and adhesion, but NAD⁺ acts independently of Paxillin to improve motility. Taken together, these data provide fundamental new insights into the adaptability of cell adhesion mechanisms *in vivo*, and the phenotypic consequences of this adaptability.

3.5.1. The ECM Microenvironment: A Dynamic Structure Sufficient to Guide Morphological Change

A fundamental question is how tissue architecture is generated and maintained during development and homeostasis. The mechanical linkage of cells to BMs, substructures in the ECM, is necessary for cell viability and physiological homeostasis.

Laminins are heterotrimeric proteins necessary for BM assembly. *laminin* mutations lead to multiple diseases including myopathies, junctional epidermolysis bullosa, laryngo-oncho-cutaneous syndrome, and microcoria-congenital nephritic syndrome (¹²⁶). Tissue specific function of Laminin isoforms arises not only through regulated expression, but also through the generation of splice variants and post-translational glycosylation and processing. Despite the apparent tissue specificity of Laminin function, multiple experiments indicate that, at least in the context of muscle biology, alternate BM components can partially compensate and restore cell-ECM adhesion when one Laminin chain is disrupted. Mutations in *laminin alpha2* cause a severe congenital muscular dystrophy, MDC1A. Overexpression of either Laminin alpha1, Laminin-111 or mini-agrin, an ECM protein that can link with the DGC, slows the progression of dystrophy in *laminin alpha2* mutant mice (^{14-16,23}). Recent data indicate that Laminin-111 protein therapy can also reverse muscle disease even when the gene mutated encodes an intracellular protein. Injection of Laminin-111 protein directly into muscle of DMD mice dramatically improves muscle structure and function by increasing *Itga7* expression (²²).

Here, we show that disorganized Laminin-111 in the MTJ BM of *Dag1*-deficient zebrafish muscle tissue can be significantly improved by exogenous NAD⁺. We implicate Laminin-111 organization in prolonging cell-ECM adhesion and fiber viability by showing that *laminin gamma1* is required for NAD⁺-mediated reduction of fiber detachment. Furthermore, we used genetic mosaic analysis to directly assess the role of a normally organized MTJ BM microenvironment on cell-ECM adhesion and muscle fiber viability in *Dag1*-deficient muscle cells. *dag1* MO-injected cells were transplanted into

control embryos. Dag1-deficient muscle cells developed normally, and sarcomeres formed in the viable Dag1-deficient fibers. Significantly, only 1.9% of Dag1-deficient fibers in control embryos detached from the wild-type ECM microenvironment. Our findings suggest that proper organization of the ECM microenvironment plays a crucial role in maintenance of cell-ECM adhesion and fiber viability and thus muscle tissue homeostasis. Another striking example of how the ECM microenvironment impacts muscle cells is seen in how sarcomere morphogenesis changes depending upon the elastic moduli of hydrogels. The highest percent of sarcomerogenesis (60%) was observed after culture on a relatively elastic hydrogel (15 kPa) ⁽¹⁶³⁾. Taken together, these data not only suggest that the composition and physical properties of the ECM influence muscle structure, but that local organization of the ECM can be dynamic and organizational state plays a critical role in muscle cell health. In addition, these data raise the possibility that a better understanding of the effects of ECM dynamics on cell and tissue morphogenesis and homeostasis, and the use of supplements like NAD⁺ to increase ECM organization, could improve *in vitro* tissue synthesis and regenerative medicine.

3.5.2. Unique and Redundant Roles for the Laminin Receptor Proteins Integrin alpha7, Integrin alpha6, and Dystroglycan

Many studies have highlighted the complex, dynamic, and redundant interactions between Integrin alpha7beta1 and the DGC in muscle disease. Although both of these Laminin receptors have unique functions ⁽¹⁴⁹⁾, they can partially compensate for each other in adhesion to Laminin. Expression of the uncompromised complex's components can be upregulated in dystrophy, mutations in both complexes exacerbate dystrophy, and

overexpression of alternate complex components can alleviate dystrophy (^{36,37,41,43,44}). Because exogenous NAD⁺ ameliorates dystrophy in embryos deficient for the DGC, we predicted that Integrin alpha7beta1 would be required for reduction of dystrophy in *dag1* morphants. In support of this, we found that the frequency of myotomes with muscle degeneration in *dag1;itga7* double morphants was not significantly improved by NAD⁺. Surprisingly, however, overall muscle structure improved in NAD⁺-supplemented *dag1;itga7* double morphants. This result suggests: (1) the existence of an additional Laminin receptor downstream of NAD⁺ in the Nr2b pathway, and (2) this receptor partially compensates when Dag1 and Itga7 are disrupted. We identified this receptor as Itga6. Compared to Itga7 and Dag1, far less is known about Itga6 function. Mutations in human *itga6* lead to epidermolysis bullosa with pyloric atresia (severe skin blistering with life threatening obstruction of the digestive tract). The mouse *itga6* mutant is even more severe; mutant embryos die at birth with severe skin blistering (¹⁶⁴). Thus, at first glance, our results implicating Itga6 in muscle development and homeostasis are surprising. However, Itga6 is downstream of Myf5 and required for Laminin assembly and normal myogenesis in mouse embryo explants (¹⁵⁸). Itga6 expression is a biomarker for highly myogenic cell populations in muscle tissue and required for normal myogenic differentiation and myotube formation of a porcine muscle progenitor cell population (^{159,160}). Itga6 and Laminin1 also play key roles in regeneration of CD117-positive cells in adult human pathological hearts (¹⁶¹). These studies, along with our data, suggest that Itga6 does play a role in muscle physiology, and may in fact be a key player in muscle tissue adaptation to stress.

Adhesion to Laminin is required for initial MTJ development: MTJs in *laminin beta1* and *gamma1* mutant embryos are significantly wider than in wild-type embryos. The Laminin receptors that mediate initial MTJ morphogenesis were not known. Our data indicate that Itga6 is the main Laminin receptor mediating MTJ morphogenesis. MTJ angles are significantly wider in *itga6* morphants or *dag1;itga6* double morphant embryos compared to controls. MTJ development is not rescued when *itga6* or *dag1;itga6* morphants are supplemented with NAD⁺, indicating that Itga6 is necessary for the role of NAD⁺ in MTJ development. Although both *dag1* and *itga7* are expressed early in zebrafish development (^{92,119}), MTJ angles are normal in *dag1* or *itga7* single morphants. However, we show that MTJ angles are wider than normal in *dag1;itga7* double morphants. This result suggests that these two Laminin receptors are required for normal MTJ development, but function redundantly. MTJ angles in *dag1;itga7* double morphants are significantly narrower when incubated in NAD⁺, suggesting that Itga6 is sufficient to compensate for the decreased adhesion to Laminin in *dag1;itga7* double morphants. Taken together, these results suggest that Itga6 is the major Laminin receptor necessary and sufficient for mediating early muscle and MTJ morphogenesis, but that Itga7 and Dag1 also contribute.

Muscle homeostasis also requires adhesion to Laminin. In this instance, however, Integrin alpha7beta1 and the DGC are the main Laminin receptors mediating muscle stability. Muscle degenerates in zebrafish embryos deficient for either *dag1* or *itga7* (^{92,119}). Exogenous NAD⁺ increases Laminin organization and reduces dystrophy in embryos deficient for either *dag1* or *itga7*. Pseudo-genetic epistasis analysis indicates

that both *itga7* and *itga6* are necessary for NAD⁺-mediated amelioration of dystrophy in *dag1* morphants. Our data suggest that all three Laminin receptors play unique roles in MTJ development and muscle homeostasis. However, when one receptor is compromised, the other receptors can partially compensate and NAD⁺ supplementation potentiates this compensatory response by facilitating increased Laminin organization in an Integrin-dependent manner.

3.5.3. Paxillin and Basement Membrane Organization

Paxillin overexpression is also sufficient to restore Laminin organization in dystrophic zebrafish. Paxillin is an essential signaling nexus that regulates cell adhesion, morphology, and migration (¹²⁵). Depending upon context, Paxillin potentiates either the assembly or disassembly of cell-ECM adhesion complexes. The robust concentration of Paxillin at MTJs during muscle development suggested a role for Paxillin in maintaining muscle structure (⁵⁸). Here we show that overexpression of Paxillin in *dag1* morphants increases organization of Laminin-111 at the MTJ and reduces dystrophy. These results clearly implicate Paxillin in playing a fundamental role in muscle homeostasis. It is very interesting that Paxillin overexpression does not rescue morphogenesis/reduce dystrophy in *itga6* or *itga7* morphants. There are at least three possible explanations for why Itga6 and Itga7, but not Dag1, are required for Paxillin overexpression-mediated restoration of muscle structure. One is that the subcellular localization of Paxillin to MTJs is critical for Paxillin function: Paxillin localization is disrupted in *dag1* morphants, but not in *itga6* or *itga7* morphants. Overexpression of Paxillin restores localization of Paxillin to MTJs in *dag1* morphants and reduces dystrophy. Another scenario that would explain these results

is that Paxillin modulates “inside-out” signaling via Itga6 and Itga7. Paxillin localization to Itga6 and Itga7 containing cell-ECM adhesions may directly or indirectly cause these Laminin receptors to adopt their high-affinity conformation, thus increasing adhesion to Laminin. Finally, Paxillin could be required to recruit the exocyst to the MTJ. The exocyst traffics vesicles to subdomains within the membrane and is critical for efficient exocytosis of Integrins. Paxillin binding to an exocyst component, Sec5, mediates proper subcellular localization of exocyst complexes (165). Thus, one mechanism by which Paxillin could function upstream of Itga6 and Itga7 is modulation of exocyst localization. Intriguingly, another component of the exocyst is Arf6, which would require NAD⁺ as a cofactor for ADP-ribosylation of its targets. Our results clearly show that MTJ-localized Paxillin is sufficient to impact local organization of the ECM microenvironment. It will be very interesting to determine the mechanism(s) of action, and elucidate why Paxillin – one of a thousand focal adhesion proteins – plays such a critical role. As Paxillin is ubiquitously expressed and necessary for early development (127,166), understanding how Paxillin improves Laminin organization in *dag1* morphants may provide insight into Paxillin function in other tissues as well.

3.5.4. Moving Toward Viable Therapeutic Options for Myopathies

Congenital muscular dystrophies are a heterogeneous group of early-onset progressive muscle wasting diseases. In animal models of CMDs where sarcolemma integrity remains intact prior to fiber detachment, BM augmentation has been proposed and implemented as a successful approach to maintain muscle fiber viability. Interestingly, multiple different methods of BM augmentation have proved beneficial. In

laminin beta2 mutant zebrafish, initial failure between muscle fibers and the MTJ BM is compensated for by newly formed ectopic BMs at the detached ends of fibers (21). Gene therapy approaches involving the expression of synthetic BM components are sufficient to reduce myopathy in mouse models (14,15). We show that modulation of the ECM microenvironment by the small molecule NAD⁺ also ameliorates muscle degeneration. In Dystrophin-deficient zebrafish, where sarcolemma integrity is compromised prior to fiber detachment, a screen of chemicals approved for human use revealed that the nonselective phosphodiesterase inhibitor aminophylline best restored muscle structure by activating cAMP-dependent PKA signaling (68). These reports highlight the importance of classifying the etiology of fiber degeneration, as different myopathies may respond better to certain treatment approaches. In addition, investigation of combinatorial therapeutic approaches may prove most useful.

Along with muscle degeneration, CMDs can also present with joint and skeletal deformities and mental retardation. In dystrophic zebrafish, we find that NAD⁺ supplementation improves both muscle structure and mobility, but Paxillin overexpression only improves muscle structure. Thus, in this system, structure does not beget function. It is perhaps not surprising that NAD⁺ contributes to the development and functioning of tissues other than muscle. Neurodegenerative disorders such as Parkinson's and Alzheimer's are associated with reduced NAD⁺ levels and increasing NAD⁺ metabolism slows neuronal degeneration *in vitro*. Although the exact mechanisms are not known, the neuroprotective effects of NAD⁺ are thought to be mediated by poly ADP-ribose polymerases (PARPs), which play critical roles in genome stability, DNA

repair, and telomere maintenance. In the case of ischemia, it is thought that the oxidative stress brought on by reperfusion with oxygen can cause DNA damage. This damage then activates the PARP-1 cascade and results in rapid depletion of NAD⁺. Energy within the cell quickly becomes limiting and may cause cell death. Evidence for this hypothesis comes from the fact that *PARP*^{-/-} mice show reduced tissue damage and protected NAD⁺ metabolism in cerebral ischemia (¹⁶⁷). In a similar vein, nicotinamide treatment has been shown to allay the effects of fetal alcohol syndrome in mice (¹⁶⁸). This may be an important intervention for early neuronal damage during fetal development. Given these data, it is tempting to speculate that NAD⁺ may contribute to neuromuscular junction development or prolong/enhance signaling through neuromuscular junctions, thus contributing to improved motility in dystrophic zebrafish. As many NAD⁺ biosynthetic enzymes and precursors/metabolites are both required and cytoprotective in muscle and neural tissues, downstream targets of NAD⁺ signaling are promising potential therapies for multiple symptoms of muscle degeneration, including fiber atrophy, reduced motor function and mental retardation.

The experiments shown here were undertaken because we had previously shown that *Nrk2b* is necessary for Laminin organization during myotendinous junction development. An alternate method to NAD⁺ supplementation *in vivo* is vitamin supplementation with a precursor to NAD⁺, such as niacin. Water-soluble Emergen-C packets that contain niacin were added to ERM and were sufficient to reduce muscle degeneration in *dag1* morphants. This result suggests the hypothesis that maternal and fetal nutrition may partly explain the variable progression and age of onset of some

dystrophies. Clearly, vitamins other than niacin in the packets could contribute to the reduction of dystrophy. However, given that the reduction in muscle degeneration is similar in NAD⁺-supplemented, Emergen-C-supplemented, and Paxillin overexpressing *dag1* morphants, it seems unlikely that other vitamins are causing this effect.

Niacin has been used clinically for decades to manage dyslipidemia (¹⁶⁹). Although the mechanism of action is not well understood, it is known that niacin increases high-density lipoprotein (HDL) independently of NAD⁺ synthesis. An extended release form of niacin, Niaspan, has been used in combination with statins that lower LDL levels to treat cardiovascular disease (¹⁷⁰). However, NIH recently aborted a clinical trial combining niacin and statin therapy because the combination therapy did not decrease cardiovascular events in patients with heart and vascular disease and the risk of stroke was slightly increased (<http://www.nih.gov/news/health/may2011/nhlbi-26.htm>). Thus, it is not clear whether niacin will continue to be prescribed for cardiovascular disease. However, recent experiments in rats suggest other possible therapeutic uses for niacin. Niaspan is neuroprotective after stroke (¹⁷¹) and slows the progression of chronic kidney disease (¹⁷²). Our data suggest that the currently tractable approach of vitamin supplementation may warrant continued investigation.

3.6. Chapter Conclusions

One of the advantages of using a “4D” system such as muscle development *in vivo* is the depth of dynamic range that cells exhibit in response to changes in cell signaling, cell adhesion, and the biophysics of the surrounding microenvironment. These processes allow cells to adapt to changing conditions during development, aging, injury response

and repair. We show that one such adaptive response – an increase in ECM organization mediated by the Nr2f1 pathway – is sufficient to improve the resilience of muscle in dystrophic zebrafish. There are three Laminin receptors expressed in muscle. The “canonical” receptors, Dag1 and Itga7, are highly expressed and, when mutated, lead to congenital muscular dystrophies. Here we implicate a “non-canonical” Laminin receptor, Itga6, in the Nr2f1 pathway. Recent findings from mouse, pig and human cells, along with our data utilizing zebrafish embryos, suggest a conserved and previously unrecognized role for Itga6 in promoting muscle regeneration and homeostasis. Genetic mosaic analysis shows that the main effect of the Nr2f1 pathway is an increase in structure of the ECM. A series of pseudo-genetic epistasis experiments with these three Laminin receptors indicate that Dag1 or Itga7 is required along with Itga6 for NAD⁺ to reduce dystrophy. Taken together, these data suggest that two out of three receptors are required in order to sufficiently bind Laminin and increase ECM organization. Our data highlight the contribution of the Nr2f1-NAD⁺-Laminin-Paxillin-Itga6/Itga7 to cellular adaptive responses and suggest that this pathway may have therapeutic potential.

CHAPTER 4

FUTURE DIRECTIONS

The best kind of answers to scientific questions are ones that beget more questions. What we have learned about the Nr2f1 pathway in muscle development and disease over the course of my graduate research project has certainly resulted in the formulation of new questions to answer and future directions to pursue. The future directions that will be discussed in this chapter are by no means an exhaustive list. Equally interesting and worthy future avenues of investigation that will not be described in this chapter include larger size scale, integrative studies, such as compensation for loss of cell-matrix adhesion by upregulation of cell-cell adhesion proteins through adhesive crosstalk, roles for NAD⁺ in neuromuscular junction development and function, and clinical epidemiological studies correlating pregnant mother's intake of NAD⁺ precursors with the timing of onset, rate of progression and severity of disease in children that were diagnosed with a congenital muscular dystrophy. The future directions that will be detailed in this chapter can be categorized into two broad areas of investigation: (1) the vertical depth of the mechanisms through which Nr2f1, NAD⁺ and Paxillin regulate Laminin organization at different size scales and (2) the horizontal breadth of the efficacy of Nr2f1 pathway manipulation in animal models of diseases associated with basement membrane disruptions. This chapter will describe potential future experiments to address questions related to these two areas of investigation, hopefully resulting in even more questions to pursue.

4.1. Molecular Functions of Zebrafish Nr_k2b

Nr_k2 (aka MIBP2, ITGB1BP3) is a little studied protein that has been implicated in regulation of muscle tissue development and function: it is upregulated in double muscled cattle (⁸⁵) and ASPS, a rare, highly metastatic cancer (⁸⁶); and its overexpression disrupts muscle differentiation in cultured mouse myoblasts (⁸⁴). MIBP2 was first identified in a yeast two-hybrid screen for proteins that directly interact with the cytoplasmic tail of human Integrin beta1 (residues 749-801(⁸⁴)). The authors of the study proposed that MIBP2 overexpression likely inhibits terminal muscle differentiation via changes in Integrin beta1 signaling, as enhanced expression of Integrin beta1 causes similar results in cell culture (^{173,174}). Interestingly, MIBP2 is a splice-variant of Nr_k2, an enzyme involved in NAD⁺ biosynthesis in multiple species (⁷¹). Therefore, MIBP2/Nr_k2 action in muscle development may occur through its role in Integrin beta1 binding, NAD⁺ biosynthesis, both, or as of yet unknown molecular functions.

This dissertation describes the first *in vivo* study of MIBP2/Nr_k2 in muscle development using a zebrafish ortholog, Nr_k2b. A reverse genetics approach and morpholino-mediated knock down of Nr_k2b protein levels revealed a role for Nr_k2b in development of the myotendinous junction basement membrane and maintenance of MTJ integrity. Provision of exogenous NAD⁺ rescued MTJ failure in *nrk2b* morphants, providing evidence that the NAD⁺ biosynthetic function of Nr_k2 enzymes may be conserved in zebrafish Nr_k2b. However, our data do not discriminate whether the role of Nr_k2b in MTJ BM development requires the catalytic function of Nr_k2b, Integrin beta1 binding or both. Experiments to address whether the enzymatic or Integrin beta1 binding

function of Nrk2b is required for normal MTJ BM development and MTJ integrity would involve generating Nrk2b mutant constructs incapable of enzymatic activity or unable to bind Integrin beta1. Aspartic acid residue 35 was identified as essential for Nrk2 enzymatic function in yeast (⁷²) and this residue is conserved in zebrafish Nrk2b and human Nrk2 (data not shown). Generation and then transgenic expression of a *nrk2b* *D35A* mutant construct in *nrk2b* morphant zebrafish could be used to determine how well catalytically dead Nrk2b rescued MTJ failure in comparison to wild-type Nrk2b. If the Nrk2b mutant construct rescued MTJ failure in *nrk2b* morphant zebrafish as well as wild-type Nrk2b, then the NAD⁺ biosynthetic function of zebrafish Nrk2b would not be required for MTJ integrity. However, if the mutant construct did not rescue boundary crossings as well as wild-type Nrk2b, it would be concluded that Nrk2b-mediated NAD⁺ biosynthesis is essential for Nrk2b's role in MTJ integrity. Similar experiments involving mutating or deleting the Integrin beta1 binding residues of Nrk2b could be done to determine whether Nrk2b-Integrin beta1 binding is required for the role of Nrk2b in MTJ integrity. However, the authors of Li et al., 1999 only determined the residues of Integrin beta1 that are involved in binding MIBP2/Nrk2, not the MIBP2/Nrk2 residues that bind Integrin beta1. These residues would have to be identified before these experiments could be conducted. Results from these experiments could show that the requirement for Nrk2b in zebrafish MTJ BM development is: (1) solely through 'inside-out' signaling via Integrin beta1, (2) through NAD⁺ biosynthesis and that Integrin beta1 binding may only function to localize this source of NAD⁺ or (3) through both or neither of these molecular functions of Nrk2b. The data from these experiments could raise the interesting

possibility that intracellular Nrk2b via Integrin beta1 signaling and provision of exogenous NAD⁺ may be two, completely independent ways of augmenting Laminin-111 organization or that the results we obtained supplementing zebrafish embryos with exogenous NAD⁺ is coupled to the NAD⁺ biosynthetic function of Nrk2b.

4.2. Molecular Functions and Regulation of NAD⁺

To begin to address how exogenous NAD⁺ affects extracellular Laminin-111 organization, the many molecular functions of intracellular and extracellular NAD⁺ must be considered. NAD⁺ is a ubiquitous metabolic factor involved in electron transfer reactions and is also a substrate in mono- and poly-ADP-ribose transfer reactions, cyclic ADP-ribose reactions regulating calcium signaling and Sirtuin deacetylase reactions. As NAD⁺ is degraded in its role as a substrate, it must be continuously synthesized via the three pathways of NAD⁺ biosynthesis. NAD⁺ can be synthesized from tryptophan via the *de novo* pathway, from nicotinamide and nicotinic acid via the Preiss-Handler salvage pathway and from nicotinamide riboside and nicotinic acid riboside via an alternative salvage pathway. This alternative salvage pathway beginning with nicotinamide riboside and involving two enzymatic steps to NAD⁺ generation is of particular interest to my graduate studies because the first reaction, phosphorylation of nicotinamide riboside, is carried out by the Nrk family of enzymes. Alternative salvage is the only means of NAD⁺ biosynthesis in bacteria that lack enzymes required in the other two pathways and the function of alternative salvage pathway enzymes was found to be conserved in eukaryotes (71). Together, this evolutionary conservation along with the fact that tryptophan alone can not maintain adequate NAD⁺ levels in rats (175) or cultured cells

(¹⁷⁶) suggest that this alternative salvage pathway of NAD⁺ biosynthesis is critical for maintenance of adequate basal levels of NAD⁺.

Due to the involvement of NAD⁺ in a myriad of cellular reactions, NAD⁺ availability and subcellular compartmentalization must be strictly regulated in order for specificity of function. Compartmentalization of NAD⁺ to mitochondria severely restricts the NAD⁺ available for reactions utilizing NAD⁺ as a coenzyme: as much as 75% of intracellular NAD⁺ can be sequestered within the mitochondria of heart muscle (¹⁷⁷). Providing NAD⁺ precursors or up regulating NAD⁺ biosynthetic enzymes can increase the availability of intracellular NAD⁺ for NAD⁺-dependent reactions through boosting overall levels NAD⁺, but can also, through as of yet unknown mechanisms, increase NAD⁺ availability without altering steady-state NAD⁺ levels (¹⁷⁸). Recently, a valuable tool was developed allowing for indirect visualization and quantification of intracellular NAD⁺ localization and levels using constitutively active PARP enzymes to generate fluorescent products in a NAD⁺ concentration dependent manner (¹⁷⁶). In this report, the authors found that extracellular nucleotides (NAD⁺, NAAD, NMN, NAMN) could not permeate the cell membrane, but that nucleosides (NA, Nam, NR, NAR) were cell permeable through nucleoside transporter-dependent or -independent routes (¹⁷⁶). Also, the authors showed that particular NAD⁺ biosynthetic enzymes localize to specific subcellular compartments, such as mitochondria, nuclei or the cytosol (¹⁷⁶). These subcellularly localized enzymes could generate localized sources of NAD⁺ that may play distinct cellular roles at different times. The study described above regarding NAD⁺ regulation in multiple cultured cell lines went a long way toward enhancing our

understanding of NAD⁺ dynamics and regulation. All together, the many molecular functions of NAD⁺, the multiple and complex layers of NAD⁺ regulation and the interconnectivity of NAD⁺ biosynthetic pathways and NAD⁺-degrading reactions with other major cell signaling pathways make for a multitude of ways in which NAD⁺ could function in organization of Laminin-111.

Adaptation of the tool described above or the development of others allowing for visualization of NAD⁺ biosynthetic components and NAD⁺ localization and levels for *in vivo* studies would certainly be a worthy endeavor. As we do not know how much, if any, of the NAD⁺ that is added to zebrafish embryo rearing media actually enters muscle cells, how it enters muscle cells or in what form it enters muscle cells, the ability to visualize changes in NAD⁺ concentrations and localizations *in vivo* would shed light on this unknown. A hypothetical tool allowing for *in vivo* visualization of NAD⁺ could also be used to assess how depletion or overexpression of Nr2b or other zebrafish Nrk orthologs, Nampt (the rate limiting enzyme in the Preiss-Handler branch of NAD⁺ biosynthesis (¹⁷⁹)) or other NAD⁺ biosynthetic enzymes affects NAD⁺ levels and localization and whether two pathways of NAD⁺ biosynthesis can compensate for the loss of one in zebrafish. Interestingly, Nampt is predominately expressed in human skeletal muscle and regulates the expression of myogenic regulatory factors and thus myogenesis in cultured chick muscle cells (¹⁸⁰). Expression of zebrafish Nampt is currently completely unknown (no data are available on ZFIN) and characterization of roles for Nampt in zebrafish muscle development would present an interesting line of investigation.

4.3. Elucidating the Molecular Function of NAD⁺ in Basement Membrane

Organization

Data presented in this dissertation show that exogenous NAD⁺ rescues MTJ break down in *nrk2b* morphants (Chapter 2) and muscle degeneration in *dag1* or *itga7* morphants (Chapter 3). Exogenous NAD⁺, however, could not rescue MTJ break down in *gup/laminin beta1* (Chapter 2) or *itga6* morphants (Chapter 3) or muscle degeneration in *sly/laminin gamma1* mutants, *dag1;itga7* or *dag1;itga6* double morphants (Chapter 3). Thus, we have not only shown a novel role for NAD⁺ in muscle development and homeostasis, but have also elucidated part of the mechanism of NAD⁺ action by showing specific requirements for Itga7, Itga6 and Laminin-111. Something our experiments did not address is the smaller size scale, molecular level mechanism of NAD⁺ action in muscle morphogenesis and homeostasis. Therefore, one future direction would be to elucidate how NAD⁺ affects Integrin receptors and how this results in organization of Laminin-111 in the MTJ BM.

We have provided a hypothesis and some preliminary data as to how we suspect extracellular NAD⁺ may be affecting Laminin-111 organization via Integrins in Section 2.5.1. We hypothesize that extracellular, NAD⁺-dependent enzymes called mono-ADP-ribosyltransferases utilize extracellular NAD⁺ to transfer ADP-ribose moieties to Integrins. ADP-ribosylation is a post-translational modification that transfers a negatively charged ADP-ribose from NAD⁺ onto target proteins. This addition frequently inactivates proteins and was historically best known for its role in bacterial pathogenesis. Within the last decade, it has become increasingly clear that ADP-ribosylation of multiple proteins is

an evolutionarily ancient and important reaction that can activate proteins. ADP-ribosylation activates Integrins to increase cell-matrix adhesion ⁽¹¹³⁾. We predict this post-translational modification will increase binding affinity between Itga7b1 or Itga6b1 and Laminin-111 and, through dynamic reciprocity, receptor recruitment and clustering would result in increased organization of the 3D structure of Laminin-111. Evidence to support our hypothesis includes increased binding affinity between Integrin alpha7beta1 and Laminin-111 upon ADP-ribosylation in *in vitro* studies ⁽¹¹³⁾ and conservation of the ADP-ribosylated region of Itga7 ⁽¹⁸¹⁾ in Itga6. This line of future investigation would be both innovative in that *in vivo* functions for mono-ADP-ribosylation in development and muscle tissue are not known as well as significant in that ecto-mono-ADP-ribosyltransferases could be novel therapeutic targets in diseases associated with disrupted BMs.

Questions and experiments to lend support to or discredit our hypothesis that extracellular NAD⁺ is utilized in mono-ADP-ribosyltransferase reactions to impact Laminin-111 organization *in vivo* are detailed below. The admittedly poorly characterized mono-ADP-ribosyltransferase genes in zebrafish include Art1 and Art4 (the Art1 gene information was recently removed from the Zebrafish Model Organism Database ZFIN for unknown reasons). We have generated preliminary data showing that *art1* and *art4* are expressed in developing zebrafish skeletal muscle in a Nr2b-dependent manner (Peterson and Henry, personal communication of unpublished data). A question of interest to pursue is whether extracellular NAD⁺ acts only through Arts to impact Laminin-111 organization or also through alternative molecular functions of NAD⁺. To

answer this question, 3D reconstructions of Laminin-111 antibody staining and the frequency of boundary crossings per embryo would be compared between *nrk2b;art* double morphants and *nrk2b;art* double morphants incubated in exogenous NAD⁺. If there is no qualitative difference in Laminin-111 organization at the MTJ BM and no quantitative difference in the frequency of boundary crossings per double morphant embryo upon NAD⁺ supplementation, it would be concluded that Arts are required and that extracellular NAD⁺ functions in Laminin-111 organization solely through mono-ADP-ribosylation reactions. If *nrk2b;art* double morphants incubated in NAD⁺ show a partial or complete rescue in Laminin-111 organization and boundary crossings compared to their unsupplemented counterparts, then Arts may or may not be required and we would conclude that the extracellular NAD⁺ provided is used in NAD⁺-consuming reactions other than mono-ADP-ribosylation to impact MTJ BM integrity. Perhaps, the best test of our hypothesis would be to show that zebrafish Art1/4 ADP-ribosylate Itga7 and Itga6 *in vivo* or in whole embryo lysates. This is currently not possible because, while antibodies for poly-ADP-ribosylation exist, antibodies to detect mono-ADP-ribosylations currently do not. Development of this tool, as well as tools to visualize Laminin-111 polymerization dynamics *in vivo* in real time, would greatly enhance rigorous testing of our hypothesis.

If it were the case that exogenous NAD⁺ could partially rescue Laminin-111 disorganization and boundary crossings in *nrk2b;art* morphants, which would not be all that surprising given the many cellular roles for NAD⁺, even more future directions would arise. This outcome could be due to mono-ADP-ribosyltransferase function of

previously unknown zebrafish Art genes that were not accounted for, but it could also implicate poly-ADP-ribosyltransferase reactions, cyclic ADP-ribose reactions regulating Calcium signaling or Sirtuin deacetylase reactions in extracellular NAD⁺-mediated organization of Laminin-111 via Integrins.

4.4. Elucidating the Molecular Function of Paxillin in Basement Membrane

Organization

As NAD⁺ is involved in multiple cellular reactions, one approach to narrowing down the possibilities of the molecular function of NAD⁺ in Laminin-111 organization is to investigate downstream of NAD⁺ in the Nrk2b pathway. Data presented in this dissertation show that the intracellular, cell-matrix adhesion protein Paxillin functions downstream of Nrk2b and NAD⁺ in zebrafish MTJ BM development. We found transgenic overexpression of Paxillin to be sufficient to reduce boundary crossings in *nrk2b* morphants (Chapter 2) and reduce dystrophic lesions in *dag1* morphant zebrafish (Chapter 3). Therefore, Paxillin likely impacts Laminin-111 organization through inside-out signaling via cell-matrix adhesion complexes. In Chapter 3, we also show that Paxillin function requires Integrin receptors for Laminin-111: Itga6 is required for Paxillin-mediated rescue of boundary crossings and Itga7 is required for Paxillin-mediated reduction of dystrophic lesions. Therefore, we have again elucidated the relevant receptors in the mechanism of Paxillin function, but not the molecular level intricacies, making another future direction to elucidate the molecular function of Paxillin in Laminin-111 organization. We hypothesize that Paxillin signaling augments Laminin-111 organization by regulating inside-out signaling via Integrins. The proposed

experiments to follow are innovative in that exceedingly little is known about regulation of BM development *in vivo* by cell-matrix adhesion proteins and significant in that molecular dissection of Paxillin function and potential links to downstream signaling pathways could elucidate novel drug targets for currently incurable diseases affecting BMs.

Experiments to address this future direction would involve generation of Paxillin mutant constructs and then either their transient expression in zebrafish or the generation of stable transgenic zebrafish lines expressing these constructs. Data analysis would involve assaying Laminin-111 antibody staining and boundary crossings in *nrk2b* morphant embryos. Dissection of Paxillin function *in vitro* has been well studied and there is a large number of potential mutant constructs to try *in vivo*. One construct of interest is a tyrosine phosphorylation-deficient variant of Paxillin, Y31F/Y118F⁽¹⁸²⁾. This construct would be co-injected along with *nrk2b* MOs and Laminin-111 antibody staining and boundary crossings would be compared between *nrk2b* morphants, *nrk2b* morphants expressing wild-type Paxillin and *nrk2b* morphants expressing Y31F/Y118F Paxillin. If this phosphorylation-deficient mutant construct rescues boundary crossings to the same degree that wild-type Paxillin does, then phosphorylation of Paxillin at these sites is not required for Paxillin function in Laminin-111 organization. If this mutant construct results in no significant change in boundary crossings compared to *nrk2b* morphants, then tyrosine phosphorylation of Paxillin is required for Paxillin action in Laminin-111 organization. Expression of this Paxillin variant could also be found to only partially rescue boundary crossings. Phosphorylation at these sites has been shown to

indirectly promote Rac1 and inhibit Rho1, has been implicated in focal adhesion maturation and modulation of Calpain activity, enhances binding of FAK to the LD motifs, promotes invadopodia (actin-rich cell membrane extensions, similar to lamellipodia, but that extend into the ECM and involve proteolysis) formation, and has been implicated in sarcomere formation (^{46,183-188}). Thus, if tyrosine phosphorylations at Y31 and Y118 are found to be required for the molecular function of Paxillin in Laminin-111 organization, the aforementioned downstream signaling pathways and proteins will be implicated and provide additional future directions to explore.

Another Paxillin variant to test is D146A/D268A, which disrupts the LD2 and LD4 domains of Paxillin and completely abrogates FAK binding (¹³¹). Binding of FAK to both LD2 and LD4 of Paxillin is necessary for maximal activation of FAK (¹³²). If the Paxillin D146A/D268A construct is unable to rescue boundary crossings in *nrk2b* morphants, FAK activation would be implicated in Paxillin-mediated Laminin-111 organization. This would open up additional future avenues of investigation into whether constitutively activated FAK is sufficient to rescue and which domains of FAK are required. Other Paxillin variants to test include phosphorylation mimics and mutated versions that affect ubiquitination, nuclear export and protein-protein interactions. It would not be surprising if multiple constructs contributed to the increased organization of Laminin-111 by Paxillin and the efficacy of rescue by certain Paxillin constructs could be prioritized.

Another line of investigation regarding Paxillin-mediated Laminin-111 organization is to ask where (in what tissues) Paxillin functions. In Chapters 2 and 3, it is shown that overexpression of Paxillin in all tissues rescues boundary crossings in *nrk2b* morphant

embryos and ameliorates dystrophy in *dag1* morphant embryos, but perhaps ubiquitous Paxillin overexpression is not necessary for this effect. It is not known if Laminin-111 polymerization at the MTJ is affected by adjacent tissues that also express Laminin (neural plate, notochord (⁹³)), if Paxillin is required within tenocytes, or if Paxillin expression in muscle cells is sufficient in order to impact Laminin-111 organization. Experiments elucidating the tissue level functions of Paxillin will provide critical information for future therapeutic applications of Paxillin in diseases with BM disruptions.

Comparison of Laminin-111 antibody staining and boundary crossings in *mrk2b* morphants either transiently or stably expressing Paxillin under the control of zebrafish muscle tissue-specific promoters (¹⁸⁹⁻¹⁹¹) vs. ubiquitous promoters (Section 2.3.1.) will elucidate whether Paxillin overexpression in muscle tissue is sufficient or whether Paxillin overexpression in other cell types is necessary for Paxillin-mediated Laminin-111 organization. Other tissue types that might be involved in Laminin-111 organization via Paxillin could include tendon progenitors or adjacent tissues, such as the notochord, that could impact the ECM of muscle. If ubiquitously expressed Paxillin provided a better rescue of the *mrk2b* morphant boundary crossings than muscle-specific Paxillin expression, investigation into the roles of these other tissues in Laminin-111 organization could be pursued. This information is critical for potential translation of Paxillin gene therapy to human applications in order to balance optimal treatment efficacy with the fewest side effects possible.

4.5. Potential of the Nr2f1 Pathway in Therapeutics

laminin mutations lead to multiple diseases including myopathies, junctional epidermolysis bullosa, laryngo-oncho-cutaneous syndrome, and microcoria-congenital nephritic syndrome (¹²⁶). Due to our limited knowledge of mechanisms regulating *in vivo* Laminin assembly and polymerization and lack of tools with which to visualize this process, effective treatments for these diseases have not yet been discovered. This dissertation describes a study elucidating a novel cell-matrix adhesion pathway that is required for normal organization of Laminin-111 in zebrafish MTJ BMs and a follow-up study beginning to test the therapeutic potential of this pathway in augmenting disrupted BMs in animal models of disease. Potential therapeutics discovered using the zebrafish model system have been successfully translated into human therapies and entered into clinical trials for the treatment of Duchenne muscular dystrophy and cancer (¹⁹²⁻¹⁹⁴). Manipulation of the Nr2f1 pathway has the potential to translate into treatments for human diseases, but many more studies still need to be conducted first and thus, another future area of investigation arises.

Data are provided in this dissertation that exogenous NAD⁺ or Paxillin overexpression rescue MTJ failure and ameliorate dystrophy in zebrafish. However, these interventions occurred around the beginning of gastrulation, approximately 40 hours before boundary crossings or fiber detachment are evident. Understanding the developmental time windows when abnormal MTJ BMs can be repaired is critical information for regenerative studies and therapies for diseases affecting BM integrity.

Important questions to resolve include when exogenous NAD⁺ or Paxillin are required for normal Laminin-111 organization, whether exogenous NAD⁺ or Paxillin are sufficient to augment Laminin-111 organization after the initial MTJ BM has formed in *nrk2b* morphants, whether exogenous NAD⁺ or Paxillin are protective at all times prior to the onset of dystrophy, and whether exogenous NAD⁺ or Paxillin can exert a protective effect subsequent to the onset of dystrophy in *dag1* morphants. In order to activate the Nrk2b pathway during different developmental windows, NAD⁺ could be added to embryo rearing media at different developmental stages and a transgenic line expressing Paxillin under control of a heat shock inducible promoter (¹⁹⁵) could be generated and embryos heat shocked at different times during development. One concern with adding exogenous NAD⁺ at later developmental time points is that it may not be able to permeate through the skin. However, changes in fat metabolism were seen in zebrafish incubated in exogenous NAD⁺ starting at 3 days post fertilization (⁹⁴), suggesting that later supplementation can cause an effect. Quantification of boundary crossings in *nrk2b* morphants and dystrophic lesions in *dag1* morphants would elucidate during which developmental windows exogenous NAD⁺ or Paxillin are able to rescue MTJ failure and dystrophy. NAD⁺ could also be injected into the skeletal muscle of older zebrafish embryos if necessary. Potential outcomes include that these interventions are protective both before and after phenotypic onset or that these interventions are only protective prior to MTJ failure or muscle fiber detachment. Regardless of the outcomes, these findings will have translational science implications. These experiments could also

uncover subtle protective roles of NAD⁺ and Paxillin after disease onset and small improvements, while not cures, could improve quality of life for patients.

Although NAD⁺ and Paxillin are sufficient to reduce MTJ failure and dystrophy in zebrafish, neither treatment is tissue-specific. Attributes that make Nrk2 an attractive therapeutic option are: (1) kinases are recognized as accessible pharmacological targets, and (2) Nrk2 is specifically expressed in human adult heart and skeletal muscle⁽⁸⁴⁾, thus potentially limiting side effects of systemic drug delivery. Asking whether overexpression of Nrk2b is sufficient to ameliorate myopathy in dystrophic zebrafish is a worthy future direction to explore. A stable transgenic line expressing Nrk2b:GFP would have to be generated in order to pursue this line of investigation. Injection of *dag1* MOs into Nrk2b transgenic embryos and quantification of dystrophic lesions would elucidate whether Nrk2b overexpression is sufficient to reduce dystrophy. If Nrk2b overexpression were found to be sufficient to reduce dystrophy, experiments as described above for Paxillin overexpression to discover when during development and in which tissues Nrk2b overexpression is required would inform the therapeutic potential of Nrk2b gene therapy as a treatment for diseases where skeletal muscle BMs are compromised. There may be a dose-dependent response to Nrk2b expression. If this were the case, the relationship between Nrk2b expression levels and the degree of rescue could be analyzed and the optimum dose determined.

The Nrk2b pathway represents an exciting new approach to BM augmentation. Testing the breadth of efficacy of Nrk2b pathway activation to treat muscular dystrophies with diverse etiologies could be easily and quickly completed using the zebrafish system

relative to other animal models. It is shown in this dissertation that activation of the Nrk2b pathway ameliorates muscle degeneration in zebrafish lacking Dag1. We predict that this pathway will also be beneficial when other DGC components, or post-translational modification of Dag1, are disrupted. This could be tested by activating the Nrk2b pathway via exogenous NAD⁺ or Paxillin in *sapje/dystrophin*, *fukutin related protein* and *large2/glycosyltransferase-like 1b* morphant or mutant zebrafish and assaying dystrophic lesions per embryo.

Mutations in subunits of Collagen VI result in Bethlem myopathy or the more severe Ullrich CMD (¹⁹⁶). Mouse models of Bethlem myopathy and patients with Collagen VI myopathies have swollen mitochondria and treatment with cyclosporine A to alter mitochondrial permeability improves mitochondria structure and reduces atrophy (¹⁹⁷⁻¹⁹⁹). However, the mouse mutant resembles Bethlem myopathy and does not model the severity of Ullrich CMD. Recent data showed that although treatment with cyclosporine A reduced mitochondrial defects and cell death in zebrafish modeling Ullrich CMD, it did not improve muscle structure or restore sarcolemma integrity (²⁰⁰). Asking whether a multifaceted approach, involving addition of both cyclosporin A and NAD⁺ to the media of Collagen VI-deficient zebrafish, improves mitochondrial and muscle structure defects would further test the breadth of Nrk2b pathway efficacy in therapeutics and potentially improve current therapeutic options being researched for treatment of Collagen VI-related myopathies.

Another multifaceted approach that could be undertaken is combining Paxillin overexpression with NAD⁺ supplementation in dystrophic zebrafish. We do not know if

either of these interventions alone maximally activates the Nrk2b pathway. If these interventions only partially activate the Nrk2b pathway, they might be more effective in combination. Alternatively, these treatments in combination could turn out to be toxic. This information would be valuable in considering the therapeutic potential of the Nrk2b pathway. A further test of the breadth of the applicability of NAD⁺ and Paxillin-mediated augmentation of Laminin-111 organization would be to look at the efficacy of these interventions in diseases associated with BM disruptions other than myopathies, such as junctional epidermolysis bullosa, laryngo-oncho-cutaneous syndrome, and microcoria-congenital nephritic syndrome.

4.6. Concluding Remarks

The future directions discussed in this chapter are only a few of the possible areas of investigation that stem from the data presented in this dissertation. The sets of experiments proposed can be conducted independently of each other with regards to space and time. However, studies at individual size scales will only elucidate pieces of the whole mechanism through which the Nrk2b pathway functions in muscle development and disease. Thus, studies at all size scales and collaboration between researchers in multiple scientific disciplines will result in the most complete understanding of the Nrk2b pathway and its implications in the basic and translational sciences.

REFERENCES

1. Lu P, Takai K, Weaver VM, Werb Z. Extracellular Matrix Degradation and Remodeling in Development and Disease. *Cold Spring Harbor Perspectives in Biology*. 2011 December 1;3(12):5058.
2. Nelson C. Of extracellular matrix, scaffolds, and signaling: tissue architecture regulates development, homeostasis, and cancer. *Annual Review of Cell and Developmental Biology*. 2006 November;22(1):287–309.
3. Rozario T. The extracellular matrix in development and morphogenesis: A dynamic view [10.1016/j.ydbio.2009.10.026](https://doi.org/10.1016/j.ydbio.2009.10.026) : *Developmental Biology* | ScienceDirect.com. *Developmental biology*. 2010.
4. Cox TR, Erler JT. Remodeling and homeostasis of the extracellular matrix: implications for fibrotic diseases and cancer. *Disease models & mechanisms*. 2011 March 1;4(2):165–178.
5. Daley WP, Peters SB, Larsen M. Extracellular matrix dynamics in development and regenerative medicine. *Journal of Cell Science*. 2008 February 1;121(3):255–264.
6. Goody MF, Henry CA. Dynamic interactions between cells and their extracellular matrix mediate embryonic development. *Molecular reproduction and development*. 2010 June;77(6):475–488.
7. Bissell MJ, Hall HG, Parry G. How does the extracellular matrix direct gene expression? *Journal of theoretical biology*. 1982 November;99(1):31–68.
8. Pedrosa-Domellöf F, Tiger CF, Virtanen I, Thornell L-E, Gullberg D. Laminin Chains in Developing and Adult Human Myotendinous Junctions. *Journal of Histochemistry & Cytochemistry*. 2000 February 1;48(2):201–209.
9. Ishii H, Hayashi YK, Nonaka I, Arahata K. Electron microscopic examination of basal lamina in Fukuyama congenital muscular dystrophy. *Neuromuscular disorders : NMD*. 1997 May;7(3):191–197.
10. Osari S, Kobayashi O, Nonaka I, 8. Basement membrane abnormality in merosin-negative congenital muscular dystrophy. *Acta Neuropathologica*. 1996 January 1;91(4):332–336.
11. Vajsar J, Ackerley C, Chitayat D, Becker LE. Basal lamina abnormality in the skeletal muscle of Walker-Warburg syndrome. *Pediatric neurology*. 2000 February;22(2):139–143.

12. Sabatelli P, Columbaro M, Mura I, Capanni C, Lattanzi G, Maraldi NM, Beltràn-Valero de Barnabè D, van Bokoven H, Squarzoni S, Merlini L. Extracellular matrix and nuclear abnormalities in skeletal muscle of a patient with Walker–Warburg syndrome caused by POMT1 mutation. *Biochimica et Biophysica Acta (BBA) - Molecular Basis of Disease*. 2003 May;1638(1):57–62.
13. Morgan JE, Zammit PS. Direct effects of the pathogenic mutation on satellite cell function in muscular dystrophy. *Experimental Cell Research*. 2010 November 1;316(18):3100–3108.
14. Moll J, Barzaghi P, Lin S, Bezakova G, Lochmüller H, Engvall E, Müller U, Ruegg MA. An agrin minigene rescues dystrophic symptoms in a mouse model for congenital muscular dystrophy. *Nature*. 2001 September 20;413(6853):302–307.
15. Bentzinger CF, Barzaghi P, Lin S, Ruegg MA. Overexpression of mini-agrin in skeletal muscle increases muscle integrity and regenerative capacity in laminin- α 2-deficient mice. *The FASEB Journal*. 2005 June 1;19(8):934–942.
16. Gawlik K, Miyagoe-Suzuki Y, Ekblom P, Takeda S, Durbeej M. Laminin α 1 chain reduces muscular dystrophy in laminin α 2 chain deficient mice. *Human Molecular Genetics*. 2004 August 15;13(16):1775–1784.
17. Gawlik KI, Akerlund M, Carmignac V, Elamaa H, Durbeej M. Distinct roles for laminin globular domains in laminin α 1 chain mediated rescue of murine laminin α 2 chain deficiency. *PLoS One*. 2010;5(7):e11549.
18. Gawlik KI, Oliveira BM, Durbeej M. Transgenic expression of Laminin α 1 chain does not prevent muscle disease in the mdx mouse model for Duchenne muscular dystrophy. *The American journal of pathology*. 2011 April;178(4):1728–1737.
19. Goudenege S, Lamarre Y, Dumont N, Rousseau J, Frenette J, Skuk D, Tremblay JP. Laminin-111: a potential therapeutic agent for Duchenne muscular dystrophy. *Molecular therapy : the journal of the American Society of Gene Therapy*. 2010 December;18(12):2155–2163.
20. Meinen S, Barzaghi P, Lin S, Lochmüller H, Ruegg MA. Linker molecules between laminins and dystroglycan ameliorate laminin-2-deficient muscular dystrophy at all disease stages. *Journal of Cell Biology*. 2007 March 19;176(7):979–993.
21. Jacoby AS, Busch-Nentwich E, Bryson-Richardson RJ, Hall TE, Berger J, Berger S, Sonntag C, Sachs C, Geisler R, Stemple DL, et al. The zebrafish dystrophic mutant softy maintains muscle fibre viability despite basement membrane rupture and muscle detachment. *Development (Cambridge, England)*. 2009 October 1;136(19):3367–3376.

22. Rooney JE, Gurple PB, Burkin DJ. Laminin-111 protein therapy prevents muscle disease in the mdx mouse model for Duchenne muscular dystrophy. *Proceedings of the National Academy of Sciences*. 2009 May 12;106(19):7991–7996.
23. Rooney JE, Knapp JR, Hodges BL, Wuebbles RD, Burkin DJ. Laminin-111 protein therapy reduces muscle pathology and improves viability of a mouse model of merosin-deficient congenital muscular dystrophy. *The American journal of pathology*. 2012 April; 180(4):1593–1602.
24. Rooney J, Gurple P. Laminin-111 Restores Regenerative Capacity in a Mouse Model for α 7 Integrin Congenital Myopathy. *American Journal of Pathology*. 2009 Jan; 174(1):256-64.
25. Yurchenco PD, Tsilibary EC, Charonis AS, Furthmayr H. Laminin polymerization in vitro. Evidence for a two-step assembly with domain specificity. *Journal of Biological Chemistry*. 1985 June 25;260(12):7636–7644.
26. Yurchenco PD, Furthmayr H. Self-assembly of basement membrane collagen. *Biochemistry*. 1984 April 10;23(8):1839–1850.
27. Schwarzbauer J. Basement membrane: Putting up the barriers. *Current Biology*. 1999 April;9(7):R242–R244.
28. Henry MD, Campbell KP. A Role for Dystroglycan in Basement Membrane Assembly. *Cell*. 1998 December 11;95(6):859–870.
29. Sasaki T, Forsberg E, Bloch W, Addicks K, Fässler R, Timpl R. Deficiency of beta 1 integrins in teratoma interferes with basement membrane assembly and laminin-1 expression. *Experimental Cell Research*. 1998 January 10;238(1):70–81.
30. Aumailley M, Pesch M, Tunggal L. Altered synthesis of laminin 1 and absence of basement membrane component deposition in (beta) 1 integrin-deficient embryoid bodies. *Journal of Cell Science*. 2000;113:259-268.
31. Williamson R, Henry M, Daniels K. Dystroglycan is essential for early embryonic development: disruption of Reichert's membrane in *Dag1*-null mice. *Human molecular genetics*. 1997;6(6):831-841.
32. Stephens LEL, Sutherland AEA, Damsky CHC, 7. Deletion of beta 1 integrins in mice results in inner cell mass failure and peri-implantation lethality. *Genes & Development*. 1995 August 1;9(15):1883–1895.

33. Henry M, Satz J, Brakebusch C, Costell M, Gustafsson E, Fässler R, Campbell K. Distinct roles for dystroglycan, α 1 integrin and perlecan in cell surface laminin organization. *Journal of Cell Science*. 2001 March 15;114(6):1137–1144.
34. Carmignac V, Durbeej M. Cell-matrix interactions in muscle disease. *The Journal of Pathology*. 2012 January;226(2):200–218.
35. Colognato H, Winkelmann D. Laminin polymerization induces a receptor–cytoskeleton network. *The Journal of Cell Biology*. 1999 May 3;145(3):619–631.
36. Rooney JE, Welser JV, Dechert MA, Flintoff-Dye NL, Kaufman SJ, Burkin DJ. Severe muscular dystrophy in mice that lack dystrophin and α 7 integrin. *Journal of Cell Science*. 2006 June 1;119(Pt 11):2185–2195.
37. Guo C. Absence of α 7 integrin in dystrophin-deficient mice causes a myopathy similar to Duchenne muscular dystrophy. *Human Molecular Genetics*. 2006 January 26;15(6):989–998.
38. Allikian MJ, Hack AA, Mewborn S, Mayer U, McNally EM. Genetic compensation for sarcoglycan loss by integrin α 7 β 1 in muscle. *Journal of Cell Science*. 2004 August 1;117(17):3821–3830.
39. Ringelmann B. Expression of Laminin α 1, α 2, α 4, and α 5 Chains, Fibronectin, and Tenascin-C in Skeletal Muscle of Dystrophic 129ReJdy/dyMice. *Experimental Cell Research*. 1999 January 10;246(1):165–182.
40. Cote PD. Dystroglycan Is Not Required for Localization of Dystrophin, Syntrophin, and Neuronal Nitric-oxide Synthase at the Sarcolemma but Regulates Integrin α 7 β 1 Expression and Caveolin-3 Distribution. *Journal of Biological Chemistry*. 2001 December 6;277(7):4672–4679.
41. Banks GB, Combs AC, Chamberlain JR, Chamberlain JS. Molecular and cellular adaptations to chronic myotendinous strain injury in mdx mice expressing a truncated dystrophin. *Human Molecular Genetics*. 2008 December 15;17(24):3975–3986.
42. Burkin DJ, Wallace GQ, Nicol KJ, Kaufman DJ, Kaufman SJ. Enhanced expression of the α 7 β 1 integrin reduces muscular dystrophy and restores viability in dystrophic mice. *The Journal of Cell Biology*. 2001 March 19;152(6):1207–1218.
43. Burkin DJ, Wallace GQ, Milner DJ, Chaney EJ, Mulligan JA, Kaufman SJ. Transgenic expression of α 7 β 1 integrin maintains muscle integrity, increases regenerative capacity, promotes hypertrophy, and reduces cardiomyopathy in dystrophic mice. *The American journal of pathology*. 2005 January;166(1):253–263.

44. Doe JA, Wuebbles RD, Allred ET, Rooney JE, Elorza M, Burkin DJ. Transgenic overexpression of the $\alpha 7$ integrin reduces muscle pathology and improves viability in the dyW mouse model of merosin-deficient congenital muscular dystrophy type 1A. *Journal of Cell Science*. 2011 July 1;124(13):2287–2297.
45. Liu J, Milner DJ, Boppart MD, Ross RS, Kaufman SJ. $\beta 1D$ chain increases $\alpha 7\beta 1$ integrin and laminin and protects against sarcolemmal damage in mdx mice. *Human Molecular Genetics*. 2011 December 30.
46. Sen S, Tewari M, Zajac A, Barton E, Sweeney HL, Discher DE. Upregulation of paxillin and focal adhesion signaling follows Dystroglycan Complex deletions and promotes a hypertensive state of differentiation. *European journal of cell biology*. 2011 January;90(2-3):249–260.
47. Durbeej M, Campbell KP. Muscular dystrophies involving the dystrophin–glycoprotein complex: an overview of current mouse models. *Current opinion in genetics & development*. 2002 June;12(3):349–361.
48. Guyon JR, Steffen LS, Howell MH, Pusack TJ, Lawrence C, Kunkel LM. Modeling human muscle disease in zebrafish. *Biochimica et biophysica acta*. 2007 February; 1772(2):205–215.
49. Steffen LS, Guyon JR, Vogel ED, Beltre R, Pusack TJ, Zhou Y, Zon LI, Kunkel LM. Zebrafish orthologs of human muscular dystrophy genes. *BMC genomics*. 2007;8:79–.
50. Bassett DI. The zebrafish as a model for muscular dystrophy and congenital myopathy. *Human Molecular Genetics*. 2003 August 19;12(90002):265R–270.
51. Lieschke GJ, Currie PD. Animal models of human disease: zebrafish swim into view. *Nature Reviews Genetics*. 2007 May;8(5):353–367.
52. Devoto S, Stoiber W, Hammond C. Generality of vertebrate developmental patterns: evidence for a dermomyotome in fish. *Evol. Dev.* 2006. 8(1):101-110.
53. Devoto S. The teleost dermomyotome. *Developmental Dynamics*. 2007.
54. Blochz W. METHODS IN CELL BIOLOGY. THE ZEBRAFISH: DISEASE MODELS AND CHEMICAL SCREENS - H William Detrich, III, Monte Westerfield, Leonard I. Zon - vol. 105, Third edition, Chapter 8. 2011.
55. Charvet B, Malbouyres M, Pagnon-Minot A, Ruggiero F, Le Guellec D. Development of the zebrafish myoseptum with emphasis on the myotendinous junction. *Cell and tissue research*. 2011 December;346(3):439–449.

56. Summers AP, Koob TJ. The evolution of tendon--morphology and material properties. *Comparative biochemistry and physiology. Part A, Molecular & integrative physiology*. 2002 December;133(4):1159–1170.
57. Hynes RO. The Evolution of Cell Adhesion. *The Journal of Cell Biology*. 2000 July 24;150(2):89F–96.
58. Crawford BD, Henry CA, Clason TA, Becker AL, Hille MB. Activity and distribution of paxillin, focal adhesion kinase, and cadherin indicate cooperative roles during zebrafish morphogenesis. *Molecular biology of the cell*. 2003 August;14(8):3065–3081.
59. Hall TE, Bryson-Richardson RJ, Berger S, Jacoby AS, Cole NJ, Hollway GE, Berger J, Currie PD. The zebrafish candyfloss mutant implicates extracellular matrix adhesion failure in laminin alpha2-deficient congenital muscular dystrophy. *Proceedings of the National Academy of Sciences of the United States of America*. 2007 April 24;104(17):7092–7097.
60. Snow CJ, Henry CA. Dynamic formation of microenvironments at the myotendinous junction correlates with muscle fiber morphogenesis in zebrafish. *Gene expression patterns : GEP*. 2009 January;9(1):37–42.
61. Sztal T, Berger S, Currie PD, Hall TE. Characterization of the laminin gene family and evolution in zebrafish. *Developmental dynamics : an official publication of the American Association of Anatomists*. 2011 February;240(2):422–431.
62. Ochi H. Signaling networks that regulate muscle development: lessons from zebrafish. *Development (Cambridge, England)*. 2007.
63. Bryson-Richardson RJ, Currie PD. The genetics of vertebrate myogenesis. *Nature Reviews Genetics*. 2008 August;9(8):632–646.
64. Berger J, Berger S, Hall TE, Lieschke GJ, Currie PD. Dystrophin-deficient zebrafish feature aspects of the Duchenne muscular dystrophy pathology. *Neuromuscular disorders : NMD*. 2010 December;20(12):826–832.
65. Bassett D, Bryson-Richardson R, Daggett D. Dystrophin is required for the formation of stable muscle attachments in the zebrafish embryo. *Development (Cambridge, England)*. 2003 December 1;130(23):5851–5860.
66. Hasegawa T, Matsumura K, Hashimoto T, Ikehira H, Fukuda H, Tateno Y. [Intramuscular degeneration process in Duchenne muscular dystrophy--investigation by longitudinal MR imaging of the skeletal muscles]. *Rinshō shinkeigaku = Clinical neurology*. 1992 March;32(3):333–335.

67. Nagao H, Morimoto T, Sano N. Magnetic resonance imaging of skeletal muscle in patients with Duchenne muscular dystrophy--serial axial and sagittal section studies]. *No to hattatsu*. 1991 January;23(1):39-43.
68. Kawahara G, Karpf JA, Myers JA, Alexander MS, Guyon JR, Kunkel LM. Drug screening in a zebrafish model of Duchenne muscular dystrophy. *Proceedings of the National Academy of Sciences of the United States of America*. 2011 March 29;108(13):5331–5336.
69. Li J, Rao H, Burkin D, Kaufman SJ, Wu C. The muscle integrin binding protein (MIBP) interacts with $\alpha7\beta1$ integrin and regulates cell adhesion and laminin matrix deposition. *Developmental biology*. 2003 September 1;261(1):209–219.
70. Belenky P, Racette FG, Bogan KL, McClure JM, Smith JS, Brenner C. Nicotinamide riboside promotes Sir2 silencing and extends lifespan via Nrk and Urh1/Pnp1/Meu1 pathways to NAD⁺. *Cell*. 2007 May 4;129(3):473–484.
71. Bieganowski P, Brenner C. Discoveries of nicotinamide riboside as a nutrient and conserved NRK genes establish a Preiss-Handler independent route to NAD⁺ in fungi and humans. *Cell*. 2004 May 14;117(4):495–502.
72. Tempel W, Rabeh WM, Bogan KL, Belenky P, Wojcik M, Seidle HF, Nedyalkova L, Yang T, Sauve AA, Park H-W, et al. Nicotinamide Riboside Kinase Structures Reveal New Pathways to NAD. *Plos Biology*. 2007;5(10):e263.
73. Geiger B, Bershadsky A, Pankov R, Yamada KM. Transmembrane crosstalk between the extracellular matrix--cytoskeleton crosstalk. *Nature Reviews Molecular Cell Biology*. 2001 November;2(11):793–805.
74. Lock J, Wehrle-Haller B. Cell–matrix adhesion complexes: master control machinery of cell migration. *Seminars in cancer biology*. 2008.
75. Schaller M, Borgman C. pp125FAK a structurally distinctive protein-tyrosine kinase associated with focal adhesions. *PNAS*. 1992 June; 89(11):5192-5196.
76. Chatzizacharias NA, Kouraklis GP, Theocharis SE. Clinical significance of FAK expression in human neoplasia. *Histology and histopathology*. 2008 May;23(5):629–650.
77. Ilić D, Furuta Y, Kanazawa S, Takeda N, Sobue K, Nakatsuji N, Nomura S, Fujimoto J, Okada M, Yamamoto T. Reduced cell motility and enhanced focal adhesion contact formation in cells from FAK-deficient mice. *Nature*. 1995 October 12;377(6549):539–544.

78. Quach NL, Rando TA. Focal adhesion kinase is essential for costamereogenesis in cultured skeletal muscle cells. *Developmental biology*. 2006 May 1;293(1):38–52.
79. Gordon SE, Flück M, Booth FW. Selected Contribution: Skeletal muscle focal adhesion kinase, paxillin, and serum response factor are loading dependent. *Journal of Applied Physiology*. 2001 March;90(3):1174–83; discussion 1165.
80. Digman MA, Brown CM, Horwitz AR, Mantulin WW, Gratton E. Paxillin dynamics measured during adhesion assembly and disassembly by correlation spectroscopy. *Biophysical journal*. 2008 April 1;94(7):2819–2831.
81. Webb DJ, Donais K, Whitmore LA, Thomas SM, Turner CE, Parsons JT, Horwitz AF. FAK-Src signalling through paxillin, ERK and MLCK regulates adhesion disassembly. *Nature Cell Biology*. 2004 February;6(2):154–161.
82. Kanagawa M, Toda T. The genetic and molecular basis of muscular dystrophy: roles of cell-matrix linkage in the pathogenesis. *Journal of human genetics*. 2006;51(11):915–926.
83. Schessl J, Zou Y, Bönnemann CG. Congenital muscular dystrophies and the extracellular matrix. *Seminars in pediatric neurology*. 2006 June;13(2):80–89.
84. Li J, Mayne R, Wu C. A novel muscle-specific beta 1 integrin binding protein (MIBP) that modulates myogenic differentiation. *The Journal of Cell Biology*. 1999 December 27;147(7):1391–1398.
85. Sadkowski T, Jank M, Zwierzchowski L, Siadkowska E, Oprzadek J, Motyl T. Gene expression profiling in skeletal muscle of Holstein-Friesian bulls with single-nucleotide polymorphism in the myostatin gene 5'-flanking region. *Journal of applied genetics*. 2008;49(3):237–250.
86. Stockwin LH, Vistica DT, Kenney S, Schrupp DS, Butcher DO, Raffeld M, Shoemaker RH. Gene expression profiling of alveolar soft-part sarcoma (ASPS). *BMC cancer*. 2009;9:22.
87. Belenky P, Bogan KL, Brenner C. NAD⁺ metabolism in health and disease. *Trends in biochemical sciences*. 2007 January;32(1):12–19.
88. Belenky P, Christensen KC, Gazzaniga F, Pletnev AA, Brenner C. Nicotinamide riboside and nicotinic acid riboside salvage in fungi and mammals. Quantitative basis for Urh1 and purine nucleoside phosphorylase function in NAD⁺ metabolism. *Journal of Biological Chemistry*. 2009 January 2;284(1):158–164.

89. Bogan KL, Brenner C. Nicotinic acid, nicotinamide, and nicotinamide riboside: a molecular evaluation of NAD⁺ precursor vitamins in human nutrition. *Annual review of nutrition*. 2008;28:115–130.
90. Kimmel CB, Ballard WW, Kimmel SR, Ullmann B, Schilling TF. Stages of embryonic development of the zebrafish. *Developmental dynamics : an official publication of the American Association of Anatomists*. 2005 February 3;203(3):253–310.
91. Kwan KM, Fujimoto E, Grabher C, Mangum BD, Hardy ME, Campbell DS, Parant JM, Yost HJ, Kanki JP, Chien C-B. The Tol2kit: a multisite gateway-based construction kit for Tol2 transposon transgenesis constructs. *Developmental dynamics : an official publication of the American Association of Anatomists*. 2007 November;236(11):3088–3099.
92. Parsons M, Campos I, Hirst E, Stemple D. Removal of dystroglycan causes severe muscular dystrophy in zebrafish embryos. *Development (Cambridge, England)*. 2002;129(14):3505–3512.
93. Parsons MJ, Pollard SM, Saúde L, Feldman B, Coutinho P, Hirst EMA, Stemple DL. Zebrafish mutants identify an essential role for laminins in notochord formation. *Development (Cambridge, England)*. 2002 July;129(13):3137–3146.
94. Jones KS, Alimov AP, Rilo HL, Jandacek RJ, Woollett LA, Penberthy WT. A high throughput live transparent animal bioassay to identify non-toxic small molecules or genes that regulate vertebrate fat metabolism for obesity drug development. *Nutrition & Metabolism*. 2008;5:23.
95. Link V, Shevchenko A, Heisenberg C-P. Proteomics of early zebrafish embryos. *BMC developmental biology*. 2006;6:1.
96. Henry CA, McNulty IM, Durst WA, Munchel SE, Amacher SL. Interactions between muscle fibers and segment boundaries in zebrafish. *Developmental biology*. 2005 November 15;287(2):346–360.
97. Arnedo A, Decoster N, Roux S. A wavelet-based method for multifractal image analysis. I. Methodology and test applications on isotropic and anisotropic random rough surfaces. *European Physical Journal B*. 2000;15(3):567–600.
98. Khalil A, Joncas G, Nekka F, Kestener P, Arnedo A. Morphological Analysis of H iFeatures. II. Wavelet-based Multifractal Formalism. *The Astrophysical Journal Supplement Series*. 2006 August;165(2):512–550.

99. Thisse B, Heyer V, Lux A, Alunni V, Degraive A, Seiliez I, Kirchner J, Parkhill J-P, Thisse C. Spatial and temporal expression of the zebrafish genome by large-scale in situ hybridization screening. *Methods in cell biology*. 2004;77:505–519.
100. Eisen JS, Smith JC. Controlling morpholino experiments: don't stop making antisense. *Development (Cambridge, England)*. 2008 May;135(10):1735–1743.
101. Robu ME, Larson JD, Nasevicius A, Beiraghi S, Brenner C, Farber SA, Ekker SC. p53 activation by knockdown technologies. *PLoS genetics*. 2007 May 25;3(5):e78.
102. Peterson MT, Henry CA. Hedgehog signaling and laminin play unique and synergistic roles in muscle development. *Developmental dynamics : an official publication of the American Association of Anatomists*. 2010 March;239(3):905–913.
103. Snow CJ, Goody M, Kelly MW, Oster EC, Jones R, Khalil A, Henry CA. Time-lapse analysis and mathematical characterization elucidate novel mechanisms underlying muscle morphogenesis. *PLoS genetics*. 2008;4(10):e1000219.
104. Lunt SJ, Chaudary N, Hill RP. The tumor microenvironment and metastatic disease. *Clinical & experimental metastasis*. 2009;26(1):19–34.
105. White ES, Baralle FE, Muro AF. New insights into form and function of fibronectin splice variants. *The Journal of Pathology*. 2008 September;216(1):1–14.
106. Hassa PO, Hottiger MO. The diverse biological roles of mammalian PARPS, a small but powerful family of poly-ADP-ribose polymerases. *Frontiers in bioscience : a journal and virtual library*. 2008;13:3046–3082.
107. Kahn RA. Toward a model for Arf GTPases as regulators of traffic at the Golgi. *FEBS letters*. 2009 December 3;583(23):3872–3879.
108. Keppler BR, Archer TK. Chromatin-modifying enzymes as therapeutic targets--Part 1. Expert opinion on therapeutic targets. 2008 October;12(10):1301–1312.
109. Koch-Nolte F, Kernstock S, Mueller-Dieckmann C, Weiss MS, Haag F. Mammalian ADP-ribosyltransferases and ADP-ribosylhydrolases. *Frontiers in bioscience : a journal and virtual library*. 2008;13:6716–6729.
110. Myers KR, Casanova JE. Regulation of actin cytoskeleton dynamics by Arf-family GTPases. *Trends in cell biology*. 2008 April;18(4):184–192.
111. Sabe H, Onodera Y, Mazaki Y, Hashimoto S. ArfGAP family proteins in cell adhesion, migration and tumor invasion. *Current opinion in cell biology*. 2006 October; 18(5):558–564.

112. Saporita AJ, Maggi LB, Apicelli AJ, Weber JD. Therapeutic targets in the ARF tumor suppressor pathway. *Current medicinal chemistry*. 2007;14(17):1815–1827.
113. Zhao Z, Gruszczynska-Biegala J, Zolkiewska A. ADP-ribosylation of integrin alpha7 modulates the binding of integrin alpha7beta1 to laminin. *Biochem J*. 2005 January 1;385(Pt 1):309–317.
114. Zolkiewska A, Moss J. The alpha 7 integrin as a target protein for cell surface mono-ADP-ribosylation in muscle cells. *Muscle Biophysics: From Molecules to Cells*. 1997;419:297–303.
115. Waller JC, Dhanoa PK, Schumann U, Mullen RT, Snedden WA. Subcellular and tissue localization of NAD kinases from Arabidopsis: compartmentalization of de novo NADP biosynthesis. *Planta*. 2010 January;231(2):305–317.
116. Tariq M, Azeem Z, Ali G, Chishti MS, Ahmad W. Mutation in the HPGD gene encoding NAD⁺ dependent 15-hydroxyprostaglandin dehydrogenase underlies isolated congenital nail clubbing (ICNC). *Journal of medical genetics*. 2009 January;46(1):14–20.
117. Bassett D, Currie P. Identification of a zebrafish model of muscular dystrophy. In: Vol. 31. 2004. pp. 537–540.
118. Nixon S, Wegner J, Ferguson C, Mery P, Hancock J, Currie P, Key B, Westerfield M, Parton R. Zebrafish as a model for caveolin-associated muscle disease; caveolin-3 is required for myofibril organization and muscle cell patterning. *Human Molecular Genetics*. 2005;14(13):1727–1743.
119. Postel R, Vakeel P, Topczewski J, Knöll R, Bakkers J. Zebrafish integrin-linked kinase is required in skeletal muscles for strengthening the integrin-ECM adhesion complex. *Developmental biology*. 2008 June 1;318(1):92–101.
120. Steffen LS, Guyon JR, Vogel ED, Howell MH, Zhou Y, Weber GJ, Zon LI, Kunkel LM. The zebrafish runzel muscular dystrophy is linked to the titin gene. *Developmental biology*. 2007 September 15;309(2):180–192.
121. Thornhill P, Bassett D, Lochmüller H, Bushby K, Straub V. Developmental defects in a zebrafish model for muscular dystrophies associated with the loss of fukutin-related protein (FKRP). *Brain : a journal of neurology*. 2008 June;131(Pt 6):1551–1561.
122. Lin Y-Y, White RJ, Torelli S, Cirak S, Muntoni F, Stemple DL. Zebrafish Fukutin family proteins link the unfolded protein response with dystroglycanopathies. *Human Molecular Genetics*. 2011 May 1;20(9):1763–1775.

123. Kudo H, Amizuka N, Araki K, Inohaya K, Kudo A. Zebrafish periostin is required for the adhesion of muscle fiber bundles to the myoseptum and for the differentiation of muscle fibers. *Developmental biology*. 2004 March 15;267(2):473–487.
124. Pagnon-Minot A, Malbouyres M, Haftek-Terreau Z, Kim HR, Sasaki T, Thisse C, Thisse B, Ingham PW, Ruggiero F, Le Guellec D. Collagen XV, a novel factor in zebrafish notochord differentiation and muscle development. *Developmental biology*. 2008 April 1;316(1):21–35.
125. Deakin NO, Turner CE. Paxillin comes of age. *Journal of Cell Science*. 2008 August 1;121(Pt 15):2435–2444.
126. Tzu J, Marinkovich MP. Bridging structure with function: Structural, regulatory, and developmental role of laminins. *The International Journal of Biochemistry & Cell Biology*. 2008 January;40(2):199–214.
127. Hagel M, George EL, Kim A, Tamimi R, Opitz SL, Turner CE, Imamoto A, Thomas SM. The adaptor protein paxillin is essential for normal development in the mouse and is a critical transducer of fibronectin signaling. *Molecular and Cellular Biology*. 2002 February;22(3):901–915.
128. Wade R, Bohl J, Vande Pol S. Paxillin null embryonic stem cells are impaired in cell spreading and tyrosine phosphorylation of focal adhesion kinase. *Oncogene*. 2002 January 3;21(1):96–107.
129. Bertolucci CM, Guibao CD, Zheng J. Structural features of the focal adhesion kinase-paxillin complex give insight into the dynamics of focal adhesion assembly. *Protein science : a publication of the Protein Society*. 2005 March;14(3):644–652.
130. Gao G, Prutzman KC, King ML, Scheswohl DM, DeRose EF, London RE, Schaller MD, Campbell SL. NMR solution structure of the focal adhesion targeting domain of focal adhesion kinase in complex with a paxillin LD peptide: evidence for a two-site binding model. *Journal of Biological Chemistry*. 2004 February 27;279(9):8441–8451.
131. Thomas JW. The Role of Focal Adhesion Kinase Binding in the Regulation of Tyrosine Phosphorylation of Paxillin. *Journal of Biological Chemistry*. 1999 December 17;274(51):36684–36692.
132. Scheswohl DM, Harrell JR, Rajfur Z, Gao G, Campbell SL, Schaller MD. Multiple paxillin binding sites regulate FAK function. *Journal of molecular signaling*. 2008;3:1.
133. Cooper WJ, Albertson RC. Quantification and variation in experimental studies of morphogenesis. *Developmental biology*. 2008 September 15;321(2):295–302.

134. Albertson RC, Yelick PC. Fgf8 haploinsufficiency results in distinct craniofacial defects in adult zebrafish. *Developmental biology*. 2007 June 15;306(2):505–515.
135. Briguët A, Courdier-Fruh I, Foster M, Meier T, Magyar JP. Histological parameters for the quantitative assessment of muscular dystrophy in the mdx-mouse. *Neuromuscular Disorders*. 2004 October;14(10):675–682.
136. Park TJ, Mitchell BJ, Abitua PB, Kintner C, Wallingford JB. Dishevelled controls apical docking and planar polarization of basal bodies in ciliated epithelial cells. *Nature genetics*. 2008 July;40(7):871–879.
137. Yin C, Kiskowski M, Pouille P-A, Farge E, Solnica-Krezel L. Cooperation of polarized cell intercalations drives convergence and extension of presomitic mesoderm during zebrafish gastrulation. *Journal of Cell Biology*. 2008 January 14;180(1):221–232.
138. Ibraghimov-Beskrovnaya OO, Ervasti JM, Leveille CJC, Slaughter CAC, Sernett SWS, Campbell KPK. Primary structure of dystrophin-associated glycoproteins linking dystrophin to the extracellular matrix. *Nature*. 1992 February 20;355(6362):696–702.
139. Gee SHS, Montanaro FF, Lindenbaum MHM, Carbonetto SS. Dystroglycan-alpha, a dystrophin-associated glycoprotein, is a functional agrin receptor. *Cell*. 1994 June 3;77(5):675–686.
140. Yamada HH, Shimizu TT, Tanaka TT, Campbell KPK, Matsumura KK. Dystroglycan is a binding protein of laminin and merosin in peripheral nerve. *FEBS letters*. 1994 September 19;352(1):49–53.
141. Ervasti JM, Campbell KP. A role for the dystrophin-glycoprotein complex as a transmembrane linker between laminin and actin. *The Journal of Cell Biology*. 1993 August;122(4):809–823.
142. Frost AR, Böhm SV, Sewduth RN, Josifova D, Ogilvie CM, Izatt L, Roberts RG. Heterozygous deletion of a 2-Mb region including the dystroglycan gene in a patient with mild myopathy, facial hypotonia, oral-motor dyspraxia and white matter abnormalities. *European journal of human genetics : EJHG*. 2010 March 17;18(7):852–855.
143. Hara Y, Balci-Hayta B, Yoshida-Moriguchi T, Kanagawa M, Beltrán-Valero de Bernabé D, Gündeşli H, Willer T, Satz JS, Crawford RW, Burden SJ, et al. A dystroglycan mutation associated with limb-girdle muscular dystrophy. *The New England journal of medicine*. 2011 March 10;364(10):939–946.
144. Inamori K-I, Yoshida-Moriguchi T, Hara Y, Anderson ME, Yu L, Campbell KP. Dystroglycan function requires xylosyl- and glucuronyltransferase activities of LARGE. *Science*. 2012 January 6;335(6064):93–96.

145. Godfrey C, Foley AR, Clement E, Muntoni F. Dystroglycanopathies: coming into focus. *Current opinion in genetics & development*. 2011 June 1;21(3):278–285.
146. Mercuri E, Messina S, Bruno C, Mora M, Pegoraro E, Comi GP, D'Amico A, Aiello C, Biancheri R, Berardinelli A, et al. Congenital muscular dystrophies with defective glycosylation of dystroglycan: a population study. *Neurology*. 2009 May 26;72(21):1802–1809.
147. Jimenez-Mallebrera C, Torelli S, Feng L, Kim J, Godfrey C, Clement E, Mein R, Abbs S, Brown SC, Campbell KP, et al. A comparative study of alpha-dystroglycan glycosylation in dystroglycanopathies suggests that the hypoglycosylation of alpha-dystroglycan does not consistently correlate with clinical severity. *Brain pathology (Zurich, Switzerland)*. 2009 October;19(4):596–611.
148. Moore CJ, Goh HT, Hewitt JE. Genes required for functional glycosylation of dystroglycan are conserved in zebrafish. *Genomics*. 2008 September;92(3):159–167.
149. Han R, Kanagawa M, Yoshida-Moriguchi T, Rader EP, Ng RA, Michele DE, Muirhead DE, Kunz S, Moore SA, Iannaccone ST, et al. Inaugural Article: Basal lamina strengthens cell membrane integrity via the laminin G domain-binding motif of α -dystroglycan. *Proceedings of the National Academy of Sciences*. 2009 August 4;106(31):12573–12579.
150. Mayer U, Saher G, Fässler R, Bornemann A, Echtermeyer F, Mark HVD, Miosge N, Pösch E, Mark KVD. Absence of integrin $\alpha 7$ causes a novel form of muscular dystrophy. *Nature genetics*. 1997 November;17(3):318–323.
151. Van Der Flier A, Gaspar A. Spatial and temporal expression of the $\beta 1 D$ integrin during mouse development. *Dev Dyn*. 1997 Dec;210(4):472-86.
152. Goody MF, Kelly MW, Lessard KN, Khalil A, Henry CA. Nr2b-mediated NAD⁺ production regulates cell adhesion and is required for muscle morphogenesis in vivo: Nr2b and NAD⁺ in muscle morphogenesis. *Developmental biology*. 2010 August 15;344(2):809–826.
153. Wiellette E, Grinblat Y, Austen M, Hirsinger E. Combined haploid and insertional mutation screen in the zebrafish. *genesis*. 2004.
154. Granato M, Van Eeden F, Schach U, Trowe T. Genes controlling and mediating locomotion behavior of the zebrafish embryo and larva. *Development*. 1996 123; 399-413.

155. Hayashi YK, Chou F-L, Engvall E, Ogawa M, Matsuda C, Hirabayashi S, Yokochi K, Ziober BL, Kramer RH, Kaufman SJ, et al. Mutations in the integrin $\alpha 7$ gene cause congenital myopathy. *Nature genetics*. 1998 May;19(1):94–97.
156. Humphries JD, Byron A, Humphries MJ. Integrin ligands at a glance. *Journal of Cell Science*. 2006 October 1;119(19):3901–3903.
157. Terpe HJ, Stark H, Ruiz P, Imhof BA. Alpha 6 integrin distribution in human embryonic and adult tissues. *Histochemistry and Cell Biology*. 1994 January;101(1):41–49.
158. Bajanca F, Luz M, Raymond K, Martins GG, Sonnenberg A, Tajbakhsh S, Buckingham M, Thorsteinsdóttir S. Integrin $\alpha 6\beta 1$ -laminin interactions regulate early myotome formation in the mouse embryo. *Development (Cambridge, England)*. 2006 May;133(9):1635–1644.
159. Wilschut KJ, van Tol HTA, Arkesteijn GJA, Haagsman HP, Roelen BAJ. Alpha 6 integrin is important for myogenic stem cell differentiation. *Stem cell research*. 2011 September;7(2):112–123.
160. Wilschut KJ, Haagsman HP, Roelen BAJ. Extracellular matrix components direct porcine muscle stem cell behavior. *Experimental Cell Research*. 2010 February 1;316(3):341–352.
161. Castaldo C, Di Meglio F, Nurzynska D, Romano G, Maiello C, Bancone C, Müller P, Böhm M, Cotrufo M, Montagnani S. CD117-positive cells in adult human heart are localized in the subepicardium, and their activation is associated with laminin-1 and $\alpha 6$ integrin expression. *Stem cells (Dayton, Ohio)*. 2008 July;26(7):1723–1731.
162. Dolez M, Nicolas J-F, Hirsinger E. Laminins, via heparan sulfate proteoglycans, participate in zebrafish myotome morphogenesis by modulating the pattern of Bmp responsiveness. *Development (Cambridge, England)*. 2011 January;138(1):97–106.
163. Serena E, Zatti S, Reghelin E, Pasut A, Cimetta E, Elvassore N. Soft substrates drive optimal differentiation of human healthy and dystrophic myotubes. *Integrative biology : quantitative biosciences from nano to macro*. 2010 April 7;2(4):193–201.
164. Georges-Labouesse E, Messaddeq N, Yehia G. Absence of integrin $\alpha 6$ leads to epidermolysis bullosa and neonatal death in mice. *Nature genetics*. 1996.
165. Spiczka KS, Yeaman C. Ral-regulated interaction between Sec5 and paxillin targets Exocyst to focal complexes during cell migration. *Journal of Cell Science*. 2008 September 1;121(Pt 17):2880–2891.

166. Mazaki Y. Paxillin Isoforms in Mouse. LACK OF THE gamma ISOFORM AND DEVELOPMENTALLY SPECIFIC beta ISOFORM EXPRESSION. *Journal of Biological Chemistry*. 1998 August 28;273(35):22435–22441.
167. Eliasson M, Sampei K, Mandir A. Poly (ADP-ribose) polymerase gene disruption renders mice resistant to cerebral ischemia. *Nature*. 1997.
168. Ieraci A, Herrera DG. Nicotinamide protects against ethanol-induced apoptotic neurodegeneration in the developing mouse brain. *PLoS medicine*. 2006 April;3(4):e101.
169. ALTSCHUL R, HOFFER A, STEPHEN JD. Influence of nicotinic acid on serum cholesterol in man. *Archives of Biochemistry and Biophysics*. 1955 February;54(2):558–559.
170. Hausenloy DJ, Yellon DM. Enhancing cardiovascular disease risk reduction: raising high-density lipoprotein levels. *Current opinion in cardiology*. 2009 September;24(5):473–482.
171. Shehadah A, Chen J, Zacharek A, Cui Y, Ion M, Roberts C, Kapke A, Chopp M. Niaspan treatment induces neuroprotection after stroke. *Neurobiology of disease*. 2010 October;40(1):277–283.
172. Cho K-H, Kim H-J, Kamanna VS, Vaziri ND. Niacin improves renal lipid metabolism and slows progression in chronic kidney disease. *Biochimica et biophysica acta*. 2010 January;1800(1):6–15.
173. Sastry SK, Lakonishok M, Thomas DA, Muschler J, Horwitz AF. Integrin alpha subunit ratios, cytoplasmic domains, and growth factor synergy regulate muscle proliferation and differentiation. *Journal of Cell Biology*. 1996 April;133(1):169–184.
174. Sastry SK. Quantitative Changes in Integrin and Focal Adhesion Signaling Regulate Myoblast Cell Cycle Withdrawal. *The Journal of Cell Biology*. 1999 March 22;144(6):1295–1309.
175. Henderson L, Deodhar T, Krehl W. FACTORS AFFECTING THE GROWTH OF RATS RECEIVING NIACIN-TRYPTOPHAN-DEFICIENT DIETS. *Journal of Biological Chemistry*. 1947.
176. Nikiforov A, Dölle C, Niere M, Ziegler M. Pathways and subcellular compartmentation of NAD biosynthesis in human cells: from entry of extracellular precursors to mitochondrial NAD generation. *Journal of Biological Chemistry*. 2011 June 17;286(24):21767–21778.

177. Di Lisa F, Ziegler M. Pathophysiological relevance of mitochondria in NAD(+) metabolism. *FEBS letters*. 2001 March 9;492(1-2):4–8.
178. Anderson RM, Bitterman KJ, Wood JG, Medvedik O, Cohen H, Lin SS, Manchester JK, Gordon JI, Sinclair DA. Manipulation of a nuclear NAD⁺ salvage pathway delays aging without altering steady-state NAD⁺ levels. *Journal of Biological Chemistry*. 2002 May 24;277(21):18881–18890.
179. Revollo JR, Grimm AA, Imai S-I. The NAD biosynthesis pathway mediated by nicotinamide phosphoribosyltransferase regulates Sir2 activity in mammalian cells. *Journal of Biological Chemistry*. 2004 December 3;279(49):50754–50763.
180. Krzysik-Walker SM, Hadley JA, Pesall JE, McFarland DC, Vasilatos-Younken R, Ramachandran R. Nampt/visfatin/PBEF affects expression of myogenic regulatory factors and is regulated by interleukin-6 in chicken skeletal muscle cells. *Comparative biochemistry and physiology. Part A, Molecular & integrative physiology*. 2011 April 22.
181. Zolkiewska A. Ecto-ADP-ribose transferases: cell-surface response to local tissue injury. *Physiology (Bethesda, Md.)*. 2005 December;20:374–381.
182. Petit V, Boyer B, Lentz D, Turner CE, Thiery JP, Vallés AM. Phosphorylation of tyrosine residues 31 and 118 on paxillin regulates cell migration through an association with CRK in NBT-II cells. *Journal of Cell Biology*. 2000 March 6;148(5):957–970.
183. Brown MC, Turner CE. Paxillin: adapting to change. *Physiological Reviews*. 2004 October;84(4):1315–1339.
184. Pasapera AM, Schneider IC, Rericha E, Schlaepfer DD, Waterman CM. Myosin II activity regulates vinculin recruitment to focal adhesions through FAK-mediated paxillin phosphorylation. *Journal of Cell Biology*. 2010 March 22;188(6):877–890.
185. Cortesio CL, Boateng LR, Piazza TM, Bennin DA, Huttenlocher A. Calpain-mediated proteolysis of paxillin negatively regulates focal adhesion dynamics and cell migration. *Journal of Biological Chemistry*. 2011 March 25;286(12):9998–10006.
186. Vindis C, Teli T, Cerretti DP, Turner CE, Huynh-Do U. EphB1-mediated cell migration requires the phosphorylation of paxillin at Tyr-31/Tyr-118. *Journal of Biological Chemistry*. 2004 July 2;279(27):27965–27970.
187. Badowski C, Pawlak G, Grichine A, Chabadel A, Oddou C, Jurdic P, Pfaff M, Albigès-Rizo C, Block MR. Paxillin phosphorylation controls invadopodia/podosomes spatiotemporal organization. *Molecular biology of the cell*. 2008 February;19(2):633–645.

188. Tsubouchi A, Sakakura J, Yagi R, Mazaki Y, Schaefer E, Yano H, Sabe H. Localized suppression of RhoA activity by Tyr31/118-phosphorylated paxillin in cell adhesion and migration. *The Journal of Cell Biology*. 2002 November 25;159(4):673–683.
189. Chen Y-H, Wang Y-H, Chang M-Y, Lin C-Y, Weng C-W, Westerfield M, Tsai H-J. Multiple upstream modules regulate zebrafish myf5 expression. *BMC developmental biology*. 2007;7:1.
190. Higashijima S, Okamoto H, Ueno N, Hotta Y, Eguchi G. High-frequency generation of transgenic zebrafish which reliably express GFP in whole muscles or the whole body by using promoters of zebrafish origin. *Developmental biology*. 1997 December 15;192(2):289–299.
191. Ju B, Chong SW, He J, Wang X, Xu Y, Wan H, Tong Y, Yan T, Korzh V, Gong Z. Recapitulation of fast skeletal muscle development in zebrafish by transgenic expression of GFP under the mylz2 promoter. *Developmental dynamics : an official publication of the American Association of Anatomists*. 2003 May;227(1):14–26.
192. Kinali M, Arechavala-Gomez V, Feng L, Cirak S, Hunt D, Adkin C, Guglieri M, Ashton E, Abbs S, Nihoyannopoulos P, et al. Local restoration of dystrophin expression with the morpholino oligomer AVI-4658 in Duchenne muscular dystrophy: a single-blind, placebo-controlled, dose-escalation, proof-of-concept study. *Lancet neurology*. 2009 October;8(10):918–928.
193. Cirak S, Arechavala-Gomez V, Guglieri M, Feng L, Torelli S, Anthony K, Abbs S, Garralda ME, Bourke J, Wells DJ, et al. Exon skipping and dystrophin restoration in patients with Duchenne muscular dystrophy after systemic phosphorodiamidate morpholino oligomer treatment: an open-label, phase 2, dose-escalation study. *The Lancet*. 2011 August;378(9791):595–605.
194. Lacadie S, Li P, Taylor A, Zon L. Small molecule screening in zebrafish: swimming in potential drug therapies. *WIREs Developmental Biology*. 2012.
195. Adám A, Bártfai R, Lele Z, Krone PH, Orbán L. Heat-inducible expression of a reporter gene detected by transient assay in zebrafish. *Experimental Cell Research*. 2000 April 10;256(1):282–290.
196. Bönnemann CG. The collagen VI-related myopathies Ullrich congenital muscular dystrophy and Bethlem myopathy. *Handbook of clinical neurology* / edited by P.J. Vinken and G.W. Bruyn. 2011;101:81–96.
197. Bernardi P, Bonaldo P. Dysfunction of mitochondria and sarcoplasmic reticulum in the pathogenesis of collagen VI muscular dystrophies. *Annals of the New York Academy of Sciences*. 2008 December;1147:303–311.

198. Merlini L, Angelin A, Tiepolo T, Braghetta P, Sabatelli P, Zamparelli A, Ferlini A, Maraldi NM, Bonaldo P, Bernardi P. Cyclosporin A corrects mitochondrial dysfunction and muscle apoptosis in patients with collagen VI myopathies. *Proceedings of the National Academy of Sciences*. 2008 April 1;105(13):5225–5229.
199. Irwin WA, Bergamin N, Sabatelli P, Reggiani C, Megighian A, Merlini L, Braghetta P, Columbaro M, Volpin D, Bressan GM, et al. Mitochondrial dysfunction and apoptosis in myopathic mice with collagen VI deficiency. *Nature genetics*. 2003 December;35(4): 367–371.
200. Telfer WR, Busta AS, Bonnemann CG, Feldman EL, Dowling JJ. Zebrafish models of collagen VI-related myopathies. *Human Molecular Genetics*. 2010 June 15;19(12): 2433–2444.

Dynamic Interactions Between Cells and Their Extracellular Matrix Mediate Embryonic Development

MICHELLE F. GOODY AND CLARISSA A. HENRY*

School of Biology and Ecology, University of Maine, Orono, Maine



SUMMARY

Cells and their surrounding extracellular matrix microenvironment interact throughout all stages of life. Understanding the continuously changing scope of cell-matrix interactions *in vivo* is crucial to garner insights into both congenital birth defects and disease progression. A current challenge in the field of developmental biology is to adapt *in vitro* tools and rapidly evolving imaging technology to study cell-matrix interactions in a complex 4-D environment. In this review, we highlight the dynamic modulation of cell-matrix interactions during development. We propose that individual cell-matrix adhesion proteins are best considered as complex proteins that can play multiple, often seemingly contradictory roles, depending upon the context of the microenvironment. In addition, cell-matrix proteins can also exert different short versus long term effects. It is thus important to consider cell behavior in light of the microenvironment because of the constant and dynamic reciprocal interactions occurring between them. Finally, we suggest that analysis of cell-matrix interactions at multiple levels (molecules, cells, tissues) *in vivo* is critical for an integrated understanding because different information can be acquired from all size scales.

[R]emodeling of the ECM allows cells to integrate signaling and differentiation with the structure of their local microenvironment.

* Corresponding author:
School of Biology and Ecology
University of Maine
5735 Hitchner Hall Room 217
Orono, ME, 04469-5735.
E-mail:
clarissa.henry@umit.maine.edu

Mol. Reprod. Dev. 77: 475–488, 2010. © 2010 Wiley-Liss, Inc.

Published online 27 January 2010 in Wiley InterScience
(www.interscience.wiley.com).
DOI 10.1002/mrd.21157

Received 13 November 2009; Accepted 10 December 2009

INTRODUCTION

The extracellular matrix (ECM) was once thought to be merely a scaffold that occupied the spaces between cells in multicellular organisms. It was thought that ECM was only required for cell proliferation and inhibition of programmed cell death. However, the ECM is now recognized as a complex and dynamic structure that is critical for normal development and physiology. Cells interact constantly with the ECM: they adhere to/disengage from the ECM and secrete proteins that modify the ECM environment. Complex and changing cell–ECM interactions mediate cell survival, apoptosis, division, differentiation, and are a hallmark of embryonic development.

Although all tissues contain ECM, the composition of the ECM in different tissues varies tremendously. The ECM provides physical support to an organism and fills the space between cells and tissues. Not only does the ECM provide a

three-dimensional substructure for cell adhesion and movement, but the ECM also acts as a storage compartment for signaling molecules. Broadly, the ECM can be thought of as a hydrated meshwork comprised of proteins with different biophysical functions. The relative proportion of proteins with different physical characteristics generates different ECMs with varying biomechanical properties. The ECM in skin is fairly elastic, the ECM in bone is very stiff, and ECM stiffness/elasticity varies in connective tissues like tendons. Thus, there is an exquisite tissue specificity to ECM components that reflects the biophysical requirements of each tissue—the epitome of coordination between form and function.

Abbreviations: CMAC = cell matrix adhesion complex; ECM = extracellular matrix; FA = focal adhesion; FB = fibrillar adhesions; FC = focal complex; FGF(R) = fibroblast growth factor (receptor); Fn = fibronectin; GAG = glycosaminoglycan; MMP = matrix metalloprotease; PCP = planar cell polarity

© 2010 WILEY-LISS, INC.

Why is regulation of the interactions between cells and the ECM critical? This can perhaps best be understood with an imperfect (but informative) analogy. Imagine a cell as a hiker who can run up a well maintained gentle slope, painstakingly scramble up a steep slope, don crampons and rope up with other hikers to climb Mt. Rainier, or anything in between. In the case of the hiker, many choices are made: where to start, where to finish, how to get there, what footwear and clothing is most appropriate for the conditions, etc. The initial decision to hike up an easy climb in good weather can turn disastrous if conditions change and the hiker must adjust their path and/or clothing and gear.

Although migrating cells do not “choose” their path and instead follow their genetic program, their behavior is complex and modified by constant interactions with the ECM. Cells can migrate individually or in groups. The speed and directionality of migration are critically dependent upon the extracellular environment. Migration tends to be slower in highly adhesive environments and faster in less adhesive environments. Cells can migrate on different matrices (the mountains) and with different receptors (the clothing and footwear of the hiker). The interaction of cells with their extracellular environment is dynamic like the conditions on a mountain and cells can adapt to perturbations, that is, a change in the weather.

ECM composition within the same tissue is also dynamic and reflects the delicate balance between ECM degradation and synthesis. The composition of the ECM within a tissue changes not only during morphogenetic events in early development, but also in aging and disease. One large focus of current research is to understand how the normal balance between ECM degradation and synthesis is maintained, with the goal being to understand how this system is deregulated during aging and disease.

The vast majority of studies investigating cellular adhesion to the ECM have been done *in vitro*. It is clear from these studies that regulation of cell–ECM adhesion occurs on many different levels including gene expression, alternative splicing, translational regulation, post-translational modification, and formation of multiprotein complexes. The next critical step for developmental biologists is to understand cell behavior *in vivo*. Pioneering efforts from a number of laboratories generated targeted mouse knockouts and showed that: (1) inhibition of cell–ECM adhesion is frequently lethal and (2) different components of the cell–ECM adhesion machinery play specific roles during embryonic development (Aszodi et al., 2006). These experiments showed that cell–ECM adhesion plays a critical role during embryonic development. However, due to early embryonic lethality, they did not elucidate many of the underlying mechanisms driving cell–ECM interactions.

The current challenge is to use new advances in technology to study the dynamics of cell–ECM adhesion *in vivo*. In particular, understanding the intimate, bi-directional relationship between cells and their local ECM environment is critical. ECM remodeling accompanies cellular shape changes, cell migration, and differentiation. ECM remodeling can also influence cell signaling via the release of secreted signaling molecules previously sequestered within the ECM. ECM remodeling is induced by many different

signals, including cellular tension and growth factor signaling. Thus, remodeling of the ECM allows cells to integrate signaling and differentiation with the structure of their local microenvironment. The term “dynamic reciprocity” was introduced to promote the view that tissue architecture is critically dependent upon reciprocal signals between cells and their extracellular environment (Bissell et al., 1982). The intent of this review is to provide the reader with a broad overview of: (1) the myriad of ways in which cell adhesion to the ECM is regulated and (2) how this regulation is critical for development and physiology. All of the proteins mentioned herein are themselves the primary subjects of multiple reviews. This review focuses more on studies that integrate dynamic interactions between cells and their ECM. For details, readers are referred to the elegant and more focused reviews and primary research papers referenced.

It is worth noting that one current trend in biology is the undertaking of “omics-type” studies. This large scale, high-throughput approach is critical and invaluable. However, one of the concepts that we would like to convey, through examples illustrated below, is that detailed analysis of cell–ECM interactions is also absolutely fundamental to understanding embryonic development as well as the transition to disease states. It is our opinion that a comprehensive picture of cell behavior will emerge only by combining the information learned from studies at all size scales, along with new imaging technologies and modeling efforts.

COMPONENTS INVOLVED IN CELL–ECM ADHESION

Cell–ECM adhesion involves: (1) ECM proteins themselves, (2) transmembrane receptors that bind ECM ligands (integrins are the major class of transmembrane ECM receptors), and (3) intracellular proteins that directly or indirectly bind to integrins and/or the cytoskeleton to affect/strengthen/maintain cell–ECM attachment and influence downstream signaling. We will discuss some of the most well-known proteins in each class.

Extracellular Matrix Proteins

Although the major structural components of different ECMs are the same, their relative proportions and types vary, resulting in strikingly different physical properties. One unifying feature of different ECMs with diverse functions is the ability to maintain shape and to flexibly respond to deformation. The major structural components of the ECM include: collagens, proteoglycans, noncollagenous glycoproteins, and elastins (Fig. 1). These components play complementary biophysical roles. Maintenance of structural integrity is predominantly via collagens, which are the most abundant protein in the human body. Collagen is a major component of connective tissues such as skin and cartilage. These tissues flexibly maintain shape by absorbing deformation. Clearly, however, skin and cartilage have different biophysical properties. There are different collagen types (fibrillar, globular) that generate varying three-dimensional scaffolds. In addition, the alignment and density of collagen are the primary determinants of the tensile strength of the ECM (Kjaer,

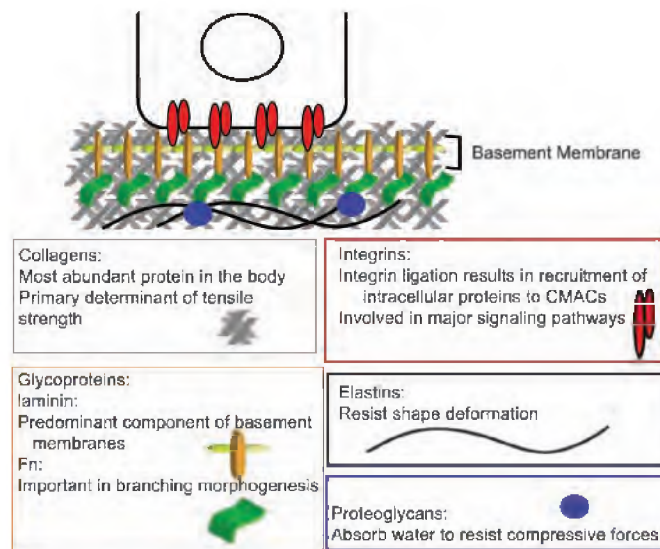


Figure 1. Extracellular matrix (ECM) components: collagens, glycoproteins, proteoglycans, and elastins. The basement membrane is an ECM structure whose major constituents are collagen type IV and the polymerized glycoprotein laminin. Cells adhere to the basement membrane through transmembrane receptors like integrins. Another glycoprotein to which transmembrane receptors adhere is fibronectin (Fn). Other ECM components include proteoglycans and elastins. Proteoglycans are proteins plus a glycosaminoglycan (GAG). The GAG portion of proteoglycans attracts water and cations and allows for the ECM to resist compression forces. Elastins resist shape deformation and give the ECM elasticity.

2004). The importance of collagen is highlighted by the fact that mutations in collagens type I, III, V, or type III procollagen can result in Ehlers-Danlos syndrome, which is characterized by skin laxity and joint hypermobility (Superti-Furga et al., 1989; Sillence et al., 1991; Nicholls et al., 1996; Toriello et al., 1996; De Paepe et al., 1997; Smith et al., 1997). Synthesized collagen scaffolds show great promise for tissue engineering and regeneration. Some current efforts directed towards understanding collagen elasticity involve applying engineering concepts to molecular mechanisms (Scott, 2003; Chaudhry et al., 2009). The potential for engineered collagen scaffolds to be used as transient and bioresorbable cartilage, skin, and cardiovascular grafts is exciting and is the focus of much research.

Proteoglycans are a protein plus a glycosaminoglycan (GAG). The GAG portion of proteoglycans has a net negative charge that attracts water (and cations) to form a hydrous gel that resists compressive forces. Proteoglycans regulate collagen fibrillogenesis. Thus, proteoglycans can indirectly regulate tissue remodeling in response to mechanical forces by modifying the amount, type, and alignment of collagen fibrils. The application of tensional or compressive loads to excised bovine tendons changed the amount and composition of proteoglycans (Robbins et al., 1997). Proteoglycan composition and amount can also change *in vivo*.

An increase in proteoglycans and GAG content was observed in tendons from 6.5 weeks old chickens that had been exercised on treadmills compared to their more sedentary counterparts (Yoon and Halper, 2005). In addition to modulating the physical properties of the ECM in response to mechanical stress, proteoglycans also modulate the movement and activity of signaling molecules through the ECM. Perlecan is an exceedingly large, ubiquitous ECM protein that surrounds cells. It has been proposed that Perlecan acts as a clearing house that controls local levels of mitogens and morphogens (Whitelock et al., 2008). The complex phenotype of mice mutant for Perlecan attests to the importance of proteoglycans for normal development (Arikawa-Hirasawa et al., 1999; Costell et al., 1999).

Glycoproteins are proteins with sugar modifications. Two prominent noncollagenous glycoproteins, fibronectin (Fn) and laminin, are discussed in further detail below. Finally, elastins, as their name suggests, are remarkable proteins that are resistant to shape deformation and are primarily responsible for the elasticity of connective tissues (DeBelle and Tamburro, 1999; Tatham and Shewry, 2000; Li and Daggett, 2002; Mithieux and Weiss, 2005; Daamen et al., 2007). Elastin-based biomaterials are becoming popular for tissue engineering due to their elastic properties, the stable nature of insoluble elastin (half-life of 70 years), and the

potential for self-assembly. Perhaps the most famous bio-elastic material is flagelliform spider silks, which can extend approximately 200% of their length without breaking (Xu and Lewis, 1990; Dong et al., 1991; Gosline et al., 1999)!

Spotlight on fibronectin. Fibronectin is a major component of many extracellular matrices and plays roles in both development and disease. Fn is perhaps most renowned for its functions during branching morphogenesis and cell migration (Roman et al., 1991; Roman, 1997; Jiang et al., 2000; Sakai et al., 2003; Trinh and Stainier, 2004; Davidson et al., 2006; Larsen et al., 2006b; Matsui et al., 2007). Fn provides an excellent example of the regulation of cell–ECM adhesion components at multiple levels. Fn transcription during embryonic development is spatially and temporally regulated (Julich et al., 2005; Koshida et al., 2005; Matsui et al., 2007). Post-transcriptionally, there are many alternatively spliced forms of Fn. The expression of different splice variants frequently correlates with disease and is regulated by multiple pathways (White et al., 2008). Fn regulation is further complicated by the fact that there are two forms of Fn: (1) plasma Fn (pFn) which circulates in the blood and is globular and (2) cellular Fn (cFn) which is assembled into fibrils that in turn polymerize to form a fibrillar matrix. Fn fibril formation is regulated on many levels, including dimerization and integrin binding, as well as stretch-mediated uncovering of a cryptic self-binding site (Leiss et al., 2008). The ability of fibrillar Fn to be stretched up to fourfold by living cells may be particularly relevant for dynamic cell movements that occur during development (Erickson, 2002).

One critical function of Fn is to regulate deposition of collagens type I and III in the ECM (Sottile and Hocking, 2002; Velling et al., 2002). Interestingly, it has recently been shown that the ability of Fn to bind to collagen is critical for Fn-stimulated cell migration during wound healing (Sottile et al., 2007). Although this study was *in vitro*, the dynamic interaction between Fn-dependent collagen deposition and Fn-dependent cell migration highlights the need for integration of multiple ECM components when studying developmental processes.

In the past decade, Fn has also been shown to be a critical regulator of branching morphogenesis. Branching occurs most frequently in epithelial tissues and involves repeated elongation and forking to generate the complex shapes of lungs, kidneys, and mammary glands, for example. As branching bears some similarities to fractals, mathematicians and biologists have long been fascinated by the morphogenic process. An excellent and entertaining book devoted to branched systems begins with Leonardo da Vinci's early studies of tree dimensions, and is highly recommended for interested readers (Davies, 2005). Here, we will focus on recent results highlighting dynamic roles for Fn during branching morphogenesis. One model for branching morphogenesis is the mouse mandibular salivary gland. Branching occurs first by the formation of localized, shallow clefts, which then deepen to become new buds (Grobstein, 1953). A key study showed that Fn expression transiently increases at cleft epithelial cells just as narrow clefts form. The increase in Fn expression correlates with a decrease in the cell–cell adhesion protein, E-cadherin

(Sakai et al., 2003). Fn expression decreases as clefts broaden. Incubation of salivary glands with an antibody against Fn inhibited branching whereas adding exogenous Fn increased branching (Sakai et al., 2003) (Fig. 2A). Thus, the authors proposed that localized Fn assembly at clefts results in the conversion of E-cadherin-based cell–cell adhesion to integrin-based cell–ECM adhesion, resulting in cleft progression. This pioneering experiment not only elucidated a key role for Fn in branching morphogenesis, but also highlights the dynamic role of ECM regulation during morphogenesis.

One key question that arose, however, was how adding exogenous Fn could promote branching if Fn was providing a local cue for cleft formation. A very elegant study addressed this issue by asking if directional Fn assembly might provide the impetus for cleft formation. Mouse mandibular salivary glands were incubated in Alexa-fluor conjugated Fn, which was then washed out and replaced by unlabeled Fn (Larsen et al., 2006b). This experiment showed that older Fn remains coherent, and is actually translocated inward as newer Fn is assembled behind it. Thus, the polarity of Fn assembly may provide a critical local cue for cleft progression (Larsen et al., 2006b) (Fig. 2B). The "wedge" of Fn would also result in conversion of cell–cell adhesion to cell–matrix adhesion (Larsen et al., 2006b). One critical question that remains to be addressed is whether Fn plays a signaling role in this adhesion conversion, or the progression of the Fn wedge mechanically breaks cell–cell adhesion. These studies, however, illustrate recurring themes of ECM regulation: ECM is dynamic, can play signaling and mechanical roles, and ECM modulation interacts with cell–cell adhesion as well as cell–ECM adhesion.

Spotlight on laminins. Laminin is necessary, along with collagen type IV, for the assembly of the basement membrane, a specialized part of ECM that provides a physical structure delineating cells from the ECM and also modulates cell signaling (Engvall, 1995; Gullberg et al., 1999; Miner and Yurchenco, 2004; Aumailley et al., 2005; Nguyen and Senior, 2006; LeBleu et al., 2007; Tzu and Marinkovich, 2008). Laminins are cross-shaped heterotrimeric proteins comprised of an α , β , and γ chain. Five α , four β , and three γ chains (Miner and Yurchenco, 2004) assemble in different combinations to generate the 16 known isoforms (Aumailley et al., 2005) whose names reflect their composition (e.g., laminin 332, which is $\alpha3\beta3\gamma2$). Assembled laminin proteins self-polymerize, along with collagen type IV, to form basement membranes. Tissue specific function of laminin isoforms during development arises not only through tissue specific expression of different laminin chains, but also through the generation of splice variants and post-translational glycosylation and processing. An excellent recent review (Tzu and Marinkovich, 2008) highlights the intricacies of laminin structure, the relationship between structure and function, and also includes a comprehensive list of knockout mice and their phenotypes.

Recent studies have provided new insight into roles for laminin during boundary formation. The formation of ECM-rich boundaries is an absolutely fundamental aspect of development. Boundary formation can separate and

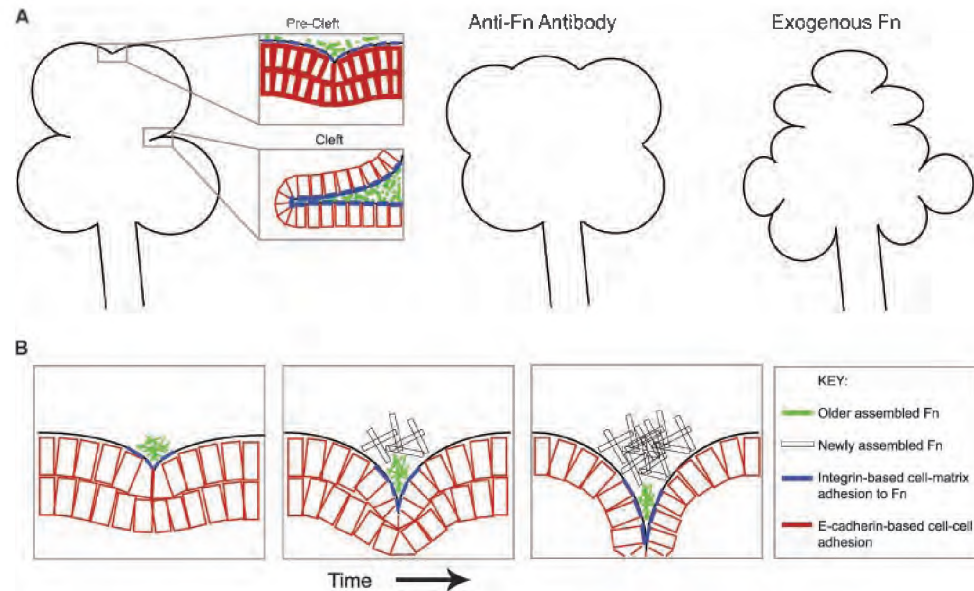


Figure 2. **A:** Outline of the experimental results obtained by Sakai et al. (2003). The expression of Fn transiently increases as narrow clefts form while the cell–cell adhesion protein E-cadherin decreases. An antibody against Fn inhibited branching whereas exogenous Fn increased branching. Localized Fn assembly at clefts results in the conversion of E-cadherin-based cell–cell adhesion to integrin-based cell–ECM adhesion, resulting in cleft progression. **B:** Outline of the experimental results obtained by Larsen et al. (2006b). Alexa-fluor conjugated Fn was washed out and replaced by unlabeled Fn. The older Fn (green) is translocated inward as newer Fn (white with black outline) is assembled behind it. This “wedge” of Fn could result in conversion of cell–cell adhesion to cell–matrix adhesion.

compartmentalize initially homologous cells. This compartmentalization occurs in the hindbrain during rhombomere formation and in the paraxial mesoderm during somite formation. Boundaries can also divide different tissues. For example, the notochord–somite boundary separates notochord cells from the paraxial mesoderm. In addition to separating structures, boundary formation contributes significantly to generating the three-dimensional shape and structure of developing organisms. The cell biology of boundary formation has been elucidated in many contexts. During *Xenopus* development, the notochord–somite boundary functions to “capture” or “trap” intercalating notochord cells. In this instance, intercalating notochord cells exhibit protrusive activity as they elongate. Upon reaching the notochord–somite boundary, protrusive activity and elongation ceases. This has been termed “boundary capture” (Keller et al., 2000). However, the ECM proteins responsible for boundary capture are not known. One hint that laminin might play a role in the formation of the notochord–somite boundary came from analysis of zebrafish mutations in two laminin chains, laminin β 1 and γ 1. In these embryos, notochords form but are not maintained (Parsons et al., 2002). Within the last year, two papers have shed new light on roles for laminin in boundary formation. In ascidians, laminin plays a role in

“trapping” or “boundary capture” of intercalating notochord cells (Veeman et al., 2008). In the absence of laminin, notochord cells invade and can cross the notochord–somite boundary. In the context of myotome boundary formation in zebrafish, laminin is required to trap elongating muscle cells. It was not known whether laminin in the basement membrane ceases elongation of muscle cells simply by providing a physical barrier, or by signaling prompted by laminin binding ceases elongation. Genetic mosaic analysis suggested that laminin signaling within the myotome boundary plays a role in trapping elongating muscle cells (Snow et al., 2008a). Future work will likely focus on the signaling mechanisms that lie downstream of “boundary capture.”

Metalloproteases. Much of the dynamic remodeling of the ECM is dependent upon matrix metalloproteases (MMPs) and members of the a disintegrin and metalloprotease (ADAM) and a disintegrin and metalloprotease with thrombospondin motifs (ADAMTS) families. Pro-MMPs lie dormant within the ECM and are activated by various signals (Murphy et al., 1999; Davidson et al., 2002; Tsuruda et al., 2004; Nagase et al., 2006; Amalinei et al., 2007; Ra and Parks, 2007; Clark et al., 2008; Filiz et al., 2008; Fu et al.,

2008). Misregulation of MMP activity contributes to multiple diseases (metastatic carcinoma, cardiovascular disease, rheumatoid arthritis, osteoarthritis, oral diseases) and is also implicated in preterm labor (Davidson et al., 2002; Abraham et al., 2005; Hofmann et al., 2005; Vadillo-Ortega and Estrada-Gutierrez, 2005; Lemaitre and D'Armiento, 2006; Liu et al., 2006; Mon et al., 2006; Cockle et al., 2007). The dynamic interaction between ECM synthesis/assembly and degradation via MMPs is an exquisite balancing act that mediates both embryonic development and tissue homeostasis. For example, a migrating cell must release sufficient proteases such that it can move, but not too many such that excessive matrix degradation leads to loss of cellular traction forces. The mechanisms that underlie the regulation of this balancing act are currently the subject of intense research with the hopes that it can be exploited for therapeutic purposes.

Transmembrane Receptors for ECM Proteins

Integrins are a major class of ECM receptors that transmit signals both from the ECM to within the cell ("outside-in" signaling) and from within the cell to the ECM ("inside-out" signaling) (Arnaout et al., 2005). Binding of integrins to the ECM results in the assembly of complexes that link to and coordinate cytoskeletal morphology. Thus, integrins and their associated proteins physically link the ECM to the intracellular cytoskeleton. As integrins do not have inherent enzymatic activity, many of the proteins involved in complex assembly are kinases or phosphatases. Integrin ligation can also result in changes in the molecular composition of the ECM. Integrins are transmembrane heterodimers comprised of an α and a β subunit. Both α and β subunits have large extracellular domains and relatively short cytoplasmic domains (Arnaout et al., 2005). Twenty-four heterodimers formed from the 18 known α and 8 known β subunits have been identified in humans (Takada et al., 2007). Although integrin receptors are notoriously promiscuous, they are receptors for a unique subset of ligands. For example, integrin $\alpha 5 \beta 1$ is a receptor for Fn, osteopontin, fibrillin, L1, thrombospondin, and ADAM family members. Conversely, integrin $\alpha 5$ is one of six known receptors for Fn (Humphries et al., 2006). Integrin expression during development is regulated both spatially and temporally, and mutant analyses indicate discrete roles for different integrins during vertebrate development (Sheppard, 2000; Bokel and Brown, 2002; Julich et al., 2005).

Integrins are highly responsive receptors that can exist in a bent (inactive) or an extended (active) state (Humphries et al., 2004). Post-translational modification of integrins can alter their affinity for ECM components and thus the overall adhesiveness of cells. One such example is the ADP-ribosylation of integrin $\alpha 7$ that occurs during myotube development in vitro. Integrin $\alpha 7$ is ADP-ribosylated at multiple sites, depending upon NAD^+ concentration. This ADP-ribosylation by an ADP-ribosyltransferase is not readily reversible (Zolkiewska and Moss, 1995) and leads to increased laminin-binding affinity of integrin $\alpha 7 \beta 1$ (Zhao et al., 2005). Given that NAD^+ is an obligatory substrate in ADP-ribosylation reactions, the authors hypothesized that integrin $\alpha 7$ ADP-

ribosylation by this ecto-ADP-ribosyltransferase might be a protective mechanism that increases integrin $\alpha 7 \beta 1$ adhesion to laminin when muscle cell membranes have been compromised (as frequently occurs in muscular dystrophies) and intracellular NAD^+ leaks into the extracellular space (Zhao et al., 2005). Although this paradigm has not yet been investigated in vivo, it is an excellent example of how post-translational modifications of integrins can affect their function.

Key Intracellular Components

Given the diverse functions of cell-ECM adhesion and the rapid assembly and disassembly of adhesion complexes, it is perhaps not surprising that different types of complexes that anchor the cell to the ECM can form. These differing classes have been defined with in vitro studies. The parameters that define the classes include the size, constituency, and signaling effects. The context in which a cell is located—the differentiation state of the cell, the specific ECM to which a cell is adhering, the physical forces of the tissue—impacts the type and size of complexes formed (Romer et al., 2006). The classes, from smaller to larger, are FCs (focal complexes), FAs (focal adhesions), and FBs (fibrillar adhesions) (Geiger et al., 2001). A recent review, noting the controversy over the definitions, suggests an overarching term for these complexes: cell matrix adhesion complexes, or CMACs (pronounced *see-macs*) (Lock et al., 2008). This review is an excellent commentary on the dynamics of cellular adhesion, and suggests a systems biology approach to studying CMACs.

CMACs contain dozens, if not hundreds, of proteins. Most of the proteins in CMACs are post-translationally regulated by phosphorylation and/or glycosylation, for example (Fig. 3). This regulation adds yet another layer of dynamic flexibility that mediates a cell's response to ECM adhesion. Some key components of CMACs (integrin-linked kinase, kindlins, paxillin, talin, zyxin) are the sole subjects of several recent reviews (Beckerle, 1997; Wang and Gilmore, 2003; McLean et al., 2005; Mitra et al., 2005; Boulter and Van Obberghen-Schilling, 2006; Legate et al., 2006; Hannigan et al., 2007; Deakin and Turner, 2008; Larjava et al., 2008; McDonald et al., 2008; Chatzizacharias et al., 2008a,b) and thus will not be discussed here in detail.

Spotlight on focal adhesion kinase (FAK) and muscle differentiation.

Attachment of muscle fibers to laminin in the basement membrane is necessary for musculoskeletal function. Mutations in genes that inactivate proteins required for adhesion to the basement membrane lead to multiple myopathies such as Duchenne, Becker, merosin-deficient, and many of the limb girdle muscular dystrophies (Hoffman et al., 1987; Tome et al., 1994; Bonnemann et al., 1995; Mayer et al., 1997; Hayashi et al., 1998). Many lines of evidence suggest that one therapeutic option for treatment of myopathies is to restore adhesion of myotubes (bundles of muscle fibrils) to the basement membrane. These studies indicate that the exact mechanism of increased adhesion is not critical. Thus, multiple studies have focused on elucidat-

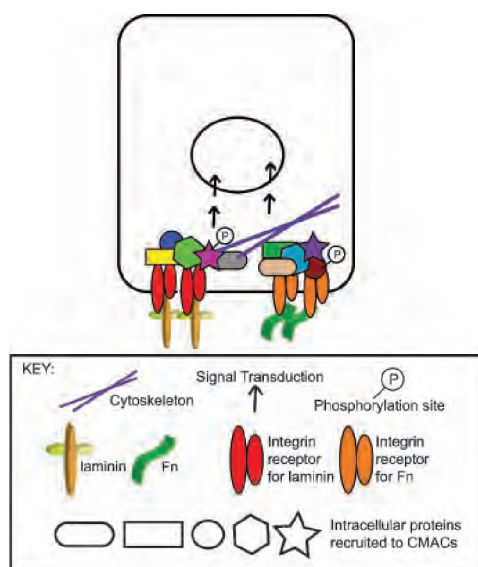


Figure 3. Simplified diagram of some cell–matrix adhesion complex (CMAC) components. When transmembrane receptors bind an ECM ligand, the receptors cluster and numerous intracellular proteins are recruited. Some of the recruited intracellular proteins bind to the cytoskeleton, some are involved in signal transduction, some function to strengthen the adhesion and some recruit or provide docking for other intracellular proteins. These clusters of proteins that form at sites of cell–matrix attachment are called CMACs. CMACs can rapidly assemble and disassemble during processes like cell migration as well as mature over the course of development. CMACs can involve different ECM ligands (i.e., laminin and Fn), their different corresponding receptors (i.e., integrin heterodimers) and different intracellular proteins (i.e., FAK). The phosphorylation of intracellular proteins regulates their activity and the signaling that occurs through CMACs.

ing the molecular mechanisms that mediate muscle fiber adhesion to laminin *in vitro*.

FAK is a highly dynamic focal adhesion protein that is not only critical for cell migration and morphogenesis *in vitro*, but is also highly upregulated in many types of cancerous cells (Hecker and Gladson, 2003; McLean et al., 2003, 2005; Nikolopoulos and Giancotti, 2005; Mon et al., 2006; Giehl and Menke, 2008; Chatzizacharias et al., 2008a). FAK is a nonreceptor tyrosine kinase that is autophosphorylated on tyrosine residue 397 (pY397) as a result of integrin signaling. This autophosphorylation generates a binding site for *src*, which then phosphorylates other tyrosine residues on FAK such as pY576/577 in the kinase domain and pY861 in the proline-rich domain (Schlaepfer and Hunter, 1998; Cary et al., 2002). Within the context of myotube adhesion to the basement membrane, several lines of evidence in cell culture systems indicate that FAK regulation is important for myotube differentiation and physiology. Interestingly, FAK

appears to be involved in the formation of strong, long-lasting CMACs that mediate muscle-tendon adhesion. FAK activation, or autophosphorylation on pY397, can also be induced by mechanical stress in cardiac myocytes (Fonseca et al., 2005). The activation of FAK correlates with many events during myotube formation in cell culture. FAK is activated via a PKC dependent pathway during insulin-mediated skeletal muscle cell spreading (Goel and Dey, 2002a,b). FAK expression and activation are modulated in response to mechanical force *in vivo*, and the response is different in predominantly slow-twitch versus predominantly fast-twitch muscles (Fluck et al., 1999; Gordon et al., 2001). During the differentiation of C2C12 myoblasts into myotubes, the ratio of inactivated FAK to activated FAK is transiently decreased, but then increases and activated FAK localizes to the tip of actin stress fibers. These data indicate roles for FAK in myotube morphogenesis *in vitro*. *In vivo* data regarding FAK function in muscle development are sparse due to the fact that FAK is required for earlier developmental processes (Ilic et al., 1995; Kragtorp and Miller, 2006). A descriptive study has shown that FAK activation correlates with myotube adhesion to the nascent myotendinous junction in Zebrafish (Snow and Henry, 2009). It is tantalizing to hypothesize that dynamic regulation of FAK may play a role during musculoskeletal development *in vivo*, however more sophisticated tools are necessary to test this hypothesis and determine the molecular and cellular consequences of FAK regulation in nascent muscle tissue.

BROAD FUNCTIONS OF CELL–ECM ADHESION

Cell–ECM Interactions Regulate Cell Signaling, Tissue Integrity, and Homeostasis

The ECM within all tissues provides a necessary scaffold for generation and maintenance of tissue architecture. It is impossible to list the plethora of functions that the ECM plays in development and physiology because virtually every developmental and physiological process relies, either directly or indirectly, on cell–ECM interactions. Cell–ECM interactions also modulate cellular responses to major signaling pathways. One major signaling pathway includes the fibroblast growth factors (FGFs) and their receptors (FGFRs). Recent experiments elucidating the extracellular “interactome” of the FGF receptor–ligand system have shown that ECM receptors act as noncanonical co-receptors that impart specificity to FGF signaling (Polanska et al., 2008). For example, inhibition of alpha V integrin can block FGF induced cell adhesion, migration, and angiogenesis (Rusnati et al., 1997; Santulli et al., 2008). This type of regulation provides mechanistic insight into how crosstalk between cell adhesion receptors and signaling pathways mediates cellular behavior.

Another mechanism for ECM-mediated regulation of growth factor signaling is the extensive crosstalk observed between growth factor and integrin signaling pathways. Integrin-based adhesion to the ECM is required for some cells to respond to growth factor signaling (Giancotti, 1996, 1997, 2000, 2003; Frisch and Ruoslahti, 1997). For example, the proliferation and/or differentiation of many cell types during development requires both adhesion to the ECM as

well as the appropriate growth factors (Sastry and Horwitz, 1996). Since the first experiments demonstrating crosstalk between growth factor signaling and integrin mediated signaling, it has become clear that crosstalk is frequent, dynamic, and involves a complex network of interactions (Schwartz and Ginsberg, 2002; Comoglio et al., 2003; Chan et al., 2006; Larsen et al., 2006a; Muller et al., 2008). Many laboratories are endeavoring to elucidate and exploit the complexity of integrin-growth factor signaling crosstalk with the hopes that more specific therapeutics with fewer side effects can be developed.

Adhesion to the ECM modulates expression and activation of growth factors and growth factor signaling can, in turn, regulate cell adhesion. One recently studied example is the pleiotropic cytokine transforming growth factor beta 1 (TGF- β 1) that is sequestered as a large latent protein complex within the ECM. Misregulated activation of this complex results in excess TGF- β 1 signaling that promotes myofibroblast differentiation and ultimately contributes to fibrosis in many organs. Activation of latent TGF- β 1 is dependent upon tension, ECM composition, and the interaction of integrin receptors with MMPs (Wipff et al., 2007; Wipff and Hinz, 2008). This paradigm is just one example of the complex regulation of growth factor release from ECM stores.

ECM receptors are both modulated and activated by signaling pathways. Notch signaling plays a major role in regulating cell fate and differentiation during development. Angiogenesis is a complex process that involves Notch signaling. Notch-4 inhibits angiogenesis by increasing integrin β 1-mediated adhesion to collagen, and thus inhibiting sprouting of endothelial cells from preexisting vessels. Interestingly, ectopic expression of activated Notch-4 does not increase the levels of integrin β 1, but rather results in more integrin β 1 molecules adopting the active, high affinity conformation (Leong et al., 2002). The mechanism underlying integrin activation by Notch-4 is not known. However, recent results suggest that Notch-1 mediates integrin activation via activating R-ras (Hodkinson et al., 2007). Thus, the "ECM interactome" is ubiquitous and may play a central role in integrating cellular responses to multiple signaling pathways.

Disrupted cell-ECM interactions can also perturb homeostasis. It is becoming increasingly recognized that disrupted interactions between cells and the ECM underlie the etiology of metastatic carcinomas, cardiovascular diseases, muscular dystrophies, kidney dysfunction, and skin disorders, among many other diseases and syndromes (Nelson and Bissell, 2006; Spinale, 2007; Stenina et al., 2007; Hamilton, 2008; Libby, 2008; Tzu and Marinkovich, 2008). Many of the less comfortable aspects of aging also result from decreased strength of cell-ECM interactions. For example, tendon failure leading to tendinopathies is exacerbated by age due to load-induced degradation of ECM (Dudhia et al., 2007). Osteoarthritis occurs when abnormal cell/ECM signaling disrupts the homeostasis of cartilage and bone tissue (Iannone and Lapadula, 2003). Age-related macular degeneration can also stem from abnormal ECM (Zarbin, 2004). Clearly, proper regulation of cell-ECM adhesion is critical for physiological homeostasis and the prevention of certain diseases.

Cell-ECM Interactions Regulate Cell Migration

The extracellular milieu influences migration, signaling, proliferation, and death of cell cohorts as well as individual cells. Cell migration requires dynamic interactions of cells with their ECM: adhesion assembly and disassembly are both necessary for migration. One classic system for studying roles for cell-ECM interactions during embryonic development is the neural crest. Neural crest cells originate from the dorsal neural tube and migrate great distances to give rise to neurons, pigment cells, cartilage, and connective tissue as well as other cell types. From the first descriptive data showing expression of cell-ECM adhesion components during neural crest migration (Krotoski et al., 1986; Krotoski and Bronner-Fraser, 1990) to functional studies shortly thereafter (Bronner-Fraser, 1986; Lallier and Bronner-Fraser, 1991, 1992, 1993; Perris et al., 1993a,b; Lallier et al., 1994; Kil et al., 1998; Peters et al., 2002), neural crest migration has proved to be an excellent model system to study cell migration. Recent advances in understanding neural crest cell migration have shown that efficient migration requires internalization and recycling of ECM receptors. Interestingly, internalization and recycling of ECM receptors is dependent upon the composition of the ECM *in vitro*—an example of dynamic reciprocity that may also function *in vivo* (Strachan and Condic, 2004). There is exquisite specificity within this system: trunk and cranial neural crest cells respond differently to varying concentrations of Fn when integrins are activated. Trunk neural crest cells are unaffected by increasing Fn concentration, whereas cranial neural crest cells slow with increasing Fn concentration (Strachan and Condic, 2008). It will be exciting to determine if similar mechanisms function *in vivo*. The complexity of cell migration *in vivo* is apparent in that another component of the ECM, laminin 111, also regulates neural crest cell spreading, migration, and survival. These different cell behaviors are regulated by the interaction of cell surface receptors with different laminin binding domains (Desban et al., 2006). Although neural crest is by no means the only paradigm of cell migration during development, neural crest migration has been an exceedingly informative model of dynamic cell-ECM interactions regulating cell behavior.

FUNCTIONS FOR DYNAMIC MODULATION OF CELL-ECM ADHESION *IN VIVO*

Many groups have devised elegant and novel techniques to elucidate the molecular mechanisms of morphogenesis during development. Unfortunately, there is only space to highlight a few recent and especially intriguing studies.

Convergent Extension During *Xenopus* Gastrulation Involves Dynamic Interactions Between Cells and Their Environment

One excellent model system for the study of how polarized interactions of cells with the ECM can drive morphogenesis is convergent extension. During convergent extension, the intercalation of cells in one plane causes elongation of the tissue in the perpendicular plane. *Xenopus*

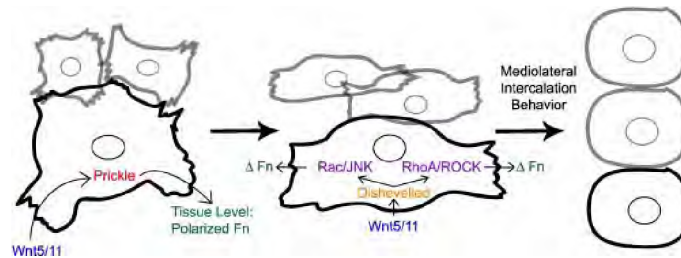


Figure 4. Schematic of the cell shape changes, signaling pathways and dynamic reciprocity involved in mediolateral intercalation behavior synthesized from the results of (Shih and Keller, 1992a,b; Habas et al., 2003; Tahinci and Symes, 2003; Goto et al., 2005). The cell outlined in black has been drawn larger than the cells outlined in gray to allow for depiction of signaling behavior while the gray cells show that groups of cells undergo these same behaviors. First, cells send out protrusions in all directions and Wnt signaling through *prickle* results in polarized Fn on a tissue level. Then, Wnt signaling through *dishevelled* and small GTPases *rac* and *rho* results in stable and oriented protrusions that generate traction and again remodel Fn. The combination of mediolaterally oriented protrusions and Fn alteration in the matrix results in mediolateral intercalation behavior. [Color figure can be viewed in the online issue which is available at www.interscience.wiley.com]

has long served as a model for the study of cell behaviors and for convergent extension in particular. In *Xenopus*, convergent extension of the embryonic axis during gastrulation is driven by mediolateral intercalation behavior (Shih and Keller, 1992a,b). Cells exhibiting mediolateral intercalation behavior become polarized in that they elongate and extend lamellipodia in the direction of interdigitation. Convergent extension depends upon this cell polarization and bipolar lamella formation.

Cell polarization during convergent extension during *Xenopus* gastrulation requires interpretation of spatial information and interactions with the ECM. Surprisingly, in this context, the planar cell polarity (PCP) signaling cascade mediates both cell polarization and interactions with the ECM. The PCP cascade activates the small GTPases *rho* and *rac* that are critical for polarized lamellipodia formation (Habas et al., 2003; Tahinci and Symes, 2003). In addition, PCP signaling modulates the ECM protein Fn in two ways: (1) to regulate normal deposition of the Fn matrix and (2) to effect cellular polarization in response to the Fn matrix (Goto et al., 2005) (Fig. 4). Thus, future studies need to consider the potential dual requirements for the PCP cascade during other morphogenetic processes (Wallingford, 2005).

At this point, the mechanisms by which Fn mediated cellular polarization were not known. Subsequent elegant experiments showed that adhesion of mesodermal cells to Fn via integrin $\alpha 5 \beta 1$ functions in two ways to promote mediolateral intercalation behavior: (1) Fn binding represses the number of cellular protrusions extended and (2) Fn binding promotes the mediolateral orientation of protrusions required for effective convergent extension (Davidson et al., 2006). An important insight derived from this study is that binding to Fn is required to initiate, but not maintain, mediolaterally polarized cell morphology. The authors used both chronic and acute disruption of Fn binding to separate initiation and maintenance (Davidson et al., 2006). Clearly, these results not only provide new molecular insight to the

regulation of cell behavior by Fn, but should also encourage researchers to design experiments to distinguish between short and long-term requirements for cell–ECM adhesion.

One common theme of the above experiments is that the same signaling cascade or protein can play more than one role within the context of the same process. The methods used to parse multiple roles differed: one study asked if a Fn surface could rescue polarity and the other used chronic versus acute disruption of Fn-mediated adhesion. The progressive nature of morphogenesis further complicates a mechanistic understanding of embryonic development. In other words, processes that occur later in development necessarily rely on earlier morphogenetic events. It is thus sometimes difficult to attribute cause and effect. Towards this end, we have recently applied a fractal-based method that quantifies cellular structure within a lattice to show that Fn plays distinct roles through time in the same tissue (Snow et al., 2008b). Taken together, these experiments all highlight the spatial and temporal complexity of cell–ECM interactions during development, and provide different tools with which to tease apart discrete requirements for cell–ECM interactions during morphogenesis.

In Vivo Observation of Fn Dynamics and Correlation With Protrusive Activity

One critical method for elucidating the dynamics of cell interactions with the ECM is high-resolution time-lapse analysis of these interactions. Recently, live imaging of Fn and cellular protrusions in *Xenopus* animal cap explants has provided new insights into Fn fibril assembly (Davidson et al., 2008). Interestingly, there was not a strong correlation between lamellipodia extension and Fn fibril movement, and Fn fibrils move without apparent contact with lamellipodia. It was shown that there are two mechanisms that underlie fibril thickening and that they occur on different time-scales. Fn polymerization can take hours, but fibrils can also shorten

and thicken within minutes. Not surprisingly, disruption of the actin cytoskeleton resulted in fibril collapse. Taken together, these novel experiments show that it is possible to visualize cell–ECM dynamics within a tissue and show that different ECM remodeling events can occur on different time-scales (Davidson et al., 2008). The lack of clear correlation between Fn fibril dynamics and cellular protrusions is somewhat confusing given the data mentioned above showing clear roles for Fn binding in regulating cell protrusions. However, different populations of cells were observed and it would be very interesting to use these newly developed tools to further study the acquisition and maintenance of mediolateral intercalation behavior. Furthermore, the use of GFP-tagged integrins in live embryos (Julich et al., 2005; DeSimone et al., 2007) concurrent with visualization of the ECM should add further insights.

But Do Cells Actually Migrate Across Fn?

“Galileo described the concept of motion relativity—motion with respect to a reference frame—in 1632. He noted that a person below deck would be unable to discern whether the boat was moving.” So begins a recent paper by Zamir, Rongish, and Little, published in *PLoS Biology* (Zamir et al., 2008). Recent time-lapse microscopy studies have described the cellular movements that result in chicken primitive streak (PS) formation (the PS is the organizing center for gastrulation) (Chuai et al., 2006; Voiculescu et al., 2007). However, the movements of cells and their ECM had not been simultaneously visualized during PS formation. Zamir and colleagues analyzed the relative movements of epiblast cells compared to the meshwork of Fn fibrils they termed SE ECM (the mesh of Fn fibrils that lie subjacent to the epiblastic epithelium). Their findings suggest that the movement of epiblast cells and the SE ECM is highly correlated. This methodology allowed them to also analyze cell autonomous movements (movements of cells relative to the SE ECM). Interestingly, although there was a small degree of cell autonomous movements, they resembled more of a “random walk” than a coordinated morphogenetic event. This exciting and highly informative study should change the way that developmental biologists investigate cell migration in different contexts. In particular, as noted by the authors, the concept of extracellular chemotactic gradients becomes exponentially more complex when it is considered that the ECM itself may move along with the cells.

SUMMARY

The studies described herein, along with many other fantastic experiments that were not discussed due to space constraints, clearly show that dynamic modulation of both the ECM and cell adhesion to the ECM are critical for development and physiology. These studies also highlight the complexity of cell–ECM adhesion complexes. CMACs contain hundreds of proteins, most of which are regulated by post-translational modification. At least two major technical issues currently hinder progress within the field. One is the paucity of technology for high resolution *in vivo* imaging of

CMAC components. Some laboratories have developed the technology for *in vivo* imaging of Fn, as described above. This is a critical step, but more remains to be done. Multiple CMACs and their post-translational modifications need to be imaged and manipulated *in vivo*. A recent, exciting paper describes a method for visualizing glycans *in vivo* during zebrafish development (Laughlin et al., 2008). One can envision refinement of this tool for visualization of proteoglycan synthesis and assembly into three-dimensional scaffolds *in vivo*. This is an area of rapidly developing technology and also rapid incorporation of excellent tools developed *in vitro* for *in vivo* use. The other major hindrance in understanding the dynamic modulation of CMAC function *in vivo* is a lack of quantitative readouts of cell–ECM signaling. Until quantitative methods are available to assess the type and amount of cell–ECM signaling, it will be quite difficult to synthesize an integrative view of CMAC function in development and physiology. Finally, in this era of deep sequencing, proteomics, and chemical genetic screens, it is important to remember that understanding the dynamics and mechanics of cell adhesion to the matrix *in vivo* is fundamentally required for true progress towards amelioration of most diseases. In this sense, cell–ECM adhesion can be thought of as fractal: detail is found at all scales analyzed.

REFERENCES

- Abraham D, Ponticos M, Nagase H. 2005. Connective tissue remodeling: Cross-talk between endothelins and matrix metalloproteinases. *Curr Vasc Pharmacol* 3:369–379.
- Amalinei C, Caruntu ID, Balan RA. 2007. Biology of metalloproteinases. *Rom J Morphol Embryol* 48:323–334.
- Arikawa-Hirasawa E, Watanabe H, Takami H, Hassell JR, Yamada Y. 1999. Perlecan is essential for cartilage and cephalic development. *Nat Genet* 23:354–358.
- Amaout MA, Mahalingam B, Xiong JP. 2005. Integrin structure, allostery, and bidirectional signaling. *Annu Rev Cell Dev Biol* 21:381–410.
- Aszodi A, Legate KR, Nakchbandi I, Fassler R. 2006. What mouse mutants teach us about extracellular matrix function. *Annu Rev Cell Dev Biol* 22:591–621.
- Aumailley M, Bruckner-Tuderman L, Carter WG, Deutzmann R, Edgar D, Ekblom P, Engel J, Engvall E, Hohenester E, Jones JC, Kleinman HK, Marinkovich MP, Martin GR, Mayer U, Meneguzzi G, Miner JH, Miyazaki K, Patarroyo M, Paulsson M, Quaranta V, Sanes JR, Sasaki T, Sekiguchi K, Sorokin LM, Talts JF, Tryggvason K, Uitto J, Virtanen I, von der Mark K, Wewer UM, Yamada Y, Yurchenco PD. 2005. A simplified laminin nomenclature. *Matrix Biol* 24:326–332.
- Beckerle MC. 1997. Zyxin: Zinc fingers at sites of cell adhesion. *Bioessays* 19:949–957.
- Bissell MJ, Hall HG, Parry G. 1982. How does the extracellular matrix direct gene expression? *J Theor Biol* 99:31–68.
- Bokel C, Brown NH. 2002. Integrins in development: Moving on, responding to, and sticking to the extracellular matrix. *Dev Cell* 3:311–321.
- Bonnemann CG, Modi R, Noguchi S, Mizuno Y, Yoshida M, Gussoni E, McNally EM, Duggan DJ, Angelini C, Hoffman EP.

1995. Beta-sarcoglycan (A3b) mutations cause autosomal recessive muscular dystrophy with loss of the sarcoglycan complex. *Nat Genet* 11:266–273.
- Boulter E, Van Obberghen-Schilling E. 2006. Integrin-linked kinase and its partners: A modular platform regulating cell-matrix adhesion dynamics and cytoskeletal organization. *Eur J Cell Biol* 85:255–263.
- Bronner-Fraser M. 1986. An antibody to a receptor for fibronectin and laminin perturbs cranial neural crest development in vivo. *Dev Biol* 117:528–536.
- Cary LA, Klinghoffer RA, Sachsenmaier C, Cooper JA. 2002. SRC catalytic but not scaffolding function is needed for integrin-regulated tyrosine phosphorylation, cell migration, and cell spreading. *Mol Cell Biol* 22:2427–2440.
- Chan PC, Chen SY, Chen CH, Chen HC. 2006. Crosstalk between hepatocyte growth factor and integrin signaling pathways. *J Biomed Sci* 13:215–223.
- Chatzizacharias NA, Kouraklis GP, Theocharis SE. 2008a. Clinical significance of FAK expression in human neoplasia. *Histol Histopathol* 23:629–650.
- Chatzizacharias NA, Kouraklis GP, Theocharis SE. 2008b. Disruption of FAK signaling: A side mechanism in cytotoxicity. *Toxicology* 245:1–10.
- Chaudhry B, Ashton H, Muhamed A, Yost M, Frankel D. 2009. Nanoscale viscoelastic properties of an aligned collagen scaffold. *J Mater Sci* 20:257–263.
- Chuai M, Zeng W, Yang X, Boychenko V, Glazier JA, Weijer CJ. 2006. Cell movement during chick primitive streak formation. *Dev Biol* 296:137–149.
- Clark IM, Swingler TE, Sampieri CL, Edwards DR. 2008. The regulation of matrix metalloproteinases and their inhibitors. *Int J Biochem Cell Biol* 40:1362–1378.
- Cockle JV, Gopichandran N, Walker JJ, Levene MI, Orsi NM. 2007. Matrix metalloproteinases and their tissue inhibitors in preterm perinatal complications. *Reprod Sci (Thousand Oaks, Calif)* 14:629–645.
- Comoglio PM, Boccaccio C, Trusolino L. 2003. Interactions between growth factor receptors and adhesion molecules: Breaking the rules. *Curr Opin Cell Biol* 15:565–571.
- Costell M, Gustafsson E, Aszodi A, Morgelin M, Bloch W, Hunziker E, Addicks K, Timpl R, Fassler R. 1999. Perlecan maintains the integrity of cartilage and some basement membranes. *J Cell Biol* 147:1109–1122.
- Daamen WF, Veerkamp JH, van Hest JC, van Kuppevelt TH. 2007. Elastin as a biomaterial for tissue engineering. *Biomaterials* 28:4378–4398.
- Davidson B, Reich R, Risberg B, Nesland JM. 2002. The biological role and regulation of matrix metalloproteinases (MMP) in cancer. *Arkh Patol* 64:47–53.
- Davidson LA, Marsden M, Keller R, Desimone DW. 2006. Integrin alpha5beta1 and fibronectin regulate polarized cell protrusions required for *Xenopus* convergence and extension. *Curr Biol* 16:833–844.
- Davidson LA, Dzamba BD, Keller R, Desimone DW. 2008. Live imaging of cell protrusive activity, and extracellular matrix assembly and remodeling during morphogenesis in the frog, *Xenopus laevis*. *Dev Dyn* 10:2684–2692.
- Davies J. 2005. Branching morphogenesis. *Landes Bioscience*. Georgetown, TX: Landes Biomedical. 170 p.
- De Paepe A, Nuytinck L, Hausser I, Anton-Lamprecht I, Naeyaert JM. 1997. Mutations in the COL5A1 gene are causal in the Ehlers-Danlos syndromes I and II. *Am J Hum Genet* 60:547–554.
- Deakin NO, Turner CE. 2008. Paxillin comes of age. *J Cell Sci* 121:2435–2444.
- Debelle L, Tamburro AM. 1999. Elastin: Molecular description and function. *Int J Biochem Cell Biol* 31:261–272.
- Desban N, Lissitzky JC, Rousselle P, Duband JL. 2006. alpha1beta1-integrin engagement to distinct laminin-1 domains orchestrates spreading, migration and survival of neural crest cells through independent signaling pathways. *J Cell Sci* 119:3206–3218.
- DeSimone DW, Dzamba B, Davidson LA. 2007. Using *Xenopus* embryos to investigate integrin function. *Methods Enzymol* 426:403–414.
- Dong Z, Lewis RV, Middaugh CR. 1991. Molecular mechanism of spider silk elasticity. *Arch Biochem Biophys* 284:53–57.
- Dudhia J, Scott CM, Draper ER, Heinegard D, Pitsillides AA, Smith RK. 2007. Aging enhances a mechanically-induced reduction in tendon strength by an active process involving matrix metalloproteinase activity. *Aging Cell* 6:547–556.
- Engvall E. 1995. Structure and function of basement membranes. *Int J Dev Biol* 39:781–787.
- Erickson HP. 2002. Stretching fibronectin. *J Muscle Res Cell Motil* 23:575–580.
- Filiz G, Price KA, Caragounis A, Du T, Crouch PJ, White AR. 2008. The role of metals in modulating metalloproteinase activity in the AD brain. *Eur Biophys J* 37:315–321.
- Fluck M, Carson JA, Gordon SE, Ziemiecki A, Booth FW. 1999. Focal adhesion proteins FAK and paxillin increase in hypertrophied skeletal muscle. *Am J Physiol* 277:C152–C162.
- Fonseca PM, Inoue RY, Kobarg CB, Crosara-Alberto DP, Kobarg J, Franchini KG. 2005. Targeting to C-terminal myosin heavy chain may explain mechanotransduction involving focal adhesion kinase in cardiac myocytes. *Circ Res* 96:73–81.
- Frisch SM, Ruoslahti E. 1997. Integrins and anoikis. *Curr Opin Cell Biol* 9:701–706.
- Fu X, Parks WC, Heinecke JW. 2008. Activation and silencing of matrix metalloproteinases. *Semin Cell Dev Biol* 19:2–13.
- Geiger B, Bershadsky A, Pankov R, Yamada KM. 2001. Transmembrane crosstalk between the extracellular matrix–cytoskeleton crosstalk. *Nat Rev* 2:793–805.
- Giancotti FG. 1996. Signal transduction by the alpha 6 beta 4 integrin: Charting the path between laminin binding and nuclear events. *J Cell Sci* 109:1165–1172.
- Giancotti FG. 1997. Integrin signaling: Specificity and control of cell survival and cell cycle progression. *Curr Opin Cell Biol* 9:691–700.
- Giancotti FG. 2000. Complexity and specificity of integrin signalling. *Nat Cell Biol* 2:E13–E14.
- Giancotti FG. 2003. A structural view of integrin activation and signaling. *Dev Cell* 4:149–151.
- Giehl K, Menke A. 2008. Microenvironmental regulation of E-cadherin-mediated adherens junctions. *Front Biosci* 13:3975–3985.
- Goel HL, Dey CS. 2002a. Focal adhesion kinase tyrosine phosphorylation is associated with myogenesis and modulated by insulin. *Cell Prolif* 35:131–142.

- Goel HL, Dey CS. 2002b. Role of protein kinase C during insulin mediated skeletal muscle cell spreading. *J Muscle Res Cell Motil* 23:269–277.
- Gordon SE, Fluck M, Booth FW. 2001. Selected contribution: Skeletal muscle focal adhesion kinase, paxillin, and serum response factor are loading dependent. *J Appl Physiol* 90: 1174–1183, discussion 1165.
- Gosline JM, Guerette PA, Ortlepp CS, Savage KN. 1999. The mechanical design of spider silks: From fibroin sequence to mechanical function. *J Exp Biol* 202:3295–3303.
- Goto T, Davidson L, Asashima M, Keller R. 2005. Planar cell polarity genes regulate polarized extracellular matrix deposition during frog gastrulation. *Curr Biol* 15:787–793.
- Grobstein C. 1953. Morphogenetic interaction between embryonic mouse tissues separated by a membrane filter. *Nature* 172: 869–870.
- Gullberg D, Tiger CF, Velling T. 1999. Laminins during muscle development and in muscular dystrophies. *Cell Mol Life Sci* 56:442–460.
- Habas R, Dawid IB, He X. 2003. Coactivation of Rac and Rho by Wnt/PCP signaling is required for vertebrate gastrulation. *Genes Dev* 17:295–309.
- Hamilton DW. 2008. Functional role of periostin in development and wound repair: Implications for connective tissue disease. *J Cell Commun Signal* 2:9–17.
- Hannigan GE, Coles JG, Dedhar S. 2007. Integrin-linked kinase at the heart of cardiac contractility, repair, and disease. *Circ Res* 100:1408–1414.
- Hayashi YK, Chou FL, Engvall E, Ogawa M, Matsuda G, Hirabayashi S, Yokochi K, Ziober BL, Kramer RH, Kaufman SJ, Ozawa E, Goto Y, Nonaka I, Tsukahara T, Wang JZ, Hoffman EP, Arahata K. 1998. Mutations in the integrin alpha7 gene cause congenital myopathy. *Nat Genet* 19:94–97.
- Hecker TP, Gladson CL. 2003. Focal adhesion kinase in cancer. *Front Biosci* 8:s705–s714.
- Hodkinson PS, Elliott PA, Lad Y, McHugh BJ, MacKinnon AC, Haslett C, Sethi T. 2007. Mammalian NOTCH-1 activates beta1 integrins via the small GTPase R-Ras. *J Biol Chem* 282: 28991–29001.
- Hoffman EP, Brown RH Jr, Kunkel LM. 1987. Dystrophin: The protein product of the Duchenne muscular dystrophy locus. *Cell* 51:919–928.
- Hofmann UB, Houben R, Brocker EB, Becker JC. 2005. Role of matrix metalloproteinases in melanoma cell invasion. *Biochimie* 87:307–314.
- Humphries MJ, Travis MA, Clark K, Mould AP. 2004. Mechanisms of integration of cells and extracellular matrices by integrins. *Biochem Soc Trans* 32:822–825.
- Humphries JD, Byron A, Humphries MJ. 2006. Integrin ligands at a glance. *J Cell Sci* 119:3901–3903.
- Iannone F, Lapadula G. 2003. The pathophysiology of osteoarthritis. *Aging Clin Exp Res* 15:364–372.
- Ilic D, Furuta Y, Kanazawa S, Takeda N, Sobue K, Nakatsuji N, Nomura S, Fujimoto J, Okada M, Yamamoto T. 1995. Reduced cell motility and enhanced focal adhesion contact formation in cells from FAK-deficient mice. *Nature* 377:539–544.
- Jiang ST, Chuang WJ, Tang MJ. 2000. Role of fibronectin deposition in branching morphogenesis of Madin-Darby canine kidney cells. *Kidney Int* 57:1860–1867.
- Julich D, Geisler R, Holley SA. 2005. Integrin alpha5 and delta/notch signaling have complementary spatiotemporal requirements during zebrafish somitogenesis. *Dev Cell* 8:575–586.
- Keller R, Davidson L, Edlund A, Elul T, Ezin M, Shook D, Skoglund P. 2000. Mechanisms of convergence and extension by cell intercalation. *Philos Trans R Soc Lond* 355:897–922.
- Kil SH, Krull CE, Cann G, Clegg D, Bronner-Fraser M. 1998. The alpha4 subunit of integrin is important for neural crest cell migration. *Dev Biol* 202:29–42.
- Kjaer M. 2004. Role of extracellular matrix in adaptation of tendon and skeletal muscle to mechanical loading. *Physiol Rev* 84:649–698.
- Koshida S, Kishimoto Y, Ustumi H, Shimizu T, Furutani-Seiki M, Kondoh H, Takada S. 2005. Integrin alpha5-dependent fibronectin accumulation for maintenance of somite boundaries in zebrafish embryos. *Dev Cell* 8:587–598.
- Kragtorp KA, Miller JR. 2006. Regulation of somitogenesis by Ena/VASP proteins and FAK during *Xenopus* development. *Development (Cambridge, England)* 133:685–695.
- Krotoski D, Bronner-Fraser M. 1990. Distribution of integrins and their ligands in the trunk of *Xenopus laevis* during neural crest cell migration. *J Exp Zool* 253:139–150.
- Krotoski DM, Domingo C, Bronner-Fraser M. 1986. Distribution of a putative cell surface receptor for fibronectin and laminin in the avian embryo. *J Cell Biol* 103:1061–1071.
- Lallier T, Bronner-Fraser M. 1991. Avian neural crest cell attachment to laminin: Involvement of divalent cation dependent and independent integrins. *Development (Cambridge, England)* 113:1069–1084.
- Lallier T, Bronner-Fraser M. 1992. Alpha 1 beta 1 integrin on neural crest cells recognizes some laminin substrata in a Ca(2+)-independent manner. *J Cell Biol* 119:1335–1345.
- Lallier T, Bronner-Fraser M. 1993. Inhibition of neural crest cell attachment by integrin antisense oligonucleotides. *Science* 259:692–695.
- Lallier T, Deutzmann R, Perris R, Bronner-Fraser M. 1994. Neural crest cell interactions with laminin: Structural requirements and localization of the binding site for alpha 1 beta 1 integrin. *Dev Biol* 162:451–464.
- Larjava H, Plow EF, Wu C. 2008. Kindlins: Essential regulators of integrin signalling and cell-matrix adhesion. *EMBO Rep* 9: 1203–1208.
- Larsen M, Artym VV, Green JA, Yamada KM. 2006a. The matrix reorganized: Extracellular matrix remodeling and integrin signaling. *Curr Opin Cell Biol* 18:463–471.
- Larsen M, Wei C, Yamada KM. 2006b. Cell and fibronectin dynamics during branching morphogenesis. *J Cell Sci* 119: 3376–3384.
- Laughlin ST, Baskin JM, Amacher SL, Bertozzi CR. 2008. In vivo imaging of membrane-associated glycans in developing zebrafish. *Science* 320:664–667.
- LeBleu VS, Macdonald B, Kalluri R. 2007. Structure and function of basement membranes. *Exp Biol Med (Maywood, NJ)* 232: 1121–1129.
- Legate KR, Montanez E, Kudlacek O, Fassler R. 2006. ILK, PINCH and parvin: The tIPP of integrin signalling. *Nat Rev* 7:20–31.
- Leiss M, Beckmann K, Giros A, Costell M, Fassler R. 2008. The role of integrin binding sites in fibronectin matrix assembly in vivo. *Curr Opin Cell Biol* 20:502–507.

- Lemaitre V, D'Armiento J. 2006. Matrix metalloproteinases in development and disease. *Birth Defects Res C Embryo Today* 78:1–10.
- Leong KG, Hu X, Li L, Noseda M, Larrivee B, Hull C, Hood L, Wong F, Karsan A. 2002. Activated Notch4 inhibits angiogenesis: Role of beta 1-integrin activation. *Mol Cell Biol* 22:2830–2841.
- Li B, Daggett V. 2002. Molecular basis for the extensibility of elastin. *J Muscle Res Cell Motil* 23:561–573.
- Libby P. 2008. The molecular mechanisms of the thrombotic complications of atherosclerosis. *J Intern Med* 263:517–527.
- Liu P, Sun M, Sader S. 2006. Matrix metalloproteinases in cardiovascular disease. *Can J Cardiol* 22:25B–30B.
- Lock JG, Wehrle-Haller B, Stromblad S. 2008. Cell-matrix adhesion complexes: Master control machinery of cell migration. *Semin Cancer Biol* 18:65–76.
- Matsui T, Raya A, Callol-Massot C, Kawakami Y, Oishi I, Rodriguez-Esteban C, Belmonte JC. 2007. miles-apart-Mediated regulation of cell-fibronectin interaction and myocardial migration in zebrafish. *Nat Clin Pract* 4:S77–S82.
- Mayer U, Saher G, Fassler R, Bornemann A, Echtermeyer F, von der Mark H, Miosge N, Poschl E, von der Mark K. 1997. Absence of integrin alpha 7 causes a novel form of muscular dystrophy. *Nat Genet* 17:318–323.
- McDonald PC, Fielding AB, Dedhar S. 2008. Integrin-linked kinase—essential roles in physiology and cancer biology. *J Cell Sci* 121:3121–3132.
- McLean GW, Avizienyte E, Frame MC. 2003. Focal adhesion kinase as a potential target in oncology. *Expert Opin Pharmacother* 4:227–234.
- McLean GW, Carragher NO, Avizienyte E, Evans J, Brunton VG, Frame MC. 2005. The role of focal-adhesion kinase in cancer—A new therapeutic opportunity. *Nat Rev* 5:505–515.
- Miner JH, Yurchenco PD. 2004. Laminin functions in tissue morphogenesis. *Annu Rev Cell Dev Biol* 20:255–284.
- Mithieux SM, Weiss AS. 2005. Elastin. *Adv Protein Chem* 70:437–461.
- Mitra SK, Hanson DA, Schlaepfer DD. 2005. Focal adhesion kinase: In command and control of cell motility. *Nat Rev* 6:56–68.
- Mon NN, Ito S, Senga T, Hamaguchi M. 2006. FAK signaling in neoplastic disorders: A linkage between inflammation and cancer. *Ann NY Acad Sci* 1086:199–212.
- Muller EJ, Williamson L, Kolly C, Suter MM. 2008. Outside-in signaling through integrins and cadherins: A central mechanism to control epidermal growth and differentiation? *J Invest Dermatol* 128:501–516.
- Murphy G, Stanton H, Cowell S, Butler G, Knauper V, Atkinson S, Gavrilovic J. 1999. Mechanisms for pro matrix metalloproteinase activation. *APMIS* 107:38–44.
- Nagase H, Visse R, Murphy G. 2006. Structure and function of matrix metalloproteinases and TIMPs. *Cardiovasc Res* 69:562–573.
- Nelson CM, Bissell MJ. 2006. Of extracellular matrix, scaffolds, and signaling: Tissue architecture regulates development, homeostasis, and cancer. *Annu Rev Cell Dev Biol* 22:287–309.
- Nguyen NM, Senior RM. 2006. Laminin isoforms and lung development: All isoforms are not equal. *Dev Biol* 294:271–279.
- Nicholls AC, Oliver JE, McCarron S, Harrison JB, Greenspan DS, Pope FM. 1996. An exon skipping mutation of a type V collagen gene (COL5A1) in Ehlers-Danlos syndrome. *J Med Genet* 33:940–946.
- Nikolopoulos SN, Giancotti FG. 2005. Netrin-integrin signaling in epithelial morphogenesis, axon guidance and vascular patterning. *Cell Cycle (Georgetown, TX)* 4:e131–e135.
- Parsons MJ, Pollard SM, Saude L, Feldman B, Coutinho P, Hirst EM, Stemple DL. 2002. Zebrafish mutants identify an essential role for laminins in notochord formation. *Development (Cambridge, England)* 129:3137–3146.
- Perris R, Kuo HJ, Glanville RW, Leibold S, Bronner-Fraser M. 1993a. Neural crest cell interaction with type VI collagen is mediated by multiple cooperative binding sites within triple-helix and globular domains. *Exp Cell Res* 209:103–117.
- Perris R, Syfrig J, Paulsson M, Bronner-Fraser M. 1993b. Molecular mechanisms of neural crest cell attachment and migration on types I and IV collagen. *J Cell Sci* 106:1357–1368.
- Peters J, Sechrist J, Luetolf S, Lored G, Bronner-Fraser M. 2002. Spatial expression of the alternatively spliced EIIIB and EIIIA segments of fibronectin in the early chicken embryo. *Cell Commun Adhes* 9:221–238.
- Polanska UM, Fernig DG, Kinnunen T. 2008. Extracellular interactome of the FGF receptor-ligand system: Complexities and the relative simplicity of the worm. *Dev Dyn* 238:277–293.
- Ra HJ, Parks WC. 2007. Control of matrix metalloproteinase catalytic activity. *Matrix Biol* 26:587–596.
- Robbins JR, Evanko SP, Vogel KG. 1997. Mechanical loading and TGF-beta regulate proteoglycan synthesis in tendon. *Arch Biochem Biophys* 342:203–211.
- Roman J. 1997. Fibronectin and fibronectin receptors in lung development. *Exp Lung Res* 23:147–159.
- Roman J, Crouch EC, McDonald JA. 1991. Reagents that inhibit fibronectin matrix assembly of cultured cells also inhibit lung branching morphogenesis in vitro. Implications for lung development, injury, and repair. *Chest* 99:20S–21S.
- Romer LH, Birukov KG, Garcia JG. 2006. Focal adhesions: Paradigm for a signaling nexus. *Circ Res* 98:606–616.
- Rusnati M, Tanghetti E, Dell'Era P, Gualandris A, Presta M. 1997. Alpha5beta3 integrin mediates the cell-adhesive capacity and biological activity of basic fibroblast growth factor (FGF-2) in cultured endothelial cells. *Mol Biol Cell* 8:2449–2461.
- Sakai T, Larsen M, Yamada KM. 2003. Fibronectin requirement in branching morphogenesis. *Nature* 423:876–881.
- Santulli RJ, Kinney WA, Ghosh S, Decorte BL, Liu L, Tuman RW, Zhou Z, Huebert N, Bursell SE, Clermont AC, Grant MB, Shaw LC, Mousa SA, Galembo RA Jr, Johnson DL, Maryanoff BE, Damiano BP. 2008. Studies with an orally bioavailable alpha V integrin antagonist in animal models of ocular vasculopathy: Retinal neovascularization in mice and retinal vascular permeability in diabetic rats. *J Pharmacol Exp Ther* 324:894–901.
- Sastry SK, Horwitz AF. 1996. Adhesion-growth factor interactions during differentiation: An integrated biological response. *Dev Biol* 180:455–467.
- Schlaepfer DD, Hunter T. 1998. Integrin signalling and tyrosine phosphorylation: Just the FAKs? *Trends Cell Biol* 8:151–157.
- Schwartz MA, Ginsberg MH. 2002. Networks and crosstalk: Integrin signalling spreads. *Nat Cell Biol* 4:E65–E68.
- Scott JE. 2003. Elasticity in extracellular matrix 'shape modules' of tendon, cartilage, etc. A sliding proteoglycan-filament model. *J Physiol* 553:335–343.
- Sheppard D. 2000. In vivo functions of integrins: Lessons from null mutations in mice. *Matrix Biol* 19:203–209.

- Shih J, Keller R. 1992a. Cell motility driving mediolateral intercalation in explants of *Xenopus laevis*. *Development* (Cambridge, England) 116:901–914.
- Shih J, Keller R. 1992b. Patterns of cell motility in the organizer and dorsal mesoderm of *Xenopus laevis*. *Development* (Cambridge, England) 116:915–930.
- Sillence DO, Chiodo AA, Campbell PE, Cole WG. 1991. Ehlers-Danlos syndrome type IV: Phenotypic consequences of a splicing mutation in one COL3A1 allele. *J Med Genet* 28:840–845.
- Smith LT, Schwarze U, Goldstein J, Byers PH. 1997. Mutations in the COL3A1 gene result in the Ehlers-Danlos syndrome type IV and alterations in the size and distribution of the major collagen fibrils of the dermis. *J Invest Dermatol* 108:241–247.
- Snow CJ, Henry CA. 2009. Dynamic formation of microenvironments at the myotendinous junction correlates with muscle fiber morphogenesis in zebrafish. *Gene Expr Patterns* 9:37–42.
- Snow CJ, Goody M, Kelly MW, Oster EC, Jones R, Khalil A, Henry CA. 2008a. Time-lapse analysis and mathematical characterization elucidate novel mechanisms underlying muscle morphogenesis. *PLoS Genet* 4:e1000219.
- Snow CJ, Peterson MT, Khalil A, Henry CA. 2008b. Muscle development is disrupted in zebrafish embryos deficient for fibronectin. *Dev Dyn* 237:2542–2553.
- Sottile J, Hocking DC. 2002. Fibronectin polymerization regulates the composition and stability of extracellular matrix fibrils and cell-matrix adhesions. *Mol Biol Cell* 13:3546–3559.
- Sottile J, Shi F, Rublyevska I, Chiang HY, Lust J, Chandler J. 2007. Fibronectin-dependent collagen I deposition modulates the cell response to fibronectin. *Am J Physiol* 293:C1934–C1946.
- Spinale FG. 2007. Myocardial matrix remodeling and the matrix metalloproteinases: Influence on cardiac form and function. *Physiol Rev* 87:1285–1342.
- Stenina OI, Topol EJ, Plow EF. 2007. Thrombospondins, their polymorphisms, and cardiovascular disease. *Arterioscler Thromb Vasc Biol* 27:1886–1894.
- Strachan LR, Condic ML. 2004. Cranial neural crest recycle surface integrins in a substratum-dependent manner to promote rapid motility. *J Cell Biol* 167:545–554.
- Strachan LR, Condic ML. 2008. Neural crest motility on fibronectin is regulated by integrin activation. *Exp Cell Res* 314:441–452.
- Superti-Furga A, Steinmann B, Ramirez F, Byers PH. 1989. Molecular defects of type III procollagen in Ehlers-Danlos syndrome type IV. *Hum Genet* 82:104–108.
- Tahinci E, Symes K. 2003. Distinct functions of Rho and Rac are required for convergent extension during *Xenopus* gastrulation. *Dev Biol* 259:318–335.
- Takada Y, Ye X, Simon S. 2007. The integrins. *Genome Biol* 8:215.
- Tatham AS, Shewry PR. 2000. Elastomeric proteins: Biological roles, structures and mechanisms. *Trends Biochem Sci* 25:567–571.
- Tome FM, Evangelista T, Leclerc A, Sunada Y, Manole E, Estournet B, Barois A, Campbell KP, Fardeau M. 1994. Congenital muscular dystrophy with merosin deficiency. *C R Acad Sci* 317:351–357.
- Toriello HV, Glover TW, Takahara K, Byers PH, Miller DE, Higgins JV, Greenspan DS. 1996. A translocation interrupts the COL5A1 gene in a patient with Ehlers-Danlos syndrome and hypomelanosis of Ito. *Nat Genet* 13:361–365.
- Trinh LA, Stainier DY. 2004. Fibronectin regulates epithelial organization during myocardial migration in zebrafish. *Dev Cell* 6:371–382.
- Tsuruda T, Costello-Boerrigter LC, Burnett JC Jr. 2004. Matrix metalloproteinases: Pathways of induction by bioactive molecules. *Heart Fail Rev* 9:53–61.
- Tzu J, Marinkovich MP. 2008. Bridging structure with function: Structural, regulatory, and developmental role of laminins. *Int J Biochem Cell Biol* 40:199–214.
- Vadillo-Ortega F, Estrada-Gutierrez G. 2005. Role of matrix metalloproteinases in preterm labour. *BJOG* 112:19–22.
- Veeman MT, Nakatani Y, Hendrickson C, Ericson V, Lin C, Smith WC. 2008. Chongmague reveals an essential role for laminin-mediated boundary formation in chordate convergence and extension movements. *Development* (Cambridge, England) 135:33–41.
- Velling T, Risteli J, Wennerberg K, Mosher DF, Johansson S. 2002. Polymerization of type I and III collagens is dependent on fibronectin and enhanced by integrins alpha 11beta 1 and alpha 2beta 1. *J Biol Chem* 277:37377–37381.
- Voiculescu O, Bertocchini F, Wolpert L, Keller RE, Stern CD. 2007. The amniote primitive streak is defined by epithelial cell intercalation before gastrulation. *Nature* 449:1049–1052.
- Wallingford JB. 2005. Vertebrate gastrulation: Polarity genes control the matrix. *Curr Biol* 15:R414–R416.
- Wang Y, Gilmore TD. 2003. Zyxin and paxillin proteins: Focal adhesion plaque LIM domain proteins go nuclear. *Biochim Biophys Acta* 1593:115–120.
- White ES, Baralle FE, Muro AF. 2008. New insights into form and function of fibronectin splice variants. *J Pathol* 216:1–14.
- Whitelock JM, Melrose J, Iozzo RV. 2008. Diverse cell signaling events modulated by perlecan. *Biochemistry* 47:11174–11183.
- Wipff PJ, Hinz B. 2008. Integrins and the activation of latent transforming growth factor beta1—An intimate relationship. *Eur J Cell Biol* 87:601–615.
- Wipff PJ, Rifkin DB, Meister JJ, Hinz B. 2007. Myofibroblast contraction activates latent TGF-beta1 from the extracellular matrix. *J Cell Biol* 179:1311–1323.
- Xu M, Lewis RV. 1990. Structure of a protein superfiber: Spider dragline silk. *Proc Natl Acad Sci USA* 87:7120–7124.
- Yoon JH, Halper J. 2005. Tendon proteoglycans: Biochemistry and function. *J Musculoskelet Neuronal Interact* 5:22–34.
- Zamir EA, Rongish BJ, Little CD. 2008. The ECM moves during primitive streak formation—computation of ECM versus cellular motion. *PLoS Biol* 6:e247.
- Zarbin MA. 2004. Current concepts in the pathogenesis of age-related macular degeneration. *Arch Ophthalmol* 122:598–614.
- Zhao Z, Gruszczynska-Biegala J, Zolkiewska A. 2005. ADP-ribosylation of integrin alpha7 modulates the binding of integrin alpha7beta1 to laminin. *Biochem J* 385:309–317.
- Zolkiewska A, Moss J. 1995. Processing of ADP-ribosylated integrin alpha 7 in skeletal muscle myotubes. *J Biol Chem* 270:9227–9233.

MIRE

Time-Lapse Analysis and Mathematical Characterization Elucidate Novel Mechanisms Underlying Muscle Morphogenesis

Chelsi J. Snow¹, Michelle Goody^{1,3}, Meghan W. Kelly^{1,3}, Emma C. Oster^{1,3}, Robert Jones^{1,3}, Andre Khalil^{2,3}, Clarissa A. Henry^{1,3*}

1 School of Biology and Ecology, University of Maine, Orono, Maine, United States of America, **2** Department of Mathematics and Statistics, University of Maine, Orono, Maine, United States of America, **3** Institute for Molecular Biophysics, The Jackson Laboratory, Bar Harbor, Maine, United States of America

Abstract

Skeletal muscle morphogenesis transforms short muscle precursor cells into long, multinucleate myotubes that anchor to tendons via the myotendinous junction (MTJ). In vertebrates, a great deal is known about muscle specification as well as how somitic cells, as a cohort, generate the early myotome. However, the cellular mechanisms that generate long muscle fibers from short cells and the molecular factors that limit elongation are unknown. We show that zebrafish fast muscle fiber morphogenesis consists of three discrete phases: short precursor cells, intercalation/elongation, and boundary capture/myotube formation. In the first phase, cells exhibit randomly directed protrusive activity. The second phase, intercalation/elongation, proceeds via a two-step process: protrusion extension and filling. This repetition of protrusion extension and filling continues until both the anterior and posterior ends of the muscle fiber reach the MTJ. Finally, both ends of the muscle fiber anchor to the MTJ (boundary capture) and undergo further morphogenetic changes as they adopt the stereotypical, cylindrical shape of myotubes. We find that the basement membrane protein laminin is required for efficient elongation, proper fiber orientation, and boundary capture. These early muscle defects in the absence of either *lamininβ1* or *lamininγ1* contrast with later dystrophic phenotypes in *lamininα2* mutant embryos, indicating discrete roles for different laminin chains during early muscle development. Surprisingly, genetic mosaic analysis suggests that boundary capture is a cell-autonomous phenomenon. Taken together, our results define three phases of muscle fiber morphogenesis and show that the critical second phase of elongation proceeds by a repetitive process of protrusion extension and protrusion filling. Furthermore, we show that laminin is a novel and critical molecular cue mediating fiber orientation and limiting muscle cell length.

Citation: Snow CJ, Goody M, Kelly MW, Oster EC, Jones R, et al. (2008) Time-Lapse Analysis and Mathematical Characterization Elucidate Novel Mechanisms Underlying Muscle Morphogenesis. *PLoS Genet* 4(10): e1000219. doi:10.1371/journal.pgen.1000219

Editor: Mary Mullins, University of Pennsylvania School of Medicine, United States of America

Received: June 3, 2008; **Accepted:** September 9, 2008; **Published:** October 3, 2008

Copyright: © 2008 Snow et al. This is an open-access article distributed under the terms of the Creative Commons Attribution License, which permits unrestricted use, distribution, and reproduction in any medium, provided the original author and source are credited.

Funding: This research was supported by the Muscular Dystrophy Association and also in part by NIH grant R01 HD052934-01A1 as well as NIH grant P20 RR-016463 from the INBRE program of the National Center for Research Resources. ECO was supported in part by a summer research fellowship from the University of Maine.

Competing Interests: The authors have declared that no competing interests exist.

* E-mail: Clarissa.Henry@umit.maine.edu

These authors contributed equally to this work.

Introduction

Muscle specification and morphogenesis during early development are critical for normal muscle physiology. In vertebrates, most of the musculature is derived from somites [1–3]. Somites are segmentally reiterated structures delineated by somite boundaries. As development proceeds, a portion of the somite gives rise to skeletal muscle fibers that comprise the myotome. The terminal ends of myotomal muscle fibers attach to somite boundaries, which then become myotome boundaries. In teleost fishes, myotome boundaries give rise to the myotendinous junction (MTJ) [4].

Myotome development is perhaps best understood in amniotes. Myogenesis in amniotes begins when muscle precursor cells translocate from the overlying dermomyotome to the myotome [3]. The first myocytes to translocate come from the dorsomedial lip, but later in development myocytes translocate from all dermomyotome borders as well as the central region [5–7].

Time-lapse analysis in the chick embryo has shown that spatial domains of the somite differ in cell behaviors that generate the primary myotome [8]. The above studies have elucidated cell movements that generate the myotome. However, although it is known that short, mononucleate, muscle precursor cells generate long, functional multinucleate muscle fibers, it is not known how this occurs. Interestingly, the early zebrafish and chick myotomes have been described as containing mononucleate muscle fibers [8,9]. Our intent in undertaking this study was to utilize the advantages of the zebrafish system to shed light on early muscle development in a vertebrate model.

Elucidation of the cellular mechanisms that underlie muscle fiber development and tendon attachment is critical for a comprehensive understanding of muscle development. Towards this end, muscle morphogenesis has been studied in different model systems. C2C12 myoblasts in culture elongate slightly prior to differentiation, align with each other, and fuse to generate a multinucleate myotube [10]. We have called this scenario elliptical

Author Summary

Despite the importance of muscle fiber development and tendon attachment, this process is incompletely understood in vertebrates. One critical step is muscle fiber elongation; muscle precursor cells are short and subsequent elongation/fusion generates long, multinucleate muscle fibers. Using a vertebrate model organism, the zebrafish, we find that single round myoblasts elongate to span the entire width of the myotome prior to fusion. Using rigorous and objective mathematical characterization techniques, we can further divide muscle development into three stages: short precursor cells, intercalation/elongation, and boundary capture/myotube formation. The second phase, elongation, occurs via a two-step mechanism of protrusion extension and filling. Myotube formation involves boundary capture, where the ends of muscle fibers anchor themselves to the myotome boundary and stop elongating. We show that the protein laminin is required for boundary capture, normal fiber length, and proper fiber orientation. Genetic mosaic experiments in laminin-deficient embryos reveal that boundary capture is a cell autonomous phenomenon. Wild-type (normal) cells capture the boundary appropriately and stop elongating in laminin-deficient embryos. Although adhesion to laminin has been implicated in muscular dystrophies where the attachment between muscle cells and tendons fails, no early developmental requirements for laminin in fast muscle morphogenesis have been shown until now.

growth. In grasshopper embryos, the first muscle cells elongate between attachment sites prior to fusion. These cells extend many processes in multiple directions while elongating [11]. We have termed this scenario branching. Elegant studies in *Drosophila* have shown that muscle morphogenesis occurs when myoblasts fuse to generate long, multinucleate myotubes and identified a number of proteins required for myoblast fusion [12,13]. Extremely exciting recent studies have shown that there is some conservation of molecular mechanisms that mediate muscle cell fusion between *Drosophila* and zebrafish [14,15]. Interestingly, however, the primary myotome in chick and zebrafish is mononucleate [8,9]. This suggests that myoblast fusion does not mediate the earliest stages of muscle morphogenesis in vertebrates, but occurs after initial muscle fiber elongation. These distinct mechanisms of morphogenesis in different systems highlight the fact that a mechanistic study of muscle fiber morphogenesis in vertebrates has not yet been undertaken. Identification of discrete morphogenetic steps that mediate muscle fiber morphogenesis in vertebrates is necessary to provide a framework for future molecular analyses.

Adhesion of muscle fibers to the basement membrane is critical for muscle function. The basement membrane attaches muscle fibers to connective tissue that then attaches to the skeletal system; this attachment is critical for force transduction from muscle to bone. One major component of the basement membrane is laminin. Laminin is a heterotrimeric protein composed of α , β and γ subunits that generate at least 15 different isoforms [16]. The importance of laminins in muscle physiology is evidenced by the fact that mutations in *lama2* result in muscular dystrophies [17–20]. Recent work has shown that muscle fibers in zebrafish mutant for *lama2* elongate and attach to the MTJ, but at 48 hours post fertilization (hpf) fibers detach before death, providing novel insight into roles for *lama2* in muscle disease [21].

Significantly less is known about spatiotemporal mechanisms of basement membrane assembly during early skeletal muscle

development and whether adhesion to the basement membrane contributes to morphogenesis. Recent data suggest that the laminin receptor Integrin $\alpha 6 \beta 1$ is necessary for both basement membrane assembly and normal expression of myogenic regulatory factors in cultured mouse explants [22]. However, Integrin $\alpha 6 \beta 1$ binds to multiple laminins with distinct affinities [23] and roles for individual laminin chains during early muscle development *in vivo* have not been identified. In order to determine whether the basement membrane is critical during early development for muscle fiber elongation and attachment, it is first necessary to understand the cellular basis of muscle fiber elongation and attachment.

The relative simplicity of zebrafish skeletal muscle, where slow and fast-twitch fibers are spatially segregated, makes it an ideal model system to study muscle cell elongation and MTJ morphogenesis. Morphogenesis of the somite boundary into the MTJ involves three stages: initial epithelial somite boundary formation, transition and myotome boundary/MTJ formation [24]. Transition encompasses the lateral displacement of slow-twitch muscle fibers and the subsequent elongation and differentiation of fast-twitch fibers [25–28]. The initial myotome forms by 26 hpf and contains long muscle fibers attached to the myotome boundary/MTJ. At this point, the extracellular matrix (ECM) proteins Fibronectin, laminin and Periostin concentrate at the MTJ [29–31]. Morpholino-mediated inhibition of Periostin disrupts MTJ formation [29,32,33], but discrete and mechanistic requirements for other ECM proteins and their receptors are not known. In addition, the precise mechanism by which elongating muscle fibers attach to the MTJ and cease elongation has not been elucidated.

The purpose of this study was to rigorously and quantitatively characterize, for the first time in vertebrate embryos, the cellular events that generate long myotubes from initially short muscle precursor cells. We focused on fast-twitch fiber morphogenesis in zebrafish embryos. Our goal was to develop methods with which discrete functions for proteins involved in muscle morphogenesis could be identified. Towards this goal, we utilized time-lapse analysis, genetic mosaic analysis, and three different mathematical tools including a powerful wavelet-based image analysis formalism to provide novel insight into cellular and molecular mechanisms that underlie muscle fiber elongation and subsequent attachment to the nascent MTJ.

Results

Three Phases of Fast-Twitch Muscle Cell Elongation

Although the elongation of somitic cells is critical for actin-mediated contractility that underlies muscle function, the cellular and molecular basis of elongation in vertebrates is not well understood. An understanding of how muscle cells elongate is critical in order to determine mechanistic roles for genes required in elongation. We used time-lapse microscopy of zebrafish embryos labeled with BODIPY-Ceramide to outline cells. This type of time-lapse analysis, where all cells are labeled, provides an initial framework with which to focus further investigation into fast-twitch fiber morphogenesis. Fast-twitch muscle cells can be identified because, in contrast to slow-twitch muscle fibers, they are not migrating medially-laterally [25]. The transition from a somite to a myotome is a dynamic process (Figure 1, Movie S1) with at least three phases. The first phase is short muscle precursor cells. Second, muscle fibers elongate by extending narrow protrusions to intercalate between other cells (Figure 1 A2 at 80 min, blue pseudocolored cell). Elongation ends when cells adhere to the anterior and posterior boundaries. The third phase is

A Time-lapse of muscle cell elongation, 22-somite stage embryo

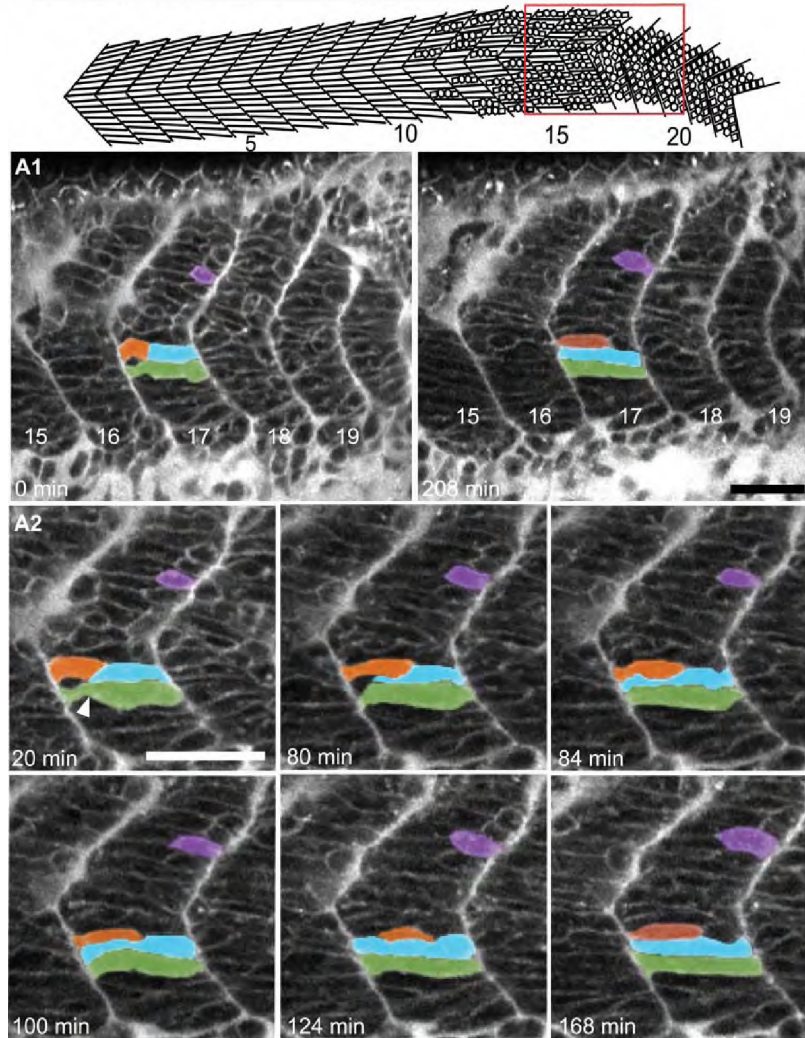


Figure 1. Myoblasts Intercalate between Each Other as They Elongate. (See also Movies S1 and S2.) A) Cartoon depicts the anterior to posterior progression of myofiber elongation in a 22 somite embryo. A1–A2) Confocal time-lapse sequence showing fast muscle cell elongation in a single focal plane of a zebrafish embryo vitally labeled with BODIPY-Ceramide. Anterior left, dorsal top, somite number denoted, time elapsed indicated on panels. The colored cells were pseudocolored to facilitate visualization. By 80 min, the blue cell is beginning to intercalate, intercalation is complete by 84 min. During this time, the orange and purple cells are elongating. The green cell transits from a long, but irregularly shaped cell (white arrowhead indicates a groove at 20 min) into a rod-shaped myotube by 124 min. Scale bars: 50 μ m. doi:10.1371/journal.pgen.1000219.g001

myotube formation. Recently elongated cells are long, but irregularly shaped (Figure 1 A1 green cell at 0 min, A2 blue cell at 84–168 min, Movie S1). During myotube formation, long cells

with grooves continue to change shape until they form a more uniformly shaped tube without grooves (Figure 1 A1 green cell at 208 min). An additional time-lapse is shown in Movie S2.

Phase 1: Short Muscle Precursor Cells

A three-dimensional quantification of cell morphology is critical to distinguish between scenarios of muscle cell elongation (Figure 2A). We transplanted dextran-filled cells into unlabeled host embryos and three-dimensionally reconstructed the behavior of labeled cells through time (Figure 2B). For each time point, the z-series was three-dimensionally projected and the area, perimeter, and major axis were measured. Thus two-dimensional parameters (area, perimeter, and major axis) were obtained from three-dimensional projections of cells. The analysis of labeled cells in an unlabeled field of cells allows unambiguous determination of cellular shape dynamics and quantification of morphometric parameters. We analyzed cell behaviors in two ways: (1) analysis of the filament index and (2) analysis of the relative dynamics of area and perimeter changes through time. As shown below, this approach supports and extends what was observed in BODIPY-Ceramide labeled embryos.

The filament index is an excellent mathematical parameter that describes cell morphology. The filament index is a measure that quantifies the departure of a shape from a circle (see methods). A circle has a filament index of 1 and a higher filament index indicates a larger departure from a circular shape. Short muscle precursor cells have a low filament index (FI) indicating that their morphology is close to a circle (Figure 2F, G1, $FI = 1.6 \pm 0.6$, Table 1).

Short muscle precursor cells extend and retract very short ($< 2 \mu\text{m}$) filopodia-like protrusions in all directions (Figure 2C, Movie S3). Small changes in the area, perimeter, and length of muscle precursor cells reflect the dynamic shape changes of precursor cells (not shown). However, their overall shape and size remains consistent.

Phase 2: Elongating Fast-Twitch Muscle Precursor Cells

Elongating cells lengthen towards their attachment site, the MTJ. Elongating cells have a higher filament index than short precursor cells (Figure 2F, 2.9 ± 0.8 , Table 1). The filament indices of elongating cells increase slightly through time (Figure 2G1, G2), reflecting their departure from a circular shape.

One purpose of this experiment was to distinguish between possible scenarios of muscle fiber elongation summarized in Figure 2A. The difference between the fusion and remaining scenarios is the timing of fusion relative to elongation. In the fusion scenario, fusion of short myoblasts is the major morphogenetic event that drives fiber elongation. Fusion of multiple short cells generates a long, multinucleate myotube in one step as in *Drosophila* [12]. In the remaining scenarios, cells elongate prior to fusion. We analyzed nuclear content of elongating and recently elongated cells and found that mononucleate fast-twitch cells elongate to the MTJ prior to fusion (Figure 4F H, $n = 108$ cells). Thus, the first fast-twitch fibers in zebrafish do not fuse prior to elongation.

The remaining scenarios are branching, elliptical growth, and protrusion (Figure 2A). The difference between the branching scenario and the elliptical growth/protrusion scenarios is the amount, size, and direction of protrusive activity. In grasshopper, the first muscle cells to elongate have extensive protrusions in many different directions [11]. This is depicted in the branching scenario (Figure 2A). In contrast, the elliptical growth and protrusion scenarios depict cells that elongate in a fixed direction. Both time-lapse analysis and analysis of cell morphology in fixed embryos indicate that fast-twitch fibers in zebrafish embryos elongate in a fixed direction and do not exhibit a branching morphology with multiple protrusions extended in different directions (Figures 2, 4). Rather, fast-twitch cells extend long ($> 4 \mu\text{m}$) protrusions along their long axis (Figure 2D, Movie S3).

These results indicate that the branching scenario does not apply to initial fast-twitch muscle morphogenesis in zebrafish.

The two remaining scenarios differ in the nature of elongation. The elliptical growth scenario depicts elongation as a continuous process reminiscent of a balloon filling. The protrusion scenario suggests that elongation is incremental and proceeds via a 2-step mechanism: protrusion extension and protrusion thickening. Time-lapse analysis suggests that fast-twitch cells extend protrusions that subsequently thicken (Figures 1, 2). Geometrical models were developed and used to determine how area and perimeter would change through time if cells were elongating via the two different scenarios. The major difference between the two models is the nature of dynamic changes in area and perimeter during elongation (see methods for details). Area and perimeter increase linearly in the elliptical growth model (Figure 3A) and incrementally in the protrusion model (Figure 3A1). The incremental nature of growth in the protrusion model is because the perimeter increases slightly more when the protrusion extends, but the area increases slightly more when the protrusion thickens (Figure 3A1). Therefore the difference between the two models is how area and perimeter values change as the cell grows: linear changes occur in the elliptical growth model and incremental changes in the protrusion model. In all cells examined, the rate of area increase is higher than the rate of perimeter increase as is predicted by both models (Figure 3B3). However, area and perimeter increase incrementally during fast-twitch muscle cell elongation (Figure 3B1, B2). Thus, analysis of area and perimeter dynamics supports the two-step intercalation model.

Phase 3: Boundary Capture/Myotube Formation

Boundary capture occurs when elongating muscle cells reach myotome boundaries and stop extending. The filament index of cells in the boundary capture/myotube formation phase is significantly higher than the preceding two phases (Figure 2F, Table 1). Their filament indices decrease slightly through time (Figure 2G1, G2). This decrease reflects the fact that a rod-shaped cell has a similar perimeter and length, but larger area than a long, irregularly shaped cell.

Recently elongated cells can be irregularly shaped and of varying diameters (Figure 2E). The thinner portions of the cell then thicken until the entire cell consists of a more uniform diameter (Figure 2E, Movie S3). Note that changes in area and perimeter of cells in the myotube formation phase are distinct: in this phase the area increases much more than the perimeter (Figure 3C, compare C3 to B3). The increase in area without a substantial increase in perimeter reflects the adoption of a more tube-shaped, regular morphology in the myotube formation phase.

Taken together, the time-lapse data along with two different quantitative analyses (area and perimeter dynamics through time and the filament index) indicates that there are three discrete morphogenetic phases that generate the first fast-twitch muscle fibers: short muscle precursor, intercalation/elongation and boundary capture/myotube formation.

Analysis of Fast-Twitch Muscle Cells in Fixed Embryos

Morphometric analysis of fixed cells corroborates the time-lapse data. Myotome formation proceeds in an anterior-posterior progression. Thus, this approach allows analysis of muscle cells in various stages of elongation within the same embryo. As observed in live embryos, fixed muscle precursor cells are short ($< 5 \mu\text{m}$) and have short protrusions (Figure 4A, F, white arrowheads). Protrusions in fixed cells are also observed to extend in all directions (Figure 4A). The filament index of live precursor cells and fixed precursor cells is similar (Figure 4E live cells

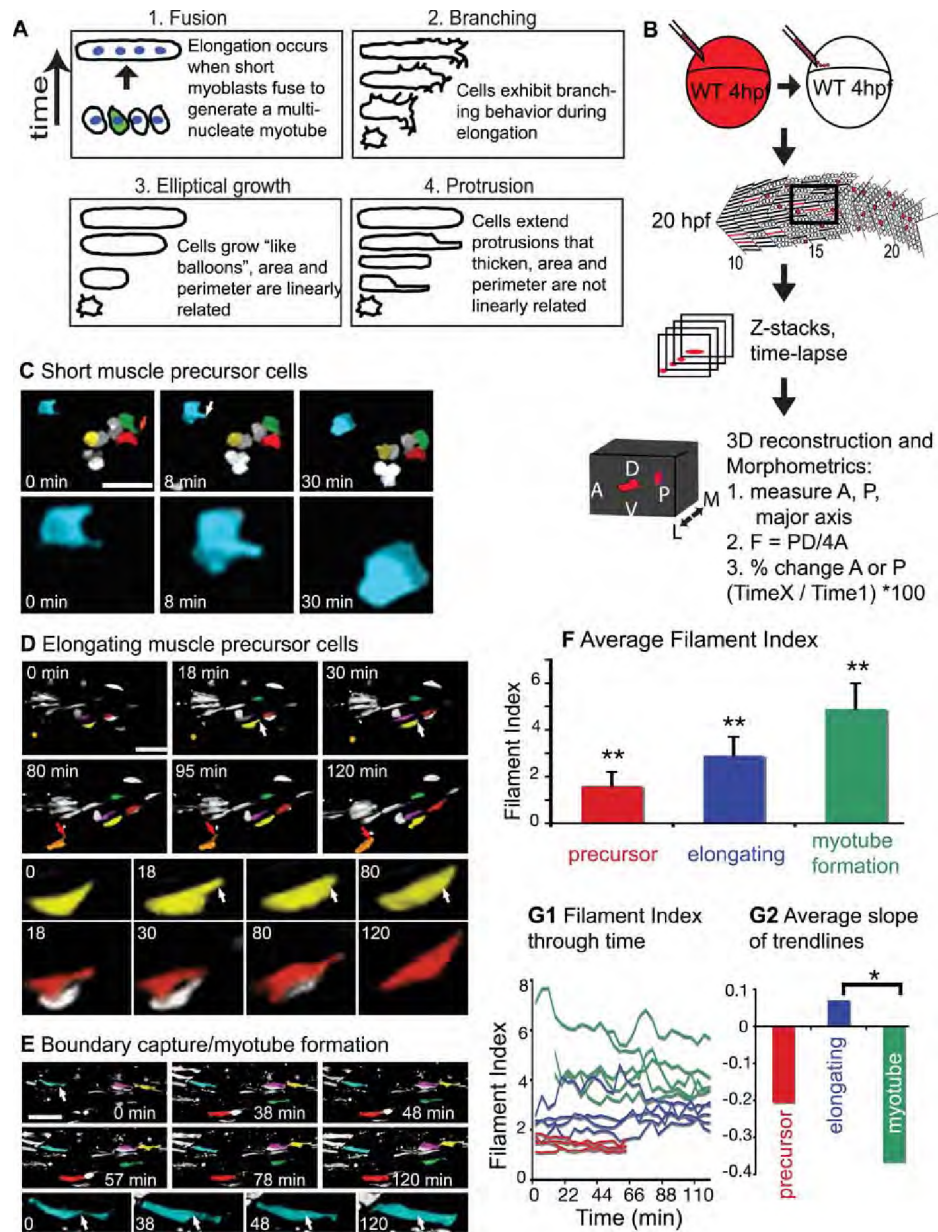


Figure 2. Three Phases of Muscle Morphogenesis: Short Muscle Precursor Cells, Intercalation/Elongation, and Boundary Capture/Myotube Formation. (See also Movie S3.) Projections of ApoTome micrographs are shown, side views, anterior left, dorsal top. Cells were pseudocolored to facilitate visualization. A) Cartoon depicting possible scenarios for elongation of myofibers. B) Cartoon depiction of the methods

used. Dextran filled WT cells (red) were transplanted into an unlabeled embryo at the blastula stage, time-lapse data was collected at 20 hpf, then Z-stacks were three dimensionally projected for morphometric analysis. C) Short muscle precursor cells do not undergo large-scale shape changes. A 21 somite stage embryo, approximate location of somite 15 at left. The blue cell extends a filopodia-like protrusion (8 min, white arrow) that is then retracted (30 min, the blue cell is enlarged in the bottom panels). The protrusion in the green cell (red arrow at 0 min) is also retracted by 30 min. D) Elongating muscle precursor cells extend protrusions along their major axis as they elongate. A 22 somite-stage embryo, somite 18 at left. The yellow cell extends a long, thin protrusion (white arrow) at 18 min that increases in thickness, resulting in a longer cell. The orange cell extends a protrusion (red arrow) at 80 min that becomes thicker by 120 min. E) Myotube formation involves the transition from an irregularly shaped cell to a more homogeneously shaped tube. At 0 min, the blue cell with a white arrow is not yet tube-shaped, i.e. part of the cell is significantly narrower than the other parts (white arrow). Over time, the narrow portion thickens, eventually generating a long tube-shaped myotube (120 min, white arrows in bottom enlarged panels are in the same location in all panels). F) The filament index is significantly different between the three phases (**, $p < 0.01$). G1) The filament index of the three phases through time. G2) Average slopes of linear trendlines from data in G1 (*, $p < 0.05$). doi:10.1371/journal.pgen.1000219.g002

1.6 ± 0.6 , fixed cells 1.4 ± 0.2). The correlation of the length with perimeter is also similar to live cells (Table 1).

Both the qualitative appearance and the morphometric properties of fixed cells presumed to have been elongating (those between $5 \mu\text{m}$ and $40 \mu\text{m}$ in fixed embryos) are similar to live elongating cells. The major axis is very strongly correlated with perimeter and area in both populations (Table 1). Similar to live cells, long narrow protrusions are only observed along the major axis (Figure 4B, G, yellow arrowheads, Movie S4). We also analyzed the nuclear content of dextran-filled cells during elongation. A z-series was taken and cells were examined in three dimensions. No elongating cells contained more than one nucleus (Figure 4G, $n > 100$ cells).

Cells that were fully elongated but irregularly shaped were presumed to be in the boundary capture/myotube formation phase (Figure 4C is a three-dimensional projection of an irregularly shaped but elongated cell). The filament index of these cells was also similar to live cells (Figure 4E). Fast-twitch cells in this phase were mononucleate (Figure 4 H shows one focal plane of a mononucleate cell that is elongated but irregularly shaped when examined in three dimensions, Movie S4, $n = 108$). Interestingly, all muscle cells that contained multiple nuclei exhibited a stereotypical tubular shape ($n = 57$, see Figure 4I). These data suggest the intriguing possibility that the transition from an irregularly shaped long cell to a rod-shaped myotube may involve fusion. Our use of dextran-labeled cells in a field of unlabeled cells clearly highlights the morphological complexity of elongating fast-twitch muscle cells and indicates that it is not possible to unambiguously identify multinucleate cells utilizing a

nuclear marker as well as a marker that denotes all cells (such as phalloidin). Thus, we do not know the exact timing of muscle cell fusion or whether fusion contributes to the morphogenesis of irregularly shaped long fibers into regularly shaped, cylindrical myotubes. However, it is evident that the first fast-twitch muscle cells do not fuse in order to elongate.

The filament index of fixed muscle cells, as in live cells, is significantly different between each phase (data not shown, two-tailed t-test, $p < 0.01$ for all comparisons). These data support the time-lapse analyses and provide new tools for analysis of morphogenetic defects in various mutant/morphant embryos.

Quantification of Anisotropy Indicates that Each Phase of Muscle Fiber Morphogenesis Is Accompanied by a Significant Increase in Ordered Structure

The identification of discrete, mathematically distinct phases provides a paradigm by which muscle morphogenesis in mutant embryos can be assessed. The above data also indicate that the morphology of fixed cells is not significantly different than live cells. However, although obtaining single labeled cells within a field of unlabeled cells in fixed embryos is easier than time-lapse analysis, it is not feasible in all model systems. We thus looked for a different mathematical tool to quantify cellular organization. Ideally such a tool would allow objective quantification of cellular structure with an easier experimental preparation such as staining with phalloidin to outline all cells. Therefore, we adapted and applied the 2D Wavelet-Transform Modulus Maxima (WTMM) method [34,35]. This method can be used to quantify the amount of structure, or order, of objects that do not necessarily have a well

Table 1. Morphometric analysis of muscle cells.

Phase	Subcategory	N	Average slope \pm SE	Major Axis vs. Perimeter R^2	Filament Index \pm SD	
Short precursor	WT live	12		0.57	1.6 ± 0.6	
	WT fixed	31		0.59	1.4 ± 0.2	
	Laminin-deficient fixed	8		0.92	1.4 ± 0.3	
Elongating precursor	WT live	6		0.9	2.9 ± 0.8	
WT live	% change in area	6	2.7 ± 0.8			
WT live	% change in perimeter	6	1.8 ± 0.8			
Forming myotube	WT fixed	255		0.90		
	Laminin-deficient fixed	166		0.89	3.0 ± 1.5	
Forming myotube	WT live	6		0.31	4.9 ± 1.1	
	WT live	% change in area	6	1.5 ± 0.5		
Forming myotube	WT live	% change in perimeter	6	0.2 ± 0.1		
	WT fixed	13		0.16	6.0 ± 0.9	
	Laminin-deficient fixed	11		0.9	5.1 ± 2.2	

doi:10.1371/journal.pgen.1000219.t001

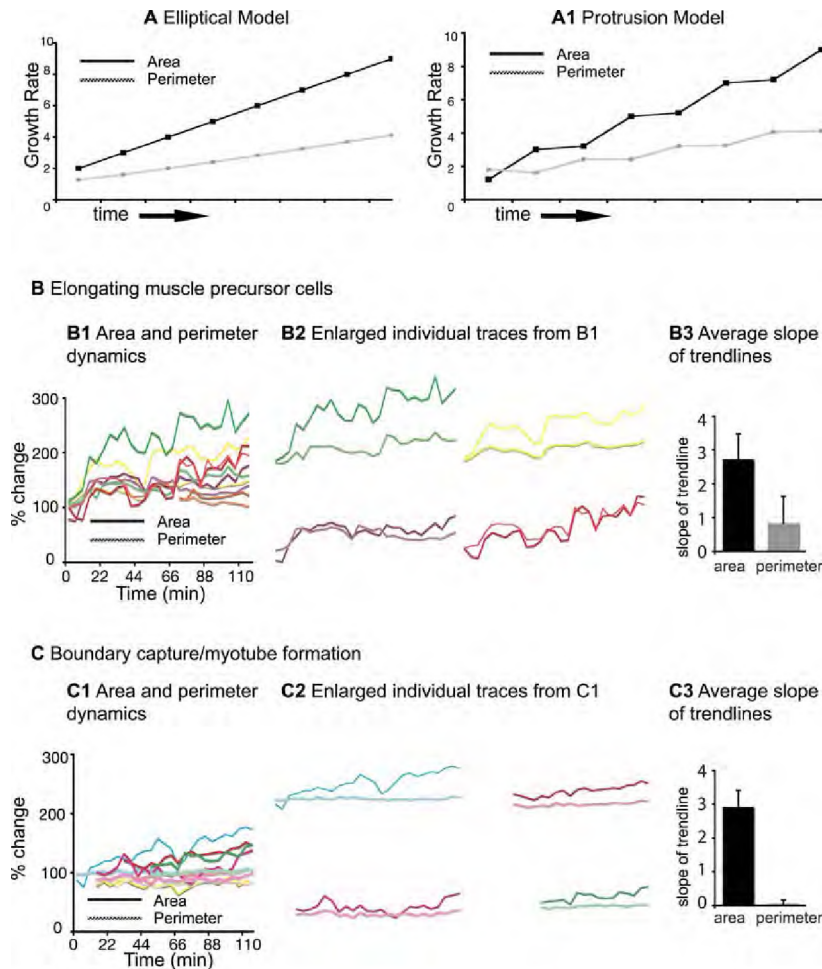


Figure 3. Mathematical Analysis of Area and Perimeter Dynamics. A) Geometric modeling of relative changes in area and perimeter that would result if cells elongated as ellipses, as if they were filling like balloons. Both area and perimeter would increase linearly. A1) Geometric modeling of relative changes in area and perimeter that would result if cells elongated via a two-step process: protrusion extension and filling. Both area and perimeter would increase incrementally. B) Area and perimeter dynamics during the elongation phase. B1) Percent change of area (solid line) and perimeter (dotted line) through time. Enlarged traces are shown in B2. B3) Average slope of linear trendlines. The area increased more than the perimeter in all cells. C) Area and perimeter dynamics during the myotube formation phase. The growth rate of area and perimeter are different in the myotube formation phase than the elongation phase. As the cell transitions from being irregularly shaped to a more homogeneously shaped myotube, the increase in area represents the filling in of an initially narrow aspect of the cell. Filling in does not dramatically increase the perimeter, but does result in an increase in area.
doi:10.1371/journal.pgen.1000219.g003

defined boundary. We used this approach to quantify the structural organization of cellular lattices during muscle fiber elongation. The WTMM analysis filters an image with the gradient of a smoothing function (i.e. a wavelet) at a given size scale. Places within the image where the intensity variation is maximal are given by the wavelet-transform modulus maxima (i.e.

the WTMM). Next, the positions of maximal intensity variation along these maxima chains are identified. These are the WTMM maxima, or WTMMM. At these nodes, the direction where the signal has the sharpest variation is calculated. An arrow that points upward has an angle of $\pi/2$ and an arrow that points down has an angle of $-\pi/2$. The anisotropy factor F_a is then calculated from

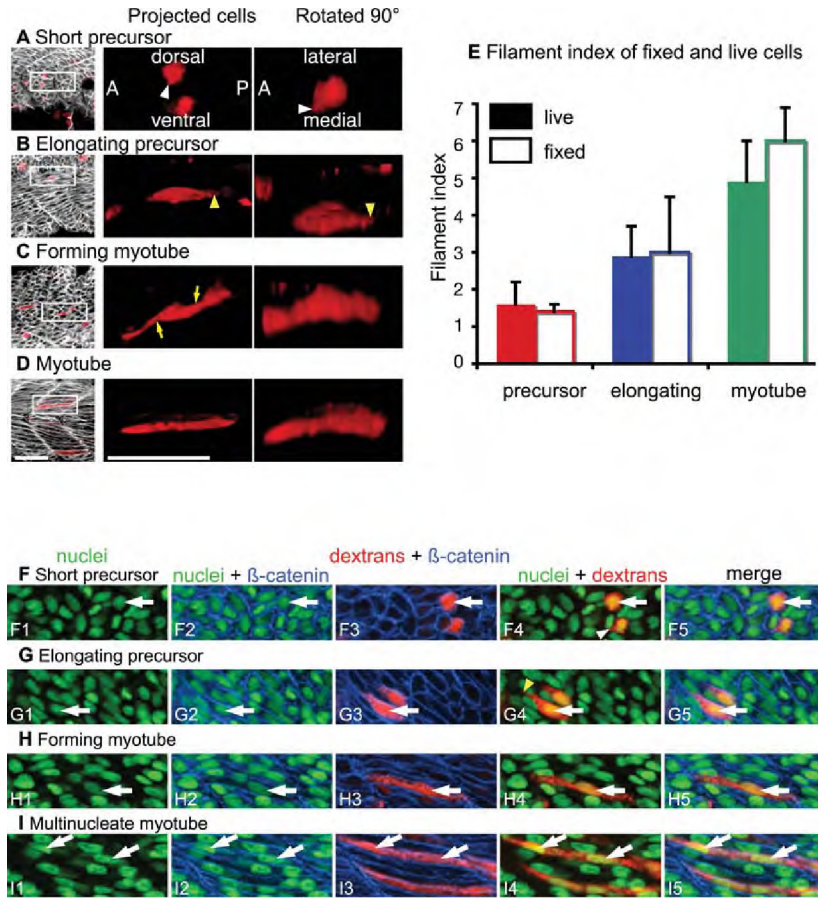


Figure 4. Mathematical Characterization of Fixed Cells Supports Time-Lapse Analysis of Live Cells. (See also Movie S4.) ApoTome images, side views, anterior left, dorsal top, 22 somite-stage fixed embryos. A–D) Dextran-labeled cells (red), β -catenin staining outlines cells (white). Rotated 90° projections were stretched ≈ 3 fold in the Z dimension due to the relative thinness of the tissue. Scale bars: 50 μ m. A) Short muscle precursor cells are short and extend small protrusions (white arrowheads). B) Long protrusions extended along the major axis of the cell are observed (yellow arrowheads). C) Irregularly shaped cells that span the entire width of the myotome are observed (yellow arrows). D) Long regularly shaped myotube. E) Graph showing that the filament indexes for live and fixed cells are similar. F–H) 22 somite-stage fixed embryo, nuclei are stained with Sytox green, dextran-labeled cells are red, β -catenin in blue outlines cells. Although the nuclear content of cells was analyzed in all focal planes, only one focal plane is shown for clarity. White arrows point to nuclei. F) Precursor cells are short and have one nucleus (white arrowhead in F4 shows short protrusion). G) Cells that were elongating when fixed were never observed to contain more than 1 nucleus (yellow arrowhead shows a long protrusion). H) An elongated cell with 1 nucleus. I) Multinucleate myotube. doi:10.1371/journal.pgen.1000219.g004

the probability density function, $P_\alpha(A)$, of the angles A of the WTMM vectors. F_α is defined in such a way that randomness, isotropy, has a value of $F_\alpha = 0$. Any value of $F_\alpha > 0$ quantifies the extent of departure from isotropy. A randomly structured cell lattice has arrows pointing in all directions and a low anisotropy factor. The arrows point in all directions because the direction of maximal intensity variation is random. A more organized cell lattice will have more arrows pointing in the same direction and a stronger anisotropic signature. More arrows will point in the same

direction in an ordered cell lattice because the direction of maximal intensity variation will be the same between multiple cells. Thus, this formalism objectively provides a quantitative assessment of morphological structure. A step-by-step explanatory diagram is presented in Figure 5.

The WTMM analysis was applied for all size scales between $a \sim 4$ and $a \sim 13 \mu$ m (see methods for details on staining and image preparation). Short muscle precursor cells have a low anisotropy factor indicating that there is only a small departure from isotropy.

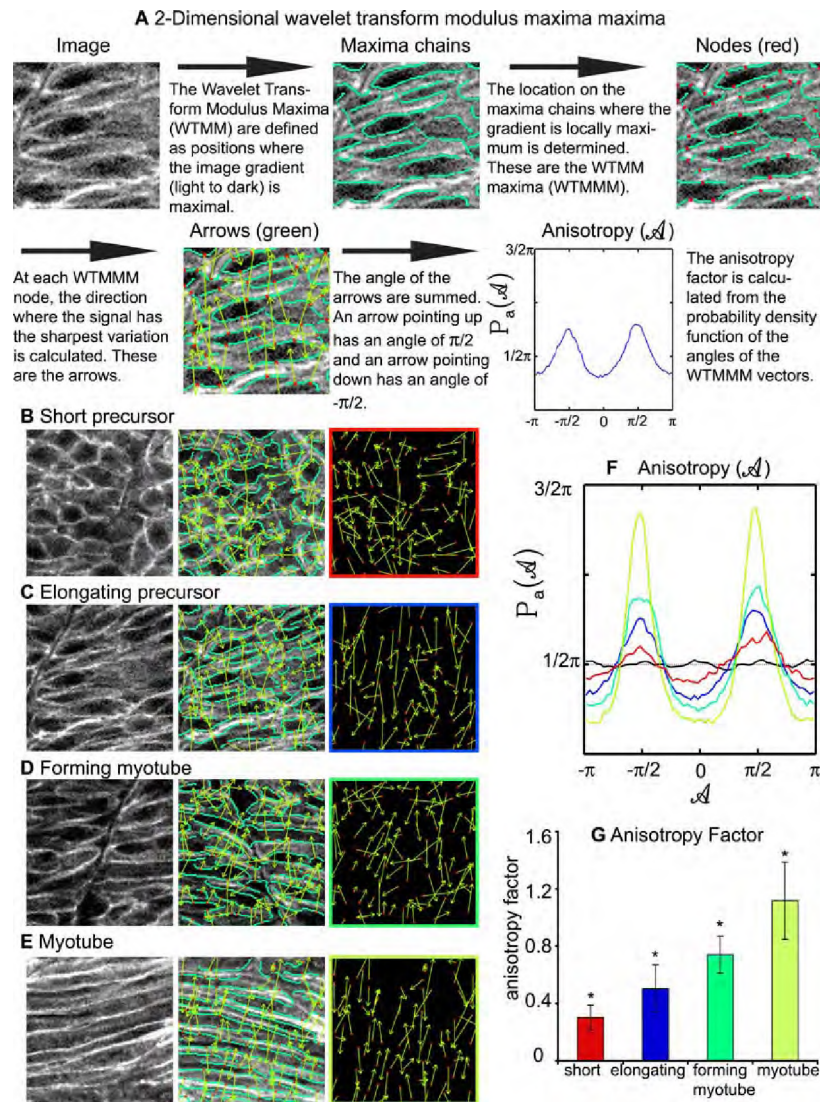


Figure 5. The 2D WTMM Method Is Used to Quantify Cellular Structure within a Lattice, and Indicates that Cellular Organization Increases during Muscle Morphogenesis. A) Description of how the 2D WTMM formalism quantifies structure. The starting image is of elongating muscle precursor cells stained for β -catenin to outline cells. B) Short muscle precursor cells have almost all WTMMM vector arrows pointing in random directions, indicating that there is only a small departure from isotropy (isotropy means randomly structured). C) Organization increases as muscle cells begin to elongate. Note more green arrows pointing either up or down in C than in B. D) Organization continues to increase during the myotube formation phase. E) Organization is readily apparent when myotubes have formed. Note that most of the green arrows are pointing either up or down indicating high levels of organization. F) Averaged $P_a(\mathcal{A})$ for one particular size scale ($a \sim 7 \mu\text{m}$) for the myotube stage (lime green curve), the forming myotube stage (dark green curve), elongating precursor stage (blue curve), short precursor (red curve) as well as for the isotropic f8m surfaces analyzed for calibration purposes (black curve fluctuating around $\pi/2$). Also shown is the flat $1/2\pi$ curve that would be obtained for a purely theoretical isotropic process (flat pointed line at $1/2\pi$). G) The anisotropy factor F_a was averaged over all size scales analyzed. An indicator of organized structure, it shows significantly distinct values for all stages of developing muscle cells. doi:10.1371/journal.pgen.1000219.g005

Organization increases throughout muscle elongation. This increase in organization through time is visible as the increase in the proportion of arrows pointing in the same directions (Compare Figure 5B to 5E). The averaged probability density functions $P_a(A)$ over all size scales a are shown in Figure 5F and the resulting averaged anisotropy factors F_a are shown in Figure 5G. Each phase of muscle development has a significantly higher anisotropy factor indicating increasing cellular organization through time (importantly, statistical significance is maintained when only single size scales are used).

Taken together, all the methods used (time-lapse analysis, area/perimeter dynamics, filament index, and 2D WTMM) show that there are discrete phases of fast muscle morphogenesis. Furthermore, the fact that the 2D WTMM analysis supports the other morphometric analyses used indicates that this is an exceedingly valuable tool that can objectively quantify how ordered/structured a field of cells is without having to isolate or segment individual cells.

lamβ1 and *lamγ1* Are Required for Normal Fast Muscle Cell Orientation

Thorough knowledge of the cellular mechanisms underlying muscle fiber elongation provides a framework for elucidating the molecular basis of muscle cell elongation. We asked if a prominent basement membrane protein, laminin, is required for muscle morphogenesis. It is known that a laminin receptor, Integrin $\alpha6\beta1$, is required for normal myofiber development in cultured mouse explants [22] but the relevant laminin ligands are unknown.

We find that muscle cell elongation in *lamβ1* and $\gamma1$ mutants and morphants is delayed. In zebrafish, slow-twitch fibers migrate laterally and trigger fast muscle cell elongation [28]. Thus, slow fiber location is an excellent marker for assaying fast muscle cell elongation: fast cells medial to slow fibers should be fully elongated. Although slow muscle fiber migration is disrupted in *lamβ1* and $\gamma1$ -deficient embryos (Figure S1), some slow fibers migrate laterally. However, fast muscle cells medial to migrating slow fibers are short in *lamβ1* or *lamγ1* mutants and morphants (Figure 6B, C, and data not shown, $n=6$ *gnumby/lamβ1* mutant embryos, 16 *lamβ1* morphant embryos, 5 *wi390/lamγ1* mutant embryos and 10 *lamγ1* morphant embryos).

Fast-twitch muscle cells belatedly elongate in *lamβ1* and $\gamma1$ -deficient embryos and the filament index of cells in all three phases is similar to control embryos (Table 1). However, fast muscle cells frequently appear misoriented in *lamβ1* and $\gamma1$ -deficient embryos (Figure 6E, note the abnormal angle of cells that are not aligning in a parallel array, data not shown). Application of the 2D WTMM method indicates that myotubes in *lamγ1*-deficient embryos are significantly more disorganized than in control embryos. Elongated myotubes in control embryos form an organized array as indicated by the strong polarization of the yellow arrows (Figure 6G3). The arrows tend to point either up or down resulting in high peaks at $\pi/2$ and $-\pi/2$ (Figure 6K lime green line) and a higher anisotropy factor (Figure 6L). In contrast, arrows in *lamγ1*-deficient embryos are far less polarized (compare Figure 6H3 to G3). The peaks at $\pi/2$ and $-\pi/2$ are lower than in wild-type embryos (Figure 6K lime green line) and the anisotropy factor is significantly lower (Figure 6L). Thus, application of the 2D WTMM formalism quantitatively supports the qualitative perception that muscle fibers are disorganized in *laminin*-deficient embryos.

The next question that follows is *when* does the anisotropic signature in *laminin*-deficient embryos become different from wild-type embryos? No overt morphological differences between control and *laminin*-deficient cells in the short precursor phase are visible to the eye (Figure 6I, J). However, there is a slight but significant difference between the anisotropy factors (Figure 6L). The difference

between anisotropy factors increases at every phase of muscle morphogenesis. These data indicate that *laminin* is required for cellular organization as early as the short precursor phase. Thus, subsequent myotube disorganization may reflect both early and late requirements for laminin during muscle morphogenesis.

Laminin Is a Molecular Cue that Stops Fiber Elongation

It has been proposed that muscle fibers elongate until they reach a small patch of ECM that functions to capture elongating muscle cells and prevent them from extending into the next myotome [24]. However, it is not known which of the many ECM components of the MTJ are required or if multiple proteins are required. We find that both *lamβ1* and *lamγ1* play a role in MTJ morphogenesis. Some fast muscle cells in *lamβ1* and *lamγ1* mutants and morphants do not stop elongating at the MTJ (Figure 6F1 white arrowhead, note that the muscle cell extends a long, thin protrusion across the boundary). The MTJ is visible in 48 hpf wild-type (WT) embryos as a dark line devoid of filamentous actin (Figure 7A, white arrow). In *wi390/lamγ1* mutant embryos, some muscle fibers inappropriately cross the MTJ and are approximately twice as long as their counterparts that did not cross the boundary (Figure 7A1 red arrowhead). These cells are multinucleate (data not shown), indicating that boundary capture is not required for fusion. The crossing of a boundary by a few muscle fibers results in an asymmetrical myotome: some of the myotome has longer fibers while the majority of fibers are an appropriate length (Figure 7A1). Fast fibers in *gup/lamβ1* mutants also cross MTJ boundaries (Figure 7A2 red arrowhead). At 48 hpf, some boundaries were crossed within every *laminin*-deficient embryo examined. Generally, 16–24% of boundaries were crossed (average % of boundaries crossed: WT, 0%, $n>100$; *gup/lamβ1*, 20% crossed, $n=12$ embryos, 3 experiments; *wi390/lamγ1*, 22% crossed, $n=9$ embryos, 1 experiment; *lamβ1* MO, 24% crossed, $n=26$ embryos, 5 experiments; *lamγ1* MO, 16% crossed, $n=18$ embryos, 3 experiments).

Boundary Capture as a Cell Autonomous Phenomenon

Our data show that *lamβ1* and $\gamma1$ play a role in boundary capture of elongating muscle fibers, but the mechanism of capture is not yet known. A dense network of polymerized laminin may function as a physical barrier that stops elongating muscle fibers. Interestingly, however, laminin polymerization can trigger changes in the organization of the matrix, ECM receptors and cytoskeletal components [36]. Cell-autonomous changes in cytoskeletal organization upon laminin binding provide an alternate hypothesis: that signaling that results from laminin binding may mediate boundary capture in a cell-autonomous fashion. We hypothesized that WT cells transplanted in *laminin*-deficient embryos might be able to secrete small amounts of laminin that would facilitate their capture and reduce the likelihood of elongating through the boundary. To test this, cells from dextran-injected control embryos were transplanted into *lamγ1* morphant hosts. Control cells were less likely than *lamγ1* morphant cells to cross the boundary (Figure 7C, D). Only 6 percent of control cells crossed boundaries (19/311 cells) whereas 25% of morphant cells crossed boundaries (407/1631 cells). Control cells undergo boundary capture even when adjacent to *lamγ1* morphant cells crossing boundaries (Figure 7B1, B2 note that the red control cell, white arrowhead respects the boundary, but adjacent morphant cells cross the boundary, red arrowhead). These data not only provide the first evidence that laminin plays a role in ceasing initial myofiber elongation, but the cell autonomous rescue of boundary integrity by WT cells suggests that boundary capture is mediated at the single cell level.

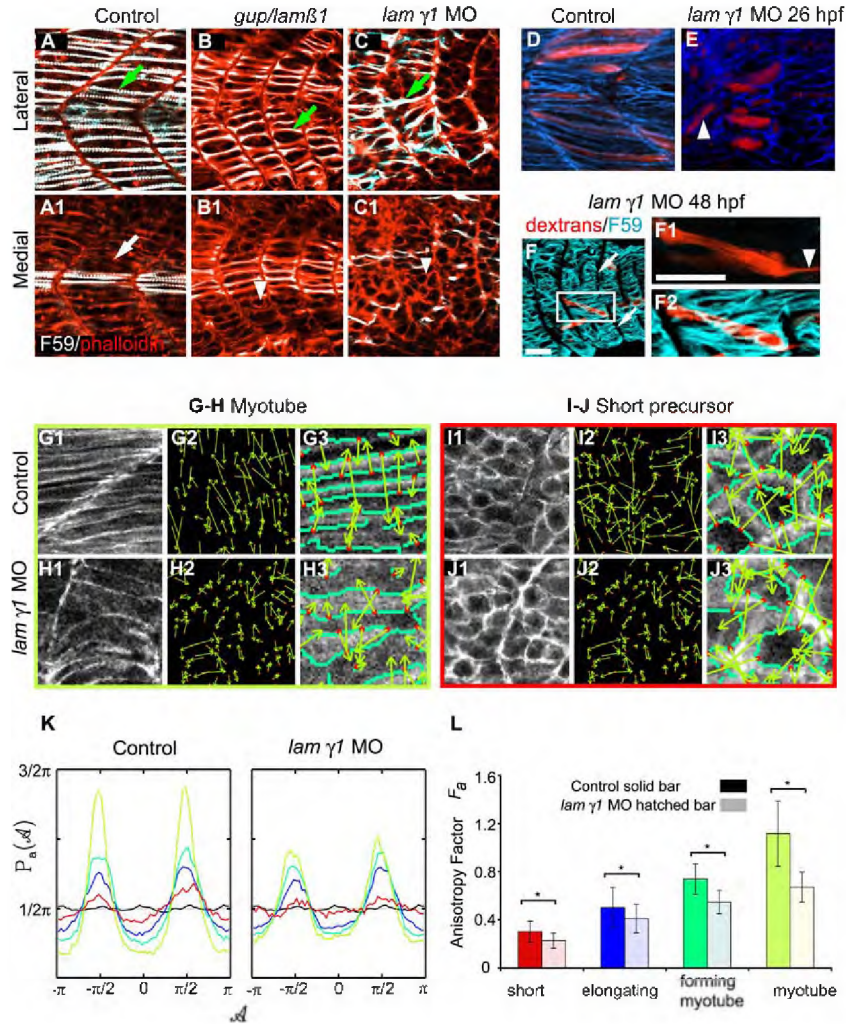


Figure 6. *lamininβ1* and *γ1* are Required for Normal Fast Muscle Cell Elongation. Panels A–C are confocal images and D–J are ApoTome micrographs. Panels A–C are side views, anterior left, dorsal top of 18 somite-stage embryos stained with F59 (white) to denote slow-twitch muscle and phalloidin (red) to outline fast muscle cells. Panels labeled 1 are lateral sections from a z-series and panels labeled 2 are medial sections from the same z-series. A) In WT embryos, fast-twitch muscle cells medial (A1, white arrow) to migrating slow-twitch fibers (A, green arrow) have elongated. B) Although some slow-twitch fibers do migrate in *gup/laminβ1* mutant embryos, not all fast muscle precursor cells have elongated (B1 white arrowhead: short cell, B green arrow: slow-twitch muscle fiber that has migrated laterally). C) Not all fast muscle precursor cells medial to migrating slow fibers have elongated in *lamγ1* morphant embryos (C1 white arrowhead: short cell, C green arrow: slow-twitch muscle fiber that has migrated laterally). Panels D–E are projected views of dextran filled cells (red) and β-catenin that outlines cells (blue). D) Elongated fibers in a WT embryo, note the organized, parallel array of fibers. E) Elongated fibers in a *lamγ1*-deficient embryo, white arrowhead denotes a fiber that is not parallel. F–F2) A dextran-filled cell in a *lamγ1* morphant embryo extends a thin protrusion across the MTJ. White arrows denote the MTJ, white arrowhead denotes thin protrusion extending across the MTJ. F59 denotes slow muscle in blue and dextrans are red. Panel F1 is a single focal plane from a z-series, panels F and F2 are projections. Scale bars F: 50 μm, F1: 20 μm. G–H) Cells in the myotube phase are less organized in *lamγ1* morphant embryos than in control embryos as shown by more randomly oriented WTMMM vector arrows. Panels numbered 3 are higher magnification views. I–J) Although differences in cellular structure are not obvious to the eye (compare I1 and J1), *lamγ1* short precursor cells are less organized than control cells as shown by more randomly oriented WTMMM vector arrows. Panels numbered 3 are higher magnification views. K: The WTMMM vector angle pdfs are displayed for all stages (color coded per panel L), the isotropic fbm surfaces (black curve fluctuating around $\pi/2$), and the flat $1/2\pi$ curve that would

be obtained for a purely theoretical isotropic process (flat pointed line at $1/2\pi$). Note the stronger (higher) peaks in control embryos. L) The anisotropy factor of muscle cells in laminin-deficient embryos is significantly lower than in control embryos at all four stages of muscle morphogenesis ($p < 0.01$). These results indicate that even though differences in organization as far back as the precursor stage are not obvious visually, they are unequivocally more disorganized than in controls when the anisotropic value is determined.
doi:10.1371/journal.pgen.1000219.g006

Discussion

A mechanistic understanding of the cellular basis of muscle cell elongation and tendon attachment is critical to elucidate underlying molecular mechanisms that mediate morphogenesis. We show here the first quantitative analysis of *individual* fast muscle cell elongation in a living vertebrate embryo. Three broad phases of morphogenesis underlie the transition from a somite comprised of short muscle precursor cells to a myotome comprised of elongated muscle fibers. First, short muscle precursor cells exhibit

dynamic protrusive activity, but do not undergo large-scale shape changes. The second phase, intercalation/elongation, occurs via a repetitive two-step process of protrusion extension and filling and requires *lamβ1* and *γ1* to proceed efficiently. The third phase encompasses boundary capture as well as shape changes that generate a more regularly shaped myotube. Although myotubes do form in *laminin*-deficient embryos, they are significantly less organized than in wild-type embryos. We find that both *lamβ1* and *γ1* are required for boundary capture and thus provide the first molecular insight into boundary capture at the MTJ. Taken

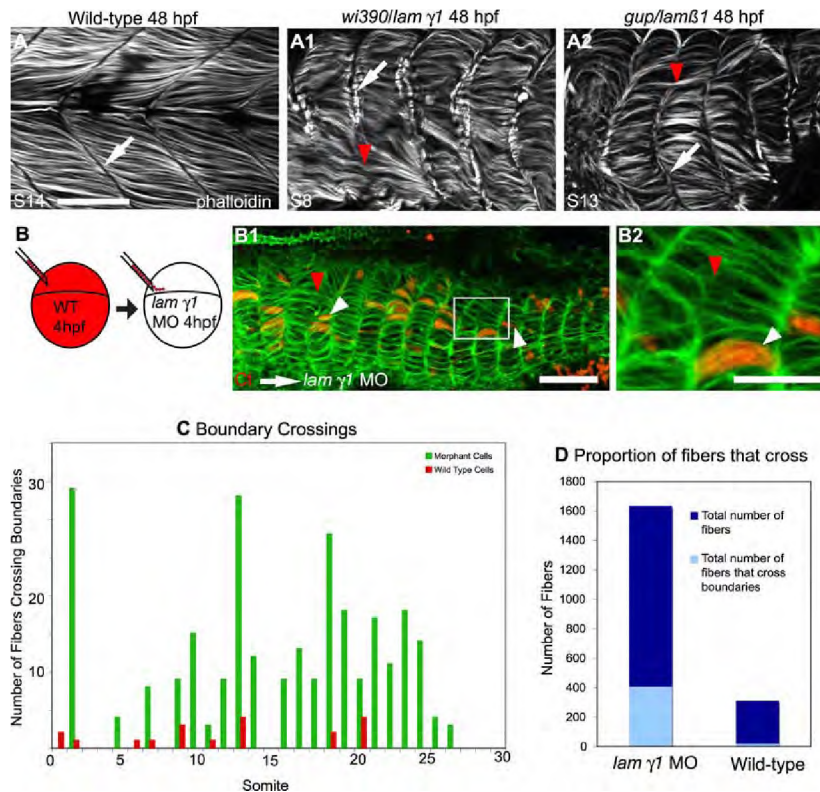


Figure 7. Laminin Plays a Role in Boundary Capture of Elongating Muscle Fibers. ApoTome micrographs, side views, anterior left, dorsal top of 48 hpf embryos. A–A2) MTJ boundaries are sometimes crossed in *lamβ1* and *lamγ1*-deficient embryos. The MTJ in WT embryos is visible as the dark line of no phalloidin staining in between myotomes (A, white arrow). In both *lamβ1* and *γ1* mutants, MTJs are observed (A1–A2, white arrows), but sometimes a portion of an MTJ is crossed by a muscle fiber (red arrowheads, A1–A2). Scale bar: 50 μ m. B–B2) Cell autonomous rescue of boundary crossing by control cells in *lamγ1* morphant embryos. White box in B1 indicates the higher magnification view in B2. Transplanted control cells do not cross the MTJ boundary (white arrowheads, only 19/311 transplanted control cells crossed MTJ boundaries in *lamγ1* morphant embryos compared to 402/1631 morphant cells). The red arrowhead indicates morphant cells that cross boundaries. Scale bars: 20 μ m. C–D) Graphs showing boundary crossing by control cells and morphant cells.
doi:10.1371/journal.pgen.1000219.g007

together, these data indicate that muscle morphogenesis is spatiotemporally complex and involves interactions between muscle fibers and the basement membrane during elongation and attachment to the MTJ. It is not yet known if there is some conservation between morphogenetic mechanisms underlying early morphogenesis between vertebrates. Given recent data indicating that the zebrafish somite has a dermomyotome and is thus more homologous to amniotes as previously thought [37–39], it is tempting to speculate that the morphogenetic mechanisms described here may apply to higher vertebrates as well.

Three Phases of Early Fast Muscle Morphogenesis

Both qualitative and quantitative assessments of early muscle development are critical to facilitate identification of molecular mechanisms that underlie morphogenesis. We find that the three phases of early fast muscle morphogenesis are qualitatively and quantitatively different. These stages are short muscle precursor cells, elongating muscle cells and myotube formation. Short muscle precursor cells have a low filament index and extend and retract short (<2 μm) protrusions in all directions. Elongating fast muscle cells extend long protrusions along the axis of elongation and have a higher filament index. Long muscle cells forming myotubes have an even higher filament index indicating yet a further departure from a circular shape. Thus, we provide a novel paradigm whereby morphometric analysis can distinguish different phases of early muscle development.

Mathematical Modeling and Time-Lapse Analysis Indicate that a Repetitive Two-Step Mechanism Underlies Fast Muscle Cell Elongation

It is not known how the first fast-twitch muscle cells elongate during vertebrate development. We utilized an experimental approach to distinguish between potential scenarios (Figure 2A). C2C12 myoblasts in culture elongate prior to differentiation and fuse to generate a multinucleated myotube [10] that we termed the elliptical growth scenario. The first muscle cells to elongate in grasshopper embryos (muscle pioneers) exhibit a morphology similar to that of pathfinding neurons [11], we have called this the branching scenario. During *Drosophila* embryogenesis, muscle cells elongate via fusion [12,13] and zebrafish homologues of genes required for muscle cell fusion in *Drosophila* are also required for normal muscle development in zebrafish [14,15]. It has also been proposed that zebrafish muscle cell elongation may be similar to notochord/neural plate cell intercalation [24], represented by the protrusion scenario. Time-lapse analysis indicates that elongating cells extend local protrusions along their long axis (Figure 8C, D). Protrusions are extended in the direction of elongation and between other cells. Protrusions then thicken, resulting in elongation of the cell. Repetition of protrusion extension/thickening results in an elongated muscle cell. Mathematical modeling of expected changes in area and perimeter supports the protrusion model of morphogenesis. Thus, we show that a novel two-step mechanism underlies elongation of the first fast muscle fibers in a vertebrate model system, the zebrafish.

Muscle Cell Fusion

Muscle development is perhaps best understood in *Drosophila*, where muscle morphogenesis is accomplished via fusion of founder cells (FCs) with fusion competent myoblasts (FCMs) [13]. Recent 3-D imaging has demonstrated that there are two phases of fusion and suggests that the spatial relationship of FCs and FCMs influences the frequency of fusion events [12]. Exciting recent studies using zebrafish suggest that molecular events underlying muscle cell fusion in vertebrates may be at least partially conserved [14,15,40]. In the

future it will be important to understand the cellular basis of fusion as well. In this regard, we show that elongating/recently elongated muscle cells possess complex 3-D shapes. Thus, a comprehensive analysis of cell behaviors underlying muscle cell fusion during zebrafish development will require development of multiple markers that label entire muscle cells such that fusion can unambiguously be analyzed. Genetic mosaic approaches such as those used previously [41] will facilitate analysis of both the timing of fusion as well as identifying what cells fuse.

Attachment to Laminin Is Necessary for Timely Fast Muscle Cell Elongation

We show that *lamβ1* and $\gamma1$ are required for efficient fast muscle cell elongation and proper organization. Application of the 2D WTMM method indicates that even in early stages of muscle development where organizational differences are not visually obvious, anisotropic signatures reveal unequivocally the morphological discrepancies between *laminin*-deficient and control embryos. This emphasizes the strength of the 2D WTMM method. This novel use of the 2D WTMM method will give researchers an invaluable tool to rigorously and quantitatively distinguish subtle differences in cellular morphology and organization.

We do not know why fast muscle cell elongation is delayed in *lamβ1* and $\gamma1$ -deficient embryos. Elongation may be delayed because fast cells are less organized than in controls. It is also possible that fast cells in *lamβ1* and $\gamma1$ mutant/morphant embryos do not elongate efficiently because slow muscle cells do not migrate efficiently. Although WT slow fibers can rescue elongation in mutant embryos that do not have slow muscle fibers [28], it is unknown if disrupted slow muscle migration and/or morphology may delay fast muscle cell elongation.

A third model is that adhesion to laminin may play a role in generation of traction forces that allow muscle cells to elongate. Muscle cells extend protrusions as they elongate and these protrusions likely attach to other cells or the ECM. Attachment would provide a mechanism for cells to stabilize an extended protrusion and continue elongation. Interestingly, adhesion to laminin via the Integrin $\alpha7\beta1$ receptor promotes migration of C2C12 and MM14 cells in culture [42]. Elongating fast muscle cells in zebrafish do not migrate per se, but future studies will address whether adhesion to laminin during fast muscle cell elongation in zebrafish promotes efficient protrusion extension and thickening. These studies would be facilitated by identification of the relevant laminin receptor (there are multiple laminin receptors) such that genetic mosaic analysis could readily be used.

Fast muscle cells do belatedly elongate in the absence of laminin. It is possible, even likely, that elongating muscle cells may utilize different modes of adhesion to the substrate and/or other cells. Thus, if one mode of adhesion is disrupted, muscle cell elongation would be delayed, but not entirely inhibited. Our results indicating that muscle cell elongation is delayed, rather than inhibited, are similar to the finding that myofiber formation is delayed, but recovers in mouse knockouts of the cell-cell adhesion protein CDO [43]. Taken together, these results suggest that muscle cells elongate by extension of protrusions that adhere both to other cells and the ECM. If one mode of adhesion is disrupted, cells are delayed in their elongation, but utilize the alternative mode of adhesion to eventually elongate (Figure 8C, D).

Laminin Participates in Boundary Capture of Elongating Muscle Cells

One fundamental process during embryonic development is boundary formation. Some of the first work describing boundary

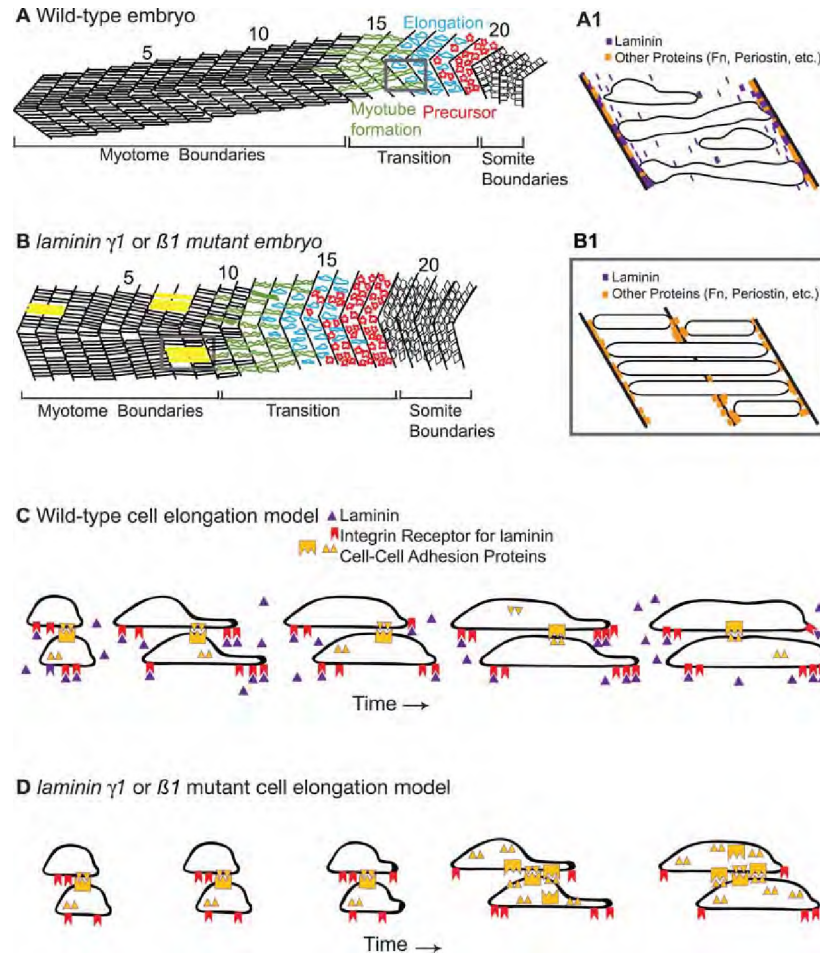


Figure 8. Model of Muscle Morphogenesis in WT and *laminin* Mutant Embryos. A–A1) Cartoon of WT embryo showing the three phases of muscle elongation. In the oldest/most anterior somites, myotubes have formed and are attached to the MTJs. The transition region contains cells intercalating by extending protrusions that are subsequently filled. Muscle precursor cells exhibit protrusive activity in all directions. A1: Magnification of a somite in panel A showing proteins concentrated at the MTJ and boundary capture of recently elongated cells. B–B1) Cartoon of *laminin* mutant embryo at the same age as WT embryo in panel A showing the same three phases of muscle morphogenesis, but with a developmental delay. Cells in yellow are aberrantly long and have invaded into neighboring myotomes. B1: Magnification of two somites in panel B that depicts a model of how boundary crossing could occur in *laminin* mutant embryos. If laminin is absent, there may be randomly spaced locations at the MTJ devoid of proteins that function in boundary capture. Elongating muscle cells would invade the MTJ at these locations. C) Cartoon model showing the two-step mechanism of elongating. We show that adhesion to the matrix is required for normal elongation and hypothesize that cells also utilize cell-cell adhesion to generate traction forces needed for protrusion extension and filling. D) Model accounting for developmental delay in muscle morphogenesis that occurs in *laminin* mutants. Cartoon depicting a *laminin* mutant cell undergoing two-step elongation via protrusion extension and filling. Lack of the cell-matrix adhesion protein laminin results in less traction and therefore slower extension and/or filling.
doi:10.1371/journal.pgen.1000219.g008

formation was done by Jacobson and colleagues [44–46], where they showed that cells that reach the notoplate/neural plate boundary remain on the boundary permanently in both axolotl and newt embryos. This phenomenon was referred to as trapping.

Keller and colleagues have since expanded upon this model and termed it boundary capture [47]. Recent work demonstrated that *laminin* plays a critical role in boundary capture during notochord morphogenesis in the ascidian *Ciona savignyi* [48]. We have

previously demonstrated that the MTJ captures elongating muscle fibers, but it was not known what ECM components were relevant [24]. It was also not known if the cessation of muscle fiber elongation is cell autonomous or mediated by community effects. Here we show that laminin is one component of the MTJ that stops elongating fibers. This result, combined with the work of Veeman et al., suggests that roles for laminin in boundary capture may be conserved, at least within chordates. We also show that wild-type cells in *lamy1* morphant embryos have a reduced ability to cross the MTJ. The fact that wild-type cells are less able to cross the MTJ, but do not rescue their *lamy1*-deficient neighbors, suggests that boundary capture is a cell autonomous process. These data also suggest that MTJ breakdown in *lamβ1* and *γ1*-deficient embryos is a local event caused by the failure of elongating muscle fibers to stop when they reach the MTJ. We do not currently know why 75% of elongating muscle cells in *lamβ1* and *γ1*-deficient embryos do stop elongating, but 25% do not. We hypothesize that the MTJ boundary is not homogenous. In this scenario, the absence of laminin would leave “holes” in the MTJ and muscle cells would elongate through these holes (Figure 8B, B1). Future experiments will be directed towards identifying additional molecular cues involved in boundary capture.

Methods

Zebrafish Husbandry

Zebrafish embryos were obtained from natural spawnings of adult fish kept at 28.5°C on a 16 h light/8 h dark cycle and were staged according to [49].

Immunocytochemistry

F59 was utilized to visualize slow fibers as previously described [25,50]. Alexa Fluor 488 and 546 phalloidin and Sytox green were obtained from Molecular Probes. We used the H2A:GFP transgenic line of zebrafish to visualize nuclei [51]. A “scatter” label of cells filled with fluoro-ruby dextrans (Molecular Probes) was obtained by microinjecting embryos at the 512–1000 cell stage with dextrans into the yolk cell close to the margin.

Antibodies used were: mouse monoclonal anti-myosin (F59) (Devoto, et al. 1996, generous gift of Frank Stockdale) 1:10, mouse monoclonal anti-β-catenin (Sigma) 1:500 and Alexa-Fluor 488, 546 and 633 conjugated goat anti-mouse and goat anti-rabbit secondary antibodies (Invitrogen) 1:200.

Imaging

Images were acquired using a Leica SP2 confocal microscope and a Zeiss ApoTome running on a Zeiss Axio Imager Z1. All mathematical analyses were done on images acquired on the Apotome using a 20× lens, NA 0.8, yielding a resolution of 1.5 pixels / μm. Images were linearly processed in Adobe Photoshop and collated in Adobe Illustrator.

Morpholinos

Morpholino-modified antisense oligonucleotides (MOs) were synthesized by Gene-Tools, LCC. The morpholinos used were previously described and recapitulate the mutant phenotypes [31].

Time-Lapse Analysis

Embryos were vitally stained and imaged with the fluorescent, lipophilic dye BODIPY-Ceramide (Molecular Probes, Eugene, OR) using the procedures outlined by [52,53]. Time-lapse recordings were made using a scanning laser confocal microscope (Leica SP2, Heidelberg, Germany). Time-lapse analysis with transplanted dextran-filled cells was performed utilizing the Zeiss ApoTome.

Morphometrics

To measure properties of dextran-filled cells, the z-series of the cell was projected such as to visualize the cell three-dimensionally. Cells were then segmented with ImageJ and the perimeter, area and major axis were measured. The major axis as determined by ImageJ is the longest length of the best fitting ellipse. The filament index was also calculated [54]:

$$F = \frac{PD}{4A}$$

where P , D and A are the perimeter, diameter and area respectively. For this study, the diameter was taken to be equal to the major axis. Note that a circle has a filament index $F = 1$ and an object having a value of F larger than 1 quantifies its departure from a circular shape. A two sample T-test was performed using SYSTAT. * denotes $p < 0.05$ and ** denotes $p < 0.01$.

Mathematical Modeling

In order to quantitatively characterize the morphology of muscle fiber growth, two geometrical models were developed. For simplicity, both the elliptical and protrusion models start with a unit circle (with radius = 1). For both models, when the cell is growing we assume that it does so only in the major direction and that the semi-minor axis stays constant, and for mathematical simplicity (and without any loss of generality), is equal to 1. Therefore, we have

$$A = \pi a \text{ and } P = 2\pi\sqrt{\frac{a^2 + 1}{2}}$$

The growth ratios for the area and perimeter of both models can be defined analytically. For the elliptical model, the growth ratio for the area at time t , $\hat{A}_{\text{elliptical}}(t)$, is equal to the major axis at time t , which grows continuously:

$$\hat{A}_{\text{elliptical}}(t) = a(t).$$

The perimeter growth ratio at time t , $\hat{P}_{\text{elliptical}}(t)$, is given by

$$\hat{P}_{\text{elliptical}}(t) = \sqrt{\frac{a(t)^2 + 1}{2}}$$

For the protrusion model, the cell grows in a two-step manner, expanding a thin protrusion of relatively small area ΔA and perimeter ΔP at time t , and then filling the area until the cell becomes an ellipse at time $t+1$. Therefore, the growth ratio for the area of the protrusion model will depend on whether it is growing a protrusion or filling that protrusion. For simplicity, we assume that the cell is growing a protrusion if t is even and it is filling the area opened by protrusion when t is odd:

$$\hat{A}_{\text{protrusion}}(t) = a(t), \text{ if } t \text{ is even or } \hat{A}_{\text{protrusion}}(t) = a(t-1) + \Delta A, \text{ if } t \text{ is odd}$$

Similarly for the perimeter of the protrusion model cell:

$$\hat{P}_{\text{protrusion}}(t) = \sqrt{\frac{a(t)^2 + 1}{2}}, \text{ if } t \text{ is even or } \hat{P}_{\text{protrusion}}(t) = \sqrt{\frac{a(t-1)^2 + 1}{2}} + \Delta P, \text{ if } t \text{ is odd.}$$

Since ΔA is relatively small with respect to the area of the whole cell, the extension of a protrusion will not significantly increase the area of the cell. Conversely, since ΔP is relatively large with respect to the perimeter of the whole cell, the perimeter of the cell will significantly increase. The evolution of the area and perimeter as a function of time for both models is shown in Figure 3A, A1.

Characterizing Anisotropy with the 2D WTMM Method

Preparation of images. Embryos were stained with β -catenin to outline all cells and fixed at 20 hpf. This stage is ideal because anterior, older somites have formed muscle but posterior somites have not. Thus, all the phases of muscle morphogenesis are represented within single embryos. Images representing all phases were obtained utilizing a Zeiss Axioimager equipped with an Apotome as mentioned above. Each image and focal plane was evaluated and the phase (short precursor, etc.) determined. The phase that was identified represented most cells within a focal plane. Because muscle cell elongation is an exceedingly dynamic process, cells within different focal planes within the same z-series are sometimes at different phases of elongation. Each image was then cropped into 256x256 pixel sub-images. This cropping is necessary to eliminate other tissues in the embryos such as residual yolk platelets and neural tissue. Cropping was also necessary because fast muscle cells in the dorsal and ventral halves of somites angle slightly towards the middle. We thus flipped all ventrally derived panels so that the WTMM vector angles for dorsal and ventral halves would not cancel each other out within a single sub-image. At least 10 images for at least 5 different embryos were analyzed for each phase.

The 2D WTMM method is a multifractal image analysis formalism introduced in [34], where the different dilations of the analyzing wavelet reveal quantitative roughness information at every length scale considered. By considering two wavelets that are, respectively, the partial derivatives with respect to x and y of a 2D smoothing Gaussian function, the Wavelet Transform is thus the gradient vector of the analyzed image smoothed by dilated versions of the Gaussian filter. A very efficient way to perform point-wise regularity analysis is to use the Wavelet Transform Modulus Maxima (WTMM) [55,56]. At a given scale a , the WTMM are defined by the positions where the Wavelet Transform Modulus is locally maximum in the direction A of the gradient vector. When analyzing rough surfaces, these WTMM lie on connected chains called *maxima chains* [34], as shown in Figure 5, green lines. One only needs to record the position of the local maxima of the gradient along the maxima chains together with the angle A at the corresponding locations. At each scale a , the wavelet analysis thus reduces to store those WTMM maxima (WTMMM) only (red dots in Figure 5). They indicate locally the direction where the signal has the sharpest variation.

An image having an anisotropic signature means that the intensity variation in the image will differ according to the direction considered. Such images having an anisotropic signature can be easily characterized from the directional information provided by the continuous 2D Wavelet Transform [35]. This is done by considering, at all size scales a , the probability density functions (pdfs), $P_a(A)$, of the angles, A , associated to each WTMMM vector. A flat pdf indicates unprivileged random directions of sharpest intensity variation (i.e. isotropy), while any departure from a flat distribution is interpreted as the signature of anisotropy. For the present study, a strong anisotropic signature is interpreted as a strongly structured cell lattice.

Anisotropy Factor

In order to obtain quantitative information from the angle pdfs $P_a(A)$, they are compared to a theoretical flat distribution

representing an ideal isotropic signature (see Figure 5F). The *anisotropy factor*, F_a , defined for each value of the scale parameter a , is given by the area between the curve corresponding to the observed pdfs and a flat distribution:

$$F_a = \int_{-\pi}^{\pi} \left| P_a(A) - \frac{1}{2\pi} \right| dA.$$

Therefore F_a has been defined in such a way that a theoretically isotropic surface will have a value of $F_a = 0$, while any value greater than 0 quantifies a departure from isotropy.

Construction of Simulated Isotropic Surfaces for Calibration Purposes

Following the standard procedures presented in [34,35], fractional Brownian motion (fBm) isotropic surfaces were generated. Two-dimensional fBm's are processes with stationary zero-mean Gaussian increments that are statistically invariant under isotropic dilations. They are therefore expected to reproduce quite faithfully the isotropic scaling invariance properties.

Genetic Mosaic Analysis

WT embryos were injected with 10,000 MW dextrans (Molecular Probes). Cells were removed at the sphere stage and placed into hosts that had been injected with *lamy1* MOs. Hosts were grown up until the appropriate stage, stained with phalloidin and the number of transplanted control cells that crossed MTJ boundaries was compared with the number of *lamy1* morphant cells that crossed MTJ boundaries.

Supporting Information

Figure S1 Somite Boundary Shape, Slow Muscle Migration and Fast Muscle Elongation are Disrupted in laminin β 1 and γ 1-deficient Embryos. All panels are ApoTome images at the 18 somite stage. Side views, anterior left, dorsal top, except panels numbered 4 that are transverse views, lateral left, medial right. Panels 2-4 are higher magnification views of the embryos shown in panels numbered 1. Panels numbered 1 and 2 are single focal planes from a Z-series and show phalloidin staining that outlines all cells. Panels numbered 3 and 4 are projections of the entire Z-series of panels numbered 2. In these panels, F59 expression denotes slow-twitch muscle fibers. All panels (A1-C1, A2-C2) are from approximately the same anterior-posterior and medial-lateral position in control and morphant embryos. A1-C1) WT control embryos contain robust, chevron shaped boundaries. *lam β 1* and *lamy1* morphants have rounder, flatter shaped boundaries. Note that initial somite boundaries, albeit less chevron-shaped, do form in *lam β 1* and *lamy1* morphant embryos. A2-C2) Whereas fast muscle cells are elongating in control embryos (A2, white arrow), fast-twitch muscle cell elongation is disrupted in both *lam β 1* (B2, white arrowhead) and *lamy1* (C2, white arrowhead) morphant embryos but some elongation does occur (white arrows). A3-C3/A4-C4) Myosin organization in slow-twitch muscle fibers is disrupted in *lam β 1* and *lamy1* morphant embryos. In control embryos, the projected (panels numbered 3) and rotated transverse views (panels numbered 4) show organized slow-twitch fibers that have migrated laterally (muscle pioneers: red asterisk). Slow-twitch fiber organization, spacing, and migration, are disrupted in *lam β 1* and *lamy1* morphant embryos.

Found at: doi:10.1371/journal.pgen.1000219.s001 (7.8 MB TIF)

Movie S1 Time-lapse confocal microscopy using BODIPY-ceramide to outline cell borders suggests that cells intercalate during elongation. Side views, anterior left. Colored cells were tracked in Image J and pseudocolored in Adobe Photoshop. The purple cell initiates elongation as does the orange cell. The blue cell elongates through time, extending a thin protrusion between the orange and green cells eventually reaching the anterior boundary. The long but irregularly shaped green cell becomes a rod shaped myotube through time.

Found at: doi:10.1371/journal.pgen.1000219.s002 (2.0 MB MOV)

Movie S2 Time-lapse analysis of three-dimensional projections from ApoTome micrographs shows the three phases of morphogenesis. Short dextran-filled cells exhibit protrusive activity as they begin elongating. Elongating cells initially extend long protrusions that subsequently grow, resulting in the elongation of the cell. Green arrowheads denote extensions. Cells in the myotube formation phase are initially irregularly shaped but become rod shaped myotubes through time.

Found at: doi:10.1371/journal.pgen.1000219.s003 (1.0 MB MOV)

Movie S3 Three-dimensional shapes of fixed cells in different phases of morphogenesis. Part 1: A lateral-medial Z-series of a

long yet irregularly shaped dextran-filled cell with one nucleus. Part 2: Rotation of a three-dimensional projection of a partially elongated dextran-filled cell in a fixed embryo showing an extension. Part 3: Rotation of a three-dimensional projection of myotube in a fixed embryo.

Found at: doi:10.1371/journal.pgen.1000219.s004 (2.7 MB MOV)

Movie S4 Time-lapse analysis of live cells.

Found at: doi:10.1371/journal.pgen.1000219.s005 (1.5 MB MOV)

Acknowledgments

We thank Yin Chiu for help with analysis. The authors would like to thank Tom Gridley for his thoughtful reading of the manuscript as well as the anonymous reviewers and their excellent suggestions. The authors would also like to thank Mary Simon, Stephen Devoto, Carol Kim, Scott Collins, and Alain Arneodo for helpful discussions and Mark Nilan for fish care.

Author Contributions

Conceived and designed the experiments: CAH. Performed the experiments: CJS ECO RJ CAH. Analyzed the data: CJS MG MWK AK CAH. Contributed reagents/materials/analysis tools: AK. Wrote the paper: CJS MG MWK AK CAH.

References

- Hollway G, Currie P (2005) Vertebrate myotome development. *Birth Defects Res C Embryo Today* 75: 172–179.
- Hollway GE, Currie PD (2003) Myotome meanderings. Cellular morphogenesis and the making of muscle. *EMBO Rep* 4: 855–860.
- Buckingham M, Bajard L, Chang T, Daubas P, Hadchouel J, et al. (2003) The formation of skeletal muscle: from somite to limb. *J Anat* 202: 59–68.
- Long JH, Adcock B, Root RG (2002) Force transmission via axial tendons in undulating fish: a dynamic analysis. *Comp Biochem Physiol A Mol Integr Physiol* 133: 911–929.
- Kahane N, Cinnamon Y, Kalcheim C (1998) The cellular mechanism by which the dermomyotome contributes to the second wave of myotome development. *Development* 125: 4259–4271.
- Denetclaw WF, Ordahl CP (2000) The growth of the dermomyotome and formation of early myotome lineages in thoracolumbar somites of chicken embryos. *Development* 127: 893–905.
- Ben-Yair R, Kalcheim C (2005) Lineage analysis of the avian dermomyotome sheet reveals the existence of single cells with both dermal and muscle progenitor fates. *Development* 132: 689–701.
- Gros J, Scaal M, Marcelle C (2004) A two-step mechanism for myotome formation in chick. *Dev Cell* 6: 875–882.
- Waterman RE (1969) Development of the lateral musculature in the teleost, *Brachydanio rerio*: a fine structural study. *Am J Anat* 125: 457–493.
- Ohtake Y, Tojo H, Seki M (2006) Multifunctional roles of MT1-MMP in myofiber formation and morphostatic maintenance of skeletal muscle. *J Cell Sci* 119: 3822–3832.
- Ho RK, Ball EE, Goodman CS (1983) Muscle pioneers: large mesodermal cells that erect a scaffold for developing muscles and motoneurons in grasshopper embryos. *Nature* 301: 66–69.
- Beckett K, Bayliss MK (2007) 3D analysis of founder cell and fusion competent myoblast arrangements outlines a new model of myoblast fusion. *Dev Biol* 309: 113–125.
- Chen EH, Olson EN (2004) Towards a molecular pathway for myoblast fusion in *Drosophila*. *Trends Cell Biol* 14: 452–460.
- Moore CA, Parkin CA, Bidet Y, Ingham PW (2007) A role for the Myoblast city homologues Dock1 and Dock5 and the adaptor proteins Crk and Crkl-like in zebrafish myoblast fusion. *Development* 134: 3145–3153.
- Srinivas BP, Woo J, Leong WY, Roy S (2007) A conserved molecular pathway mediates myoblast fusion in insects and vertebrates. *Nat Genet* 39: 781–786.
- LeBleu VS, Macdonald B, Kalluri R (2007) Structure and function of basement membranes. *Exp Biol Med* (Maywood) 232: 1121–1129.
- Hoffman EP, Brown RH Jr, Kunkel LM (1987) Dystrophin: the protein product of the Duchenne muscular dystrophy locus. *Cell* 51: 919–928.
- Bonnemann CG, Modi R, Noguchi S, Mizuno Y, Yoshida M, et al. (1995) Beta-sarcoglycan (A3b) mutations cause autosomal recessive muscular dystrophy with loss of the sarcoglycan complex. *Nat Genet* 11: 266–273.
- Noguchi S, McNally EM, Ben Othmane K, Hagiwara Y, Mizuno Y, et al. (1995) Mutations in the dystrophin-associated protein gamma-sarcoglycan in chromosome 13 muscular dystrophy. *Science* 270: 819–822.
- Nigro V, de Sa Moreira E, Piluso G, Vainzof M, Belsito A, et al. (1996) Autosomal recessive limb-girdle muscular dystrophy, LGMD2F, is caused by a mutation in the delta-sarcoglycan gene. *Nat Genet* 14: 195–198.
- Hall TE, Bryson-Richardson RJ, Berger S, Jacoby AS, Cole NJ, et al. (2007) The zebrafish *candyloss* mutant implicates extracellular matrix adhesion failure in laminin α 2-deficient congenital muscular dystrophy. *Proc Natl Acad Sci U S A* 104: 7092–7097.
- Bajanca F, Luz M, Raymond K, Martins GC, Sonnenberg A, et al. (2006) Integrin α 6 β 1-laminin interactions regulate early myotome formation in the mouse embryo. *Development* 133: 1635–1644.
- Nishiuchi R, Murayama O, Fujiwara H, Gu J, Kawakami T, et al. (2003) Characterization of the ligand-binding specificities of integrin α 3 β 1 and α 6 β 1 using a panel of purified laminin isoforms containing distinct alpha chains. *J Biochem* 134: 497–504.
- Henry CA, McNulty IM, Durst WA, Munchel SE, Amacher SL (2005) Interactions between muscle fibers and segment boundaries in zebrafish. *Dev Biol* 287: 346–360.
- Devoto SH, Melancon E, Eisen JS, Westerfield M (1996) Identification of separate slow and fast muscle precursor cells in vivo, prior to somite formation. *Development* 122: 3371–3380.
- Blagden CS, Currie PD, Ingham PW, Hughes SM (1997) Notochord induction of zebrafish slow muscle mediated by Sonic hedgehog. *Genes Dev* 11: 2163–2175.
- Cortes F, Daggett D, Bryson-Richardson RJ, Neyt C, Maule J, et al. (2005) Cadherin-mediated differential cell adhesion controls slow muscle cell migration in the developing zebrafish myotome. *Dev Cell* 5: 865–876.
- Henry CA, Amacher SL (2004) Zebrafish slow muscle cell migration induces a wave of fast muscle morphogenesis. *Dev Cell* 7: 917–923.
- Kudo H, Amizuka N, Araki K, Inohaya K, Kudo A (2004) Zebrafish perostin is required for the adhesion of muscle fiber bundles to the myoseptum and for the differentiation of muscle fibers. *Dev Biol* 267: 473–487.
- Crawford BD, Henry CA, Clason TA, Becker AL, Hille MB (2003) Activity and distribution of paxillin, focal adhesion kinase, and cadherin indicate cooperative roles during zebrafish morphogenesis. *Mol Biol Cell* 14: 3065–3081.
- Parsons MJ, Pollard SM, Saude I, Feldman B, Coutinho P, et al. (2002) Zebrafish mutants identify an essential role for laminins in notochord formation. *Development* 129: 3137–3146.
- Julich D, Geister R, Holley SA (2005) Integrin α 5 and delta/notch signaling have complementary spatiotemporal requirements during zebrafish somitogenesis. *Dev Cell* 8: 575–586.
- Koshida S, Kishimoto Y, Ustumi H, Shimizu T, Furutani-Seiki M, et al. (2005) Integrin α 5-dependent fibronectin accumulation for maintenance of somite boundaries in zebrafish embryos. *Dev Cell* 8: 587–598.
- Arneodo A, Decoster N, Roux S (2000) A wavelet-based method for multifractal image analysis. I. Methodology and test applications on isotropic and anisotropic random rough surfaces. *European Journal of Physics B* 15: 567–600.
- Khalil A, Joncas G, Nekka F, Kestener P, Arneodo A (2006) Morphological analysis of HI features. II. Wavelet-based multifractal formalism. *Astrophysical Journal Supplement Series* 165: 512–550.

36. Colognato H, Winkelmann DA, Yurchenco PD (1999) Laminin polymerization induces a receptor-cytoskeleton network. *J Cell Biol* 145: 619–631.
37. Stellabotte F, Devoto SH (2007) The teleost dermomyotome. *Dev Dyn* 236: 2432–2443.
38. Hammond CL, Hinitz Y, Osborn DP, Minchin JE, Tettamanti G, et al. (2007) Signals and myogenic regulatory factors restrict pax3 and pax7 expression to dermomyotome-like tissue in zebrafish. *Dev Biol* 302: 504–521.
39. Devoto SH, Stoiber W, Hammond CL, Steinbacher P, Haslett JR, et al. (2006) Generality of vertebrate developmental patterns: evidence for a dermomyotome in fish. *Evol Dev* 8: 101–110.
40. Krauss RS (2007) Evolutionary conservation in myoblast fusion. *Nat Genet* 39: 704–705.
41. Roy S, Wolff C, Ingham PW (2001) The u-boot mutation identifies a Hedgehog-regulated myogenic switch for fiber-type diversification in the zebrafish embryo. *Genes Dev* 15: 1563–1576.
42. Yao CC, Ziober BL, Sutherland AE, Mendrick DL, Kramer RH (1996) Laminins promote the locomotion of skeletal myoblasts via the alpha 7 integrin receptor. *J Cell Sci* 109 (Pt 13): 3139–3150.
43. Cole F, Zhang W, Geyra A, Kang JS, Krauss RS (2004) Positive regulation of myogenic bHLH factors and skeletal muscle development by the cell surface receptor CDO. *Dev Cell* 7: 843–854.
44. Jacobson AG, Moury JD (1995) Tissue boundaries and cell behavior during neurulation. *Dev Biol* 171: 98–110.
45. Jacobson AG, Oster GF, Odell GM, Cheng LY (1986) Neurulation and the cortical tractor model for epithelial folding. *J Embryol Exp Morphol* 96: 19–49.
46. Moury JD, Jacobson AG (1989) Neural fold formation at newly created boundaries between neural plate and epidermis in the axolotl. *Dev Biol* 133: 44–57.
47. Keller R, Davidson L, Edlund A, Ehrl T, Ezin M, et al. (2000) Mechanisms of convergence and extension by cell intercalation. *Philos Trans R Soc Lond B Biol Sci* 355: 897–922.
48. Veeman MT, Nakatani Y, Hendrickson C, Ericson V, Lin C, et al. (2008) Chongmague reveals an essential role for laminin-mediated boundary formation in chordate convergence and extension movements. *Development* 135: 33–41.
49. Kimmel CB, Ballard WW, Kimmel SR, Uhlmann B, Schilling TF (1995) Stages of embryonic development of the zebrafish. *Dev Dyn* 203: 253–310.
50. Crow MT, Stockdale FE (1986) Myosin expression and specialization among the earliest muscle fibers of the developing avian limb. *Dev Biol* 113: 238–294.
51. Pauls S, Geldmacher-Voss B, Campos-Ortega JA (2001) A zebrafish histone variant H2A.F/Z and a transgenic H2A.F/Z-GFP fusion protein for in vivo studies of embryonic development. *Dev Genes Evol* 211: 603–610.
52. Cooper MS, D'Amico LA, Henry CA (1999) Analyzing morphogenetic cell behaviors in vitally stained zebrafish embryos. *Methods Mol Biol* 122: 185–204.
53. Cooper MS, D'Amico LA, Henry CA (1999) Confocal microscopic analysis of morphogenetic movements. *Methods Cell Biol* 59: 179–204.
54. Khalil A, Grant JL, Caddle LB, Atzema E, Mills KD, et al. (2007) Chromosome territories have a highly nonspherical morphology and nonrandom positioning. *Chromosome Res* 15: 899–916.
55. Mallat S, Hwang WL (1992) *IEEE Trans on Information Theory* 38: 617.
56. Mallat S, Zhong S (1992) *IEEE Trans on Pattern Analysis and Machine Intelligence* 14: 710.

BIOGRAPHY OF THE AUTHOR

Michelle F. Goody was born in Portland, ME in May of 1985. She graduated as the Valedictorian from Orono High School in Orono, ME in 2003. In 2007, she graduated *summa cum laude* from the University of Maine with a Bachelor of Science degree in Biology. Michelle worked in the research laboratories of Dr. Mary Rumpho and Dr. Seanna Annis as an undergraduate student at UMaine. During Graduate School, Michelle was a Teaching Assistant for the Developmental Biology course and laboratories. Michelle has two first author publications, one co-second author publication and two manuscripts in preparation. The titles of her published manuscripts are: “Nr2f1b-mediated NAD⁺ production regulates cell adhesion and is required for muscle morphogenesis *in vivo* (*Dev Biol* 2010)”, “Dynamic interactions between cells and their extracellular matrix mediate embryonic development (*Mol Reprod Dev* 2010)”, and “Time-lapse analysis and mathematical characterization elucidate novel mechanisms underlying muscle morphogenesis (*PLoS Genet* 2008)”. Her manuscripts in preparation will likely be titled: “NAD⁺ ameliorates muscular dystrophy in zebrafish” and “Compensation between cell adhesion molecules mediates muscle homeostasis.” Michelle won the 2011 College of Natural Sciences, Forestry and Agriculture Graduate Research Excellence Award scholarship. She is a candidate for the Doctor of Philosophy degree in Biomedical Sciences from the University of Maine in August, 2012.